FLAME PROPAGATION OF PREMIXED GAS MIXTURES DEFLAGRATION IN TEE PIPELINES

SINA DAVAZDAH EMAMI

THESIS SUBMITTED IN FULFILMENT OF THE REQUIREMENTS FOR THE DEGREE OF DOCTOR OF PHILOSOPHY

DEPARTMENT OF CHEMICAL ENGINEERING/
FACULTY OF ENGINEERING

UNIVERSITY OF MALAYA

KUALA LUMPUR

2016

UNIVERSITY OF MALAYA
ORIGINAL LITERARY WORK DECLARATION

Name of Candidate: SINA DAVAZDAH EMAMI

Registration/Matric No: KHA120141

Name of Degree: DOCTOR OF PHILOSOPHY

Title of Project Paper/Research Report/Dissertation/Thesis ("this Work"):

FLAME PROPAGATION OF PREMIXED GAS MIXTURES DEFLAGRATION IN TEE PIPELINES

Field of Study: HEALTH, SAFETY AND ENVIRONMENT-PROCESS SAFETY

I do solemnly and sincerely declare that:

(1) I am the sole author/writer of this Work;
(2) This Work is original;
(3) Any use of any work in which copyright exists was done by way of fair dealing and for permitted purposes and any excerpt or extract from, or reference to or reproduction of any copyright work has been disclosed expressly and sufficiently and the title of the Work and its authorship have been acknowledged in this Work;
(4) I do not have any actual knowledge nor do I ought reasonably to know that the making of this work constitutes an infringement of any copyright work;
(5) I hereby assign all and every rights in the copyright to this Work to the University of Malaya ("UM"), who henceforth shall be owner of the copyright in this Work and that any reproduction or use in any form or by any means whatsoever is prohibited without the written consent of UM having been first had and obtained;
(6) I am fully aware that if in the course of making this Work I have infringed any copyright whether intentionally or otherwise, I may be subject to legal action or any other action as may be determined by UM.

Candidate's Signature Date:

Subscribed and solemnly declared before,

Witness's Signature Date:

Name:

Designation:

ABSTRACT

Explosions in chemical, gas and petroleum industries are still a significant problem leading to injuries, death, destruction of equipment and downtime. In the chemical, hydrocarbon and gas process industries, a large variety of cases can be found where internal gas explosions, confined explosion, may occur. As a consequence there is a need to protect gas pipelines against propagation of unwanted combustion phenomena such as deflagrations to detonations transmission (DDT). However, a review of the literatures revealed that flame acceleration of hydrocarbons/air, hydrogen/air, hydrocarbons-hydrogen/air and hydrogen-inhibitors/air mixtures with wild range of concentration in tee pipelines are still unclear. Thus, given the gaps in the literature, this research was carried out to investigate the dynamics of flame propagation of premixed gas mixtures deflagration in tee pipelines for determining the most critical point(s) of tee pipelines based on the rate of pressure rise with respecting ignition positions. In this research study, the fuel/air mixtures were ignited at six different ignition positions in two different tee pipes' configuration. The results of pure hydrocarbons/air and hydrogen/air mixtures show that, while there is no significant difference in the maximum pressure and rate of pressure rise in both the tee-pipe arrangements investigated, the bending pipe consistently produces the worst set of results in terms of maximum pressure and flame speeds, in pipe explosions involving the most reactive mixtures. In addition, the detailed records of pressure traces and blast waves show that the duration of flame acceleration, the flame direction and the initial ignition point depend on the tee junction placement along the pipe length, as this gives a different overall profile of the flame acceleration mechanism. Moreover, for the overall observation of hydrocarbons-hydrogen/air mixture, it can be said that the flame reactivity of ethylene-hydrogen/air and NG-hydrogen/air was much higher. The kinetic reaction of these mixtures contributed to the overall explosion development. However, the dynamics of flame deployment in the tee junctions had a

significant effect on the recorded maximum overpressure and flame speeds along the pipes. The obtained data show that the lower distance between tee junction and the ignition point caused a higher explosion severity in terms of the rate of pressure rise. The results show that, when ignited at the furthest distance, the tee junction area is most vulnerable to the critical pressure impact of gas explosion. However, no similar trend was observed at the other ignition positions. In addition, mixtures with compositions of 95% H_2-2.5% Ar-2.5% N_2/air, 95% H_2-5% N_2/air, H_2/air and 95% H_2-5% Ar/air showed the highest risks due to the higher diffusivity ratio and the associated rate of pressure rise. The results show that mixtures with CO_2 lead to lower severity than other hydrogen-inhibitors/air mixutures (~ 50% reduction), as the average recorded maximum flame speed for this particular mixture was lower at all of the ignition points. This suggests that the effectiveness of the inhibitors should be in the order of Ar < N_2 < CO_2.

ABSTRAK

Kejadian letupan di industri petroleum, kimia dan gas adalah isu signifikan yang mengakibatkan kerosakan kepada peralatan, masa henti operasi, kecederaan dan kematian. Pelbagai kes letupan gas dalaman dan letupan dalam ruang terkurung mungkin berlaku di industri-industri ini. Oleh yang demikian, perlindungan terhadap fenomena perambatan pembakaran tidak dikehendaki seperti *deflagrations to detonations (DDT)* dalam proses industri adalah perlu. Namun begitu, berdasarkan kajian literatur, fenomena pecutan nyalaan campuran hidrokarbon/udara, hidrogen/udara, hidrokarbon-hidrogen/udara dan hidrogen-perencat/udara dengan pelbagai kepekatan di dalam saluran paip Tee masih tidak jelas. Justeru, kajian ini dijalankan bagi mengkaji dinamik perambatan nyalaan gas pracampuran di dalam saluran paip Tee. Kedudukan paling kritikal di dalam saluran paip ditentukan berdasarkan kadar peningkatan tekanan yang bergantung kepada kedudukan pencucuhan. Dalam kajian yang dijalankan, campuran bahan api/udara dinyalakan pada enam titik nyalaan yang berbeza di dua tatarajah salur paip Tee berlainan. Hasil kajian terhadap campuran tulen hidrokarbon/udara dan campuran hidrogen/udara mendapati bahawa tekanan maksimum dan kadar peningkatan tekanan tidak menunjukkan perbezaan signifikan antara kedua-dua tatarajah saluran paip. Selain itu, pembengkokan paip juga didapati tidak mempengaruhi tekanan maksimum dan laju nyala dalam letupan paip yang mengandungi campuran sangat reaktif. Berdasarkan data gelombang bagas dan tekanan yang direkodkan, tempoh pecutan nyalaan, arah nyalaan dan titik mula pencucuhan bergantung kepada kedudukan persimpangan Tee yang juga memberi kesan berbeza kepada profil keseluruhan mekanisme pecutan nyalaan. Di samping itu, hasil kajian terhadap campuran hidrokarbon-hidrogen/udara mendapati reaktiviti nyalaan ethylene-hidrogen/udara dan gas asli-hidrogen/udara adalah lebih tinggi berbanding campuran gas lain. Tindak balas kinetik campuran-campuran ini memberi kesan kepada keseluruhan pengorakan letupan.

Namun begitu, dinamik nyalaan di persimpangan tee memberi kesan yang signifikan terhadap tekanan lebih maksimum dan laju nyala sepanjang saluran paip. Berdasarkan data yang diperoleh, tahap keterukan letupan yang bergantung kepada kadar peningkatan tekanan semakin tinggi apabila jarak persimpangan Tee semakin hampir ke titik pencucuhan. Persimpangan Tee merupakan kawasan paling terdedah kepada kesan tekanan kritikal letupan gas apabila titik pencucuhan terletak paling jauh (titik A). Walau bagaimanapun, tiada trend yang sama diperolehi di titik pencucuhan lain. Di samping itu, komposisi campuran 95% H_2-2.5% Ar-2.5% N_2/udara, 95% H_2-5% N_2/udara, H_2/udara dan 95% H_2-5% Ar/udara didapati merupakan campuran paling berisiko disebabkan oleh nisbah kemeresapan yang lebih tinggi dan kadar peningkatan tekanan berkaitan. Hasil kajian menunjukkan campuran karbon dioksida memberi kesan kepada tahap keterukan yang lebih rendah berbanding campuran hidrogen-perencat/udara (~50% penurunan) memandangkan purata laju nyala maksimum campuran ini adalah lebih rendah di kesemua titik pencucuhan. Oleh itu, susunan perencat mengikut keberkesanan ialah $Ar < N_2 < CO_2$.

ACKNOWLEDGEMENTS

I would like to express my deepest gratitude to both supervisors Dr. Mahar Diana and Associate Professor Dr. Che Rosmani Che Hassan and my external Co-supervisor Rafiziana Md. Kasmani from UTM university for their astute support, encouragements and valuable advices and guides throughout the study period.

The author would like to express the gratefulness and appreciation to PPP grant (Project No: PG105-2013A), and UMRG grant (Project No: RP015-2012H) from University of Malaya (UM).

I would like to share my deepest and sincerest thankfulness to my family for their kindness, love and supports during my life. I also want to share my purest feeling to never put out of my mind their dedication and unwavering affections in my journey.

TABLE OF CONTENTS

LIST OF FIGURES

LIST OF TABLES

LIST OF ABBREVIATIONS

DNS - DIRECT NUMERICAL SIMULATION
CFD - COMPUTATIONAL FLUID DYNAMICS
RNG - RENORMALIZATION GROUP
NPT - NORMAL PRESSURE AND TEMPERATURE
DDT - DEFLAGRATION TO DETONATION TRANSITION
MILD - MODERATE OR INTENSE LOW-OXYGEN DILUTION
CNG - COMPRESSED NATURAL GAS
BSEC - BRAKE SPECIFIC ENERGY COMBUSTION

LIST OF SYMBOLS

Y_M - Fluctuating dilatation in compressible turbulence

u_b - Burning velocity

U_0 - Jet velocity

$t_{ig.ad}$ - Adiabatic ignition delay time

t_{flow} - Flow time

T - Absolute temperature

S_i - Rate of creation

S_g - uUnburnt gas velocity

S_f - Flame speed

R - Universal gas constant (8.314 J/kmol .K)

P - Relative pressure

n - Temperature exponent

N - Total number of fluid phase chemical species

M - Molar mass

L_e - Lewis number

k - Von karman constant (=0.4187)

K - Turbulence kinetic energy

K - Thermal conductivity

H_L - Lift-off height

E - Activation energy for the reaction

E - Expansion factor and

E - Empurical constant (= 9.793)

D - Mass diffusivity

Cp - Specific heat capacity

A - Pre-exponential factor

U_p - Mean velocity of the fluid at point P

μ - Dynamic viscosity of the fluid.

Y_i - Local mass fraction of each species

C_μ - Constant=0.09

$C_{1\epsilon}$ - Constant=1.44

$C_{2\epsilon}$ - Constant=1.92

G_k - Turbulence kinetic energy due to the mean velocity gradients.

G_b - Turbulence kinetic energy due to buoyancy.

S_k - User-defined source terms

S_ϵ - User-defined source terms

R_i - Net rate of production of species i by chemical reaction

u, ϑ, w - Normal stresses in different direction

ρ - Density

k_P - Turbulence kinetic energy at point P

y_P - Distance from point P to the wall

y^* - Mean velocity

σ_ϵ - Constant=1.03

σ_k - Constant=1

Sc_t - Turbulent Schmidt number

μ_t - Turbulent viscosity

$\delta_{i,j}$ - Kronecker delta

Φ - Equivalence ratio

μ_t - Turbulent (or eddy) viscosity

ϵ - Rate of dissipation

f - Constant value

α - Thermal diffusivity

CHAPTER I: INTRODUCTION

1.1. Background of Study

Explosions in the chemical, gas and petroleum industries are still a significant problem leading to injuries, death, destruction of equipment and downtime. In the chemical, hydrocarbon and gas process industries, there is a large variety of cases of internal gas explosions or confined explosions (Hadjisophocleous & Mehaffey, 2016). Such explosions can be caused by uncontrolled leaks, simply by accidental purging with air or unpredictable failures (Khan & Abbasi, 2001). As a consequence, there is a need for protection of gas pipelines against propagation of unwanted combustion phenomena such as deflagration to detonation transmission (DDT) (including decomposition flames) in the process (Blanchard et al., 2010; Grossel, 2010).

To ensure safety precautions in pipeline gas carriers, it is essential to fully characterize and quantify their explosion behaviour. In particular, information regarding the maximum pressure, maximum rate of pressure rise (i.e., the deflagration index) and flame speed, which are among the most important parameters for the assessment of process hazards, and the safe design of process equipment are required (Hawkes & Chen, 2004; Salzano et al., 2012). Studies on flame propagation and explosion mechanisms in pipes have been extensively discussed and reported (Blanchard et al., 2010; Chatrathi et al., 2001; Emami et al., 2013; Jianliang et al., 2005; Oh et al., 2001; Phylaktou et al., 1993; Thomas et al., 2010), but most are focused on specific applications, i.e., different pipe diameters, effects of obstacles, bending pipes or straight pipes. For this reason, holistic studies should be performed on flame propagation in different pipe configurations, considering the complicated problems involved in the interaction between fluid dynamics, heat transfer and turbulent combustion. For instance, Zhu et al. (2010) used a single-bend, U-shaped pipe and a Z-shaped pipe in their experimental setup, to investigate the effect of roadway turning on methane-air explosion propagation. The results showed that, by increasing the number of turnings the explosion strength was significantly enhanced, while the flame speed and peak overpressure increased dramatically. In addition, the values of flame speed and maximum overpressure were enhanced by increasing the concentration of methane in the mixture in a horizontal pipe (Zhu et al., 2010). Another study on a straight pipe with a 60 L/D (length/diameter) showed that pressure and velocity waves accelerate with the increasing reaction rate of methane-air (Zhu et al., 2015). More examples of flame acceleration of fuels are presented in Section 2.4.2 in Chapter II. Yet, what is lacking is a comprehensive study of the governing parameters involved in flame propagation in different pipe configurations, by considering the physics and dynamics of the flame and pressure development of hydrocarbon-air and hydrogen-air explosions in a wide range of equivalence ratios (lean, stoichiometric and reach concentrations).

The point at which ignition takes place is another important factor during the initial stages of combustion (Phylaktou & Andrews, 1991). When the ignition source is further from a sealing flange or vessel wall, the flame will have a longer period to spherically propagate, leading to an initially higher overall flame speed and rate of pressure rise. Changes in these initial conditions will also affect the continuation of combustion further along the pipe, particularly when the pipe has different configurations, i.e., obstructed, bending and branched. Investigations of fuel transfer in pipes have shown that 36.5% v/v hydrogen in air has the potential to develop DDT (Heidari & Wen, 2014; Thomas et al., 2010). Blanchard et al. (2010) also reported that the ignition position had a significant effect on DDT development in the hydrogen/air explosion. In their study, the shortest run-up distance to DDT relative to the end pipe was recorded when the ignition source was placed 0.7 m from the pipe ends. From the discussion above, it can be postulated that there is a direct relationship between the changes of ignition positions and gas fuel on the pressure-development mechanism and flame dynamics during gas explosion inside a branched pipe.

Transporting hydrogen to end users could affect the integrity or durability of a pipeline network. This is because the existing gas pipeline network is designed, constructed and operated using natural gas. Once it is introduced into the pipeline, the hydrogen mixes with other gases such as hydrocarbons and inhibitors. Hence, for the safe use of hydrogen fuels, it is essential to fully characterize and quantify their explosion behaviour to insure that hydrogen application is safer. Extensive reports in the literature on the development of partial or total replacement of hydrocarbon fuels with hydrogen in power plants and vehicle engines have significantly highlighted society's awareness of environmental pollution and the declining supply of fossil fuels (Verhelst & Wallner, 2009; Vu et al., 2011a). These are broadly discussed in Chapter II.

A review of the literature revealed that the flame acceleration of hydrocarbons/air, hydrogen/air, hydrocarbons-hydrogen/air and hydrogen-inhibitors/air mixtures with wide range of concentration in tee pipes have not been extensively studied. Thus, the objective of this work is to report some new experimental and numerical data and provide an understanding of the explosion development in tee-pipe geometry on a medium-scale system, where ignition occurs at different locations. This work intends to present and discuss the effect of ignition position and tee-junction placement on the physics and dynamics of the explosion mechanism.

1.2. Problem statement

Industries commonly use pipes to connect vessels handling or storing flammable gas such as interconnected reactors, tanks and adjacent buildings (Di Benedetto & Salzano, 2010). After an explosion, the flame can propagate from one vessel to others through interconnected pipes, which increases the risk on the systems by enhancing the peak pressures and rates of pressure rise inside the vessels (Khan & Abbasi, 2001).

Consequently, paying attention to the flame acceleration of flammable fuels in the fuel-transferring process, especially in pipelines, are undeniable.

Moreover, due to growing environmental concerns and the deteriorating supply–demand scenario for fossil fuels (Abbasi et al., 2011), the idea of partial or complete replacement of hydrocarbon fuel with hydrogen in power plants and transportation engines, because of its unique properties (Das, 1996; Ikegami et al., 1982; Jamal & Wyszynski, 1994), is discussed in the literature (Verhelst & Wallner, 2009; Vu et al., 2011a). Hydrogen is a promising fuel for the future and is massively utilized in industries, especially in refineries and petrochemical industries. However, storing and transporting hydrogen in a pipeline is a complicated and subtle process. To avoid anomaly accidents, this process needs to take into account the numerous safety considerations and follow safety procedures (de Goey et al., 2011; Emami et al., 2013). Hydrogen is considered dangerous due to its properties of low ignition temperature, small ignition energy, wider explosion limits and fast combustion speeds [3,4]. In a confined space hydrogen is dangerous, like any other flammable gas. Moreover, the presence of inhibitors in hydrogen fuels can be considered a solution for preventing unexpected incidents. However, only scarce data about the effectiveness of inhibitors on hydrogen-explosion behaviour are available for different systems (Di Benedetto et al., 2009; Kwon & Faeth, 2001; Sabard et al., 2013; Shih, 2009). Consequently, it is required to fully understand the phenomena of flame propagation of hydrocarbons/air and hydrogen-hydrocarbon/air and hydrogen-inhibitors/air mixtures in fuel-transferring process to reduce unexpected incidents in systems.

1.3. Objectives

Based on the above-mentioned problems and gaps in the literature, the overall aim of the project is to develop and evaluate methodologies for classifying flame acceleration and deflagration to detonation hazard in pipe facilities that are filled with hydrocarbon/air, hydrogen/air, hydrocarbon-hydrogen/air and hydrogen-inhibitors/air mixtures. To undertake the main objective successfully, several tasks will be carried out to:

1. measure the associated maximum over pressure, explosion severity rate, flame speed and unburnt gas velocity of the flame front of hydrocarbon/air and hydrogen/air explosions in the tee pipes;
2. quantify the influence of pipe configuration, ignition position and the flame acceleration mechanism on explosion development in straight, bending and tee-junction pipes for hydrocarbon/air and hydrogen/air mixtures in different concentrations;
3. quantify the effect of hydrogen enrichment on flame propagation and explosion severity of hydrocarbon/air mixtures in tee pipelines;
4. determine the effect of inhibitor gases on flame propagation of hydrogen/air mixtures in tee pipes; and

determine the overall dynamic of flame acceleration and flame appearance of hydrocarbon/air and hydrogen/air explosions in tee pipelines using the FLUENT software.

1.4. Research Questions

Consequently, to achieve the above-mentioned objectives the research questions are:

- ✓ What is the maximum pressure, flame speed, rate of pressure rise and unburnt gas velocity ahead of the flame during explosion development in tee pipes?
- ✓ What is the influence of hydrogen addition on flame acceleration and over pressure during hydrocarbon explosion in tee junctions?
- ✓ What are the effects of adding inhibitors on the overall pressure and flame propagation of hydrogen/air explosion in tee junctions?

- ✓ Is the ignition position one of the governing factors influencing explosion development in a tee junction?
- ✓ Do obstacles in pipes, i.e. bending and tee junctions, result in an increase of the explosion severity compared to a straight pipe?

1.5. Significance of the Study

Although many studies have been conducted to identify the explosion behaviour of hydrocarbon/air, hydrogen/air, hydrogen-hydrocarbon/air and hydrogen-inhibitors/air mixtures, most are focused on specific applications, i.e., bending or straight pipes (Blanchard et al., 2010; Chatrathi et al., 2001; Emami et al., 2013; Jianliang et al., 2005; Oh et al., 2001; Phylaktou et al., 1993; Thomas et al., 2010). For this reason, holistic studies should be performed on flame propagation in different pipe configurations, considering the complicated problems involved in the interaction between fluid dynamics, heat transfer and turbulent combustion. This study is conducted to investigate the dynamic flame behaviour of gas fuel in the tee pipelines, which would generate new data.

Hydrogen has been promoted for several decades as an energy carrier of the future. As a secondary energy carrier with a lower heating value of 120 MJ/kg and density of 0.0899 kg/m^3, it can be used in many applications, particularly in refineries and petrochemicals (Barreto et al., 2003). However, hydrogen explosion hazards have constantly been a concern for its storage and transportation through pipelines; it is essential to address safety issues related to pipeline gas carriers by characterizing and adequately quantifying their explosion behaviour to protect against the propagation of unwanted combustion phenomena such as deflagrations and detonations (including decomposition flames) (Grossel, 2002; Xiao et al., 2012; Zhou et al., 2006). Extensive reports in the literature on the development of partial or total replacement of hydrocarbon fuels with hydrogen in power plants and vehicle engines have significantly highlighted society's awareness of environmental pollution and the declining supply of fossil fuels (Verhelst & Wallner, 2009; Vu et al., 2011a). To safely use hydrogen-hydrocarbon and hydrogen-inhibitors mixtures, knowledge of the explosion hazard of these fuels is vital. Thus, this work also aims to develop new experimental data and provide an understanding of the explosion development of these mixtures in tee-pipe geometry on a medium-scale system.

As mentioned earlier, the point at which ignition takes place is an important factor during the initial stages of combustion (Phylaktou & Andrews, 1991). Therefore, six ignition positions have been applied on experimental rigs to determine the most critical area of tee pipelines for these mixtures to cause explosion from the respective ignition position. It intends to explore data that are reported in the literature in terms of maximum pressures (P_{max}), rates of pressure rise (dP/dt) and flame speeds observed. The findings are more significant for gas fuel transferring and mining processing due to controlling the unexpected incidents that come about from unpredictable gas explosions in systems.

1.6. Scope of Study

To address the gaps in the literature, a study of flame propagation in tee pipelines at two different configurations resulting from the combustion of different concentrations of ethylene/air propane/air, NG/air, hydrogen/air NG-hydrogen/air, propane-hydrogen/air, ethylene-hydrogen/air, hydrohen-CO_2/air, hydrohen-N_2/air, hydrogen-Ar/air, hydrohen-CO_2-N_2/air, hydrohen-Ar-N_2/air and hydrohen-CO_2-Ar/air mixtures were carried out experimentally and numerically in this research. In addition, six ignition positions have been applied on experimental rigs. The full details of rigs' configuration and applied fuel are presented in Chapter III.

It is noticeable that the current research thesis has been divided into five main chapters. In the first chapter, the importance of the current research is discussed and the objectives of the research are defined. In Chapter II, the related previous research studies are summarized and discussed fairly to find out the available gaps in fuel transferring process. This chapter is divided into four main subsections: flame acceleration mechanisms in pipes, deflagration to detonation transmission in pipelines, the effects of the initial condition on flame acceleration of fuels and the flame evolution during explosion in different combustor systems. In Chapter III, the full details of the experimental and numerical setups and the experimental procedure are presented.

The experimental and numerical data are presented and discussed in Chapter IV. This chapter is divided into four main sections. In the first, the flame acceleration of hydrocarbon/air and hydrogen/air mixtures in different pipe configurations (e.g., straight, bending and tee pipes) is highlighted and explored. In the second section, the flame development of hydrocarbon-hydrogen/air mixtures in the tee pipes by considering the influence of ignition positions are discussed. In the following section, the effectiveness of inhibitors on the flame acceleration of hydrogen/air is discussed in detail. In Chapter V, the main achievements of the current research are summarized and some recommendations for both academic and industrial concepts for improvement of piping processing are given.

CHAPTER II: LITERATURE REVIEW

2.1. Introduction

Nowadays the need for energy is soaring significantly among conventional energy sources including oil, gas and coal. Among all sources, hydrocarbons and hydrogen fuel gases are the common fuel sources as they are playing significant roles to drive the economy’s wheels (Bradley et al., 2008; Ciccarelli & Dorofeev, 2008; Gamezo et al., 2008; Liberman et al., 2010). However, the processing industry has raised a major concern in terms of safety due to accidental gas explosions that have frequently happened and caused serious damage. Table 2.1 shows some associated gas explosion accidents.

Table 2. 1 Previous gas explosion accidents

Location	**Year(s)**	**reports**
Ethylene accidents (Ethylene is Explosive!, 2015)		
Sidon, Lebanon,	2013	Fatality: 1 Injury: 14 Reason: A reaction between chemicals used at the plant to treat bananas
Los Angeles, CA,	1999	Fatality: 1 Injury: 1 Reason: An ethylene cylinder was left open in a ripening room. Consequently, the LEL exceeded over 27,000 ppm, likely from a door opening, caused a spark, which ignited the explosion.

Fort Pierce, FL	late 1970's	Fortunately, this explosion did not kill anyone Reason: A reaction between chemicals used at the plant
Lantanna, FL,	1976	Fortunately, this explosion did not kill anyone Reason: This blast caused by cylinders of ethylene gas.
Camarillo, CA,	1987	Injury: 1 Reason: Inappropriate response for changing ethylene cylinders
Naples, FL	late 1970's	Injury: 1 Reason: Inappropriate response by releasing too much ethylene into the ripening area
Athens, Greece,	1997	Fatality: 2 Reason: Leaking ethylene cylinders in banana ripening rooms.
Natural gas disasters (List of pipeline accidents, 2015)		
Belgium	2004	A major natural gas pipeline exploded in Ghislenghien, Belgium near Ath (50 kilometres southwest of Brussels), killing 24 people and leaving 122 wounded.
Canada	1962	An explosion on a gas pipeline occurred on a lateral line, about 50 kilometers northwest of Edson, Alberta. 8 people were killed.
	2014	A Trans Canada Corporation gas transmission pipeline exploded and burned, causing a natural gas shortage in Manitoba and parts of the United States.
	2009	A refined product pipeline rupture near Farran's Point, Ontario on Ottawa Lateral, from Trans

		Northern Pipelines Inc. system, unknown petroleum product, unknown quantity.
	2009	A refined product pipeline rupture near Farran's Point, Ontario on Ottawa Lateral, on 2009 Oct 05, from Trans Northern Pipelines Inc. system, unknown petroleum product, unknown quantity.
	2003	A backhoe punctured a pipeline in Etobicoke, Ontario. The resulting explosion killed 7 people.
	1965	An explosion & fire involved the Albert Gas Trunk Line LTD. near Sundre, Alberta, killing 2 pipeline workers.
	1996	A gas pipeline, owned and operated by TransCanada Corporation ruptured at a crossing of the La Salle River in St. Norbert, Winnipeg resulting in an explosion, fire and loss of one home. There were no injuries or deaths reported.
	1965	An explosion from a gas line destroyed several apartments in the LaSalle Heights Disaster in LaSalle, Quebec killing 28 people, the worst pipeline disaster in Canadian history.
Malaysia	2014	Petronas gas pipeline explosion in the state of Sarawak, Malaysia ripped apart a portion of the RM3bil Sabah to Sarawak interstate gas pipeline between Lawas town and Long Sukang in the northernmost district of Sarawak at 2 a.m., resulting in the evacuation of nearby villagers; some houses and vehicles were damaged.
Kenya	2011	Nairobi pipeline fire killed approximately 100 people and hospitalized 120.
Mexico	1978	A gas pipeline exploded and burned, killing 52 people in Colonia Benito Juarez, Mexico, and

		injuring 11 in a town of only 100 people. The Failure created a crater 300 feet wide and 20 feet deep.
Nigeria	2000	Pipeline explosion near the town of Jesse killed about 250 villagers.
	2000	At least 100 villagers died when a ruptured pipeline exploded in Warri.
	2000	A leaking pipeline caught fire near the fishing village of Ebute near Lagos, killing at least 60 people.
	2003	A pipeline punctured by thieves exploded and killed 125 villagers near Umuahia, Abia State.
	2004	A pipeline punctured by thieves exploded and killed dozens of people in Lagos State.
USA	1994-2013	The U.S. had 745 serious incidents with gas distribution, causing 278 fatalities and 1059 injuries, with $110,658,083 in property damage. There were an additional 110 serious incidents with gas transmission, resulting in 41 fatalities, 195 injuries, and $448,900,333 in property damage.
Propane accidents		
Canada	1998	An 18,000-gallon propane tank exploded at the Herrig Brothers farm in Albert City, Iowa. Fatality: 2 Injury: 7 Several buildings were also damaged by the blast (Herrig Brothers Farm Propane Tank Explosion, 1998).

	2008	The explosions occurred at the Sunrise Propane Industrial Gases propane facility, located in Torento Injury: 40 Fatality: 1 (Toronto propane explosion, 2008)
	1963	The Indianapolis Coliseum Explosion (now known as the Pepsi Coliseum) occurred during the opening night for the Holiday on Ice show. Injury: 400 Fatality: 74 The cause was an explosion following a propane tank leak (Gas explosion, 2012).
USA	2012	A propane leak explosion Injury: 2 Fatality: 1 (Gas explosion, 2012)
	Hydrogen accidents	
All over the word	1908-1937	22 Hydrogen Airship Disasters (Hydrogen Airship Disasters, 2015)
Canada	1994	Chemical accident with hydrogen due to low concentration of hydrogen Injury: 1
Japan	2011	Hydrogen Explosions in Nuclear Reactors (Buxbaum, 2011) No fatality

USA	2007	Hydrogen explosion at the Muskingum River Power Plant's (Hamza, 2010) Injury: 11

These phenomena can take place in a confined area within a vessel, pipes, channels or tunnels, and the use of a pipeline to convey the reactive material from one vessel to another could possibly lead to the development of an explosion and potentially damaging overpressures (Blanchard et al., 2010; Grossel, 2010). Consequently, experimental and theoretical studies have been done to understand the gas explosion phenomena as well as to identify the ignition and transmission laws in the flammable gases with oxygen or air in different systems that have been fairly reviewed in this chapter.

2.2. Flame Acceleration Mechanism in Pipes

Flame acceleration mechanism, in relation to the pressure development in closed pipeline has recently been discussed by Solberg et al. (1979). They mentioned that some flame acceleration is caused by a feedback mechanism involving flame instabilities. In such a feedback mechanism, for instance, pressure waves generated by a propagating flame may be reflected from a vessel wall back to the flame, binging about an increase in burning rate. It is necessary to mention that flame acceleration also can happen due to turbulence regime which is discussed later.

These statements emphasize that in order to ensure that better precautions are taken in relation to pipeline gas carriers, it is essential to fully characterize and quantify their explosion mechanisms. In particular, knowledge is required about the maximum pressure, the maximum rate of pressure rise and the flame speed, which are among the most important parameters for the assessment of process hazards and the safe design of process equipment (Hawkes & Chen, 2004; Salzano et al., 2012). Studies on flame propagation and explosion mechanisms in pipes have been widely discussed (Blanchard et al., 2010; Chatrathi et al., 2001; Emami et al., 2013; Jianliang et al., 2005; Oh et al., 2001; Phylaktou et al., 1993; Thomas et al., 2010), but most of these are focused on specific applications (i.e., bending or straight pipes).

2.3. Deflagration to Detonation Transition in Pipeline

Flame may be accelerated through a series of regimes depending on the fuel concentration and the flow geometry, as illustrated in Figure 2.1. For the case of mild ignition, in the first phase the flame propagates laminar by the laminar burning velocity and the density ratio across the flame front. The laminar flame propagation regime has a short-live and it is quickly replaced by a "wrinkled" flame regime. Wrinkled regime can persist over moderately large flame propagation distances in many accidental explosions. Therefore, the flame propagation velocity in the wrinkled flame regime can be several times higher than the laminar flame due to the increase in flame area and the burning rate. In the next phase, the wrinkled flame ultimately transforms into a turbulent flame due to associated obstacles or boundary layers inside the systems. This phenomenon causes further flame acceleration due to the increase in surface area of the laminar flamelets inside the flame. Higher level of turbulence also causes that a distributed reaction zone may destroyed and then replaced the flamelet structure which it leads the deflagration to detonation transition (DDT) happened via shock ignition or the shock wave amplification mechanism (Gamezo et al, 2008).

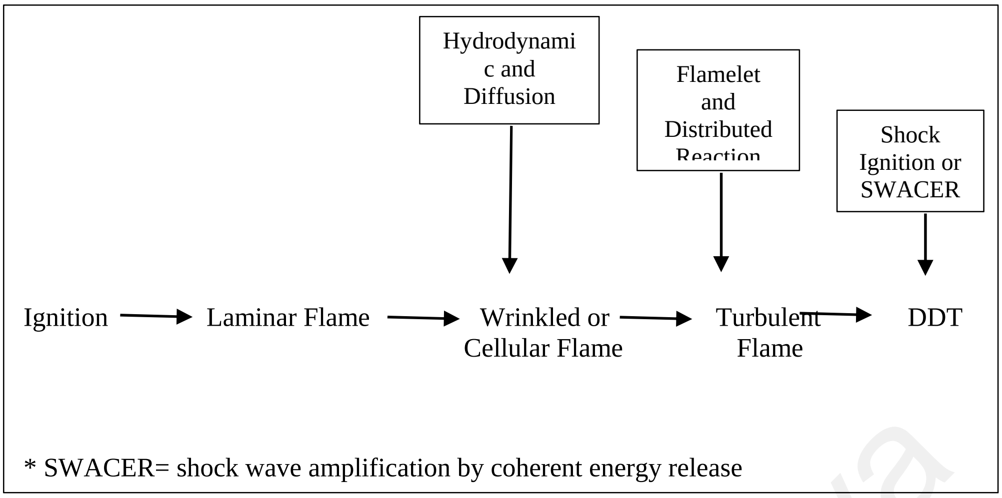

* SWACER= shock wave amplification by coherent energy release

Figure 2. 1 Regimes of flame propagation (Gamezo et al, 2008)

According to Thomas et al. (2010), an early review of flame acceleration and a deflagration to detonation transition (DDT) were produced by Smith in 1948 who considered explosion pressures in industrial piping, with a particular interest in acetylene. In later studies, much effort was concentrated on determining the distance from the ignition source to the point at which detonation was observed, the run up or transition distance, DDT, and how it correlated with pipe diameter, D. Moreover, for flames that have achieved choked velocities (velocity of the flame equals the sonic velocity of the burned gas), the pressure between the precursor shock and the reaction zone is three times the initial pressure of the mixture. In laboratory experiments with relatively sensitive mixtures, unusually high pressures resulting from DDT in the end gas were observed. It has been also observed that the pressure generated in pipelines during some accidents could be extremely high, capable of causing damage to the pipeline. In these accidents, DDT often occurred in the end gas region of the pipeline (Chan & Dewit, 1996).

It is valuable to know that the flame could behave as a thrust resource for the unburned mixture to generate or induce very complex flow fields (Zhou et al., 2006). When the flame travels across the pipe the shape of the flame front changes due to interaction between the flame front and the flame-induced. In fact, this is an interaction between burned gas and unburned gas. Also the static pressure gradient could play a role in the shape of flame front but a difference of velocity can be a large item in this issue. Below Figures (a-h) show the evolution of the flame section by section. These figures show the flame front and the complex flame induced velocity fields near the flame front.

In the first phase of flame propagation, the flame formed an oval cylinder-like shape (Figure 2.2. (a), t = 0.01 s) with the flow of the unburned gas around the flame. Later, the front was almost cylindrical with a parabolic frontal section (Figure 2.2. (b), t = 0.02 s). At that instance, the flow of the unburned gas near the lateral region tended to be parallel to the side walls while that of the burned and unburned gases near the frontal region remained in the downstream direction. Then, due to the effect of the sidewalls of the duct, the lateral regions flattened while the frontal region remained curved (Figure 2.2. (c) t= *0.06* for instance). When the lateral regions of the flame front were quenched at the walls, the front section was flattened (Figure 2.2. (c) for t = 0.06 s and Figure 2.1. (d) for 0.07 s).

There are three noticeable points about Figures 2.2 (a-d):

a. In the burned region there are two vortex about the middle line;
b. The vortex area is increased with time;
c. There is a clear velocity gradient across the lateral area of the flame front.

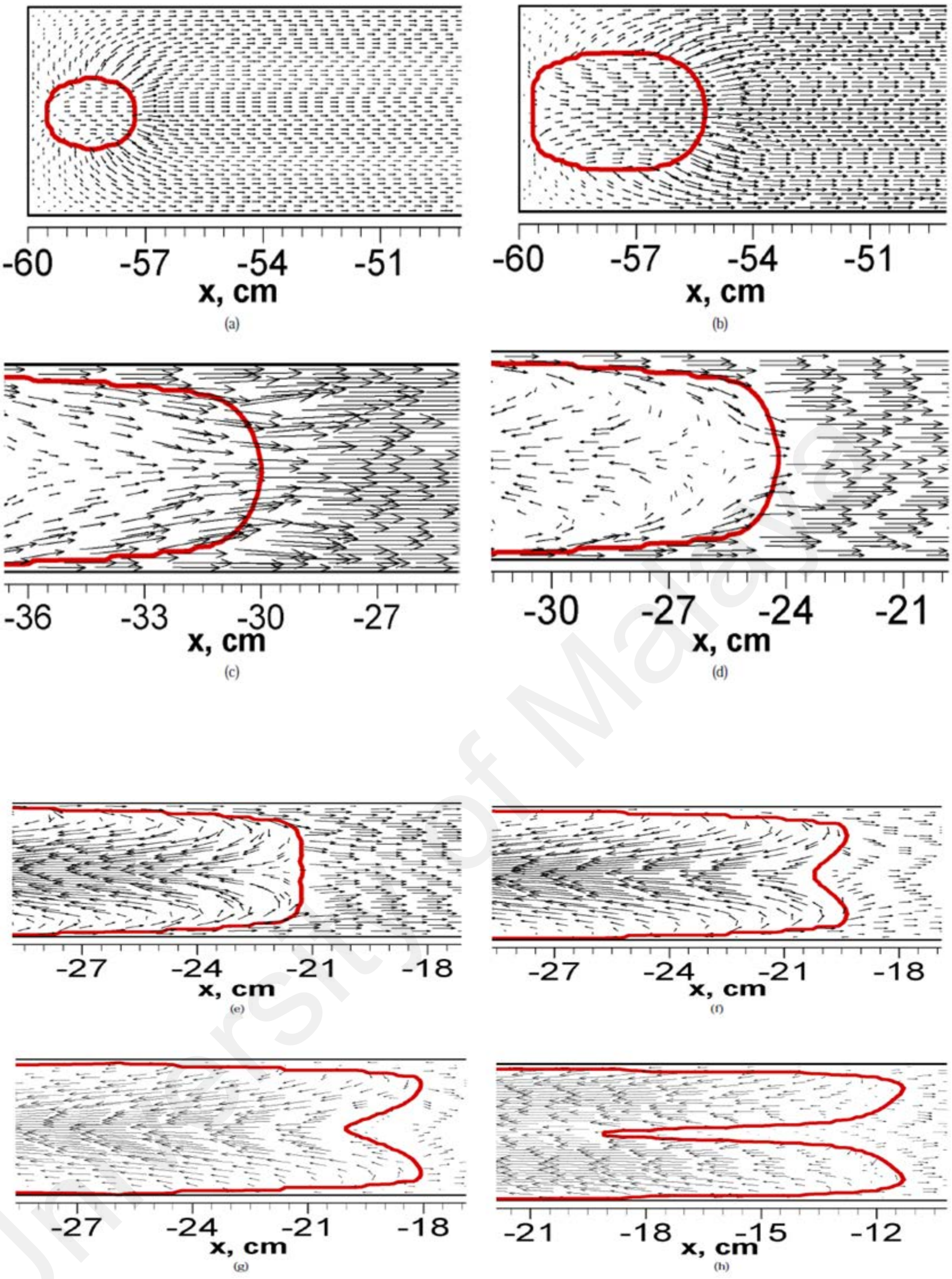

(a) (b) (c) (d) (e) (f) (g) (h)

Figure 2. 2 Flame front and the velocity fields in the vicinity of the flame front at the middle plane of the pipe (Zhou et al., 2006).

When the lateral regions of flame were quenched and reminding the leading section was nearly completely flat (Figure 2.2. (e)). At *t* = 0.09 s and 0.10 s (Figure 2.2. (f) and (g)), at which time the corner section of the flame traveled faster than the central region, the flame front was folded, with a backward directed dome. From *t* = 0.11 s to *t* = 0.14 s, the folding of the flame front increased and a tulip flame developed more clearly and the magnitude of the velocity around the cusp in the unburned region approached zero (Figure 2.1. (h)) (Zhou et al., 2006).

An investigation showed that the transition to detonation in pure ethylene can sustain a detonation by a decomposition reaction at pressures greater than atmospheric (Thomas et al., 2010). Moreover, while the energy of the ethylene sphere explosion was estimated to be about (2.4–3.2)×10^7 kJ (Wang et al., 2000), an experimental study on flame acceleration and deflagration to detonation transition in representative process piping indicated that the initial pressure does not have a significant effect on flame acceleration of ethylene/air mixture, however, the initial pipe wall temperature or possibly mixture humidity could affect (Thomas et al., 2010). For more clarification, Figure 2.3 shows pressure histories of ethylene at ambient condition in a straight pipeline tests with 150 mm diameter.

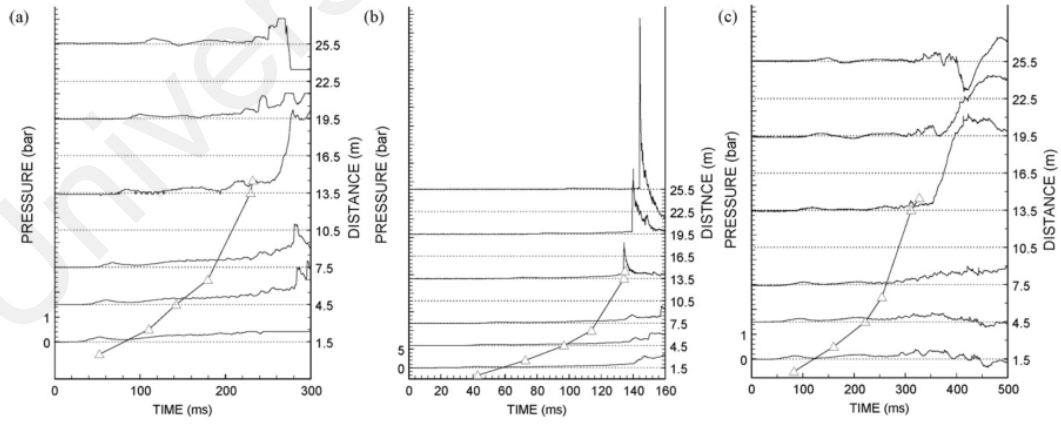

Figure 2. 3 Pressure histories at various gauge locations for ethylene–air mixtures: (a) 5.2%, (b) 6.45% and (c) 10.1% in air at ambient atmospheric pressure (Thomas et al., 2010)

Blanchard et al. (2011) showed that there is no possibility for ethylene/air mixture to present shock waves since its overdriven detonations were not strong enough to enable confident measurement of its velocity. As shown in Figure 2.4, after DDT, flame speed decreases during the transition process in both straight and bend pipe with 159 mm initial diameter. However, the maximum flame speed was observed at approximately 80% for the straight pipe and, at approximately 70% for the two configurations containing obstacles. This phenomenon indicated that the reflected pressure waves from the closed end of the pipe has a significant effect to slow down the flame/pressure front.

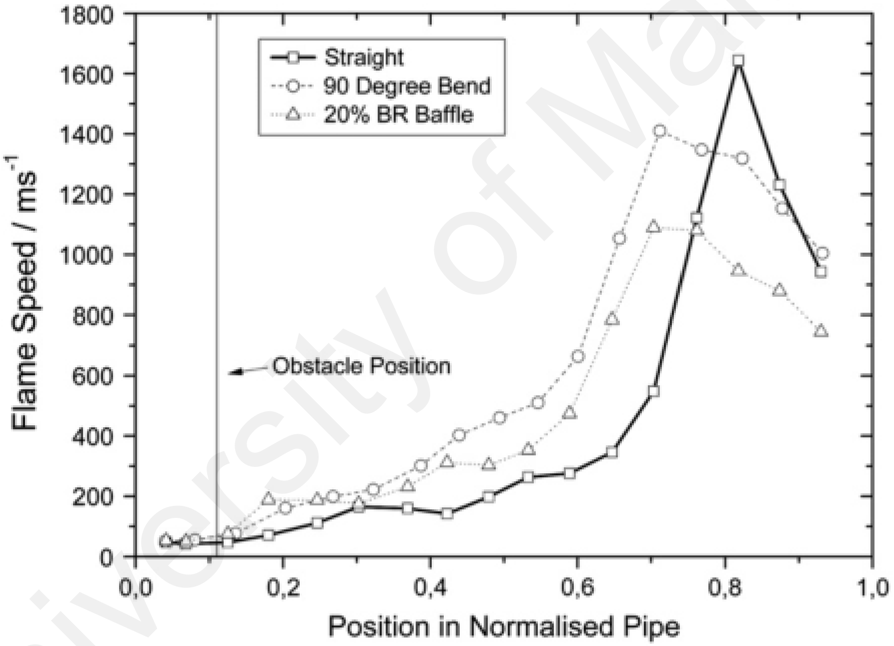

Figure 2. 4 Flame speeds for ethylene–air explosions (Blanchard et al., 2011)

On the other hand, the investigation on the behaviors and shape changes of premixed hydrogen–air flames at various equivalence ratios propagating in half-open and closed horizontal ducts showed that the premixed hydrogen–air flame undergoes more complex shape changes and exhibits more distinct characteristics than that of other gaseous fuels (Xiao et al., 2011). The previous investigation reported that hydrogen is susceptible to deflagration to detonation transition (DDT) (Ciccarelli & Dorofeev, 2008) and it is important that this parameter can be calculated and predicted with a reasonable degree of accuracy in order to affect the end goal; control over flame acceleration and the process of DDT. An extensive amount of work has therefore been devoted to understand the phenomena related to a flame acceleration and transition from deflagration to detonation (DDT) in pipes (Markstein, 2014). Investigation on fuel transferring in pipes showed that 36.5% hydrogen in air has the capability to develop DDT (Heidari & Wen, 2014; Thomas et al., 2010) as presented in Figure 2.5.

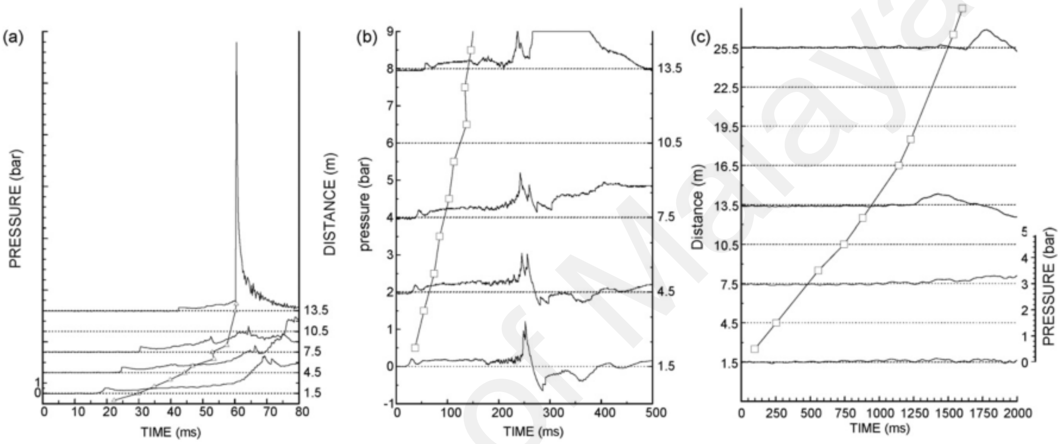

Figure 2. 5 Pressure histories at various gauge locations and superimposed flame front arrival time for hydrogen in air: (a) 35.6% H_2, (b) 19.7% H_2 and (c) 14% H_2 (Thomas et al., 2010).

These previous works discussed and illustrated the fact that the changes of the flame front shape and the propagation in a tube depend on numerous parameters, such as aspect ratio, initial pressure, the tube with open or closed ends, equivalence ratio of the mixture, etc. (Markstein, 2014). Yet, dynamics of flame mechanism during gas explosion development of premixed hydrogen–air flames at various equivalence ratios undergoes a complex flame inversion and exhibits more distinct characteristics than that of other gaseous fuels (Xiao et al., 2011).

2.4. Effect of Initial Condition on Flame Acceleration of Fuels

Considering the safety aspects on fuel transferring cause researchers to give more attention on the influence of the initial conditions on the overall maximum overpressure, rate of pressure rise, flame speed, burning velocity and time arrival. The investigations showed that the initial fuel, pressure, temperature, ignition source and pipe/tube configuration have significant influence on flame acceleration in pipes.

2.4.1. Influence of Fuel Reactivity and Concentration

Natural gas mainly contain light hydrocarbons including methane, ethane, propane, etc. but methane is the primary component with a concentration of 82% (Akansu et al., 2004). Due to the numerous advantages of natural gas, including high fuel octane number (Shiga et al., 2002), clean energy with the lowest C/H ratio and user-friendly for internal combustion engines (Ma et al., 2007; Papagiannakis et al., 2010; Shiga et al., 2002; Turrio-Baldassarri et al., 2006), industry has given more attention to it, especially, applying as a fuel for engines. However, utilizing natural gas contains unavoidable problems/disasters which are coming across with combustion (Jo & Ahn, 2005; Jo & Crowl, 2008; Jo & Ahn, 2002; Wiser et al., 2004). Therefore, many studies have been done to fully understand the combustion behavior including flame instability and ratio of the laminar burning velocity of methane/air and natural gas/air mixtures at different equivalence ratios (Gu et al., 2000; Liao et al., 2004).

Moreover, among all hydrocarbon fuels, propane has been used as a domestic, agricultural, industrial, and commercial fuel for many years due to its extensive use as an alternative “clean” fuel. Specifically, after gasoline and diesel, it is the third most popular vehicle fuel due to its undeniable advantages including being liquefied at a moderate pressure, fast refill times, less engine wear and no need diluting engine oil (Liu et al., 2015). However, due to unpredictable disasters/accidents that could happen in fuel transporting/usage of propane, many research studies have been conducted to fully characterize propane explosion phenomenon. For instance, Razus et al. (2011) examined the influence of the initial composition, temperature and pressure of propane/air mixtures on pressure evolution in spherical vessel deflagrations. In other investigation, Liu et al. (2015) studied the flame propagation and gas explosion in propane/air mixtures.

Ethylene (C_2H_4) is the simplest alkene among all hydrocarbons which is a colorless flammable gas with a faint "sweet and musky" odor. Ethylene is commonly used in the chemical industry, and its production surpassed that of any other organic compounds. Ethylene is widely applied as a raw material for ethylene oxide, ethylene glycol and polyethylene manufacture (Movileanu et al., 2013). Furthermore, ethylene has been promoted the interest among researchers for applying numerical methods of kinetic modeling to find a suitable mechanism for ethylene oxidation at a wide range of temperatures, pressures, and equivalence ratios (Bergthorson & Dimotakis, 2007; Egolfopoulos et al., 1991; Jomaas et al., 2005). Based on severe consequences of ethylene explosions, a number of experimental and numerical studies on flammable parameters of ethylene have been done (Kumar et al., 2007; Movileanu et al., 2011a, 2011b). However, same as propane, for fuel transferring process, only a few research have been done.

Hydrogen explosion hazards have for many years been a concern within its use in storage and transportation using pipelines and it is essential to address the related safety issues on pipeline gas carriers by characterizing and adequately quantifying their explosion behaviour to protect against propagation of unwanted combustion phenomena such as deflagrations and detonations (including decomposition flames) in the process (Grossel, 2002; Xiao et al., 2012; Zhou et al., 2006). Some unique properties of hydrogen, such as lower ignition energy, wider flammability range, higher laminar burning velocity and higher diffusivity, smaller quenching distance and greater extinction strain rates than other typical gaseous fuels, make its flame behavior and propagation different from other gases such as methane, butane and etc. For instance, the lean premixed hydrogen-air flame is more susceptible to a variety of flame-induced hydrodynamic and combustion instabilities (Sarli & Benedetto, 2007). Therefore, the study on these unique features is becoming more demanding (Xiao et al., 2011). Hydrogen has a very high burning rate compared to other flammable gases. The possibility of a significant flash fire or vapour cloud explosion resulting from delayed remote ignition is extremely low due to the buoyant nature of the hydrogen, which generally precludes the formation of a persistent vapour cloud at ground level (Jo & Ahn, 2006). However, due to a relatively high burning velocity, hydrogen can easily make the transition from deflagration to detonation (Wooley et al., 2008), should a fire incident occur. Moreover, hydrogen has been feared in the popular press as a relatively more dangerous fuel, and in fact it has the widest explosive/ignition mix range compared to all fuel gases except acetylene (Thomas et al., 2010). Moreover, field-scale experiments on the high pressure release of hydrogen gas inside a 6 m long horizontal channel presented that the pressure started to build up as the flame moved closer towards the jet, and the deflagration taking place closer to the jet resulting in the highest pressure peak (Rai et al., 2014).

Initial fuel concentration is another important factor that has been given attention by researchers. The fuel/oxidant ratio is normally reported in terms of a non-dimensional variable called equivalence ratio (Φ). Equivalence ratio is the actual fuel/oxidant ratio normalized by the stoichiometric fuel/oxidant ratio (Eq 2.1) (Lee et al., 2000).

$$\phi = \frac{(Fuel/Oxidant)_{Actual}}{(Fuel/Oxidant)_{\mathrm{Stoichiometric}}} \qquad \text{(Eq 2.1)}$$

Stoichiometric concentration is defined as $\Phi = 1.0$. “Lean” and “Rich” conditions are also identified as an excess of oxidant present ($\Phi < 1.0$) and an excess of fuel ($\Phi > 1.0$) in the mixture, respectively (Lee et al., 2000). Fundamental studies on explosion behavior of hydrogen/air (Kim et al., 2013) and methane/air (Kindrachi et al., 2007) mixtures showed that the flames in lean condition propagated by artless flame instabilities. However, the flames propagated smoothly in the early stage, and wrinkled and accelerated in the later stage, intensively, by different type of instabilities in stoichiometric and rich conditions (Figure 2.6 and 2.7).

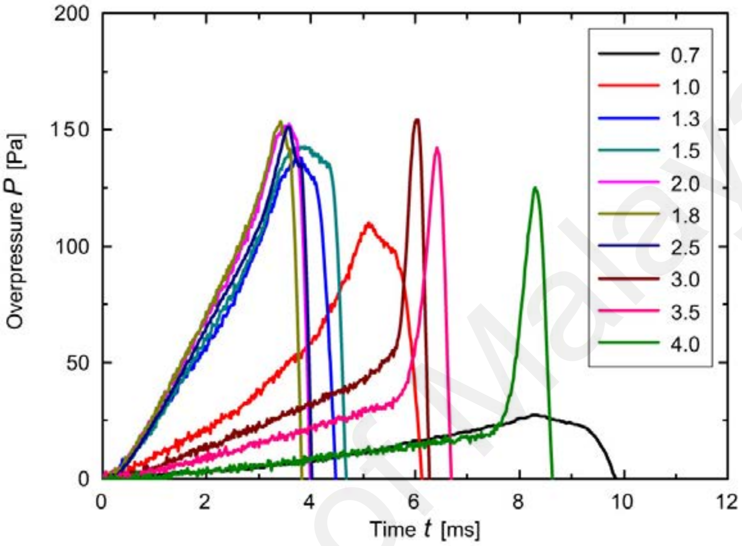

Figure 2. 6 Pressure wave histories of hydrogen/air with different equivalence ratio in a spherical soap bubble (Kim et al., 2013)

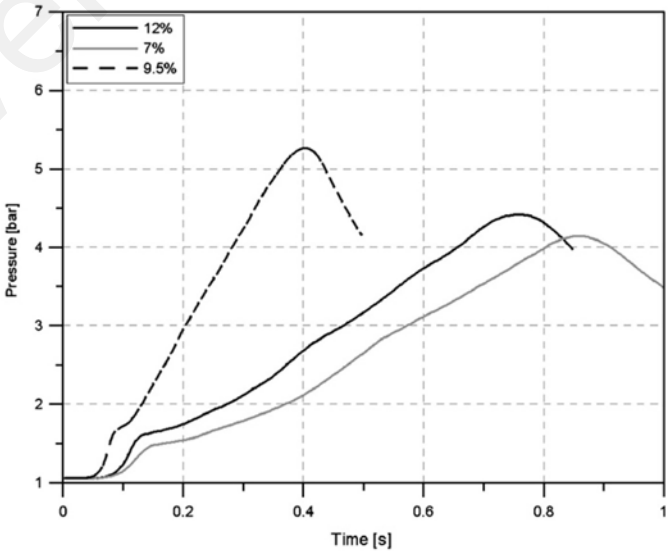

Figure 2. 7 Pressure wave histories of methane–air mixture with different equivalence ratio in a horizontal tube (without obstacle) (Kindrachi et al., 2007)

For giving more clarification, Figure 2.8 illustrates a series of representative high-speed schilieren images of premixed hydrogen-air flame shape changes during propagation at various equivalence ratios in a closed duct. Xiao et al. (2011) found that in the experiments when the $\phi<0.42$ tulip flame would not be initiated anymore and when $0.49\leq\phi<0.84$ and $4.22\leq\phi<7.14$ a classical tulip flame, which has been widely studied, will be produced without obvious distortion. Moreover, squish flow can drive the flame to propagate faster near the walls than in the central region; although it is not the essential cause that initiates the tulip formation. In the amplitude of equivalence ratio should be $0.67 \leq \phi < 1.17$ and $\phi > 4.05$ though the squish flow is active. Another research study showed that a stratified mixture even may posed a greater problem than homogeneous for lean overall global concentration ($\phi<1$). It is due to the increased mixture reactivity at the ignition site and the concentration gradient in the vessel, which would let explosion to create the more severe condition (Willacy et al., 2007).

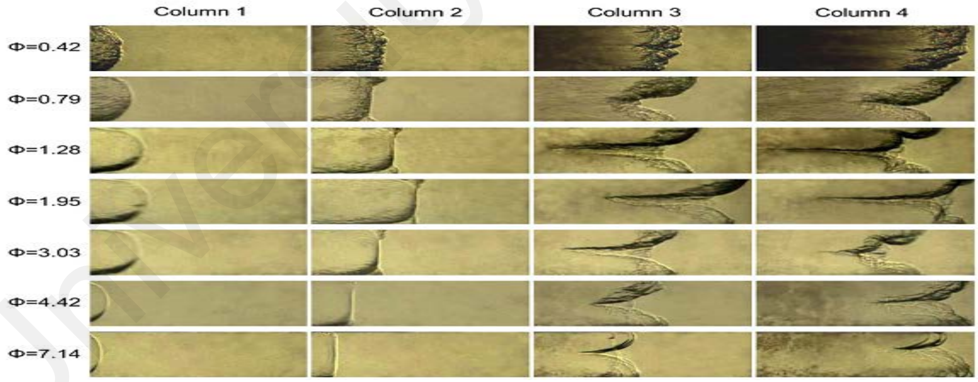

Figure 2. 8 High-Speed schiliren of flame premixed hydrogen- air shape changes during propagation in closed duct at various equivalence ratios (Xiao et al., 2011).

The conducted research on an incident shock wave of hydrogen–oxygen mixture also showed that associated incidents are following the respective sequences: first, reflected shock, second, wave structure of medium behind these waves, third and fourth, the centers of ignition, fifth, own luminescence of combustion waves and sixth, extending from ignition centers (Petukhov et al., 2009). However, the hazard assessment on these phenomena is still debatable, even though this concern has attracted researchers' attention. It is essential that reliable and cost-effective prevention and mitigation methods are available to practitioners and researchers to assess the hydrogen explosion hazards in the pipeline, in order to ensure that a loss of containment and hydrogen leakage during transportation does not occur (Middha et al., 2007). One possible means for mitigating the hazards associated with unintended hydrogen release or DDT in a pipe is through the use of inhibitors and adding to hydrocarbon fuels that are discussed in sections 2.4.1.1 and 2.4.1.2.

2.4.1.1. Hydrogen Enrichment

Extensive reports in the literature on the development of partial or total replacement of hydrocarbon fuels with hydrogen in power plants and vehicle engines have given increasing impact on awareness of environmental pollution and the declining supply of fossil fuels (Das, 1996; Ikegami et al., 1982; Jamal & Wyszynski, 1994; Verhelst & Wallner, 2009; Vu et al., 2011a). However, the benefits of using hydrogen as a source of fuel seem to be limited due to some difficulties, particularly on storage issues. These difficulties are relating to its low density (0.08 kg/m^3 at 300 ^{o}K and 1 atm), wider range of flammability limits (from 4 to 75%), higher laminar flame velocity (2.3 m/s at normal conditions) and very low ignition energy (0.02 mJ) (Frolov et al., 2013) and this drawback properties would make hydrogen becoming a second alternative compared to hydrocarbons. From previous studies, hydrocarbon-hydrogen fuel mixtures would be the best substitution to overcome these drawbacks (local flame extinction, combustion instabilities, lower power output, etc.), as the blending would synergistically resolve the problems associated with the combustion of hydrogen and fossil fuels combustion

(Briones et al., 2008), both stationary and mobile systems (Cammarota et al., 2009; Ernesto Salzano et al., 2012; Tahtouh et al., 2009).

The fundamental and practical aspects of the usage of hydrogen-hydrocarbon mixtures in both transportation and power generation (in terms of their mechanical and chemical properties) in different systems, such as *engines* (Hu et al., 2009d; Kahraman et al., 2009; Mohammed et al., 2011; Nguyen & Mikami, 2013; Ozcan, 2010; Shirk et al., 2008; Wang et al., 2008a;), *burners* (Boushaki et al., 2012; Choi & Chung, 2012; de Ferrières et al., 2008; Mardani & Tabejamaat, 2010; Sepman et al., 2011; Zhen et al., 2012a,), combustion bombs (; Di Sarli et al., 2012; Di Sarlia et al., 2013; Hu et al., 2009c; Miao et al., 2008; Tinaut et al., 2011), *vessels* (Azatyan et al., 2005; Cammarota et al., 2009; Cammarota et al., 2010; Di Benedetto et al., 2009; Emami et al., 2013; Ernesto Salzano et al., 2012; Tang et al., 2008) and *chambers* (Aggarwal et al., 2011; Dinkelacker et al., 2011; Hu et al., 2009b; Miao et al., 2011;; Tahtouh et al., 2011;; Vu et al., 2011a), have been broadly investigated. The parameters affecting hydrogen-hydrocarbon mixtures have been studied, including flame configurations, e.g., laminar premixed (F. Halter et al., 2005; Yu et al., 1986), non-premixed (Guo & Neill, 2009) and partially premixed flames (Briones et al., 2008; Sayangdev Naha & Aggarwal, 2004), as well as burner-stabilized (Choudhuri & Gollahalli, 2003; Halter et al., 2007) and swirl-stabilized turbulent flames (Kim et al., 2009; Schefer et al., 2002; Strakey et al., 2007).

As far as authors' concern, literature studies have focused on the effect of the addition of hydrogen to: **(a) chemical characteristics** (*kinetics* (Hu et al., 2009b; Masri et al., 1992; S. Refael & E. Sher, 1989), *flame stability* (Hu et al., 2009c; Lafay et al., 2008; Miao et al., 2008; Tuncer et al., 2009; Vu et al., 2011b), *NOx* (Bauer & Forest, 2001; Guo et al., 2005b; Hawkes & Chen, 2004; Hu et al., 2009e; Miao et al., 2009; Mohammed et al., 2011; Sayangdev Naha & Aggarwal, 2004; S. Naha et al., 2005; Tinaut et al., 2011; Tuncer et al., 2009), *CO* (Bauer & Forest, 2001; Burbano et al., 2008; de Ferrières et al., 2008; Tinaut et al., 2011; Zhen et al., 2012b) and *CO_2 emissions* (Bauer & Forest, 2001; de Ferrières et al., 2008; Mardani & Tabejamaat, 2010; Miao et al., 2009; Mohammed et al., 2011; Shih, 2009), *Markstein length* (Briones et al., 2008; Hu et al., 2009b; Hu et al., 2009c; Huang et al., 2006;; Miao et al., 2008, 2009; Tahtouh et al., 2011; Tang et al., 2008; Vu et al., 2011a), *kernel development* (Dunstan & Jenkins, 2009)), and **(b) physical characteristics** (*flame shape and structure* (Di Sarli & Di Benedetto, 2013; Di Sarli et al., 2012), *flammability limits* (Guo et al., 2005b; Miao et al., 2011), *laminar* (Azatyan et al., 2010; Boushaki et al., 2012; F Cammarota et al., 2010; Coppens et al., 2007; Di Sarlia & Di Benedettob, 2013; Halter et al., 2007; Hu et al., 2009b; Huang et al., 2006; Ilbas et al., 2006; Law & Kwon, 2004; Li et al., 2012; Miao et al., 2008, 2009; Salzano et al., 2012; Tahtouh et al., 2009; Tang et al., 2008; Vu et al., 2011a; Yu et al., 1986) and *turbulent* (Cammarota et al., 2009; Dinkelacker et al., 2011; Hawkes & Chen, 2004; Mandilas et al., 2007; Shy et al., 2008) *burning velocities*, flame propagation characteristics including *flame speed* (Boushaki et al., 2012; Conte & Boulouchos, 2006; Emami et al., 2013; Guo & Neill, 2009; Hu et al., 2009c; Li et al., 2012; Miao et al., 2009; Tang et al., 2008; Tuncer et al., 2009), *auto-ignition* (Choi & Chung, 2012; Frolov et al., 2013) *maximum overpressure* (Azatyan et al., 2005; Cammarota et al., 2010; Di Benedetto et al., 2009; Emami et al., 2013; Li et al., 2012; Mohammed et al., 2011; Salzano et al., 2012; Tinaut et al., 2011; Tuncer et al., 2009), *maximum rate of pressure increase* (Azatyan et al., 2005; Cammarota et al., 2009; Emami et al., 2013; Salzano et al., 2012), *flame temperature* (Boushaki et al., 2012; A. Di Benedetto et al., 2009; Guo & Neill, 2009; Hawkes & Chen, 2004; Hu et al., 2009e; Li et al., 2012; Tuncer et al., 2009; Zhen et al., 2012b), *resistance to strain-induced extinction* (Halter et al., 2005; Halter et al., 2007; Ren et al., 2001; Schefer et al., 2002), *flashback* (Briones et al., 2008; Tuncer et al., 2009), *small-scale flame-front wrinkling* (Conte & Boulouchos, 2006; Di Sarli et al., 2012; Halter et al., 2007; Hawkes & Chen, 2004; Vu et al., 2011b), *lean blowout limits*

(Schefer et al., 2002; Schefer, 2003; Strakey et al., 2007; Tuncer et al., 2009) and *length* (Burbano et al., 2008; Choi & Chung, 2012; Dinkelacker et al., 2011; Hawkes & Chen, 2004; Zhen et al., 2012a) of flames).

Moreover, for the diffusion of combustion, hydrogen-enrichments can suppress the formation of soot particles (Gülder et al., 1996; Guo et al., 2007) and reduce ignition delay (Aggarwal et al., 2011; Choi & Chung, 2012; Frolov et al., 2013; Ju & Niioka, 1994).

Tuncer et al. (2009) showed that hydrogen-enrichment allows the combustion to be sustained at a much leaner equivalence ratio than those possible with methane. The kinetic analyses show that the addition of H_2 to natural gas mainly benefits the methane and ethane oxidation sequence initiated by H-abstraction by H, OH and O (de Ferrières et al., 2008; R. Schefer et al., 2002):

$$CH_4 + OH \rightarrow CH_3 + H_2O \tag{2.1}$$

$$CH_4 + O \rightarrow CH_3 + OH \tag{2.2}$$

$$CH_4 + H \rightarrow CH_3 + H_2 \tag{2.3}$$

The supplementary kinetic mechanism shown below provides evidence on why the addition of more hydrogen to methane would lead to higher levels of OH, CH_3O and HCO in the mixtures (Hu et al., 2009b):

$$HO_2 + CO \leftrightarrow HCO + O_2 \tag{2.4}$$

$$H + CO + H_2O \leftrightarrow HCO + H_2O \tag{2.5}$$

$$HO_2 + CH_3 \leftrightarrow OH + CH_3O \tag{2.6}$$

$$H + O_2 \leftrightarrow O + OH \tag{2.7}$$

As a consequence, the reaction rate, the mixture-ignitability and the rate of heat release (Mardani & Tabejamaat, 2010) as well as the burning rate (Hu et al., 2009b) would increase significantly. These large positive sensitivities were promoted by the development of the following reactions (Hu et al., 2009b):

$$H + O_2 \leftrightarrow O + OH \tag{2.8}$$

$$OH + CH_3 \leftrightarrow CH_2(S) + H_2O \tag{2.9}$$

$$OH + CO \leftrightarrow H + CO_2 \tag{2.10}$$

$$HO_2 + CH_3 \leftrightarrow OH + CH_3O \tag{2.11}$$

$$HCO + H_2O \leftrightarrow H + CO + H_2O \tag{2.12}$$

Lafay et al. (2008) also showed that the following reactions have a crucial effect on the increased heat release rate from CH_4+H_2 flames:

$$O + CH_3 \leftrightarrow H + CH_2O, \qquad (10\%) \tag{2.13}$$

$$O + CH_3 \leftrightarrow H + H_2 + CO, \qquad (9.0\%) \tag{2.14}$$

$$H + CH_3(+M) \leftrightarrow CH_4(+M), \qquad (8.5\%) \tag{2.15}$$

$$OH + H_2 \leftrightarrow H + H_2O, \qquad (8.5\%) \tag{2.16}$$

$$HCO + O_2 \leftrightarrow HO_2 + CO, \qquad (6.0\%) \tag{2.17}$$

$$OH + CO \leftrightarrow H + CO_2, \qquad (5.7\%) \tag{2.18}$$

$$OH + CH_4 \leftrightarrow CH_3 + H_2O, \qquad (5.3\%) \tag{2.19}$$

The links between major heat release rate reactions and the reaction (2.8) showed that this particular reaction plays a significant role on the global increase of the heat release rate and temperature gradient. Moreover, the reaction (2.20) increases the mixture reactivity and heat release rate at lower temperatures, and this causes higher OH concentrations in early flame development (Dagaut & Nicolle, 2005; Lafay et al., 2008). In other words, by adding H_2, the OH production in this flame zone is mainly due to reaction chain of (2.20) (36%), whereas the influence of (2.8) reaction is only 24% based on report by Lafay et al. (2008).

$$H + HO_2 \leftrightarrow 2OH \tag{2.20}$$

However, the following reactions have negative sensitivities due to the reduction of active radicals during the combustion process (Hu et al., 2009b):

$$H + O_2 + H_2O \leftrightarrow HO_2 + H_2O \tag{2.21}$$

$$H + CH_3 + (M) \leftrightarrow CH_4 + (M) \tag{2.22}$$

$$HCO + O_2 \leftrightarrow HO_2 + CO \tag{2.23}$$

In the literature, numerous reports show that NOx formation would be almost double if hydrogen were added to hydrocarbon mixtures (Bauer & Forest, 2001; Das, 1996; Guo & Neill, 2009; Guo et al., 2007; Guo et al., 2005b; Hawkes & Chen, 2004; Hu et al., 2009e; Jackson et al., 2003; Miao et al., 2009; Mohammed et al., 2011; Sayangdev Naha & Aggarwal, 2004; S. Naha et al., 2005; Ren et al., 2001; Sankaran & Im, 2006; Tinaut et al., 2011; Tuncer et al., 2009; Zhen et al., 2012a, 2012b). Tuncer et al. (2009) in their work have explained how hydrogen-enrichment allows the combustion to become more sustainable at the linear equivalence ratios than those with methane (Tuncer et al., 2009). The NO formation is influenced by the CH mole fraction, and the addition of H_2 to methane, propane and ethane mixtures led to a dramatic decrease in NO formation for an atmospheric pressure-stabilized burner (Hawkes & Chen, 2004; Sepman et al., 2011). However, some works have reported that there is an increase in NOx formation in CH_4+H_2/air mixtures with lower concentrations of H_2 (0-35 % v/v), and this phenomenon is similar to methane/air flames in a flat burner (Guo & Neill, 2009). Guo and Neill (2009) have shown that this observation is in good agreement with numerical analysis. They indicated that lower concentrations of hydrogen in methane/air mixture lead to an increase in NO formation at moderate or higher strain rates. Work by Coppens et al. (2007) supported the hypothesis made, indicating that the Zeldovich thermal–NO mechanism and enriched mixtures are the reason for higher NOx formation in stoichiometric mixtures, in a circa of 1.3–1.4 due to the Fenimore prompt–NO mechanism (Coppens et al., 2007). A kinetic analysis done by Guo et al. (2005a) showed that N_2O and NNH are the two main routes on the NO formation in pure CH_4/air. By adding hydrogen into pure CH_4/air mixture, the contribution of the NNH intermediate route significantly increases, while the other route showed only minimal change, except for the mixtures with $\phi<0.47$ at lower hydrogen fraction. At equivalence ratio of 0.47, the contribution of the N_2O intermediate route rises much faster than another route when the hydrogen fraction is 0.2. A sensitivity analysis on CH_4-H_2/air mixture with ultra-lean counter flow (Guo et al., 2005a) indicates that the two most significant initiation reactions of the NNH intermediate route are:

$$N_2 + H \leftrightarrow NHH \tag{2.31}$$

$$NHH + M \leftrightarrow N_2 + H + M \tag{2.32}$$

and the most important NNH destruction reaction is:

$$NNH + O_2 \leftrightarrow HO_2 + N_2 \tag{2.33}$$

Mainly, NO_2 formation reaction in CH_4-H_2/air mixture is:

$$HO_2 + NO \leftrightarrow NO_2 + OH \tag{2.34}$$

Since the activation energy of this particular reaction is negative, the rate of NO_2 formation is very slow yet, the contribution of these radical reactions cause higher NO formation and flame temperature, simultaneously (Guo et al., 2005a). At other perspectives, an experimental study carried out by Ng and Gan (2010) suggested the potential use of palm oil biodiesels in small-scale liquid fuel burners. Their investigation showed that the optimum combustion in a non-pressurized burner system at an equivalence ratios ranging between 0.75 and 0.85 of the biodiesel-diesel blends is either too rich or lean to endure a complete combustion consequently, the level of NO was the highest as temperature became elevated from the overall stoichiometric combustion.

From this work, it was also found that the recombination of H and C_2H_5 molecule structures caused vigorous reinforcement of the ethane sequence and the richness of H atoms in natural gas-hydrogen mixtures. This reinforcement would implicitly convert fewer radicals into ethylene via the thermal decomposition reaction, which is unfavourable to the C_5 sequence (de Ferrières et al., 2008). To support the argument, Sepman et al. (Sepman et al., 2011) have done series of experiments involving H_2+CH_4/air, H_2+C_2H_6/air and H_2+C_3H_8/air flames. A realistic agreement is successfully obtained between the experimental and quick loading (QL) mechanism calculations' profiles on NO and temperature in H_2+CH_4/air, H_2+C_2H_6/air and H_2+C_3H_8/air flames (Sepman et al., 2011).

Basically, it can be said that the reactions with a positive sensitivity rate affect not only the thermodynamic parameters but also the dynamic properties of flame propagation in hydrogen-hydrocarbon fuel mixtures. For example, in H_2-air system, the addition of a hydrocarbon, like propane, at an appropriate concentration (ϕ=0.8) can suppress the instability of H_2-air flames by reducing the laminar burning velocities of the fuel. When the mixture is ignited, it tends to form a spontaneous cell on expanding low concentration of H_2 spherical flames; in a consequence, retarding the intensity of the flames (Tang et al., 2008). The kinetic analysis of propane shows that if the pre-exponent coefficient is lower at high pressure, the following reactions have an insignificant effect on the burning velocity, leading to the consumption of the free H radicals (Refael & Sher, 1989):

$$C_2H_3 + H + M \rightarrow C_2H_4 + M \tag{2.24}$$

$$C_2H_2 + H + M \rightarrow C_2H_3 + M \tag{2.25}$$

$$CO + H + M \rightarrow HCO + M \tag{2.26}$$

$$OH + H + M \rightarrow H_2O + M \tag{2.27}$$

$$O_2 + H + M \rightarrow HO_4 + M \tag{2.28}$$

Furthermore, there are no apparent changes in the reaction in co-flow air, though some reactions are reported at the fuel reaction zone when hydrogen is added, implying the dominance of H radicals over OH radicals in the system. Accordingly, the last sequence implies that the H-abstraction is mainly conducted by OH radicals as presented in reaction (2.29), although H-abstraction by H atoms will dominate when hydrogen is added (de Ferrières et al., 2008). This favourable interaction of H atoms in the chemical reaction of CO conversion to CO_2 indicates that the CO level increases with co-flow oxygen enrichment, a finding which has been said to be an unforeseen observation (Burbano et al., 2008; de Ferrières et al., 2008; Mardani & Tabejamaat, 2010). It should be noted that the reaction (2.30) is temperature sensitive. On this basis, the contrary observation of CO and CO_2 can be assumed based on the measurement of the temperature (de Ferrières et al., 2008). It is also shown that the higher concentration of hydrogen in methane (Burbano et al., 2008; Zhen et al., 2012a) and LPG (Zhen et al., 2012a, 2012b) would considerably decrease the air-free CO emissions. The addition of hydrogen dramatically affects the concentration of OH radicals by raising and promoting CO oxidation to CO_2 sequences, as shown in the kinetic reaction above (Burbano et al., 2008; Hawkes & Chen, 2004; İlbas et al., 2005; Schefer, 2003).

$$CH_4 + OH \rightarrow CH_3 + H_2O \tag{2.29}$$

$$CO + OH \rightarrow CO_2 + H \tag{2.30}$$

In order to safely use hydrogen-hydrocarbon mixtures, knowledge of the explosion hazard of these fuels is vital. Experimental investigations into the laminar flame characteristics of hydrogen-hydrocarbons/air flames which have been validated by numerical analyses have disclosed a number of key changes that take place with the addition of H_2, namely: extended flammability limits (a lower lean limit and a higher stretch extinction limit) (Miao et al., 2011), a reduced laminar flame thickness, a higher adiabatic flame temperature, a reduced stretch response (a lower Markstein number), increased laminar flame speed (with a greater increase at lower equivalence ratios) (Dunstan & Jenkins, 2009), improved combustion stability (Schefer, 2003) and reduced pollutant emissions (Sankaran & Im, 2006). Investigations into combustion bombs also emphasize the potential effectiveness of adding hydrogen to hydrocarbon fuels in relation to laminar burning velocity (Hu et al., 2009c; Miao et al., 2008, 2009; Tinaut et al., 2011), flame speed (Miao et al., 2008), CO_2 (Miao et al., 2008), CO (Tinaut et al., 2011) and NOx (Tinaut et al., 2011) emissions, flame stability (Hu et al., 2009c; Lafay et al., 2008; Miao et al., 2009) and flame shape, and vortex (Di Sarli & Di Benedetto, 2013; Di Sarli et al., 2012; Di Sarlia & Di Benedettob, 2013) at different initial conditions. Experimental results demonstrate that the mole fraction, equivalence ratio, initial pressure (Miao et al., 2008) and initial temperature (Hu et al., 2009c) unify the effects of hydrogen-enriched NG on the mentioned parameters (Miao et al., 2008) as well as the optimum ignition timing (Tinaut et al., 2011). The results indicate that an increase of initial pressure could be either favourable or unfavourable to the flame propagation. In other words, a higher initial pressure reduces the concentration of H and OH radicals, as a result of which the flame speed tends to decrease. On the other hand, with the growth of initial pressure, the temperature of the reaction zone and the flame speed will be enhanced (Miao et al., 2008). The flammability limits of hydrogen-enriched natural gas and hydrogen-methane in both lean limit and rich limit mixtures show that the upper flammability limit increases with the escalation of the hydrogen fraction. It can be said that while a higher hydrogen fraction has an insignificant effect on the lower flammability limit, the upper flammability limit is governed with the addition of more hydrogen in both mixtures. It indicates that the upper flammability limit can be applied for hydrogen-enriched natural gas for hydrogen fractions at the same value since their flammability data are closer to each other. Moreover, the ignition source and experimental setup have a significant effect on the lower flammability limit results while the upper flammability limit results tend to agree with each other (Miao et al., 2011). The addition of H_2 also extends the flammability limits associated with CH_4–air triple flames by the improving interactions between the reaction zones (Briones et al., 2008). No more experimental data are available for the flammability limits of other enriched hydrocarbon-hydrogen mixtures. Similarly, there is no discussion of whether the same phenomena occur in other mixtures, especially those containing reformer gases, such as N_2, Ar, CO and CO_2.

Moreover, Fotache et al. (1997) investigated the ignition characteristics of hydrogen-enriched methane flames at various pressures and identified three ignition limits: (i)hydrogen-assisted ignition, (ii)transition, and (iii)hydrogen-dominated ignition. The auto-ignited lifted flames of methane-hydrogen mixture fuels in laminar jets were investigated experimentally in heated co-flow air. By adding a small amount of hydrogen to methane, the lift-off height of the auto-ignited lifted flames increases with the jet's velocity under a high temperature hydrogen-assisted auto-ignition regime (Choi & Chung, 2012). However, a higher hydrogen fuel fraction is required to auto-ignite the flame under the temperature regime. The addition of hydrogen to hydrocarbon/air plays the role of a self-ignition inhibitor at temperatures lower than 1050 ^{o}K. This is mainly caused by the formation of fewer active species, like HO radicals, which in turn hinder the chain-branching processes (Frolov et al., 2013). Moreover, even by adding hydrogen and maintaining the condition of mild combustion, the critical auto-ignition with tri-brachial flames still contains the linear relation between the flow time and the square of the adiabatic ignition delay time (Choi & Chung, 2012).

2.4.1.2. Effectiveness of Inhibitors on Hydrogen Flame Acceleration

From the previous studies, the investigations are more focused on the discussions that the presence of inhibitors in hydrocarbon and hydrogen fuels affect the laminar flame propagation velocity, laminar combustion velocity, Markstein length, flame stability and the maximum combustion pressure (Kwon & Faeth, 2001; Zeng et al., 2014). Nevertheless, these investigations analyse different aspects and there are still a lot of open questions due to various assumptions, different fuel-inhibitors concentrations, tube/vessel system application and different condition boundaries on responding to the inhibitors effects. For example, Qiao et al. (2005) look for the flame stretching effects on the laminar burning velocities of H_2-O_2-diluent (N_2, Ar or He) in a small scale system (a spherical windowed chamber). They reported that these flames were very sensitive to flame stretching, exhibit the ratio of unstretched-to-stretched laminar burning velocities in the range of 0.6 to 3.0, with corresponding Markstein numbers ranging between ±3-7. They also indicated that diluents, i.e., N_2, Ar, and He, tend to have a significant effect on the preferential-diffusion/stretch interactions due to their dynamic and kinetic characteristics i.e. argon and helium have a higher laminar burning velocity ratios, compared to nitrogen based on their higher flame temperatures and transport rates (Qiao et al., 2005). Further, a study on the flame propagation of H_2-O_2-N_2 using an International Thermonuclear Experimental Reactor (ITER) showed that both the overpressure and laminar flame speed increased as the initial pressure and temperature increased. It also showed that this condition was more preferable on a higher nitrogen concentration (Sabard et al., 2013). Different view was given by Di Benedetto et al. (2009) on the effectiveness of CO_2 on the H_2-O_2-N_2-CO_2 mixtures. They suggested that the burning velocity of the fuel-inhibitors mixtures is mainly due to their kinetic mechanism as the rapid reaction of O, H, CO, HCO, OH, HO_2 and CO_2, gives a negligible effect on the transport rate. However, the explosion behaviour of a stoichiometric H_2-O_2-N_2-CO_2 mixture at NTP (normal temperature and pressure) condition showed a significant stability on the flame and apparently, no ignition if CO_2 presence is higher than 40%. It could be depicted that the explosion was mainly affected by the CO_2 and O_2 concentration (Di Benedetto et al., 2009). On the other hand, investigations also show that adding N_2 to both methane-hydrogen and iso-octane-hydrogen mixtures (Tahtouh et al., 2011; Tahtouh et al., 2009), as well as adding CO to methane-hydrogen (Masri et al., 1992; Vu et al., 2011a) and propane-hydrogen mixtures (Vu et al., 2011a), significantly reduced the rate of the laminar burning velocity for every hydrogen mole fraction due to the enhancement of the flame inheritor groups; increase in H_2 fractions, the carbon fraction declined in the methane-hydrogen blends and the combustion temperature increased. Moreover, CO_2 had a significant radiation and dilution effect on the quenching and blow-off limits, as reported by Shih (2009). Yet, the effectiveness of all of these inhibitor gases on Markstein numbers were insignificant, due to their virtually similar dynamic properties (Di Benedetto et al., 2009; Kwon & Faeth, 2001; Qiao et al., 2005). Despite such extensive studies, discussion on the influence of the inhibitors concerning explosion in the pipe is still crucial particularly on the unsteady propagation of flames under branched pipe conditions.

2.4.2. Effectiveness of Pipe Configuration on Flame Acceleration

As mentioned earlier, studies on flame propagation and explosion mechanisms in pipes have been widely discussed (Blanchard et al., 2010; Chatrathi et al., 2001; Emami et al., 2013; Jianliang et al., 2005; Oh et al., 2001; Phylaktou et al., 1993; Thomas et al., 2010), but most of these focused on specific applications (i.e., bending or straight pipes). For this reason, holistic studies should be performed on flame propagation in different pipe configurations, considering the complicated problems involved in the interaction between fluid dynamics, heat transfer and turbulent combustion.

2.4.2.1. Flame Acceleration in Straight Pipes

Razus et al. (2006) studied the explosion pressures of hydrocarbon-air mixtures in closed vessels. They showed that the initial pressure, fuel concentration and heat losses have a significant effect on the maximum overpressure during flame propagation. Gu et al. (2000), and Liao et al. (2004), investigated the flame instability and ratio of the laminar burning velocity of methane-air and natural gas-air mixtures at different equivalence ratios. Liu et al. (2015) studied flame propagation and explosion development in propane-air mixtures, in a 1.16 m^3 vessel with central ignition, to evaluate the burning velocity of the fuel by considering the history of flame-front trajectory and pressure in the vessel. From their work, flame instability was observed at the equivalence ratio of 1.2 and above, suggesting that the flame instability is due to the effect of thermal-diffusion instability and hydrodynamic instability. Rich mixtures are known to be more susceptible to developing surface instabilities (flame cellularity), which can lead to higher burning rates and hence higher flame speeds. This in turn could result in a more severe explosion than might otherwise be expected (on the basis of its laminar burning velocity alone). In addition, the values of flame speed and maximum overpressure are enhanced by increasing the concentration of methane in the mixture in a horizontal pipe (Zhu et al., 2010). Another study on a straight pipe with a 60 L/D (length/diameter) showed that the pressure and velocity waves accelerate with the increasing reaction rate of methane-air (Zhu et al., 2015).

On the other hand, Xiao et al. (2011) have carried out an experimental study on half-open and closed horizontal ducts, and found that premixed hydrogen-air mixtures undergo different phases of flame shapes, indicating pronounced characteristics compared to other gaseous fuels. Research on the estimation of shock waves in hydrogen-oxygen mixtures in a 12-metre diameter volume has also shown that wave intensification from a small [initial] amount of energy could create secondary combustion explosion centres, whose parameters exceed the values predicted by the Chapman-Jouguet condition (Petukhov et al., 2009). This contradicts the normal assumption that detonation is stimulated by a significant power effect. However, experimental researchers report a number of common findings, including the fact that when an explosion uses hydrogen fuels, DDT has the potential to be achieved at a magnitude of greater severity, compared to hydrocarbon fuels (Heidari & Wen, 2014; Thomas et al., 2010).

2.4.2.2. Flame Acceleration in 90 degree Pipes

Little research has been carried out on explosions through pipe bends as well as round pipes, a complicated problem involving the interaction between fluid dynamics, heat transfer and (turbulent) combustion. An investigation by Qing et al. (2009) showed that the bend curvature, duct diameter and the duct end condition (open or closed) has significant effect on the propagation characteristics. Moreover, Blanchard et al. (2010; 2011) showed that at a moderately short distance from the ignition point in a long tube had the ability to increase flame speeds and overpressures, and shorten the run-up distance to DDT in 90 degree pipe. Observations of the flame front when travelling through a rectangular 90 degree bend were made by Zhou et al. (2006), who showed that after initially propagating as a flat flame the flame front takes on a tulip configuration. Investigation on flame acceleration of propane/air mixture also showed that both the flame tip speed and pressure dynamics are in close connection with the flame front evolution in 90 degree pipe. As presented, the flame propagates exponentially in the early stages, and decelerate quickly after touching the sidewalls (Xiao et al., 2014). It was also shown that amount of mole fraction has significant effect on dynamic of flame propagation in terms of flame speed, maximum overpressure and rate of pressure rise in this configuration (Emami et al., 2013). Emami et al. (2013) study on the flame acceleration of methane-hydrogen/air for an ambient initial pressure and temperature in a 90-degree pipeline showed that hydrogen at a concentration below 10% in methane-hydrogen/air mixtures would dramatically affect the maximum overpressure, rate of pressure increase and flame speed due to the energy release and chaotic combination of mixture reactivity.

Numerical simulation and experimental study on flame propagation in a duct with a 90◦ curved section also showed good agreement for the basic physical phenomena, such as, the tulip flame, flame shedding, pressure evolution trends, flame propagation speed trends and vortex development in the bend (Emami et al., 2013; Zhou et al., 2006). As shown, the unburned mixture flow development in the bend was marked by an imbedded transient secondary flow in a form of two or more stream wise vortices (Zhou et al., 2006). Moreover, the representative results from propane/air explosions utilizing the straight pipe configuration, 90 degree bend and a 20% BR baffle at 2 m from the ignition source also showed that the utilized maximum overpressures and rates of pressure rise in baffle and bend were slightly higher compared to the straight configuration due to the higher flame speeds (Figure 2.9) (Blanchard et al., 2010).

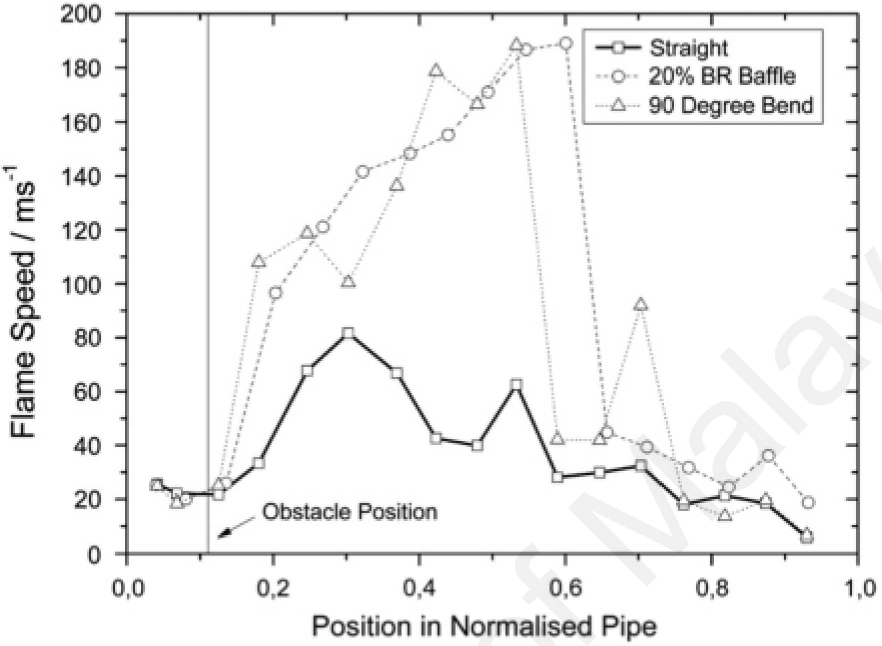

Figure 2. 9 Flame speeds for propane–air explosions (Blanchard et al., 2010)

Explosions in pipes and ducts, flame acceleration and the transition from deflagration to detonation are well researched subjects (Ciccarelli & Dorofeev, 2008). However, research in this area tends to concentrate on the effects of baffle type obstacles or items in the path of the flow (Ibrahim & Masri, 2001). Tube bends, for example, are obstacles used extensively in industrial applications, however little is known about their effects on flame acceleration, overpressure enhancement and their contribution to DDT therefore a complicated problem involving the interaction between fluid dynamics, heat transfer and (turbulent) combustion. Phylaktou, et al. (1993) showed that with a short tube, a 90 degree bend can enhance to both the flame speed and the overpressure for methane–air explosions compared to similar experiments carried out in straight pipes. The flame speed in these experiments was enhanced by a factor of approximately five and was equated to the effects of a baffle with a blockage ratio of 20% at the same position. Observations of the flame front when travelling through a rectangular 90 degree bend were made by Zhou et al. (2006), who showed that after initially propagating as a flat flame the flame front takes on the tulip configuration (Clanet & Searby, 1996a). As the flame reached the bend, the upper tongue (the one propagating towards the outside of the bend) of the tulip slowed down, Whereas the lower tongue the one propagating towards the inside of the bend began propagating more quickly around the inside of the bend, an effect named ‘‘flame shedding’’ by the authors. 3-D particle modeling of the flow around the bend showed that large vortexes were created just downstream of the inside wall of the bend while flow followed a more streamlined pattern around the outside of the bend. Lohrer et al. (2008) demonstrated that a bend induced a significant increase in turbulence over the first 30% of the inner diameter of the pipe immediately after the bend whereas only a relatively small amount of turbulence regime was induced around the outer side (Blanchard et al., 2010).

2.4.2.3. Explosions in Other Systems

Investigation on enriched hydrogen mixtures in chambers showed that the chamber volume has no significant effect on the burning velocity, opposite to initial pressure and hydrogen concentration (Figure 2.10). It illustrates that a less stable flame will occur at a higher initial pressure and hydrogen fraction for relatively lean conditions (Miao et al., 2008). Moreover, for a fixed initial pressure, the laminar burning velocity is increased with the increase in the hydrogen fraction (Cammarota et al., 2009; Cammarota et al., 2010; Hu et al., 2009b; Salzano et al., 2012; Tahtouh et al., 2011; Tahtouh et al., 2009; Tang et al., 2008; Vu et al., 2011a) in all mixtures. One study also suggests an empirical correlation to estimate the laminar burning velocity of CH_4–H_2–N_2/air mixtures for all hydrogen mole fractions under stoichiometric conditions, at 1 bar pressure and ambient temperature, for vast dilution levels ($0 < \beta < 0.35$) (Tahtouh et al., 2009).

Several findings also show the modification of the triple flame structure (Briones et al., 2008) and flame dynamics (Azatyan et al., 2005; Briones et al., 2008; Cammarota et al., 2009; Cammarota et al., 2010; Di Benedetto et al., 2009; Emami et al., 2013) of methane by H_2 enrichment and transition phenomenon of laminar burning velocity into turbulent burning velocity (Ciccarelli & Dorofeev, 2008), yet only fair discussion is offered. Adding hydrogen to methane increases the flame curvature, the mixture fraction gradient near the triple point, and the total stretch (Briones et al., 2008). It can be said that a higher value of the H_2 mole fraction (Azatyan et al., 2005; Cammarota et al., 2010; Emami et al., 2013; Salzano et al., 2012), a higher initial pressure (Cammarota et al., 2009; Cammarota et al., 2010; Salzano et al., 2012) and greater flame turbulence (Cammarota et al., 2009) also increase the maximum pressure and maximum rate of pressure-increase in confined systems. The combined effects of initial pressure and turbulence on the maximum pressure rate of the pressure increase and burning velocity are insignificant for methane-hydrogen at lower concentrations of H_2 (lower than 10%), since the fuel has a negligible effect on the flame reactivity (Cammarota et al., 2009). For any initial pressure, the effect of hydrogen-substitution to methane is dramatic in relation to both the maximum rate of pressure increase and the laminar burning velocity for hydrogen molar fractions higher than 50% (Cammarota et al., 2010; Salzano et al., 2012). The inhibitor gases if added into hydrogen-hydrocarbon fuel mixtures would significantly decrease the burning velocity values as shown in Figure 2.10 b and c. For instance, the presence of N_2 and CO in CH_4-H_2 and C_3H_8-H_2 mixtures in constant initial pressure declines the burning velocity up to two times at the same equivalence ratio. It is understood that the initial conditions have a significant effect on the hydrogen-enrichment mixtures, though it requires further investigation of the dynamic and chemical analysis of the explosive behaviour of hydrogen-hydrocarbon mixtures. However, researchers have not yet paid attention (whether experimentally or numerically) to the dynamic properties in question, especially to the flame propagation of hydrogen-hydrocarbon mixtures in other types of junctions, which is an important safety issue for future fuel transmission and distribution.

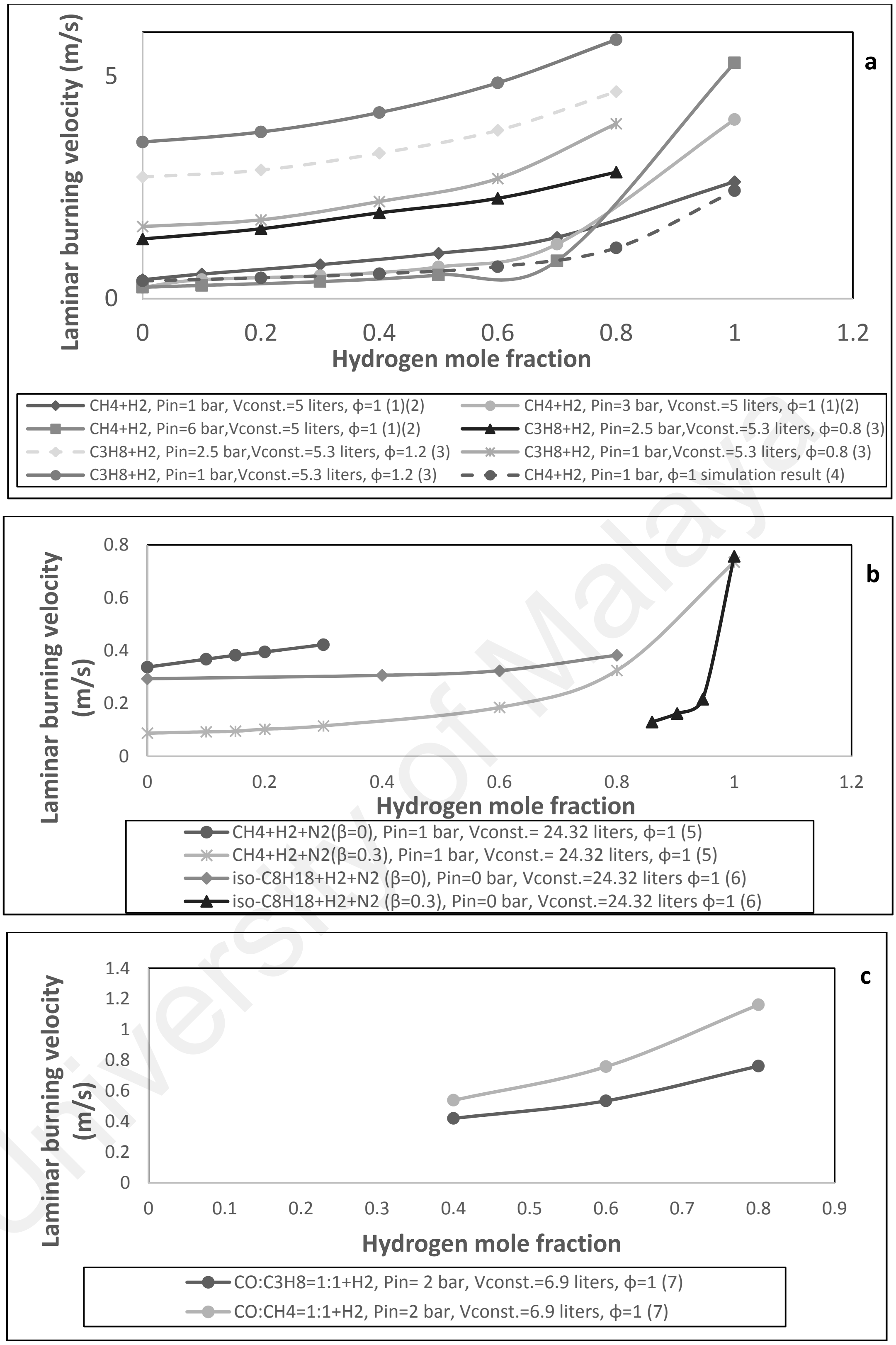

Figure 2. 10 Laminar burning velocity Vs. hydrogen mole fraction: (1) (Salzano et al., 2012), (2) (Cammarota et al., 2010), (3) (Tang et al., 2008), (4) (Hu et al., 2009), (5) (Tahtouh et al., 2009), (6) (Tahtouh et al., 2011), (7) (Vu et al. 2011)

2.4.3. Effectiveness of Ignition Source on Flame Acceleration of Fuels

The point at which ignition takes place is an important factor during the initial stages of combustion (Phylaktou & Andrews, 1991), especially in closed vessels (Inaba et al., 2004; Kindracki et al., 2007; Qingwu et al., 2013). When the ignition source is further from a sealing flange or vessel wall, the flame will have a longer period to spherically propagate, leading to initially higher overall flame speed and rate of pressure rise.

Cho et al.(2007) reviewed the effectiveness of the spark ignition on some indexes such as emissions, combustion efficiency, and strategies to get stable combustion of the natural gas in engines. As shown in Figure 2.11, the central ignition causes higher maximum pressure due to a shorter time of the heat exchange between hot combustion products and cold vessel walls. Moreover, the presence of obstacles in vessels cause higher pressure and rate of pressure rise due to shorter time of combustion process. A comparison study between interconnected closed vessels and an isolated close vessel of the same size also showed that ignition position affects on the peak pressure and the rate of pressure rise in the interconnected vessels. In overall, the results indicate that explosion in interconnected vessels presents strongly destructive power to secondary vessel, especially transmission from big vessel to the small one (Zhang et al., 2013).

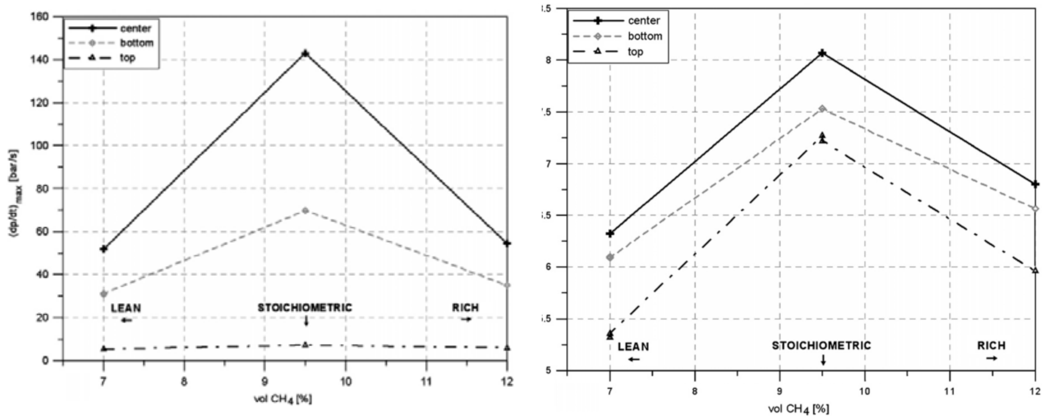

Figure 2. 11 Maximum rate of the pressure rise of methane–air mixture in cylindrical vessel, a)without obstacle and b)with obstacle for various ignition positions (Kindracki et al., 2007)

Blanchard et al. (2011) also shows that ignition position has a significant effect on DDT development of hydrogen/air mixture. For instance, the shortest run-up distance to DDT relative to the end of the pipe was recorded when the ignition source was placed 4.4 pipe diameters or 0.7 m from the pipe end (Figure 2.12).

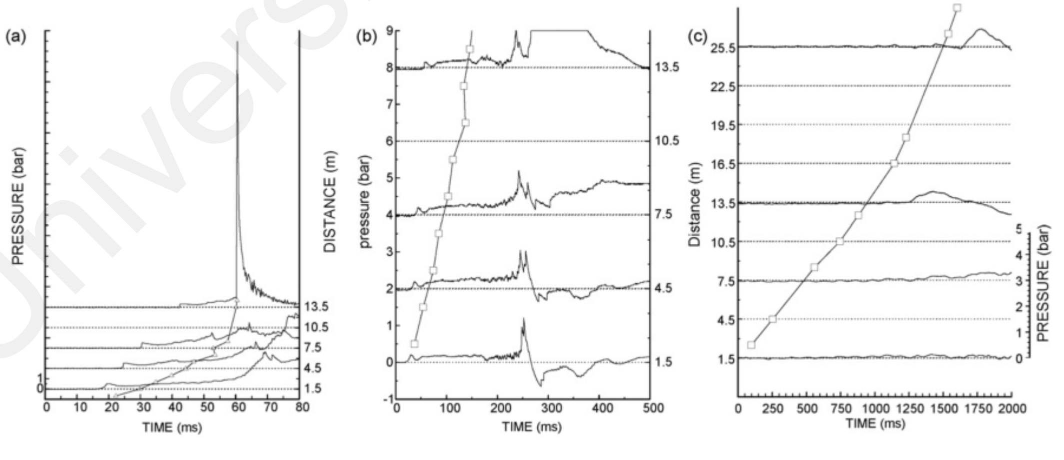

Figure 2. 12 Pressure histories at various gauge locations and superimposed flame front arrival time for hydrogen in air: (a) 35.6% H_2, (b) 19.7% H_2 and (c) 14% H_2 (Thomas et al., 2010).

However, Willacy et al. (2007) showed that effectiveness of ignition position on flame acceleration of propane/air mixture compared to initial concentration is negligible in a duct vented vessel. But, the results showed that the severity of the system is higher if the ignition position was allocated at end point compared to central ignition point. Moreover, another study showed that the minimum required ignition energy by using laser sparks as an ignition source are reliably larger than electrical sparks for propane/air mixtures at 1 atm and lower pressures (Eckhoff et al., 2010; Lee et al., 2001). It is due to the different electromagnetic and thermal conditions that exist within and near the spark plasmas (Lee et al., 2001).

Spark duration is another issue in methane explosion in closed vessels that investigated by Zhang et al. (2012). They illustrated that for the weaker ignition, the spark durations in the range from 6.5 μs to 40.6 μs had insignificant effect on explosion parameters of methane/air mixtures in the 5 L or 20 L vessels while the vessel volumes had a significant impact on the flame temperatures near the vessel wall in the same ignition and the volume fractions of methane/air.

2.5. Flame Instabilities

2.5.2. Hydrodynamic Instabilities

The results on stability envelopes in micro-scale combustion showed that propane/air flames could be stabilized in narrow channels by applying specific conditions for common ceramics such as alumina and silica. As known, the wall material thermal conductivity acting a conflicting role in flame stability. Regarding to material lifetimes, the wall temperature gradients and hotspots are declined by higher wall thermal conductivities. It was also shown that thicker walls cause further upstream heat propagation and faster flows before blowout which give this opportunity to use less conductive materials (Norton

& Vlachos, 2004). However, another study showed that heat recirculation has insignificant effect on flame stability of propane/air mixture in the extinction mode. It makes the internal channel warmer while it increases the heat loss (Federici & Vlachos, 2008).

The determination of burning velocity is another important issue that should be considered for hazardous waste explosion. Consequently, Huzayyin et al.(2008) and Razus et al. (2010b) determined laminar burning velocity of propane/air mixture at NPT condition in different systems. The normal burning velocities at NTP condition versus the equivalence ratio present a good agreement in published data, especially when inherent differences between the accuracies of different methods are considered (Figure 2.13). Moreover, an investigation on effect of the burning velocity behaviour on blast wave intensity of propane/air mixture showed that the enhancement of the blast wave intensity is due to the burning velocity increasing and the acceleration ratio (Kim et al., 2014). It was also found that the explosion times at constant initial pressure decrease by increasing of the preheating temperature in all propane/air concentrations (Razus et al., 2010a). It also showed that propane/air mixtures at higher equivalence ratios (1.2-1.4) will be exploded in shorter time (Razus et al., 2010a).

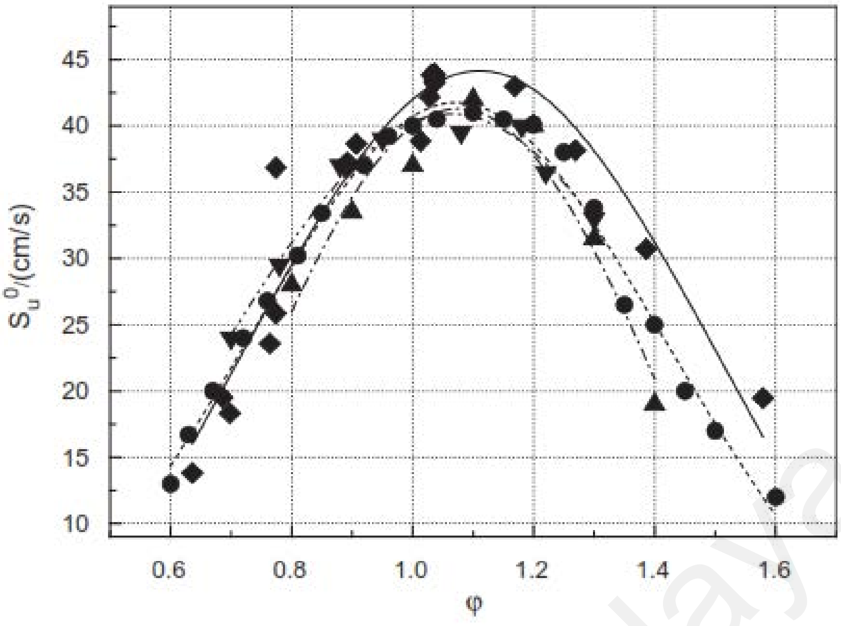

Figure 2. 13 Normal burning velocities of propane–air mixtures at 298 K and 1 bar: ♦ (Razus et al., 2010b); ▲(Metghalchi & Keck, 1980); ●(Vagelopoulos C, 1994); ▼(Zhenwei Zhao et al., 2004).

Moreover, Razus et al. (2006) and Tang et al. (2014) studied explosion pressures of hydrocarbon–air mixtures in closed vessels. They showed that initial pressure, fuel concentration and heat losses have significant effects on the maximum overpressure during flame propagation. Hu et al. (2009a) also showed that with the increase of equivalence ratio of hydrogen in air, laminar burning velocity increases in the case of fuel-lean mixture combustion and decreases in the case of fuel-rich mixture combustion. Laminar burning velocity increases with the increase of initial temperature initial pressure. Investigation on other systems also showed same phenomenon (Bauwens et al., 2012; Dahoe, 2005).

Sabia et al. (2014) also analyzed the auto-ignition of propane mixtures under a moderate or intense low-oxygen dilution (MILD) by varying the mixture composition from, fuel-lean to fuel-rich conditions, and the dilution level over a wide range of temperatures (850-

1250 K) at atmospheric pressure. The results showed an obvious change in the slopes of the Arrhenius plot at stoichiometric concentration. Moreover, another investigation showed that the auto-ignition for 40 mol% propane–air mixtures at atmospheric pressure occurs in 300°C in a closed vessel. However, if the temperature declines up to 250 °C, it is required to increase initial pressure up to 14.5 bar to let auto-ignition occurs for this particular mixture at same concentration ratio (Norman et al., 2006). It can be found that the propane sensitivity to auto-ignition mainly depends on the initial pressure. Prince et al. (Prince & Williams, 2012) also showed an ignition possibility and negative-temperature-coefficient (NTC) behavior at low temperature for propane/air mixture by adding a small number of appropriate elementary steps. Figure 2.14 is giving an example of predictions of two-stage ignition with San Diego mechanism for propane. As shown in the transition from the first stage to the second stage, the ignition-time reversal clearly occurred in the center of the two-stage regime at initial temperatures between 725 K and 825 K (Prince & Williams, 2012).

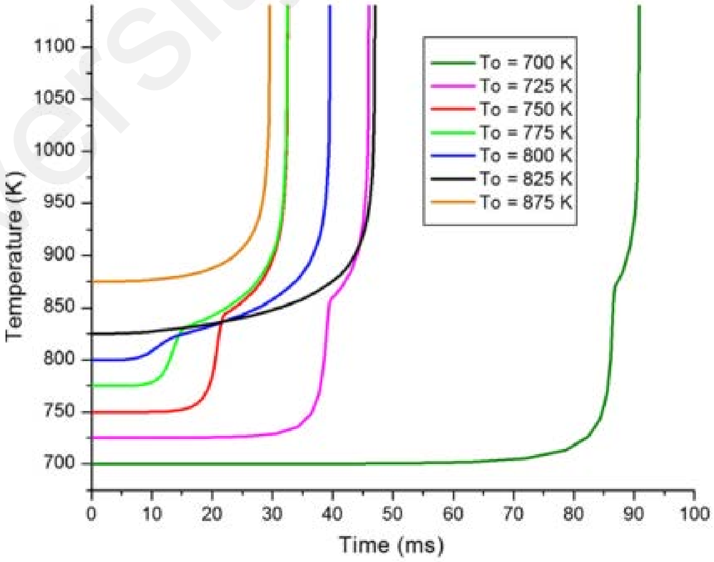

Figure 2. 14 prediction of two-stage ignition for stoichiometric propane–air mixtures at 30 bar pressure using San Diago mechanism (Prince & Williams, 2012)

On the other hand, the investigations (Bauwens et al., 2011; Razus et al., 2011) showed that the maximum rates of pressure rise and deflagration are slightly influenced by the initial temperature at constant initial pressure and composition. Moreover, an experimental study in long closed pipes showed that maximum overpressures and flame speeds occurred at near the stoichiometric concentration for propane/air fuel while they were decreased by increasing the length-to-diameter ratio of the steel pipe (at a constant diameter) (Lohrer et al., 2008).

Studies of single-port atmospheric (Burbano et al., 2008), drilled-port atmospheric (Burbano et al., 2008) and Bunsen (Zhen et al., 2012a, 2012b) burners demonstrate the significant effect of additional hydrogen in methane (Burbano et al., 2008; Zhen et al., 2012a) and LPG (Zhen et al., 2012a, 2012b) in terms of the height of the blue cone of the flames. At a constant Reynolds number, an increase in the hydrogen concentration in both LPG and methane led to a rise in the volume flow rate of the fuel/air mixtures. Therefore, the reduction in the height of the inner reaction cone suggests an increase in the laminar burning speed of the flame under stoichiometric conditions in all burners (Burbano et al., 2008; Zhen et al., 2012a, 2012b). However, one study shows that if the middling of the local reaction rates is done over the total flame brush then the influence of the Lewis number is negligible, since the curvature distribution is naturally symmetric for highly turbulent flames (Dinkelacker et al., 2011). For consolidating these achievements, more analytical and experimental investigations on the flame stability of hydrogen-hydrocarbon mixtures in other burners are required.

From the literature, the peak temperature (in non-stoichiometric conditions) was increased by adding more hydrogen into methane/air under a moderate or intense low-oxygen dilution (MILD) combustion regime at an L/D (length per diameter) higher than 10. However, the mixture fraction, strain rate and radial velocity are dramatically decreased at L/D of between 10 and 25 (Mardani & Tabejamaat, 2010). On the other hand, the addition of hydrogen into hydrocarbon fuel also induces a slight increase in flame temperature, and the effect is more prominent at ambient conditions. The slight linear modification of the temperature of all hydrocarbon-hydrogen mixtures is due to the linear increase in the energy input at higher hydrogen contents (Burbano et al., 2008; Zhen et al., 2012a, 2012b). Noted that, due to a faster decrease in flame height and a higher increase in the laminar burning speed in the CH_4 flames, a significant increase in the flame temperature and heat transfer of the CH_4 flames over LPG flames was experienced (Dinkelacker et al., 2011; Zhen et al., 2012a). Under the same conditions, the higher initial pressure of CH_4-H_2 flames also showed a substantial increase in the initial temperature (up to 225°K) (Zhen et al., 2012a). This indicates the effectiveness of initial pressure on flame propagation. Moreover, investigation of combustor shells show that there is a close relation between the pressure cycle, the periodic flashback behaviour and the emission of NO. The presented data show that higher hydrogen concentrations cause fewer pressure fluctuations and lower levels of flashback formation (Tuncer et al., 2009). Yet, the highest equivalence ratio corresponds to the flashback limits, the increase that takes place due to the reactant preheats, and the higher pressure of the combustor (Noble et al., 2006).

Investigations on the flame characteristics of various enriched-hydrogen mixtures have been done in different chambers with different values of hydrogen. The results show that the un-stretched flame propagation speed (Azatyan et al., 2005; Briones et al., 2008; Emami et al., 2013; Li et al., 2012; Strakey et al., 2007; Tang et al., 2008) and laminar burning velocity (Azatyan et al., 2010; Li et al., 2012; Refael & Sher, 1989; Tang et al., 2008) increased parallel to any increase in the initial temperature (Azatyan et al., 2010; Hu et al., 2009b; Hu et al., 2009c; Miao et al., 2008; Refael & Sher, 1989; Tang et al., 2008; Tinaut et al., 2011) and hydrogen fraction (Azatyan et al., 2005; Cammarota et al., 2009; Cammarota et al., 2010; Emami et al., 2013; Hu et al., 2009c; Li et al., 2012; Miao et al., 2008; Salzano et al., 2012; Tang et al., 2008; Tinaut et al., 2011). However, the values declined with an increase in the initial pressure, as this condition will reduce the H and OH radical concentrations at elevated pressures (Cammarota et al., 2009; F Cammarota et al., 2010; Hu et al., 2009b; Hu et al., 2009c; Miao et al., 2008; Salzano et al., 2012). Based on numerical analysis (Hu et al., 2009b; Hu et al., 2009e), it was also found that the increase in the burning velocity is more significant in hydrogen-hydrocarbon mixtures when the hydrogen mole fraction is higher than 40%. It can be said that the burning velocity increased exponentially with the increase of the equivalence ratio, as clearly illustrated in Figure 2.10. These phenomena are induced by a chemical mechanism as explained by Westbrook et al. (2007). As the can be seen, this is more significant for propane-hydrogen mixtures due to the higher inhibiting reaction, reaction (2.47), and a delaying effect is, therefore, inflicted on the overall progress of the reaction with increasing pressure (Azatyan et al., 2005; Tang et al., 2008). Apparently, a study on burning velocities of CH_4+H_2/air mixtures with wide range of equivalence ratio (from 0.8 to 1.4) in adiabatic condition was in a good agreement with the literature results given at atmospheric pressure (Konnov et al., 2010). The mechanisms and phenomena of H_2+C_3H_6 and H_2+iso-C_3H_6 combustions are also in agreement with definition of inhibition offered by encyclopaedias, chemical kinetics and monographs (Azatyan et al., 2005). In one study, the flame stability of the lean blow-off limit was assessed by the turbulent flame speed. The results showed that the turbulent flame speed for the enriched flame was higher than that the pure methane flame, due to a faster laminar burning rate, a greater area and the mean effect of the turbulence on the local structure, leading to a different burning rate per unit area. Consequently, the higher turbulent flame speed promotes a greater resistance to flame blow-off, which leads to greater stability in the flame (Hawkes & Chen, 2004) and is significantly greater for kernels by a factor of 1.38 (Dunstan & Jenkins, 2009).

$$H + O_2 + M \rightarrow HO_2 + M \qquad (2.47)$$

The simulation studies prove that the non-equidiffusion has an insignificant effect on controlling the unsteady flame propagation of the hydrogen-methane/air mixture, which is mainly controlled by the laminar burning velocity. As a result, it causes faster flame propagation and higher velocities ahead of the moving flame, which focuses on the burning-rate growth by interacting with flame-flow (Di Sarli & Di Benedetto, 2013; Di Sarli et al., 2012). The result is also in agreement with the experimental results, confirming that adding lower concentrations of hydrogen to methane will lead to transition from a regime in which the vortex only wrinkles the flame front to a more vigorous regime (Di Sarli et al., 2012; Di Sarlia & Di Benedettob, 2013). Moreover, the higher mole fraction in the fuel causes a growth in the intensity of the flame-vortex interaction and the flame surface area (Di Sarli et al., 2012).

Moreover, the higher equivalence ratio (ϕ up to 1.2) increases the burning velocity caused by hydrodynamic instability. The critical radius and Markstein length decrease with an increase in the hydrogen fraction (Tang et al., 2008; Vu et al., 2011b); however, this phenomenon is reversed for a equivalence ratio of more than 1.3 (Vu et al., 2011c). It should be noted that the explosion behaviour of a stoichiometric H_2+O_2+N_2+CO_2 mixture at NTP (normal temperature and pressure) condition was different. Significant stability in the flame and no ignition behaviour were observed, since the explosion was clearly affected by the CO_2 and O_2 concentration (Di Benedetto et al., 2009). The numerical studies show that CO_2 dilution chemically affects the H_2+O_2 flame structure under a counter-flow diffusion conditions. Moreover, CO_2 has a significant radiation and dilution effect on quenching and blow-off limits, respectively. A higher CO_2 concentration decreases the extinction limits and flame temperature, which in turn reduce the overall reaction rate (Shih, 2009). However, this proposition was not examined for other inhibitory gases.

2.5.3. Thermal and Mass Instabilities

Consider the combustion of gas-air mixture within a vessel a short time after ignition. It is assumed that before ignition the unburnt gases are at rest and that during combustion the burnt gases are at all-time trapped behind the advancing flame front. Consequently, in linear condition the relation between flame speed and burning velocity is as follow (Harris, 1983):

$$S_f = Eu_b \qquad \text{(Eq. 2.2)}$$

S_f is defined as flame speed, E is expansion factor and u_b is burning velocity.

The expansion factor is equal to ratio of densities of unburnt and burnt gas (Eq. 2.3),

$$E = \rho_u/\rho_b = N_u/N_b \qquad \text{(Eq. 2.3)}$$

Consequently, unburned gas velocity (Sg) can be also calculated as below:

$$S_g = S_f\,(E-1)/E \qquad \text{(Eq. 2.4)}$$

Where E is the expansion factor.

Lewis numbers were calculated as a basic analysis of the diffusivity rate of involved species in the unburnt gases, corresponding to the mass burning rate. This is the most important factor that affects the burning velocity and heat release rate during flame propagation (Movileanu et al., 2013). The Lewis number calculation is as following (Lide & Haynes, 2009):

$$Le = \frac{\alpha}{D} \qquad \text{(Eq. 2.5)}$$

Where, α is thermal diffusivity and D is the mass diffusivity. Thermal diffusivity is the thermal conductivity divided by density and specific heat capacity at constant pressure:

$$\alpha = \frac{k}{\rho C_p} \qquad \text{(Eq. 2.6)}$$

Where, k is thermal conductivity (W/(m·K)), ρ is density (kg/m³) and Cp is specific heat capacity (J/(kg·K)). Moreover, for current system, the mass diffusivity dependence of the diffusion coefficient on temperature for gases can be expressed using Eq 2.7:

$$D = \frac{1.858.10^{-3} T^{3/2} \sqrt{\frac{1}{M_1} + \frac{1}{M_2}}}{P} \qquad \text{(Eq. 2.7)}$$

where; 1 and 2 index the two kinds of molecules present in the gaseous mixture, T is the absolute temperature (K), M is the molar mass (g/mol) and P is the relative pressure referring to $(\frac{P_x}{P_{\text{atmosphere}}})$ where P_x is the pressure on each measured point.

Liu et al. (2015) investigated the flame propagation and explosion in propane/air mixtures in a 1.16m^3 vessel with central ignition to evaluate the burning velocity of the fuel be considering the history of flame-front trajectory and pressure in vessel. The results showed that at equivalence ratios 0.7-1.0, 1.2 and 1.0 instability occurs within a flame radius of 125, 24 and 30 mm with corresponding Lewis numbers 1.6-1.25, 1.1 and 0.95, respectively. It indicates that the flame instability results are due to effect of thermal-diffusion instability and hydrodynamic instability. A similar situation was observed by Kim et al. (2014), who demonstrated that the flame for a Le < 1 mixture was wrinkled by diffusional-thermal instability, accelerating the flame speed and consequently increasing the overpressure with time. The studies report that a higher hydrogen mole fraction is not only causing stretched flame propagation speeds and an increase in the burning velocity, but also reducing the burned gas Markstein lengths (L_b) (Hu et al., 2009b; Tahtouh et al., 2011; Tahtouh et al., 2009; Tang et al., 2008; Vu et al., 2011a, 2011b; Vu et al., 2011c), which in turn results inane increase in the instability of the flame (Hu et al., 2009c; Miao et al., 2008; Tahtouh et al., 2011; Tahtouh et al., 2009; Vu et al., 2011a, 2011b; Vu et al., 2011c).

The numerical analysis indicates that the effectiveness of the Lewis number on flame temperature is undeniably important, particularly when the hydrogen mole fraction is higher. Furthermore, the flame temperature increases faster than the adiabatic equilibrium and a super-adiabatic flame temperature at the same operation due to the effect of the Lewis number (Guo & Neill, 2009). Nevertheless, radioactive losses at a lower mass flux gave the opposite effect on temperature at atmospheric pressure burner-stabilized H_2+CH_4/air, H_2+C_2H_6/air and H_2+C_3H_8/air flames (at φ=1.3), suggesting an advantage of burner stabilization over the fuel mentioned (Sepman et al., 2011). This can be justified based on the kinetic mechanism discussed previously.

Hydrogen-enrichment also swings the flame’s centre of mass more towards the dump plane since the burning velocity is increased with the addition of hydrogen (Tuncer et al., 2009). Nevertheless, these phenomena are distinct with the achievements for the combustion of syngas in a pressurized combustor system. A study showed that for a syngas fuel mixture including hydrogen 79.5% and 29.5% carbon monoxide, no combustion instabilities such as auto-ignition, flashback, dynamic instability or blow-off (non-deliberate) were observed and the level of CO and NOx were lower than expected (Delattin et al., 2010). It was due to the fact that the combustion of syngas has higher level of linearity.

The properties of hydrogen/air combustion are broadly discussed in various thermal systems (Das, 1996). However, few studies have investigated the performance of engines using hydrogen-hydrocarbon mixtures (Jamal & Wyszynski, 1994). Experiments have shown that by fuelling hydrogen-enriched natural gas, engines can operate smoothly at lean conditions with improved engine performance (up to 14%) (Bauer & Forest, 2001), increased thermal efficiency (Choi & Chung, 2012; Conte & Boulouchos, 2006; Karim et al., 1996; Ma & Wang, 2008; Ma et al., 2008; Sher & Ozdor, 1992; Zhen et al., 2012a, 2012b) and reduced emissions (Bauer & Forest, 2001; Burbano et al., 2008; Coppens et al., 2007; de Ferrières et al., 2008; de Goey et al., 2007; İlbas et al., 2005; Karim et al., 1996; Ma & Wang, 2008; Ma et al., 2008; Mandilas et al., 2007; Mardani & Tabejamaat, 2010; Mohammed et al., 2011; Saravanan & Nagarajan, 2008; Sepman et al., 2011; Zhen et al., 2012a, 2012b). Therefore, it provides a feasible solution for the high-efficiency and environmentally friendly usage of both hydrogen and natural gas.

The effect of additional hydrogen on the combustion of gasoline-air mixtures depends significantly on the quality of the mixtures' preparation and the presence of residual combustion products (Bortnikov, 2007; Conte & Boulouchos, 2006). A report by Bortnikov (2007) showed that by adding 3-5% (as with the addition of10-15% hydrogen) it was possible to reduce the gasoline combustion value under the throttle-operation conditions of a reciprocating internal combustion engine cylinder. Moreover, by adding reformer gas (H_2+CO+N_2) to gasoline, the process of combustion would develop faster and a higher amount of heat would be released compared to pure gasoline, since the flame front reaches the furthest wall more quickly in an engine with two cylinders (Conte & Boulouchos, 2006). A similar observation is made for a single-cylinder stationary diesel engine for diesel-hydrogen mixtures (Saravanan & Nagarajan, 2008). Furthermore, adding 10% hydrogen greatly contributes to a decrease in combustion noise with late diesel-fuel injection timings due to a dramatic increase in the maximum combustion impact energy of the mixture (Nguyen & Mikami, 2013). The laminar flame speed of the addition of reformer gas to gasoline also qualifies the different fuel behaviours regarding flame curvature and stretch during the early phase of flame propagation in the engine. By adding reformer gas, the flame speed of the fuel increases significantly due to the higher flow rate through the engine and the combination of different spark timings and flame propagation speeds. Further, when the concentration of the initial component is too high, its impeding thermal effect overcomes the accelerating chemical effect of the hydrogen (Conte & Boulouchos, 2006).

A study on a single-cylinder engine shows that adding a small amount of hydrogen into compressed natural gas (CNG) improves engine performance at low engine speeds. At higher concentrations of hydrogen, the thermal brake efficiency and cylinder pressure are increased while the engine torque and brake specific energy combustion (BSEC) decay due to the higher heating value of hydrogen (Mohammed et al., 2011). The detailed analysis of the driving cycle of a S.I. (spark ignition) engine showed that adding H_2 to methane (up to 60%) leads to a lower partial burn limit from an equivalence ratio from 0.58 to 0.34 in comparison to methane alone. It also corresponds to a reduction in braking power up to 8% (at $\varphi=1$) and maximum to 14% ($\varphi=0.58$-1) in brake-specific fuel consumption. However, the increase in engine speed showed no significant difference as regards fuel consumption and pollutant production (Bauer & Forest, 2001).

However, the results in the CNG engine indicate that the turbulence intensity of the fuel mixture is already higher at high engine speeds (e.g., 3,000 and 4,000 rpm). Therefore, a lower concentration of H_2 does not contribute any significant effect to the flame's development or the duration of rapid combustion (Mohammed et al., 2011). The kinetic analysis showed that reactions (2.44-2.46) are important reactions in the ignition of n-C_7H_{16}/H_2 blends at engine-relevant conditions. The sensitivity to these reactions increased with an increase of the H_2 value (Aggarwal et al., 2011). This is in contribution with the addition of H_2 to CNG, which improves the optimal ignition timing, consequently leading to improved engine efficiency (Tinaut et al., 2011). The effectiveness of hydrogen-enrichment in relation to the availability of lean burning in a natural gas engine showed that the percentage of fuel availability exchanged through irreversibility. Clearly, it appeared near the lean limit with the addition of H_2 to NG. This phenomenon occurred due to an increase in combustion temperatures and a decrease in combustion duration and entropy generation during oxidation (Ozcan, 2010). Another study also showed that the addition of a relatively small amount of n-$C_7H_{16}$to H_2/air mixtures significantly modifies their ignition characteristics by decreasing and increasing the ignition delays at low and high temperatures, respectively (Aggarwal et al., 2011). The high lower-heating value of the hydrogen increase the energy input in the cylinder (Ozcan, 2010); it is in a contribution to the second law point view.

$$C_7H_{14} + O_2H+O_2 \rightarrow C_7H_{14} + O_2 + HO_2 \quad (2.44)$$

$$H_2O_2+m \rightarrow OH+OH+m \quad (2.45)$$

$$C_7H_{15}\text{-}2 \rightarrow C_4H_9+C_3H_6 \quad (2.46)$$

On the other hand, the relation between exhaust emission and engine speed showed that the total unburned hydrocarbon (THC), CO and NOx decayed for all CNG-hydrogen mixtures under the same conditions when the engine speed was increased. However, at a low engine speed of 2,000 rpm, the reduction rate of the THC was almost negligible for all values of H_2 (Mohammed et al., 2011). Due to the increase in H_2 fractions, the carbon fraction declined in the fuel blends and the combustion temperature increased. Thus, the THC reduction is more significant with higher concentrations of H_2 in mixtures. Moreover, particulate emissions are reduced by hydrogen-enrichment due to the absence of carbon in hydrogen. A study of a diesel engine showed that the reduction of particulates is more significant, especially for NOx (about 70%), with 90% hydrogen-enrichment

(Saravanan & Nagarajan, 2008). This phenomenon is in agreement with the numerical analysis investigation (Hu et al., 2009e). It also verifies that the burning velocity can be enhanced at low engine speeds with the addition of a small amount of hydrogen into pure CNG. However, this condition might not be suitable for application at high engine speeds because of the high turbulence intensity of the mixtures (Mohammed et al., 2011). Additionally, the released brake specific CO_2 and CO values declined up to 26% and 40%, respectively, with the addition of 60% hydrogen to methane in an I.S. engine. This statement also holds in relation to the temperature and pressure drop in the cylinder due to the closing throttle plate and lower oxidization of the unburned fuel (Mohammed et al., 2011).

2.6. Remarks

1. Adding hydrogen to hydrocarbons leads to an increase of the flame temperature and the heat release rate in burners due to the higher release of OH, CH_2O and HCO radicals. The interaction on these species is mainly kinetically related. However, the initial conditions (including pressure, temperature and initiated hydrocarbons, etc.) are also effective for burners' processing.
2. The CO and CO_2 emission rates significantly decay while the NOx rate slightly increases in the combustion of hydrogen-hydrocarbon mixtures, since the addition of hydrogen dramatically increases the concentration of OH radicals.
3. Adding a small amount of hydrogen improves engine performance at lower engine speeds. With higher concentrations of hydrogen, the brake thermal efficiency and cylinder pressure increase while the engine torque and brake specific energy combustion (BSEC) decline due to the higher heating value of hydrogen.
4. The addition of 10% hydrogen to a diesel engine system contributes significantly to a decrease in the combustion noise of late diesel-fuel injection timings, thanks

to the dramatic increase in the maximum combustion impact energy of the mixture. However, while lower concentration of H_2 does not have any significant effect on flame development or rapid combustion duration, the lift-off height of auto-ignited lifted flames significantly increases.

5. Adding H_2 affects the dynamic parameters, namely the extended flammability limits (lower lean limit and higher stretch extinction limit), reduced laminar flame thickness, higher adiabatic flame temperature, reduced stretch response (lower Markstein number), increased laminar flame speed (with a greater increase at lower equivalence ratios), and improved combustion stability.
6. Different dynamic behaviours have been observed in each system due to the different initial conditions of hydrogen-hydrocarbon mixtures. In other words, the initial pressure, temperature, mixture and system have a vivid effect on the burning velocity, the flame speed, pollutant emissions, auto-ignition and flame stability.

CHAPTER III: RESEARCH METHODOLODY

3.1. Introduction

In this chapter, the methodology of the research is discussed. The research utilized a quantitative methodology. The main purpose of this study is to investigate pre-mixed-mixture flame propagation in confined tee pipelines and identify the associated risks for systems. For this study, different concentrations of pre-mixed mixtures were exploded to evaluate the maximum overpressure, rate of pressure rise, flame speed, blast wave, Lewis number and unburnt gas velocity in tee pipelines. Consequently, the effectiveness of ignition positions and tee junction positions have been considered in this research.

3.2. Test Operation Location

The experiments were carried out in building N06a, which was designed for medium-scale gas explosion tests, at the University of Technology (UTM) in Skudai, Malaysia. To ensure the safety of the experiment, the experimental rig was stablished in a semi-confined area following the safety procedures of UTM and Malaysian safety law (Act 1994 and FMA 1967), as presented in Figure 3.1.

Figure 3. 1 Actual pictures of tee pipes configuration

3.3. Primary Preparation of Equipment

Initially, preparation of the equipment and mixtures was completed before the start of the actual tests on explosion properties. Some of the preparation includes the rig installation, which involved the setup of the piping system, installation of additional fittings and the igniter switch system, setting the sensor and data collection system and preparing the mixture pressure at different concentrations. Knowledge about the equipment, understanding the important theories to be referred to and purchasing skill were vital in making sure this research study started and finished smoothly. Moreover, before the actual data collection period, a pilot study was conducted to assess the validity of the research instruments.

On the other hand, the non-experimental variables that affect the dependent variable were checked in this research. Variables such as initial pressure, temperature and amount of mixture, which all affect the dependent variables, were controlled. In this study, the effect of the initial mixture on flame propagation was investigated to evaluate the maximum overpressure, rate of pressure rise, flame speed, blast wave, Lewis number and unburnt gas velocity after explosion in pipelines.

3.4. Experimental Setup

Tee pipe rig configurations consisting of 4.12 m horizontal and 1.275 m junction lengths, with an 0.1 m initial diameter were set up as shown in Figure 3.1. The pipes had several segments ranging from 0.5 to 1 m in length, bolted together with a gasket seal in-between the connections and blind flanges at both ends by fallowing an ASTM Standard with a Schedule 40 pipe. Moreover, a digital pressure gauge with accuracy ±0.001 bar was used to monitor the initial mixtures. The full details of the experimental setup are listed in Table 3.1.

Table 3. 1 Details of the experimental rig

Internal diameter (m)	0.1
Length (m):	
- Long in horizontal (normal) (m)	4.12
- Long in junction (normal) (m)	1.275
Wall thickness (m)	0.005
Design pressure (bar)	20
Flanges	
Flange thickness (m)	0.05
Number of bolts on each two flanges	8
Bolt-hole diameters (m)	0.042
Bolt-hole PCD (m)	0.67
Diameter of bolts (m)	0.038
Assembled test-vessel	
Length-to-diameter ratio(L/D)	53.95
Volume (m^3)	0.042

Measurements of flame speed and overpressure were recorded from the pipe using an array of exposed junction, mineral insulated, type-k thermocouples (CHAL OMEGA, with accuracy ±0.001s) and piezoresistive pressure transducers (Keller series 11, with accuracy ±0.001s), respectively, positioned along the centre line (as presented in Figure 3.2 and Table 3.2). The data generated were collected using a 34-channel transient data recorder by NI Compact DAQ (NI 9220, 100 kS/s per channel sample rate). An ignition source and vacuum pump (VACUUBRAND RE 2.5) were also used in the research. More discussion about the application of the equipment is included in Sections 3.6 and 3.7.

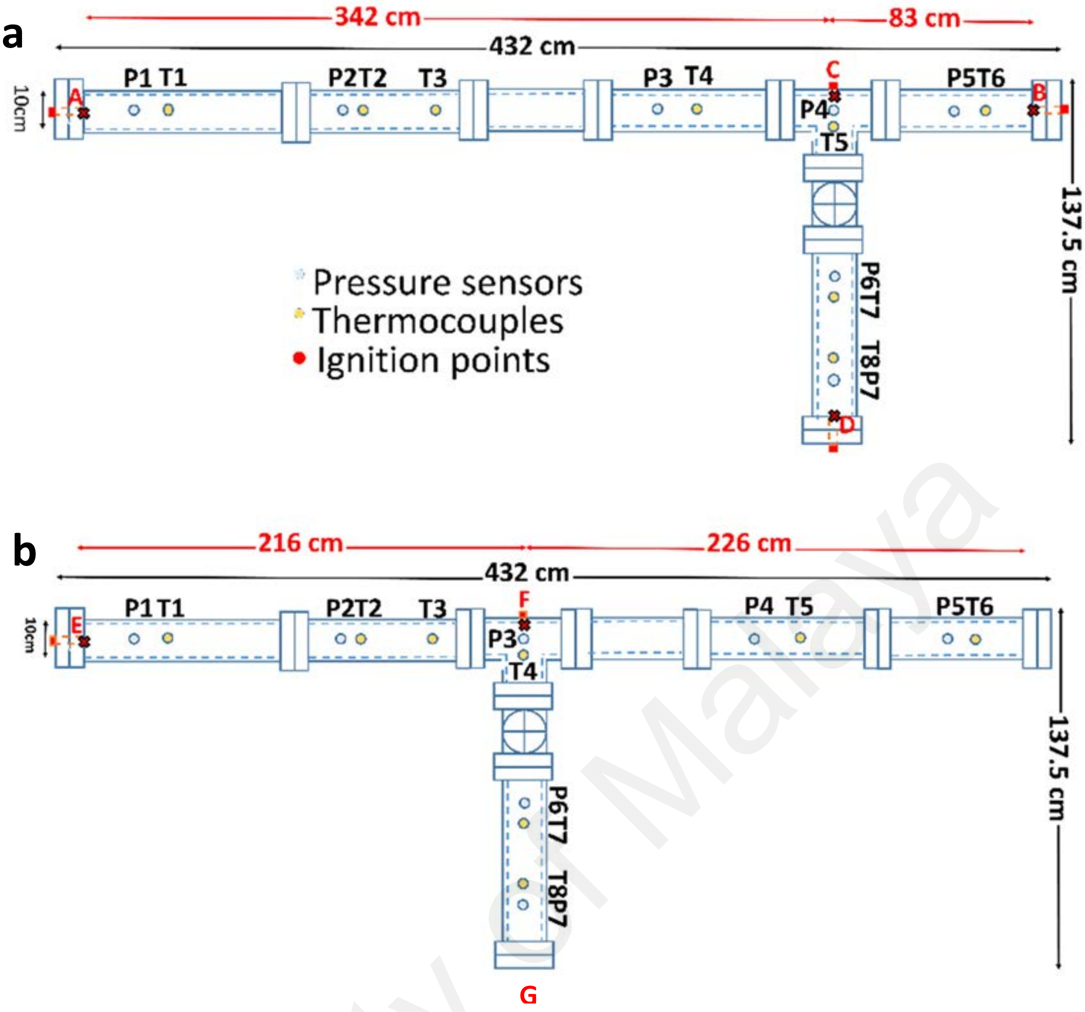

Figure 3. 2 Tee pipes configuration

3.5. Mixtures Preparation

Mixtures of C_2H_4/air, NG/air, C_3H_8/air, H_2/air, C_2H_4-H_2/air, NG-H_2/air, C_3H_8-H_2/air and H_2-inhibitors/air (in wide range of concentrations) were applied and prepared using a partial pressure method, with an accuracy of 0.1 mbar (0.01% of the composition) at normal temperature and pressure (NTP) conditions. Mathematically, the total initial pressure of the fuel gases mixture can be defined as:

$$P_{total} = P_1 + P_2 + ...P_n \qquad \text{(Eq. 3.1)}$$

where P_1, P_2, ..., P_n represent the partial pressures of each component. It should be mentioned that the overall pressure of pipeline must not be more than 1 atm (equal to 0 bar) at the NTP condition. Therefore, it was assumed that the initial pressure of the pipeline before inserting the fuel gases was -0.5 bar using vacuum pump.

3.5.1. Single Gases

For single gases (C_2H_4/air, NG/air, C_3H_8/air and H_2/air), five equivalence ratios (φ=0.6, 0.8, 1.0, 1.2 and 1.4) were considered. For more clarification on the preparation of single mixtures, an example on the preparation of hydrogen/air mixtures described as:

$$2H_2+O_2 \rightarrow 2H_2O \qquad (3.1)$$

As shown in reaction 3.1, the stoichiometric ratio of hydrogen for 1 mole oxygen is 2 moles. Consequently, as shown below, since the stoichiometric concentration of hydrogen based on the constant volume is equal to 30%, the initial injected hydrogen into the system was 180 mbar at equivalence ratios of 0.6 by considering equation of stoichiometric (Eq. 3.2) at normal pressure and temperature condition.

$$\phi = \frac{\left(\frac{nH_2}{nO_2}\right)_{\text{stoichiome tric concentrat ion}}}{\left(\frac{nH_2}{nO_2}\right)_{\text{stoichiome tric}}} \text{ (Lee et al., 2000)} \qquad \text{(Eq. 3.2)}$$

$$0.6 = \frac{\left(\frac{1H_2}{0.5O_2}\right)}{0.3\left(\frac{nH_2}{0.5O_2}\right)} \rightarrow nH_2 = 0.18mole$$

Based on Daltown's law, the initial pressure (P_{in}) is in proportion with initial mole fraction for ideal gases. Therefore:

$$P_{in} = 0.18bar = 180mbar$$

Consequently, the initial hydrogen injected into the system was 240, 300, 360 and 420 mbars at equivalence ratios of 0.8, 1.0, 1.2 and 1.4, respectively. The same phenomenon applied to other mixtures by considering the stoichiometric concentrations of C_2H_4, NG and C_3H_8 is 6.5%, 8% and 4%, respectively.

3.5.2. Hydrocarbon-Hydrogen/Air and Hydrogen-Inhibitors/Air Mixtures

Mixtures of C_2H_4-H_2/air, NG-H_2/air and C_3H_8-H_2/air in wide ratio ranges (90:10, 70:30, 50:50, 30:70 and 10:90) were applied by considering hydrocarbon fuels as the primary fuel at their stoichiometric concentration. Moreover, H_2-Ar/air, H_2-CO_2/air, H_2-N_2/air, H_2-Ar-CO_2/air, H_2-Ar-N_2/air and H_2-N_2-CO_2/air mixtures with a constant ratio (95:5=H_2:inhibitors) were used at a stoichiometric equivalence ratio ($\phi=1$) by considering hydrogen as the primary gas.

For more clarification, the preparation of 90%NG-10%H_2/air is described as follows:

Since the stoichiometric concentration of the primary gas (NG) is 8% v/v, the initial pressure at stoichiometric ratio for this particular gas is 80 mbars at the NTP condition (for more clarification refer to Section 3.5.1). Consequently, when applying the 90%NG-10%H_2/air mixture, 72 mbars NG and 8 mbars H_2 must be injected into the system.

3.6. Experiment Procedure

As a first step, a check-list operation (Appendix A) was done to ensure leakages were not present in the pipes during the tests. Moreover, all gases were initially stored in different storage tanks and kept at higher pressures to create a pressure difference to facilitate gas flow from the tank into the vessel using the partial pressure method, with an accuracy of 0.1 mbar (0.01% of the composition) at different concentrations. It should be mentioned that the overall pressure of the pipeline must not be more than 1 atm so we can assume the partial pressure of pipeline can be -0.5 bar using vacuum pump (more clarification is given in Section 3.5). The injected gases were left for 10 minutes in each run to achieve a homogeneous composition. This method of mixture preparation ensured complete mixing, as the initial vacuum condition rapidly dispersed the fuel added and the subsequent addition of air was still at very low pressure, which together with the turbulence from the air injection ensured rapid mixing.

In the next step, the flammable mixtures were ignited by an electrical spark, which gave energy of 16 J at six ignition positions (A-F) for the gas explosion tests, separately. It should be noticed that in previous investigations on the flame propagation of fuels (Hassan et al., 2012; Kolbe & Baker, 2005; Phylaktou, 1993) in tee pipes, the tee junction was placed in the central part of the horizontal pipe (such as Figure 3.2b at G point). This showed that if the ignition happens in the G point, the flames propagate almost symmetrically along both sides of horizontal part. Consequently, the ignition point at the tee junction for the second configuration (Figure 3.2b) was not used in the current research. The ignition positions and location of each sensor are presented in Figure 3.2 and Table 3.2. Moreover, each explosion was repeated at least three times for accuracy and reproducibility.

Table 3. 2 Position of each pressure transducer and thermocouple from ignition points

		Ignition Position (m)					
		A	**B**	**C**	**D**	**E**	**F**
Pressure transducers	**P1**	0.26	3.99	3.2.2	4.45	0.26	1.9
	P2	1.18	3.07	0.23	3.53	1.18	0.98
	P3	2.53	1.72	0.95	2.18	2.16	0.06
	P4	3.42	0.83	0.06	1.29	3.08	0.92
	P5	3.9	0.35	0.54	1.77	4.07	1.91
	P6	4.03	1.44	0.67	0.6.	2.77	0.67
	P7	4.52	1.93	1.16	0.19	3.26	1.16
Thermocouples	**T1**	0.45	3.84	3.09	4.25	0.45	1.51
	T2	1.26	3.03	2.28	3.44	1.26	0.7
	T3	1.65	2.64	1.89	3.05	1.65	0.31
	T4	2.75	1.54	0.79	1.95	2.06	0.12
	T5	3.42	0.87	0.12	1.23	3.13	1.17
	T6	3.99	0.26	0.69	1.85	3.9	1.94
	T7	4.12	1.54	0.79	0.56	2.73	0.79
	T8	4.38	1.8	1.05	0.3	2.99	1.05

The circuit diagram before ignition included various safety interlocks including:

- A gate valve used to fully confine the pipe during the mixture preparation had to be closed before ignition.
- The mixture inlet line and pumping line had to be disconnected from the test vessel. This effectively meant the fuel supply was isolated before ignition.

Finally, the data generated were collected using a 34-channel transient data recorder by NI Compact DAQ. The collected data was transferred to the operation computer using Signal Express software.

To make the experimental rig ready for the next round of experiments, the vacuum pump was re-connected to the system and turned on for 15 minutes to ensure the system was cleaned of combustion products.

3.6.1. Nitrogen Purging System

In some cases, the fuel-air mixtures were not ignited due to failures that may be associated with the ignition spark plug, an electrical fault in the ignition circuit or the sediment of exhausts in the system, which led to a relatively large volume of explosive mixture remaining inside the test vessel. Consequently, the experimental rig needed to be purged of the gas mixtures before any repairs could be made. One of the methods was to use a 'nitrogen purging system' in which high-pressure nitrogen was injected into the system and the gate valve left open to release the mixtures and exhaust to the atmosphere outside. Afterwards, the vacuum pump was turned on for 20 minutes to purge the system and safely release the leftover gases and exhaust to the atmosphere.

3.7. Method of Calculations for Required Parameters

3.7.1. Flame Speed

Measurements of flame speed were recorded from the pipe using an array of exposed junction, mineral insulated, type-k thermocouples positioned along the centre line. Flame-speed data were generated from the thermocouple flame arrival times (marked as an abrupt change in the thermocouple output). The flame-speed data were generated from the thermocouple flame arrival times, the time of travel between two adjacent thermocouples and the distance between them. The flame speed was plotted at the position midway between the thermocouples or, in the case of the first flame speed, the time between the spark and the arrival at the first thermocouple (Table 3.3). This technique did not measure the flame temperature as the thermocouple junction was too large (~0.5 mm), but there was no dead time and the flame was detected as a sudden increase in temperature from the near-ambient base temperature. The thermocouple flame arrival time in the pipe was taken to be the first point at which the reading started to rise. For the thermocouples in the pipe, this was hindered by a pre-compression wave ahead of the flame (and the associated high flow velocity around the thermocouple) giving rise to two distinct gradients on the thermocouple trace (Emami et al., 2013; Na'inna et al., 2015). In this case, the point at which the second (steeper) gradient became apparent was taken as the flame arrival time.

Table 3. 3 Procedure in calculating the flame speed from raw data

Flame arrival time, t	**Thermocouples positions, x**	**Flame speed**
t_0 (ignition)	X_0	----------
t_1	X_1	$(X_1-X_0)/(t_1-t_0)$
t_2	X_2	$(X_2-X_1)/(t_2-t_1)$
t_n	X_n	$(X_n-X_{n-1})/(t_n-t_{n-1})$

3.7.2. Pressure

Pressure within the pipe was monitored using an array of piezoresistive pressure transducers (Keller 11), with high sensitivity combined with stability and shock resistance, at points around the outer wall in each section, shown as P in Figure 3.2. All the pressure transducers were calibrated using a standard hydraulic dead-weight calibrator. This was performed with the transducers connected to the data acquisition system. Calibration of this integrated system eliminated any errors that might arise from the electronic circuit connecting the instrumentation to the data logging system.

3.7.3. Unburnt Gas Velocity

Equations 2.1–2.3 were used to calculate unburnt gas velocity. The details of calculation are presented in Section 2.5.3.

3.7.4. Rate of Pressure Rise

On the other hand, when considering the most critical point(s) of the pipes after explosion, the rate of pressure rise based on the deferential of maximum overpressures at reached times (dp/dt) were calculated as follows:

$$\frac{dp}{dt} = \frac{P_j - P_i}{t_j - t_i} \qquad \text{(Eq. 3.3)}$$

Where P_i and P_j are the primary and secondary maximum overpressures along the tee pipe, respectively. For instance, the rate of pressure rise at P_2 point for ignition position A is calculated as follows:

$$\frac{dp}{dt} = \frac{P_2 - P_1}{t_2 - t_1} \qquad \text{(Eq. 3.4)}$$

P1 and P2 allocation were presented in Table 3.2.

3.7.4. Lewis Number

To justify the associated maximum rate of pressure rise, the Lewis number was calculated using equations 2.5–2.7. The details of calculation are presented in Section 2.5.3.

3.8. Simulation

3.7.1. Problem Formulation and Simulation

The review showed that the theoretical and simulation analysis investigations on flame propagation of different fuel gases in tee joints are well studied (Chen-hua, 2008; CHEN et al., 2011; Fang, 1996; Ferrara et al., 2006; S. LIU et al., 2011; Muramatsu, 2004; Remennikov & Rose, 2005; Smith & Rose, 2006; Xianli, 1995; Yang et al., 2002; L.-w. ZHANG et al., 2010). Among all simulator software, ANSYS FLUENT can model the mixing and transport of fuels by solving conservation equations describing convection, diffusion and reaction sources. Multiple simultaneous chemical reactions can be modelled, with reactions occurring in the bulk phase (volumetric reactions) and/or on the wall or particle surfaces, and in the porous region. Consequently, for investigating the capability of ANSYS FLUENT software on flame acceleration of the fuels in medium-scale piping size, the combustion of the hydrogen/air and hydrocarbon/air mixtures at the three most critical ignition points in tee pipes, which were consistent in the experimental rig and initial conditions, were applied for simulation.

.

3.7.2. Software

The software used in this study was ANSYS FLUENT15. It has a capability for modelling fluid flow, heat transfer, and chemical reactions of hydrocarbons/air and hydrogen/air combustion in pipelines as well as other combustor systems that suits the purpose of this study. It provides complete mesh flexibility, including the ability to solve flow problems using structured mesh and also using adaption in meshing during the calculation in simulation, which can generate complex hydrogen combustion.

3.7.3. Computer Workstation

The simulation was carried out in the Process Safety and Risk Assessment laboratory, on a computer with CORE i7 4820K (4C/8T) CPU and DDR3 RAM 16G.

3.7.4. Geometry and Mesh

Simulation was conducted in 2D Cartesian dimensions, where the size of tee pipe was similar to the experimental rig. Moreover, quadrilateral meshing size was used, with mapped face meshing. For increasing the accuracy of FLUENT's prediction, a different grid size was adopted. However, by comparing different meshing size, 1×1 mm gave a reasonable prediction on explosion properties, therefore, it was used in simulations. Moreover, during the solution, the 'adaption meshing size' was carried out to find the independent mesh sizing influence on the results (Figure 3.2).

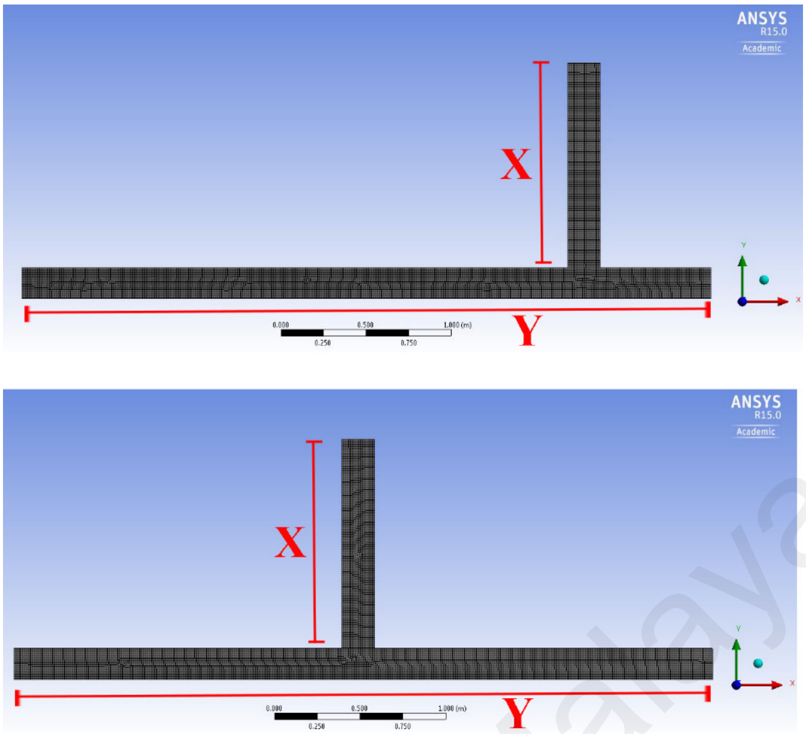

Figure 3. 3 Meshing in Ansys

3.7.5. Boundary and initial conditions

To define a problem that results in a unique solution, the dependent variables including fluxes of mass, momentum and energy, etc., must be specified at the domain boundaries.

FLUENT predicts the local mass fraction of each species, Y_i, through the solution of a convection-diffusion equation for the i^{th} species using the following conservation equation:

$$\frac{\partial}{\partial t}(\rho Y_i) + \nabla.\left(\rho\vec{\vartheta}Y_i\right) = -\nabla.\vec{J_i} + R_i + S_i \qquad \text{(Eq. 3.2)}$$

where R_i is the net rate of production of species i by chemical reaction (described later in this section) and S_i is the rate of creation by addition from the dispersed phase plus any user-defined sources. It is noticeable that this form of equation is solving N-1 species where N is the total number of fluid phase chemical species present in the system.

Consequently, the Nth mass fraction is determined as one minus the sum of the N-1 solved mass fractions since the mass fraction of the species must sum to unity.

On the other hand, two-equation models are the simplest complete models of turbulence in FLUENT which allows the turbulent velocity and length scales to be independently determined. The standard $k-\epsilon$ model is also classified in this class of turbulence model and has become the workhorse of practical engineering flow calculations in the time since it was proposed by Launder and Spalding. Based on well-known the strengths and weaknesses of the standard $k-\epsilon$ model, the RNG $k-\epsilon$ and the realizable $k-\epsilon$ models also add up to software to improve its performance. Based on model transport equations, the standard $k-\epsilon$ model is a semi-empirical model for the turbulence kinetic energy (k) and its dissipation rate (ϵ) which are obtained from the following transport equations:

$$\frac{\partial}{\partial t}(\rho k)+\frac{\partial}{\partial x_i}(\rho k u_i)=\frac{\partial}{\partial x_j}\left[\left(\mu+\frac{\mu_t}{\partial k}\right)\frac{\partial k}{\partial x_j}\right]+G_k+G_b-\rho\epsilon-Y_M+S_k \qquad \text{(Eq. 3.3)}$$

And,

$$\frac{\partial}{\partial t}(\rho t)+\frac{\partial}{\partial x_i}(\rho\epsilon u_i)=\frac{\partial}{\partial x_j}\left[\left(\mu+\frac{\mu_t}{\partial \epsilon}\right)\frac{\partial \epsilon}{\partial x_j}\right]+c_{1\epsilon}\frac{\epsilon}{k}(G_k+G_b C_{3\epsilon})-C_{2\epsilon\rho}\frac{\epsilon^2}{k}+S_\epsilon \qquad \text{(Eq. 3.4)}$$

In these equations,

G_k : represents the generation of turbulence kinetic energy due to the mean velocity gradients.

G_b : is the generation of turbulence kinetic energy due to buoyancy.

Y_M : represents the contribution of the fluctuating dilatation in compressible turbulence to the overall dissipation rate.

$C_{1\epsilon}$, $C_{2\epsilon}$ and $C_{3\epsilon}$ are constants σ_k and σ_ϵ and are the turbulent Prandtl numbers for k and ϵ , respectively $S_k$and S_ϵ are user-defined source terms.

In turbulent flows, FLUENT computes the mass diffusion in the following form:

$$\vec{J_i} = -(\rho D_{i,m} + \frac{\mu_t}{\rho D_t})\nabla Y_i \qquad \text{(Eq. 3.5)}$$

where Sc_t is the turbulent Schmidt number ($\frac{\mu_t}{\rho D_t}$) where μ_t is the turbulent viscosity and D_t is the turbulent diffusivity). The default $Sc_t$is 0.7 Note that turbulent diffusion generally forces laminar diffusion and the specification of detailed laminar diffusion properties in turbulent flows is generally not warranted.

Defining boundary conditions involves: identifying the location of the boundaries (e.g., inlets, walls, symmetry) and supplying information at the boundaries that have been discussed in following sections:

3.7.5.1.Boundary conditions at inlet

The boundary conditions set at the inlet plane were as follows: k epsilon module with turbulent intensity equal to 5%, 300 ^{o}K as input temperature and species mass fraction on the basis of stoichiometric concentration ratio and active the ‘Spark’ in central point of inlets with 16 j energy.

3.7.5.2.Wall boundary conditions

The thermal boundary condition was set at a fixed heat flux of zero (adiabatic condition), while the walls were not moving. The no slip conditions were prescribed for the wall shear stress. The treatment of the boundary conditions concerned with turbulent flows was the same as for laminar flows except in the case of walls.

3.7.5.3.Standard wall functions

In the part of the flow near to walls there exist regions in which the local Reynolds number of turbulence (Eq. 3.6) is so small that the viscous effects become more significant than the turbulent ones. In this viscous sublayer very steep gradients occur; so for accurate modeling many grid points were applied in this region. However, it is not necessary to discretize the k and ϵ conservation equations over this region as there exist suitable laws, called law-of-the-wall which relates the wall conditions to values of the dependent variables just outside the viscous sublayer.

$$Re_t = k^2/(\vartheta\epsilon) \qquad \text{(Eq. 3.6)}$$

3.9. Summarize of Research Frame Work

All carried out steps in current research are summarized in Figure 3.4.

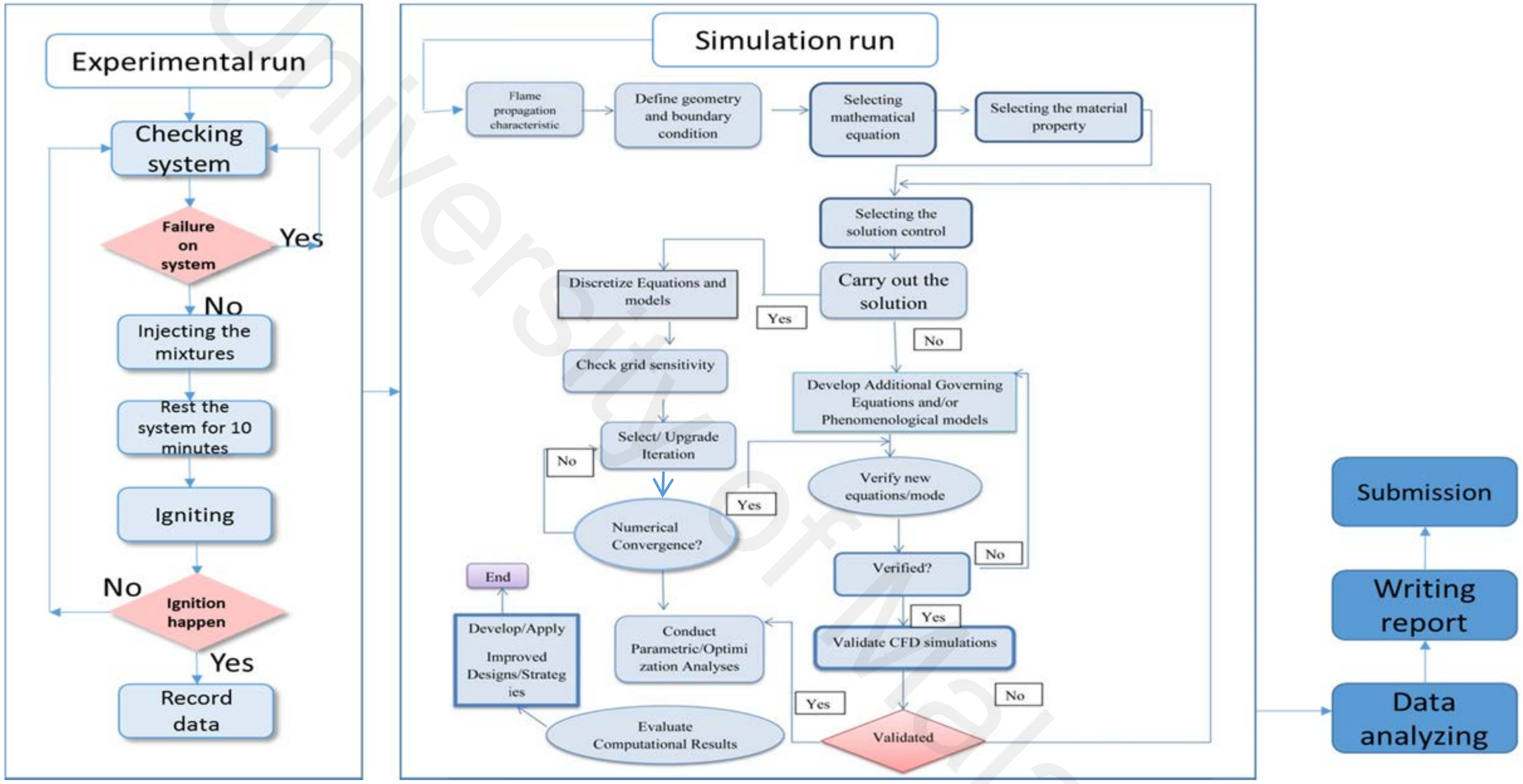

Figure 3. 4 Summarized of research frame work

CHAPTER IV: RESULTS AND DISCUSSIONS

4.1. Introduction

As mentioned earlier, in order to ensure that better precautions are taken in relation to pipeline gas carriers, it is essential to fully characterize and quantify their explosion mechanisms. In particular, knowledge is required about the maximum pressure, the maximum rate of pressure rise and the flame speed, which are among the most important parameters for the assessment of process hazards and the safe design of process equipment (Hawkes & Chen, 2004; Salzano et al., 2012). However, what has been lacking is a comprehensive study of the governing parameters involved in flame propagation in different configurations, by considering the physics and dynamics of the flame and pressure development of fuels-air mixtures in a wide range of concentration. For this reason, the physics and dynamics of explosion development of applied mixtures in two different Tee pipe configurations are discussed in this chapter with respecting the Tee junction and ignition positions.

This chapter has been divided into four main sections (4.2-4.5). In section 4.2, the flame acceleration of hydrocarbons/air and hydrogen/air mixtures, as reference mixtures, in the tee pipes are discussed. Moreover, for giving detailed and comprehensive discussion about flame development of hydrocarbons/air and hydrogen/air mixtures in tee pipes, the obtained data has been compared with associated data from the straight and 90 degree pipes with similar initial conditions from the literature (Sulaiman, 2015). The pipes configuration and details of recorded points in straight and 90 degree pipe configurations are presented in Figure 4.1 and Table 4.1.

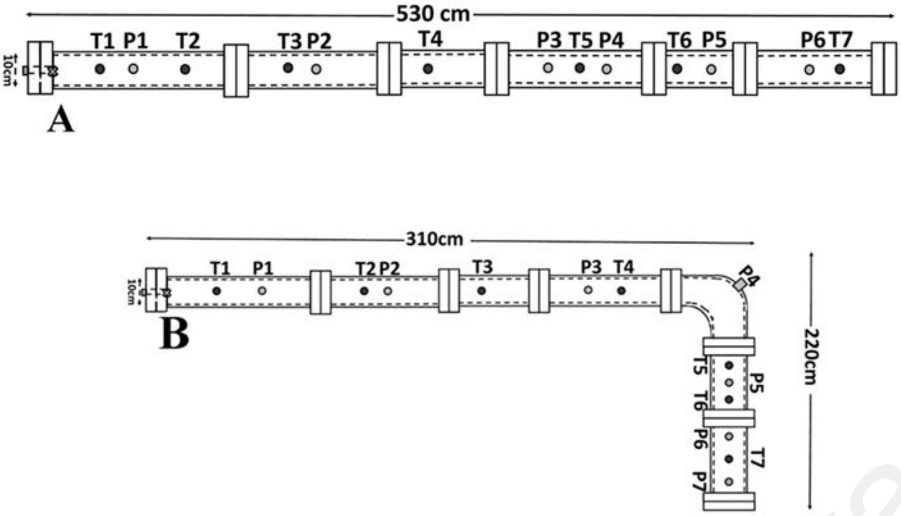

Figure 4. 1 Scheme of pipes: (a) straight; (b) 90-degree (Sulaiman, 2015)

Table 4. 1 Position of each pressure transducer and thermocouple from the ignition points (Sulaiman, 2015)

		Ignition Position	
		straight	**90 degree**
Pressure transducers	**P1**	0.32	0.32
	P2	1.35	1.35
	P3	2.02	2.02
	P4	2.58	2.58
	P5	3.33	3.33
	P6	4.16	4.16
	P7	------	4.44
Thermocouples	**T1**	0.26	0.26
	T2	0.705	0.75
	T3	1.065	1.61
	T4	1.485	2.17
	T5	2.14	2.62
	T6	3.2	3.48
	T7	4.345	4.26

In the next section (4.3), the flame acceleration of hydrocarbons-hydrogen/air mixtures in the tee pipes have been analyzed with different ignition positions. Continuously, the findings on effectiveness of inhibitors on flame acceleration of hydrogen in Tee pipes are presented in section 4.4. Finally, the flame acceleration of hydrocarbons/air and hydrogen/air mixtures in experimental study have been compared with simulated results from FLUENT 15 software at four ignition positions.

4.2. Flame acceleration of hydrocarbons/air and hydrogen/air

4.2.1. The effect of maximum overpressure on the pipe configuration

Figures 4.2 and 4.3 illustrate the recorded maximum overpressures for all hydrocarbons/air and hydrogen/air fuels at straight, 90 degree and tee pipe configurations. The pressure traces are presented with respect to times. For hydrocarbon explosions, typical explosion profiles are shown, giving a highest maximum pressure value at the bending region when ignited at the rear positions. From the hydrogen-air pressure results, it was found that the maximum overpressure of a hydrogen explosion is greater than that of hydrocarbon fuels: twice as high for all pipe configurations. Surprisingly, the maximum pressure of hydrogen-air mixtures experienced its highest value (~7.2 bars) at the bending region, rather than the tee junction position for both the longer obstacles position and the equal distance position (2.22 bars and 2.67 bars, respectively).

From previous investigations, the burning area was found to increase when the flame front travelled through the 90-degree bend (Clanet & Searby, 1996b; Zhou et al., 2006). Consequently, the flame speed also increases, thus giving a higher overpressure when compared to similar experiments carried out in a straight pipe and tee junction (Blanchard et al., 2010; Cheng et al., 2009; Emami et al., 2013; Phylaktou et al., 1993). Figure 3d shows the overpressure development along the pipe at different positions for hydrogen-air mixture. It is clearly shown that the two overpressure peaks were observed at two different positions—first, at the bending position, and second, near the end wall (0.9 m from the pipe's end wall)—for the 90-degree pipe explosions. There is no doubt that the first pressure rise is due to the influence of an obstacle: in this case, the presence of the 90-degree bend in the closed pipe. Strong reflection and diffraction acoustic/shock waves enter into the reaction zone, enhancing the burning rate and increasing the flame speed. This phenomenon causes the overpressure to increase by about 7.2 barg (at an equivalence ratio of 1). It is a known fact that the presence of an obstacle in the pipe will randomize the flow, thus increasing the flame speed and overpressure when compared to the straight pipe/tube (Phylaktou et al., 1993). However, in a closed pipe/tube, the end wall also acts as an obstacle with a propensity to initiate flame perturbation, and hence, affect the explosion behaviour (Liberman et al., 2010; Thomas et al., 2010; Zhu et al., 2012). Figure 4.2a also shows the pressure development as influenced by the distance from the ignition position, for ethylene-air mixture in straight and 90 degree pipes. It shows that the pressure decayed after the bending position, which is inconsistent with other fuel explosion profiles. For propane and natural gas (NG) explosions, the pressure rose after the bend/obstacle, whether in the 90-degree or tee pipes. It is suspected that the quenching effect of the preferential-diffusion mechanism promoted the flame dissipation at the pipe wall, giving a lower overall adiabatic temperature inside the pipe. According to Aung et al. (2002), the turbulent flame propagation decreases progressively with the increase of the preferential-diffusion region. The preferential-diffusion concept is relative to the flame-stretch interaction. Thus, it can be suggested that, when the preferential-diffusion effect is apparent, it tends to retard the flame distortion through excessive flame stretching and causes the flame to partially quench (Bradley et al., 2008). Due to the various flame instability mechanisms involved in the flame propagation (e.g., hydrodynamic instability, thermal diffusion, Darrieus-Landau), turbulent flame also develops as a result of interactions between the flame front and the acoustic waves (Bradley et al., 2008; Ciccarelli & Dorofeev, 2008; Gamezo et al., 2008; Liberman et al., 2010). However, the findings confirm that the maximum overpressure attained at the bending position for most fuels (except for propane and NG) are as shown in Figure 4.2. This inconsistent trend can be explained based on fuel reactivity itself. The diffusivity of propane is significantly smaller than its thermal conductivity, allowing the fuel to be preferentially heated more rapidly at the preheated zone (Aspden et al., 2011). For propane, the highest maximum pressure was observed at x = 2.02 m (P3), before the 90-degree bend position shown in Figure 4.2c. At the same time, the acoustic/shock wave—which was diffracted and reflected due to the bending effect—travelled back toward the hot flames to amplify the burning rate. Due to the slower burning rate and heat losses to the wall, the flame tends to quench after point P3. However, a second acceleration was observed at a distance of 4.16 m from the ignition position (P5), due to the end wall's effect relative to the flame-reflective wave interaction. For NG-air mixtures, the pressure at P3 was approximately 0.41 barg, as exhibited in Figure 4.2b. The second peak overpressure was shown to be located at P5 (after the bending position), due to the flame-wave interaction, which was comparable to the other fuels. This could suggest that the effect of bending was more pronounced in the NG-air explosions. As expected, the methane-air mixture exhibited the lowest pressure development along the pipe, because of its lower reactivity behaviour.

The results clearly show that, in the straight pipe, the trend is consistent for all fuels, with the maximum overpressure occurring at a distance of x = 2.02 m (P3) from the ignition position (Figure 4.2). The associated maximum overpressure, resulting from the highest burning rate, is due to the flame cellularity/wrinkling, i.e., the distortion of the flame surface increasing the flame area and, hence, enhancing the burning velocity. In this instance, the tulip formation attenuates the turbulence, due to its vortex creation, and the reflective wave promotes a strong interaction between the fast flame and turbulence which increases the flame speed, followed by a pressure rise. However, at x > 2.02 m (P4 onwards), the trend was inconsistent for reactive fuels. For instance, hydrogen-air gave a gradual pressure development, yet there were no similar observations for ethylene-air, propane-air or methane-air explosions, which displayed an abrupt pressure drop to around two to five times lower than the overpressure at x = 2.02 m. This inconsistent trend can be related to the nature of fuel reactivity. This will be discussed further in the next section.

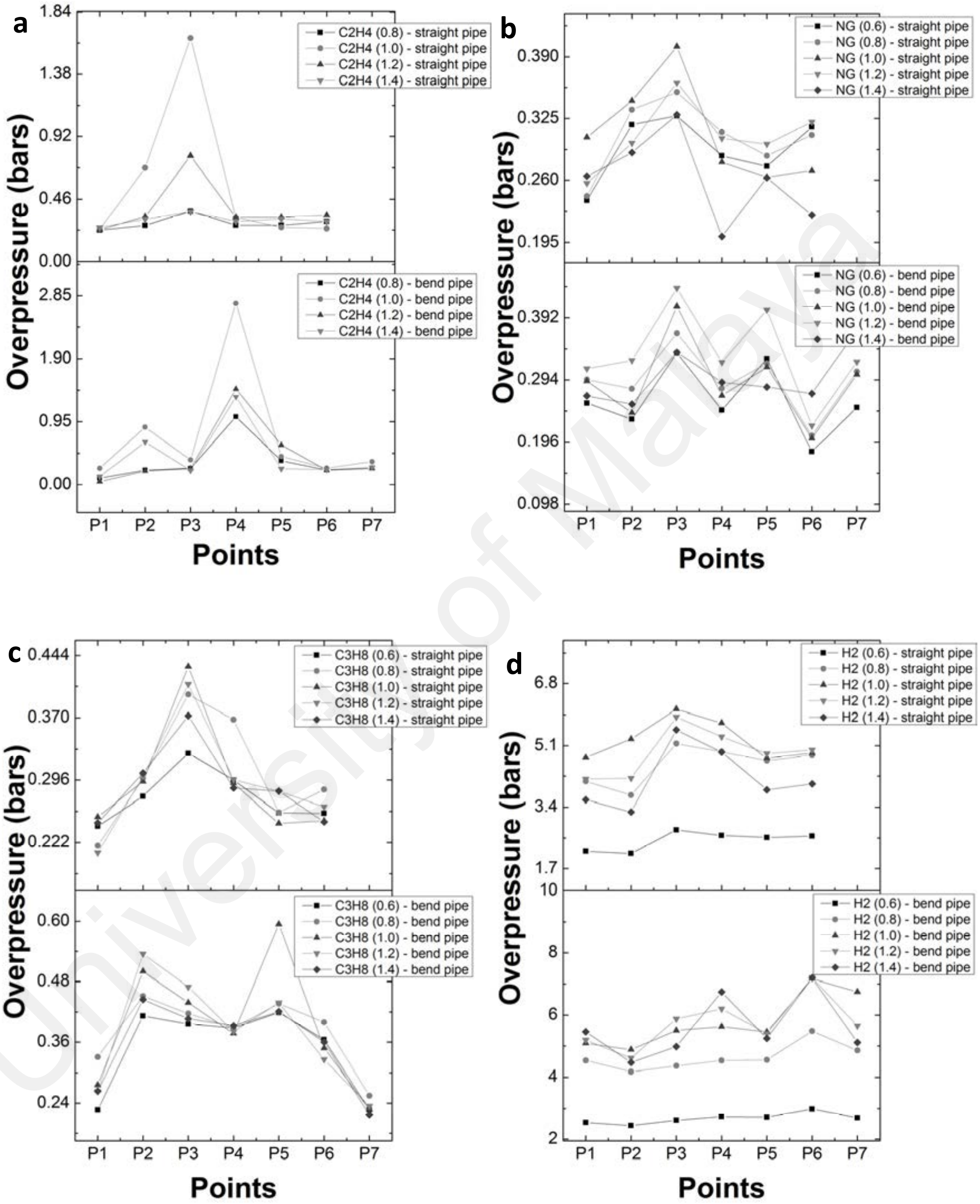

Figure 4. 2 Maximum overpressure vs. the recorded points in straight and 90 degree pipes (Sulaiman, 2015)

Within the examined range of hydrocarbons-air and hydrogen-air concentrations, the value of the maximum overpressure was almost the same for both tee pipe configurations

(Figure 3.1 a and b), only it was attained at different locations. As Figure 4.3 shows, the highest overpressure for hydrogen-air mixture was observed at the tee junction region (P7) for the Figure 3.1a configuration, whereas P5 gave the maximum peak pressure for another tee pipe (Figure 3.1b). As seen, the propagated flames in both tee pipes experienced a higher acceleration rate after the tee region, leading to a higher pressure at the pipe end, by considering ignition A and E as the reference points. As mentioned earlier, the flames for the various mixtures were susceptible to flame wrinkling, particularly for the more reactive fuels, due to the diffusional-thermal instability effect. Consequently, this wrinkled flame causes an increase in the mass burning rate, giving a higher overall flame speed and overpressure intensity (Kim et al., 2014).

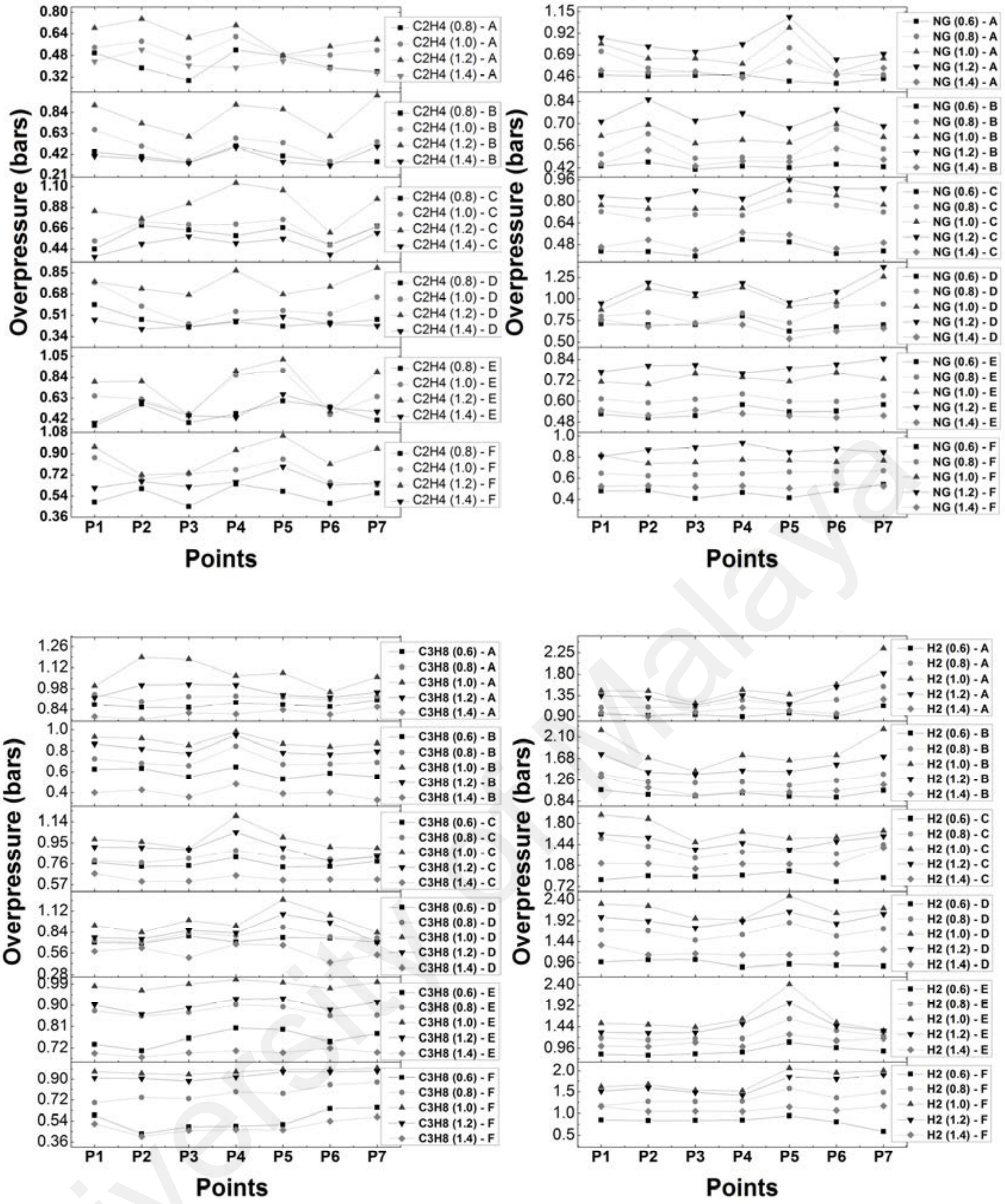

Figure 4. 3 Maximum overpressure vs. the recorded points in tee pipes

Giving attention into overpressure trends of all mixtures in all configurations, it can be found that the maximum overpressures of all mixtures were recorded at their stoichiometric concentration ratio while it was recorded at equivalence ratio 1.2 for C_2H_4/air mixture. It is due to this fact that flame reactivity of the mixtures at the mentioned equivalence ratio range is higher than lean concentrations (ϕ<1 and ϕ>1.2).

This statement is also in agreement with previous research studies (Hjertager et al., 1988; Lewis et al., 2012)

From Figure 4.4d, we can see that it took a shorter amount of time for the hydrogen flames to reach the maximum overpressure, towards the end pipe, giving a net result of a higher pressure rise and higher flame speeds when the explosion occurred inside the pipe Figure 3.1a configuration. On the other hand, when the mixtures were exploded inside the tee pipe Figure 3.1b configuration, the flame propagation of this particular mixture was inconsistent with the others. The appearance of multiple peak overpressures indicates that, at a shorter distance between the ignition point and obstacles, the flame experiences a strong interaction with the transverse pressure waves from the tee junction effect, inducing more turbulence and, consequently, attenuating the acceleration of the burning of the unreacted mixtures, which were trapped along the tee junction region. This, again, will increase the combustion rate and thus increase the flame speed and overpressure. The findings of this study are in good agreement with previous studies (Kim et al., 2014). It appears that hydrocarbons-air flames have the most minimal fluctuations along the tee pipes, both in terms of overpressure and flame speed (Figures 4.2-4.5). However, the relationship between the overall maximum pressure and its explosion severity in both tee pipe configurations, can be substantiated by the unburned gas velocity’s Sg profile, as shown in Figure 4.6. The Sg for both the tee pipe configurations was at an average of 208.18 m/s, indicating that there is no possibility of these particular gases presenting shock waves since their overdriven detonations were not strong enough (Blanchard et al., 2011). This statement is also in agreement with previous investigations of the flame acceleration of hydrocarbon fuels (Cho & He, 2007; Kumar et al., 2007; Movileanu et al., 2011a, 2011b; Prince & Williams, 2012). Moreover, the plotted blast waves of the flames at multiple locations (given in Figure 4.7) also suggest a linearity of flame acceleration for the hydrocarbons-air fuels in tee pipes. It is interesting to note that the duration of flame acceleration, the flame direction and the initial ignition points all depended on the tee junction placement along the pipe length, as this gives a different overall profile to the flame acceleration mechanism in general.

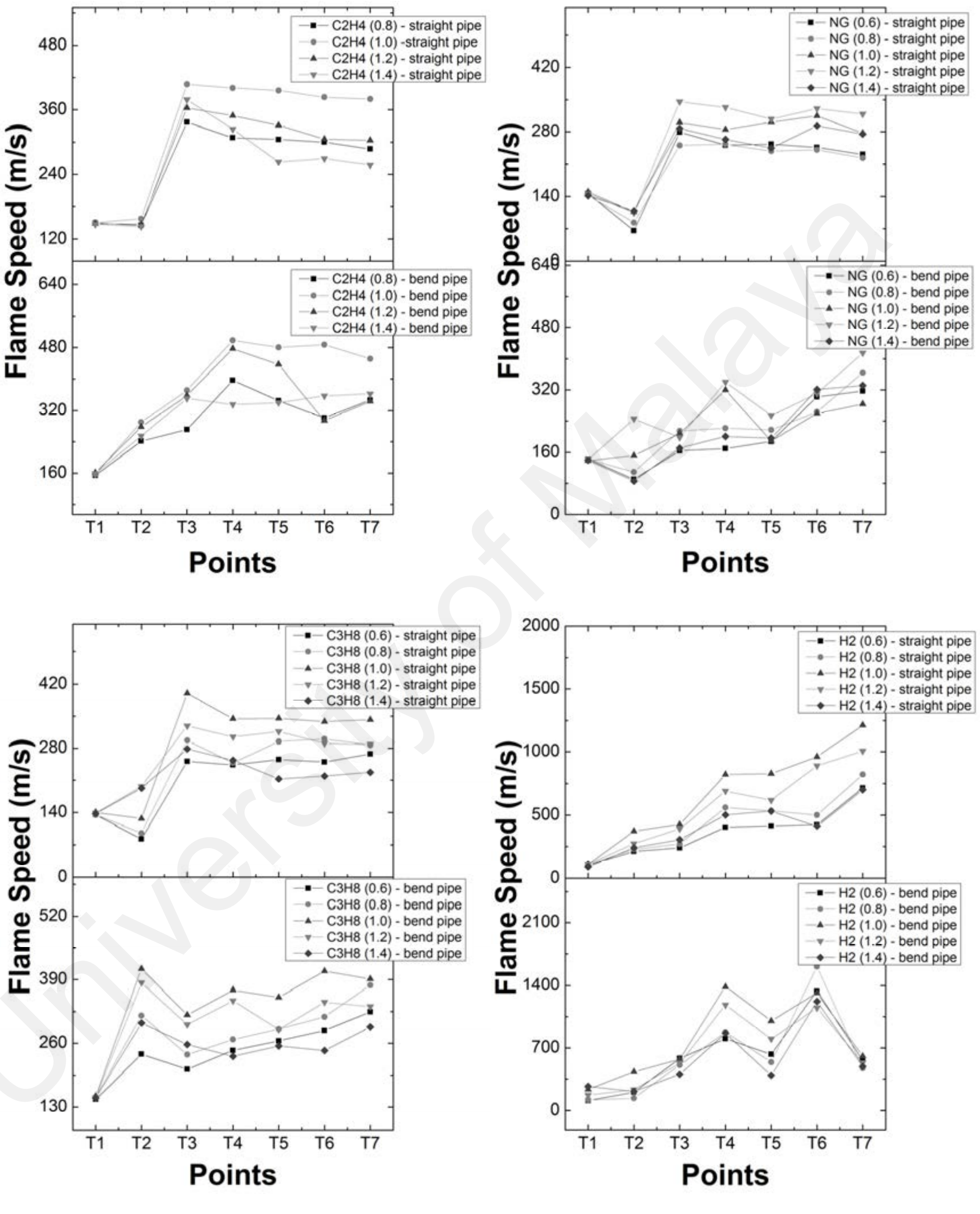

Figure 4. 4 Maximum flame speed vs. the recorded points in straight and 90 degree pipes (Sulaiman, 2015)

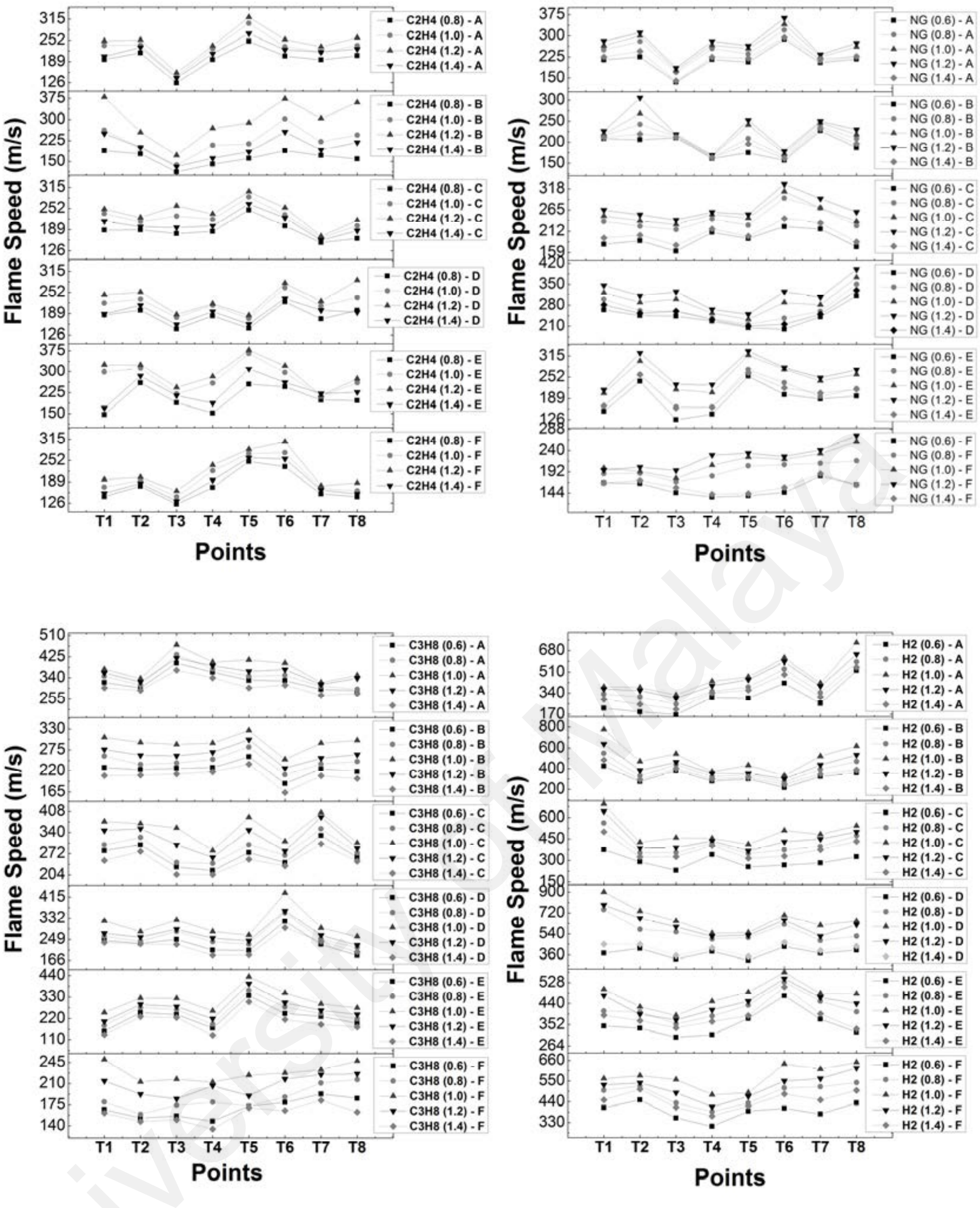

Figure 4. 5 Maximum flame speed vs. the recorded points in tee pipes

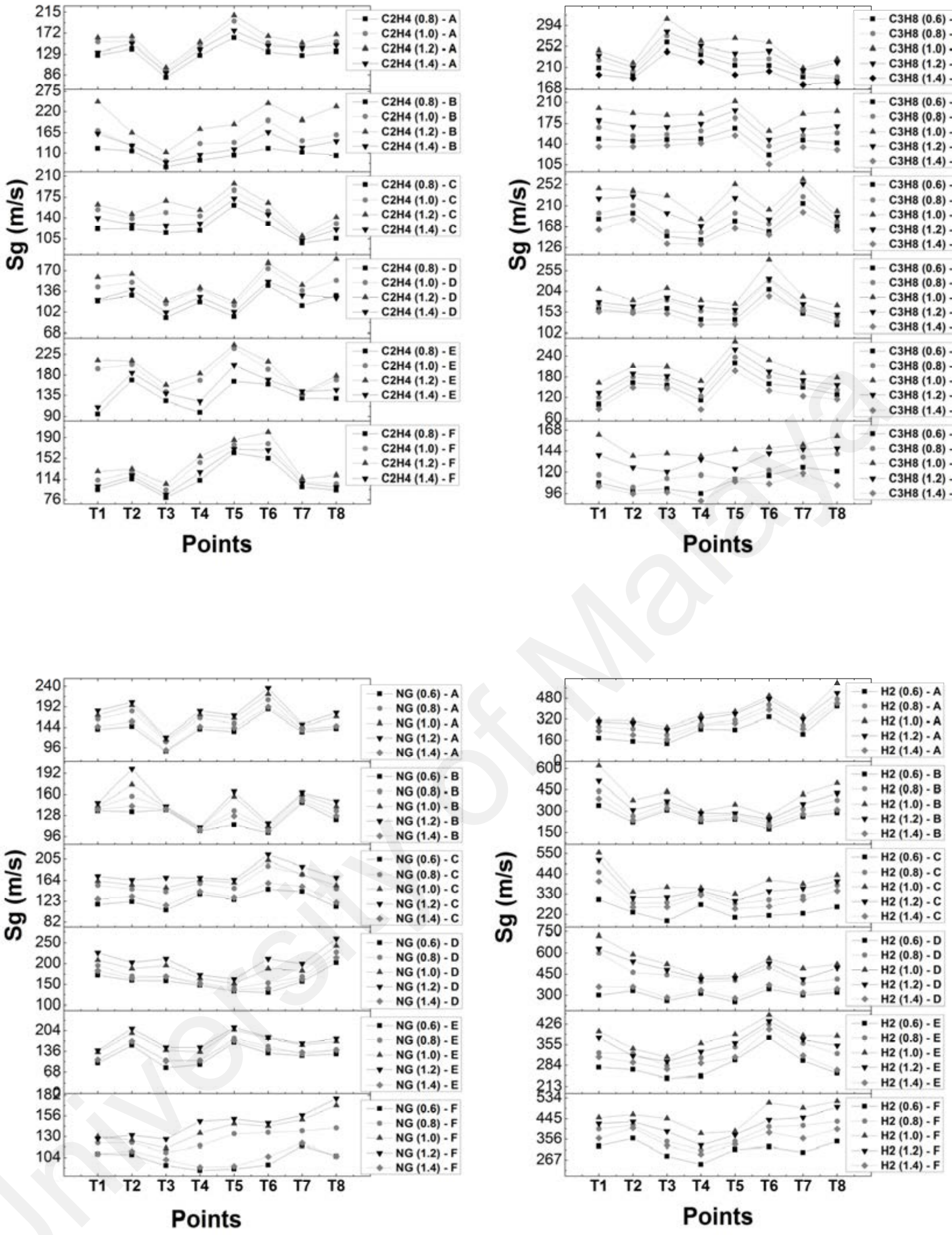

Figure 4. 6 Unburned gas flame speed vs. the recorded points

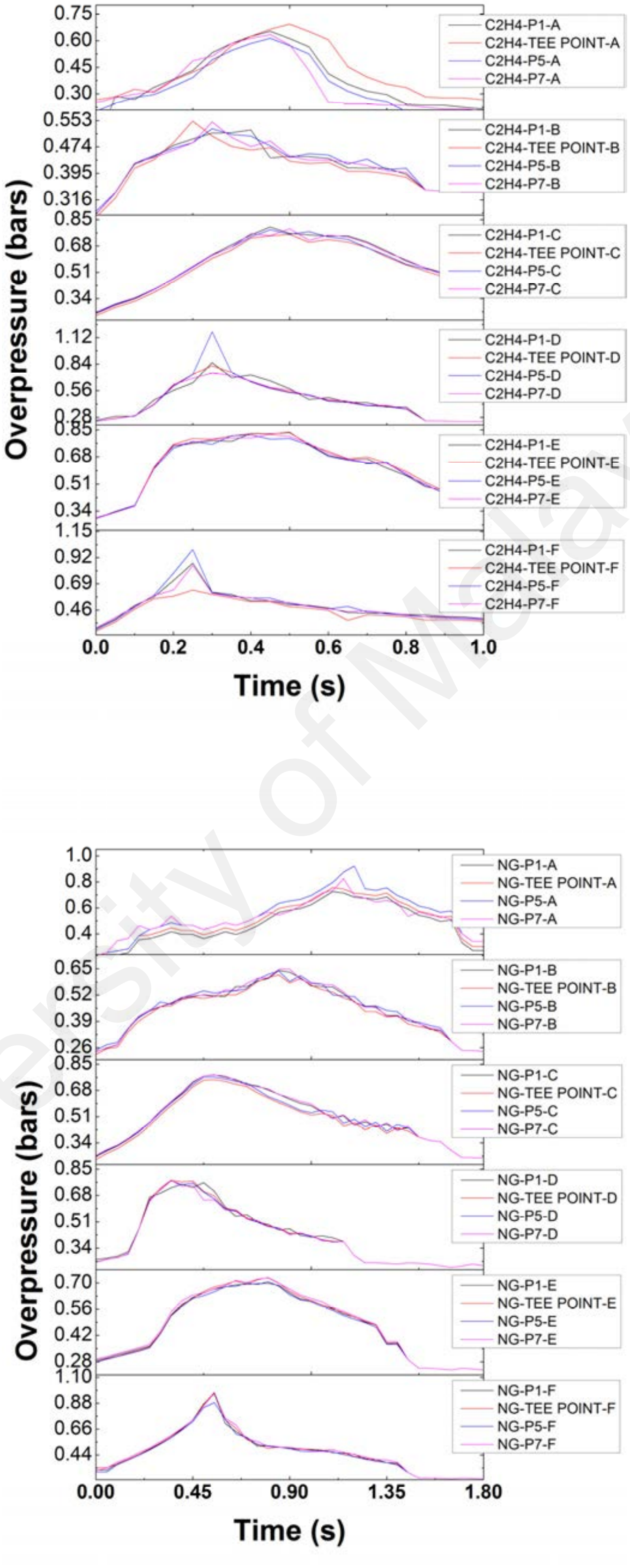

Figure 4. 7 Blast waves

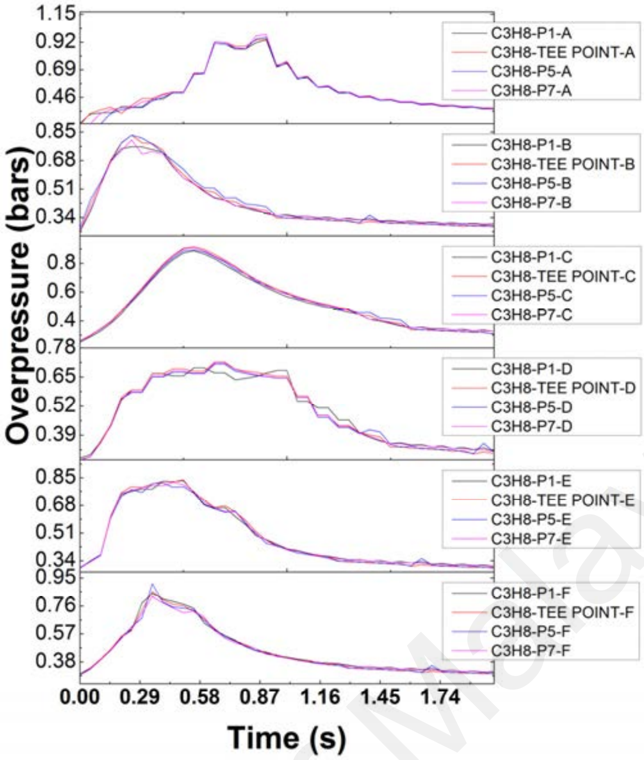

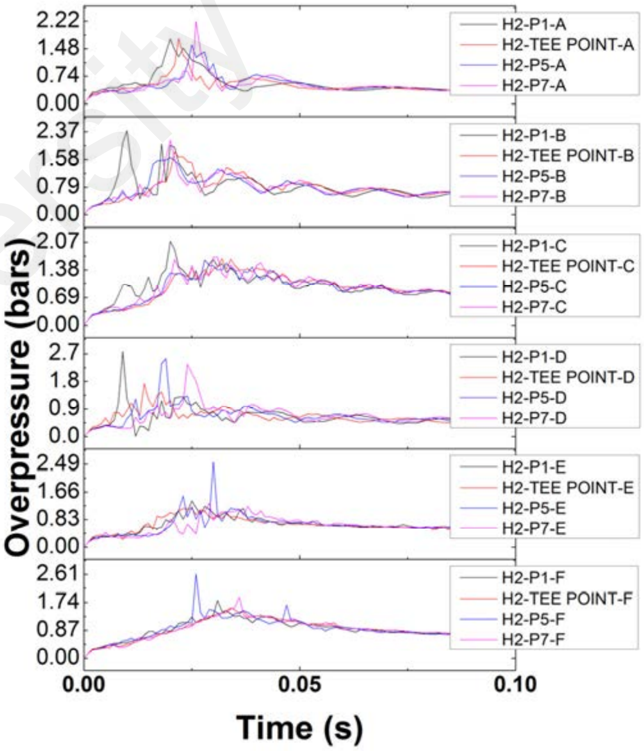

Figure 4. 7 continued

4.2.2. Flame speeds inside the pipe

Figures 4.4 and 4.5 illustrate the flame speed as a function of flame arrival points, represented by the thermocouple positions (denoted by T1–T8 in Figures 3.1 and 4.1). For the straight pipe, natural gas, propane and ethylene gave consistent flame speed profile: i.e., the maximum flame speeds occurred at x = 1.0 m from the ignition position (T3). However, two peaks were observed in the hydrogen flame speed figures, occurring at x = 1.48 m (T4) and 3.20 m (T7) from the ignition position, as shown in Figure 4.1A. It should be noted that the laminar burning velocity (SL) of hydrogen, at a stoichiometric concentration (Φ=1.0), is approximately 3.15 m/s (Harris, 1983), and the adiabatic spherical flame speed is 28 m/s (Alekseev et al., 2014). The measured flame speeds were much higher than SL, and at least seven times higher than the adiabatic flame speed. The significant increase in flame speed could be due to the self-acceleration of the flame resulting from the thermal-diffusive instabilities of the flame-front mechanism. The first peak reached a speed of 172.4 m/s, an increment of approximately 13 times the initial speed, indicating a very high turbulence experienced in the pipe. This flow creates turbulence ahead of the flame, inducing the flame to speed up rapidly. Coupled with the formation of flame wrinkling, flame folding and vorticity generation, the rapid flame propagation would draw the flame expansion preferentially in the direction of the end of the pipe. Furthermore, the reflective wave from the end of the pipe would attenuate the mass burning rate at the maximum, resulting in a rise to the second peak at ~1000 m/s, at T7 from the ignition position. It can be suggested that the flame speed development, seen between the ignition point and a distance of x =2.14 m (T5), is due to the unsteady flow caused by the tulip flame phenomenon, the quenching effect and the flame-wave interaction in confined pipes (Ciccarelli & Dorofeev, 2008). The high flame speeds for hydrogen-air were due to the flame's self-acceleration, resulting from the interaction between the shock wave, the fast flame and the flame front during the onset of a vortex, in accordance with the baroclinic effect (Petchenko et al., 2007). Such vortices induce the stretching of the flame surface area and cause the flame to cellularize/distort, intensifying the turbulence flame. To the contrary, for ethylene-air, propane-air and methane-air mixtures, the flame speeds had decreased slightly at x = 1.5 m (T5), before propagating at a constant velocity towards the end pipe. It is suspected that the flame starts to quench, resulting in a weaker flame turbulization.

The recorded flame speed in the 90-degree pipe indicated that the presence of bending would promote the flame stretch around it, intensifying the turbulence vortex and thus increasing the flame surface area through the strong mixing of burned and unburned gas. As Figure 4.4d shows, the peak flame speed of hydrogen-air was approximately 1384 m/s: a steep increase of up to 4.8 times before entering the bend. Meanwhile, ethylene-air, propane-air and methane-air experienced maximum flame speeds of about 496 m/s, 407 m/s and 339 m/s, respectively, before the bending position. Furthermore, it also shows that the second acceleration occurred at 3.49 m (T6) from the ignition point, giving an increase of flame speeds to 1311 m/s, 487 m/s, 407 m/s and 310 m/s for hydrogen-air, ethylene-air, propane-air and methane/air, respectively, before reaching the end wall. The increased flame speeds at this position were approximately twice as high as the flame speeds at distance 2.62 m (T5). This is possibly caused by the complicated interaction between flame acceleration, the quenching effect and flame shape, which affects the mass burning rate (Phylaktou & G. E. Andrews, 1991; Phylaktou et al., 1993). It is worth noting that the interaction of hot flame with pressure waves, which are reflected from the end wall, plays an important role in contributing to the second acceleration.

For the tee pipe, the flame speeds were lower than those of the straight and 90-degree pipes, due to the free paths available after the tee region (figure 4.5). An investigation of parallel pipes also showed a similar observation (Zhu et al., 2012). However, there is no doubt of the explosion severity posed by the tee pipe configuration. The data from both tee pipe configurations (Figures 3.1a and b) show that a shorter distance of the tee junction from the ignition position gives a higher severity magnitude, compared to a longer distance of the tee junction placement. However, at a longer distance of tee junction, different flame speed profiles were recorded. The higher flame speed observed at T3 (~500 m/s) was due to the dynamic effect experienced by the flame propagation; mass diffusivity, the rapid mixing of the induced turbulence, fast flame downstream, a strong interaction between reflective waves and fast flames from the end points, on the one hand, and flame acceleration of the fuels, on the other, can cause retonation and detonation, as discussed by Qiao and Faeth (2005). When the tee junction was placed at an equal distance along the pipe, as shown in Fig. 1d, the flame acceleration of the fuel gases gave the lowest flame speed intensity, since the flames accelerate at almost the same distance after the tee junction region. In this instance, the interaction between the reflective waves and fast flames from the end points was insignificant; this phenomenon has been fairly widely discussed in the literature (Hassan et al., 2012; Kolbe & Baker, 2005).

4.2.3. Maximum rate of pressure rise

The maximum rate of pressure rise at all equivalence ratios for all fuels is presented in Figures 4.8 and 4.9. As shown, the associated maximum rates of pressure rise from the ignition point were recorded at the end of the second of the three parts of the straight pipe (P3), and at the bend point in the 90-degree pipe (P4). However, it was localized at different points in the tee pipes, with respect to the tee junction allocation. As mentioned earlier, flame cellularity causes distortion to the flame surface, giving a larger area and thus increasing the ratio of burning velocity. Consequently, the tulip formation reduces the turbulence due to the vortex creation, and the reflective wave leads to a strong interaction between the fast flame and turbulence, increasing the flame speed as well as the rate of pressure rise (Bougrine et al., 2014; Merlin et al., 2012). These conditions can be substantiated by associated blast wave (Figures 4.7) and calculated Lewis number (Figure 4.10). The fluctuation rate at each pressure transducer point suggests that the flame has a tendency to become cellular as it is progressively stretched, particularly in bending and tee junction regions, giving it more room to grow larger and thus increasing the mass-burning rate. The rate of pressure rise data appear to be more repeatable than the maximum overpressure results, and show that the hydrogen fuel produced a more severe explosion for all the configurations tested. For instance, it took the shortest time for the hydrogen-air to reach maximum overpressure in all configurations. This was not only an effect of the kinetic reaction for each mixture, but also of the dynamic properties of the flame (i.e., diffusional-thermal instability also has a significant influence on this phenomenon) which it has been presented by Lewis number in Figure 4.10. This is the most important factor affecting the burning velocity and heat release rate during flame propagation (Movileanu et al., 2013); consequently, it is associated with flame wrinkling. This wrinkled flame causes an increase in the mass-burning rate, giving a higher overall flame speed and overpressure intensity (Kim et al., 2014). This was the reason for the highest and lowest rates of pressure rise observed in hydrogen-air and propane-air explosions, respectively.

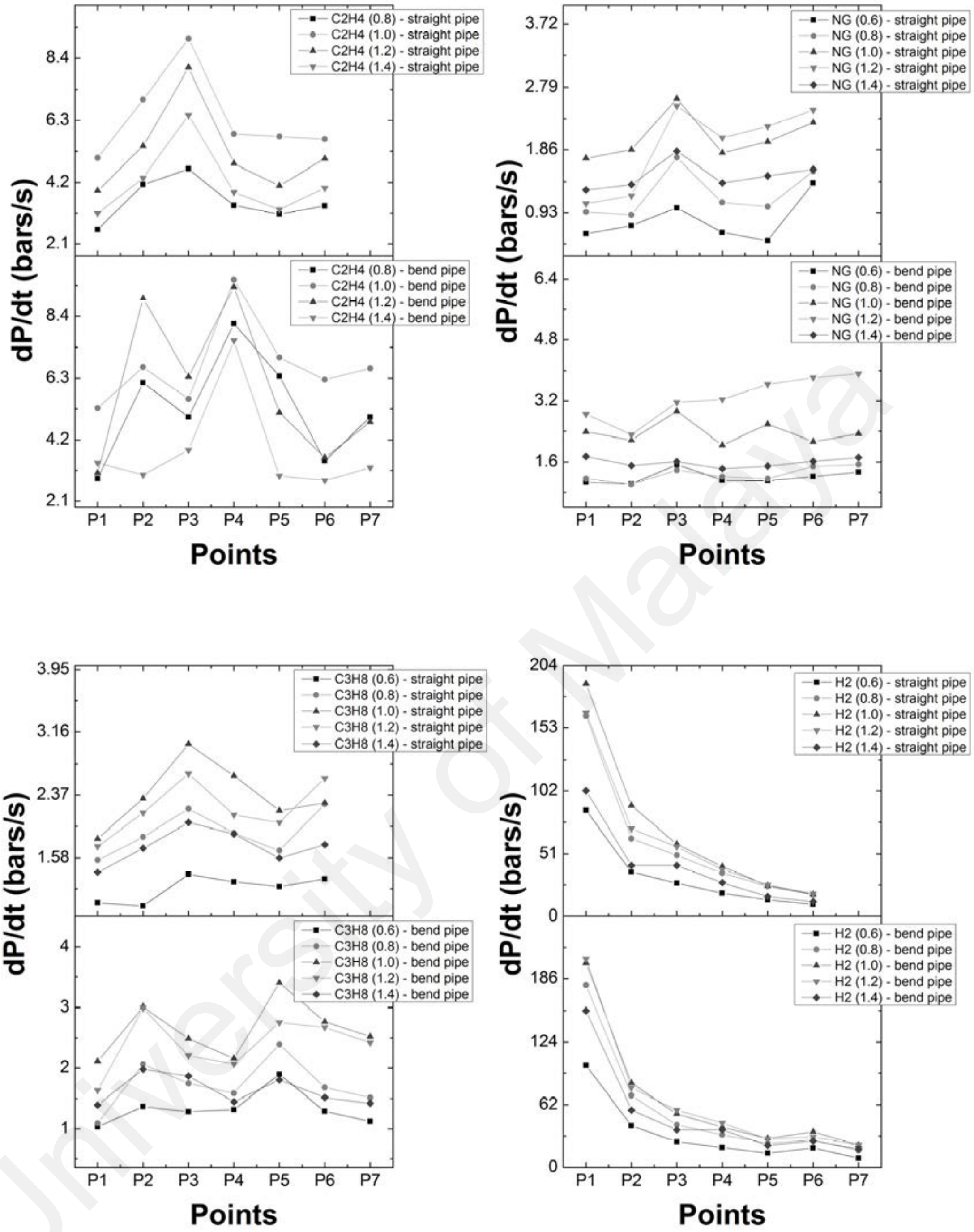

Figure 4. 8 Rate of pressure rise vs. the recorded points in straight and 90 degree pipes (Sulaiman, 2015)

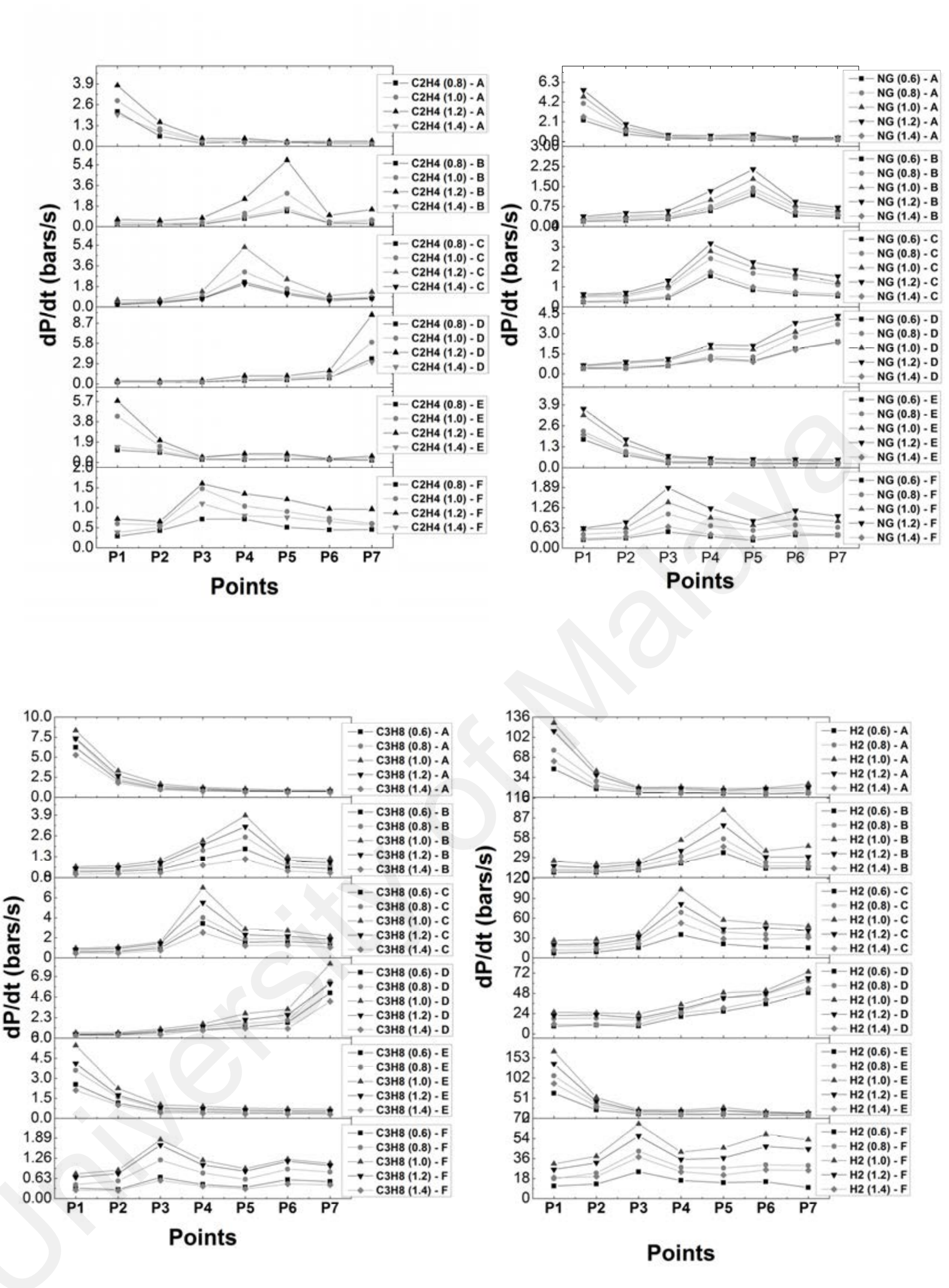

Figure 4. 9 Rate of pressure rise vs. the recorded points in tee pipes

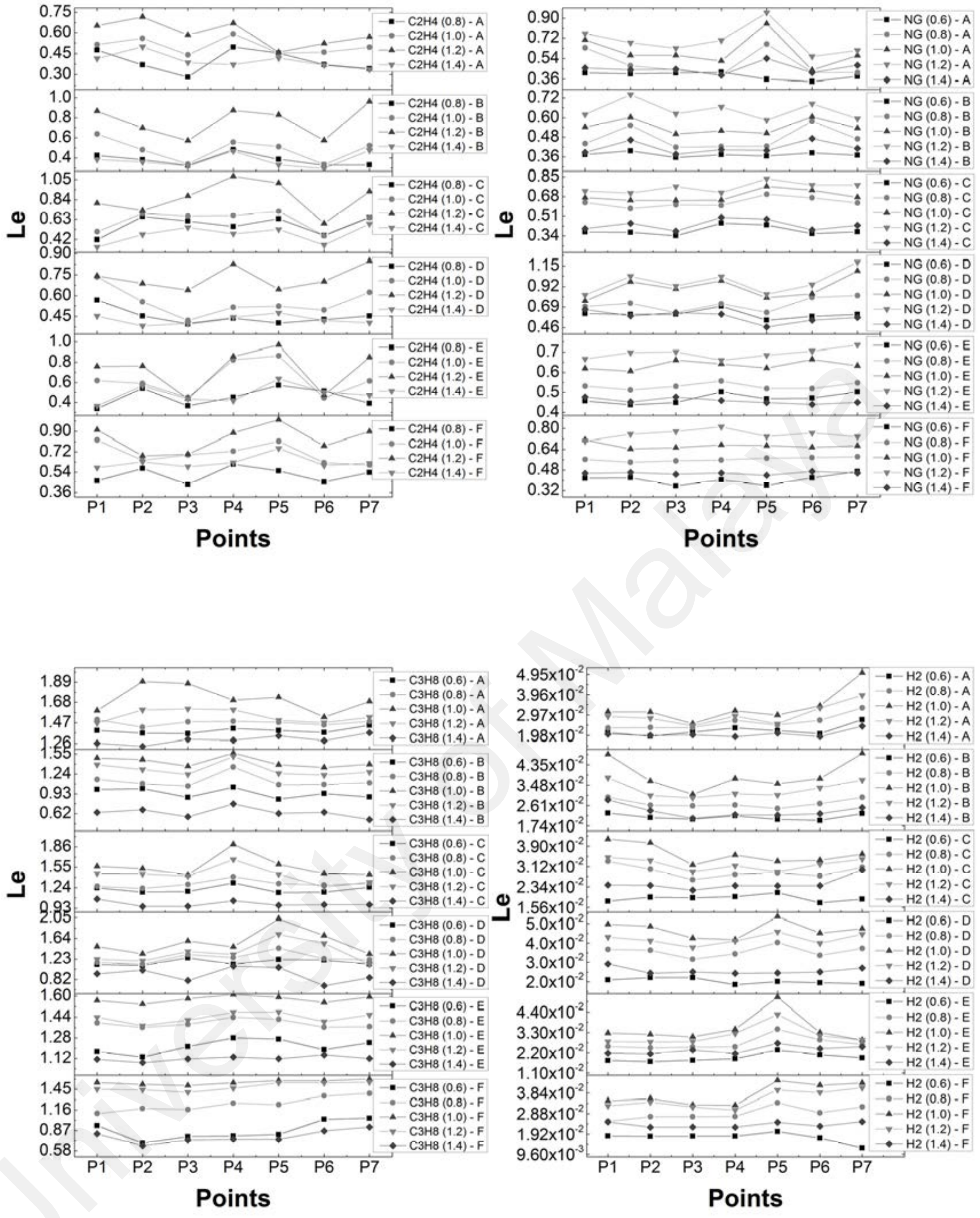

Figure 4. 10 Lewis number vs. the recorded points in tee pipes

It is noticeable that the effectiveness of ignition points and associated Lewis number on flame acceleration of hydrocarbons/air and hydrogen/air mixtures have been deliberated in following sections due to avoiding repetitive discussion.

4.3. Flame acceleration of Hydrocarbons-hydrogen/air mixtures

4.3.1. Pressure and Flames Acceleration Mechanism

Figures 4.11-4.13 describe the overpressure as a function of the pressure transducers' points. By giving overall attention to all of the ignition points, as shown in Figure 4.11 and 4.12, the maximum overpressure for the ethylene-hydrogen/air and NG-hydrogen/air mixtures were higher than the pure ethylene/air and NG/air fuels, with an addition of 10-30% v/v hydrogen in the mixtures. In details, by adding 10-30% hydrogen into pure ethylene/air and NG/air fuels, maximum overpressure increased up to 0.7 and 0.8 bars, respectively, which they are almost two times higher than the recorded maximum overpressure for pure ethylene/air and NG/air fuels. However, the overpressure was lower when the hydrogen enrichment was 50% v/v and above. Furthermore, there were no significant changes on the pressure development along the pipe. It can be said that the interaction between the flame front and unburnt gases in the lower hydrogen content was much higher due to the oxidation reactions of ethylene-hydrogen/air and NG-hydrogen/air mixtures. Tuncer et al. (2009) have shown that hydrogen-enrichment allows the combustion to be sustained at a much leaner equivalence ratio than is possible with methane. The supplementary kinetic mechanism that is shown below provides evidence for why the addition of hydrogen leads to higher levels of OH and HCO in these mixtures (Hu et al., 2009b):

$$HO_2 + CO \leftrightarrow HCO + O_2 \tag{4.1}$$

$$H + CO + H_2O \leftrightarrow HCO + H_2O \tag{4.2}$$

$$H + O_2 \leftrightarrow O + OH \tag{4.3}$$

As a consequence, the reaction rate, the mixture-ignitability and the rate of heat release (Mardani & Tabejamaat, 2010), as well as the burning rate (Hu et al., 2009b), increases significantly. This affects the overall dynamic parameters including the overpressure and flame speeds. This also applies for ethylene. The presence of double bands in its structure causes a higher expansion ratio (Cortright et al., 1991; Huntress Jr, 1972). Consequently, the researchers recorded a higher value of overpressure in ethylene-hydrogen/air mixtures. Moreover, they showed that the reaction (4.4) promotes higher mixture reactivity and heat release rate at lower temperatures. This causes higher OH concentrations at early flame development (Dagaut & Nicolle, 2005; Lafay et al., 2008). However, the following reactions have negative sensitivities due to the reduction of active radicals during the combustion process (Hu et al., 2009b):

$$H + HO_2 \leftrightarrow 2OH \tag{4.4}$$

$$C_2H_3 + H + M \rightarrow C_2H_4 + M \tag{4.5}$$

$$C_2H_2 + H + M \rightarrow C_2H_3 + M \tag{4.6}$$

$$CO + H + M \rightarrow HCO + M \tag{4.7}$$

$$OH + H + M \rightarrow H_2O + M \tag{4.8}$$

$$O_2 + H + M \rightarrow HO_4 + M \tag{4.9}$$

$$H + O_2 + H_2O \leftrightarrow HO_2 + H_2O \tag{4.10}$$

$$HCO + O_2 \leftrightarrow HO_2 + CO \tag{4.11}$$

Less active radicals significantly reduce the overpressure of ethylene-hydrogen/air and NG-hydrogen/air mixtures in the presence of a higher concentration of hydrogen. This is a possible explanation for lower, maximum overpressure and flame speed with 50% v/v and above hydrogen content (Figures 4.11-4.14). However, the pressure profile for propane is different. In the present work, the value of maximum overpressure and flame speed of this particular mixture in all of the ratios were lower than the pure propane/air mixture. Maximum overpressure was recorded at 50% C_3H_8-50%H_2/air mixtures. A kinetic analysis showed that the hydrogen radicals on the primary and secondary sites of propane favourably occurred at one side and the reactions of propyl radicals on the other side (Refael & Sher, 1989). This kinetic reaction plays an important role in the overall reaction mechanism due to its thermal decomposition. Therefore, by adding hydrogen into propane/air, the H and OH radicals broke down the propane molecules, forming the products of combustion at a lower temperature. This has already been adequately discussed in previous literature (Levy, 1955; Refael & Sher, 1989). The kinetic analysis of propane-hydrogen showed that the following reactions have an insignificant effect on the flame development, leading to the consumption of the free H radicals (Refael & Sher, 1989):

$$C_2H_3 + H + M \rightarrow C_2H_4 + M \tag{4.12}$$

$$C_2H_2 + H + M \rightarrow C_2H_3 + M \tag{4.13}$$

$$CO + H + M \rightarrow HCO + M \tag{4.14}$$

$$OH + H + M \rightarrow H_2O + M \tag{4.15}$$

$$O_2 + H + M \rightarrow HO_4 + M \tag{4.16}$$

Furthermore, there are no apparent changes in the reaction in the co-flow air. However, some reactions have been reported at the fuel reaction zone when hydrogen is added into the propane. This implies the dominance of H atoms over the OH radicals in the system. Accordingly, the last sequence implies that the H-abstraction was mainly conducted by OH radicals, although the H-abstraction by the H atoms dominated when the hydrogen was added (de Ferrières et al., 2008). This favourable interaction of H atoms in the chemical reaction of CO conversion to CO_2 indicates that the CO level increases with the co-flow oxygen enrichment. In such studies, this finding was an unforeseen observation (Burbano et al., 2008; de Ferrières et al., 2008; Mardani & Tabejamaat, 2010). With regard to what is discussed above, in the current study, the presence of hydrogen in propane/air caused the value of the burnt gases to increase at all of the compositions. This was more significant for the ratios of 90:10 and 70:30, respectively. Consequently, the overall maximum overpressure and flame speed declined, compared to the pure propane/air mixtures.

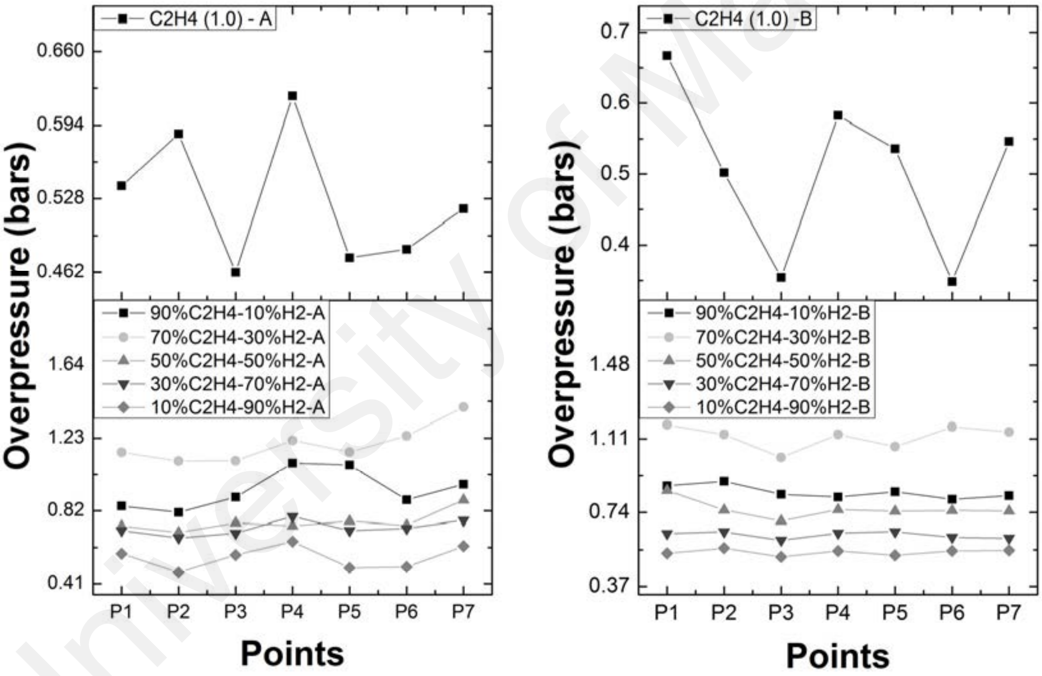

Figure 4. 11 Maximum overpressure vs. the recorded points at different ignition positions – C_2H_4/air and C_2H_4-H_2/air mixtures

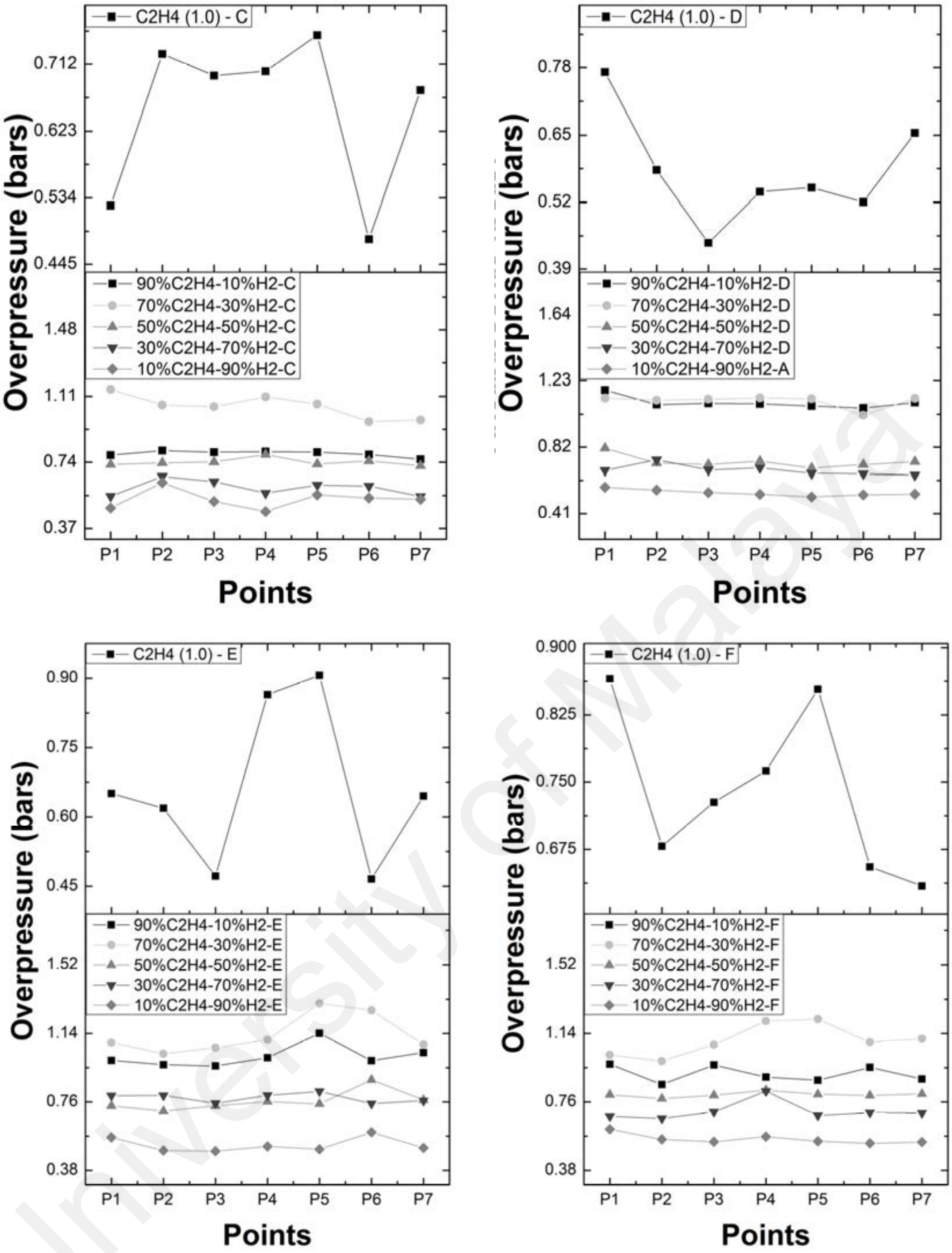

Figure 4. 11 Continued

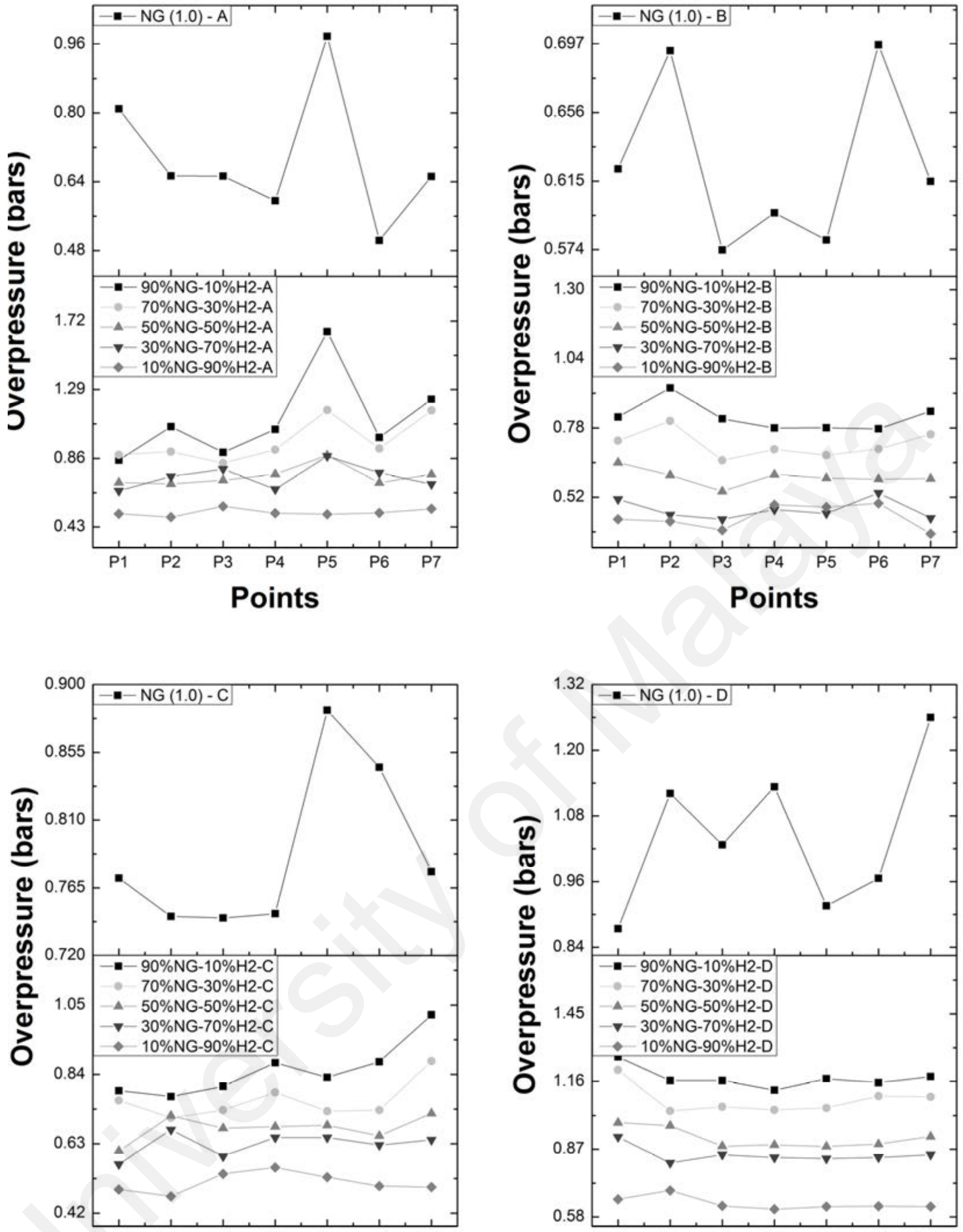

Figure 4. 12 Maximum overpressure vs. the recorded points at different ignition positions – NG/air and NG-H_2/air mixtures

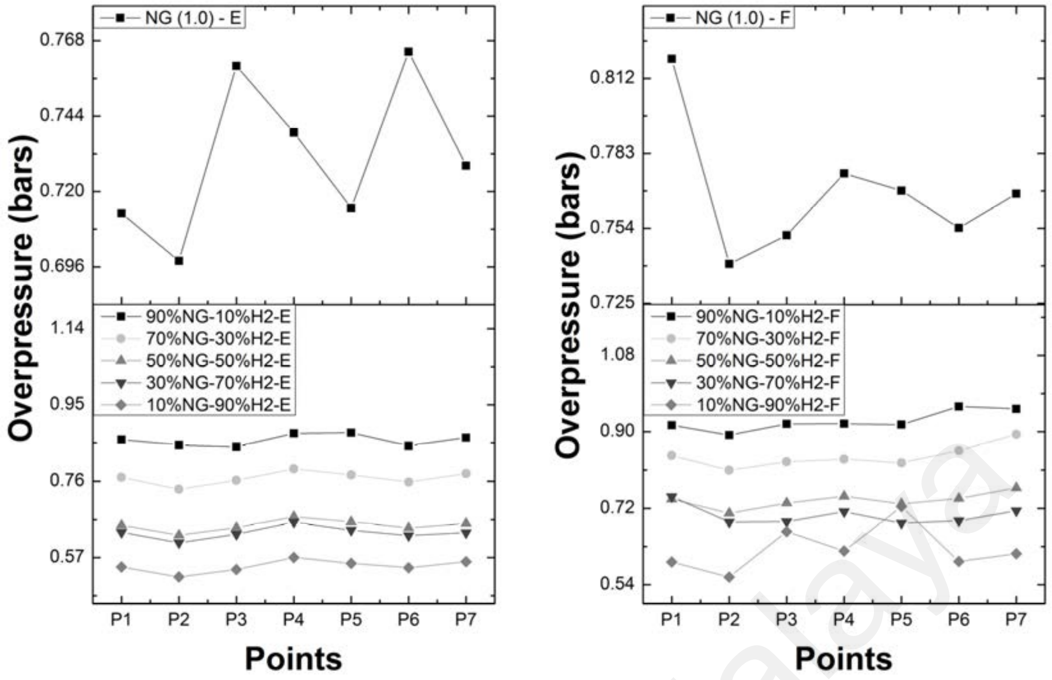

Figure 4. 12 Continued

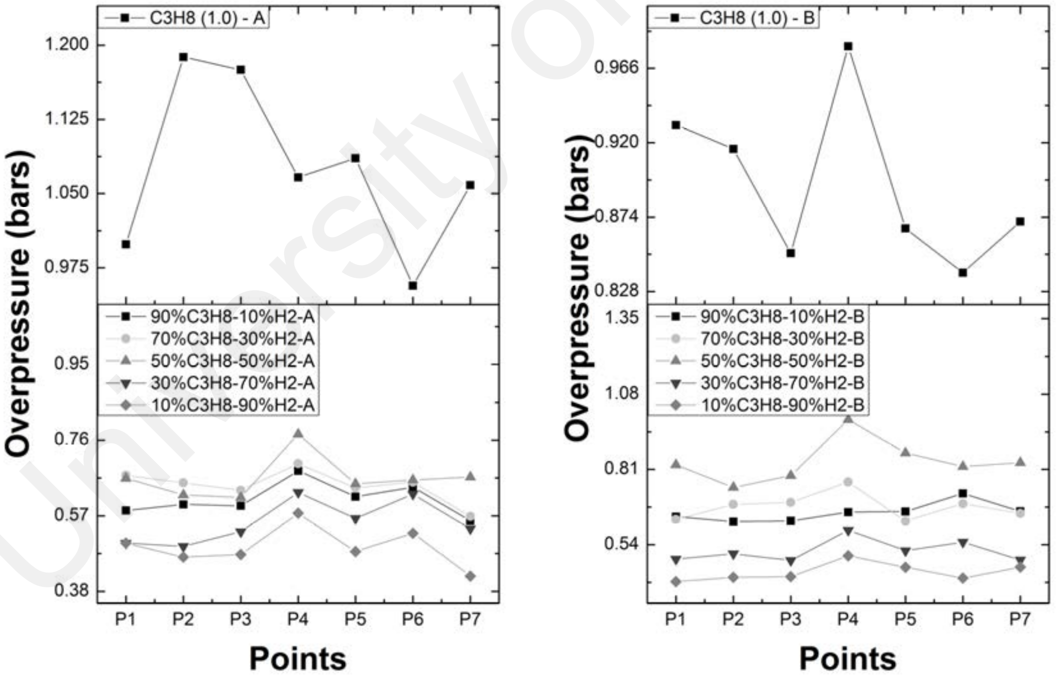

Figure 4. 13 Maximum overpressure vs. the recorded points at different ignition positions – C_3H_8/air and C_3H_8-H_2/air mixtures

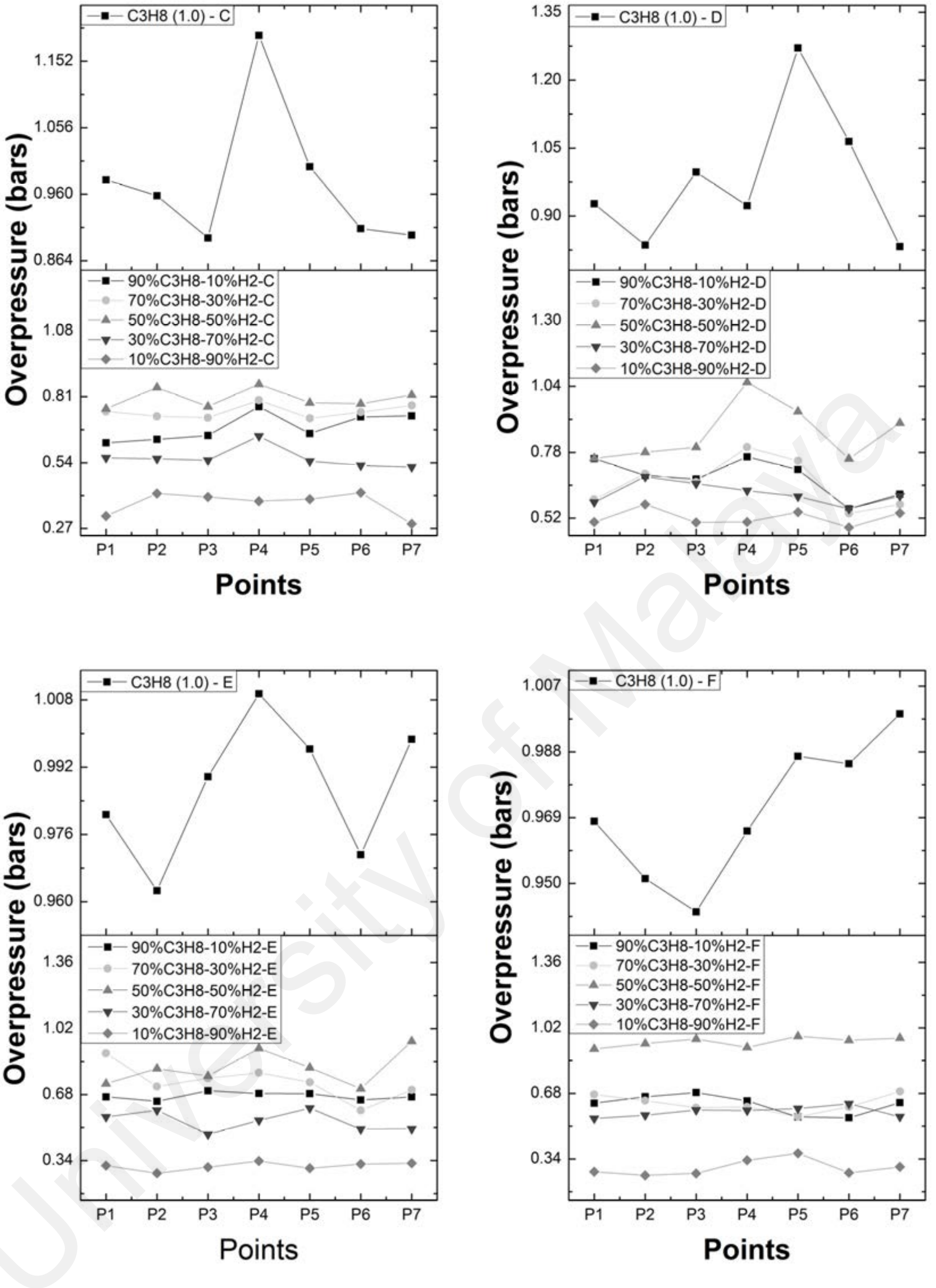

4. 13 Continued

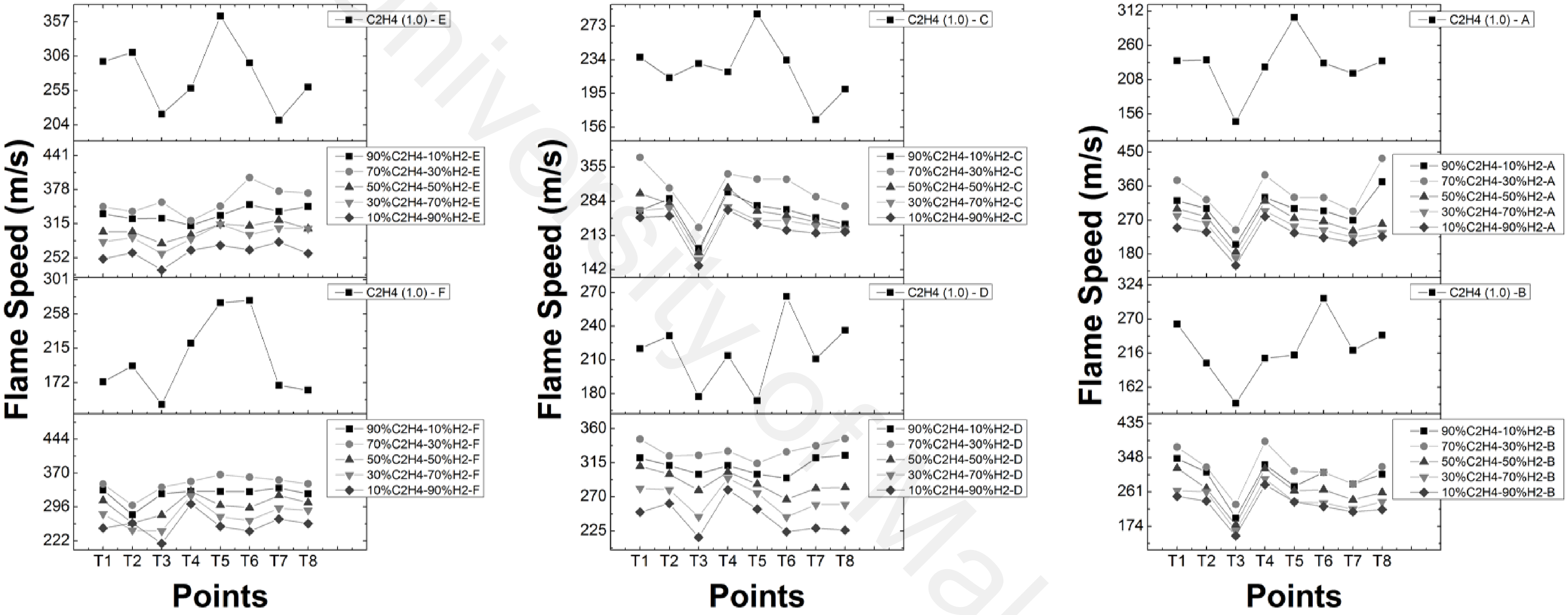

Figure 4. 14 Maximum flame speed vs. the recorded points at different ignition positions

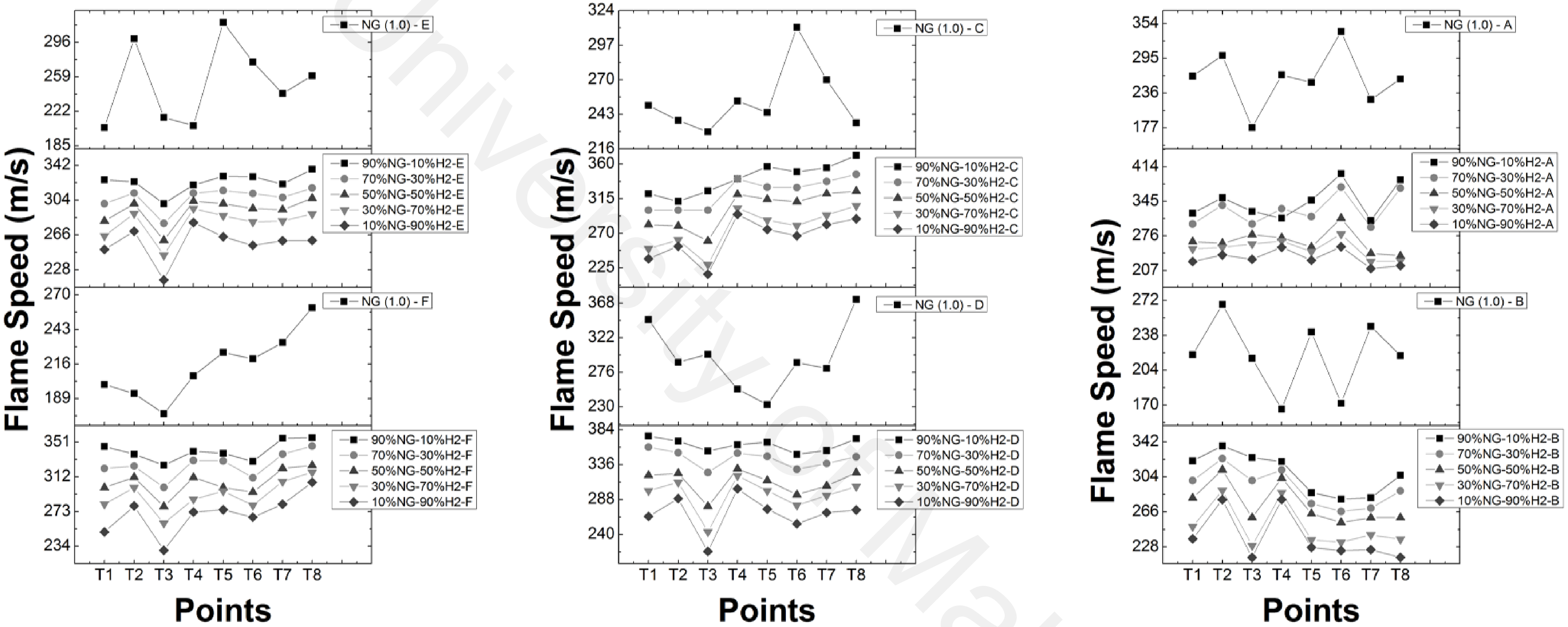

Figure 4. 14 Continued

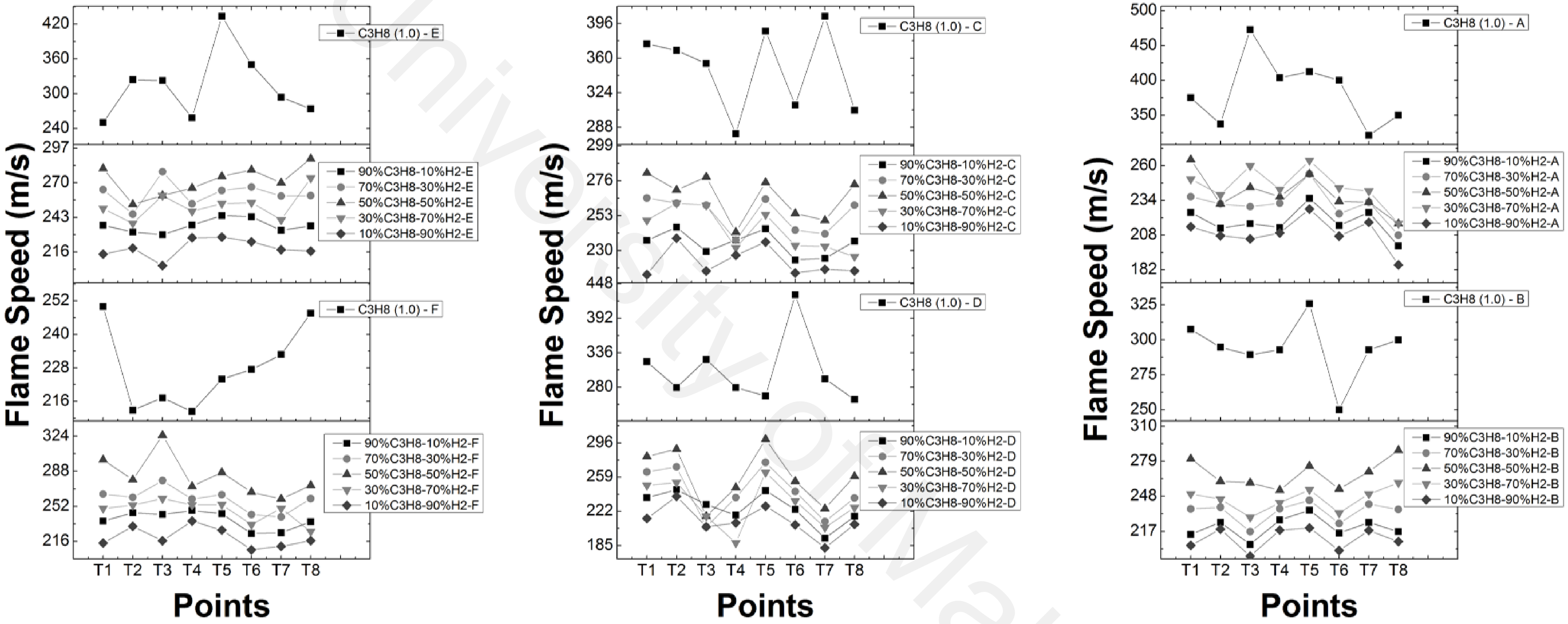

Figure 4. 14 Continued

4.3.2. Influence of Ignition Positions on Explosion Development

Previous investigations (Blanchard et al., 2011; Kasmani et al., 2007; Kindracki et al., 2007) have shown that the position of the ignition source has a significant effect on the initial flame propagation and the resulting flame speeds and overpressures. Within the examined range of hydrocarbons/air and hydrocarbons-hydrogen/air concentrations, the value of the maximum overpressure and flame speed were almost the same at all of the ignition positions. There was only a different location on the recorded peak overpressure and flame speeds (refer to Table 3.2). For instance, the highest overpressures for the ethylene/air and ethylene-hydrogen/air mixtures were observed at the tee point (P4) for the ignition positions A, C and F. Meanwhile, P1 gave maximum pressure for the ignition position at B and D. Furthermore, P5 gave the highest value of pressure when it was ignited at E. It can be depicted that the differences in the maximum overpressure and flame speed of each of the mixtures at all of the ignition points may have been due to the stratification of gases on the pipe bed or what is known as sedimentation phenomenon. This has been discussed in previous literature (Di Benedetto et al., 2011; Sanchirico et al., 2011).

To further support the justification that is mentioned above, the maximum rate of pressure rise, dP/dt and blast wave for all of the fuels mixtures at all of the concentrations are presented in Figures 4.15-4.18. From Figure 4.15, it can be seen that, compared with the pure fuel explosions, there were different dP/dt profiles, when ignited at B, D and F. Position D and F were located at the tee junction, while B was at the shortest distance from the ignition to tee junction. It can be said that the addition of hydrogen to the fuel mixtures and ignition position gives different physics and kinetic mechanisms to the overall tee junction explosion development. As mentioned above, the additional OH radicals encourage the diffusivity process to become shorter, causing the flame to distort and the flame area to increase. Hence, it increases the burning rate and enhances the flame speeds and pressures (Bougrine et al., 2014; Merlin et al., 2012).

To further clarify this condition, the blast wave plots of all of the mixtures at P1, tee point (P4), P5 and P7 at t =1 s are presented in Figure 4.16-4.18. From the figures, the oscillation instabilities are apparent when the mixtures were ignited at B and D. This associates with the lower Lewis number for the ethylene /air and NG /air, and a higher Lewis value for the propane. As mentioned earlier, the mixtures with a lower Lewis number than one were susceptible to flame wrinkling, due to the diffusional-thermal instability. This wrinkled flame causes an increase in the mass burning rate, giving a higher overall flame speed and overpressure intensity (Kim et al., 2014). With a Lewis number that is higher than one, rich propane is susceptible to flame cellularity. This indicates that the mass thermal diffusivity was dominant in this condition. The appearance of the multiple peak overpressures indicates that, at a shorter obstacles distance and, in this case, when ignited at B, the flame experienced a strong interaction of transverse pressure waves from the tee junction. This interaction induced more turbulence and, consequently, attenuated the acceleration of the burning of the unreacted mixtures, which were trapped along the tee junction. This, again, increased the combustion rate and hence, increased the flame speeds and overpressure in the ethylene-hydrogen/air and NG-hydrogen/air, compared to others. These statements are also in agreement with previous research studies (Kim et al., 2014). From the findings, it can be said that the flame dynamic mechanism at the tee junction mainly depends on the ignition positions.

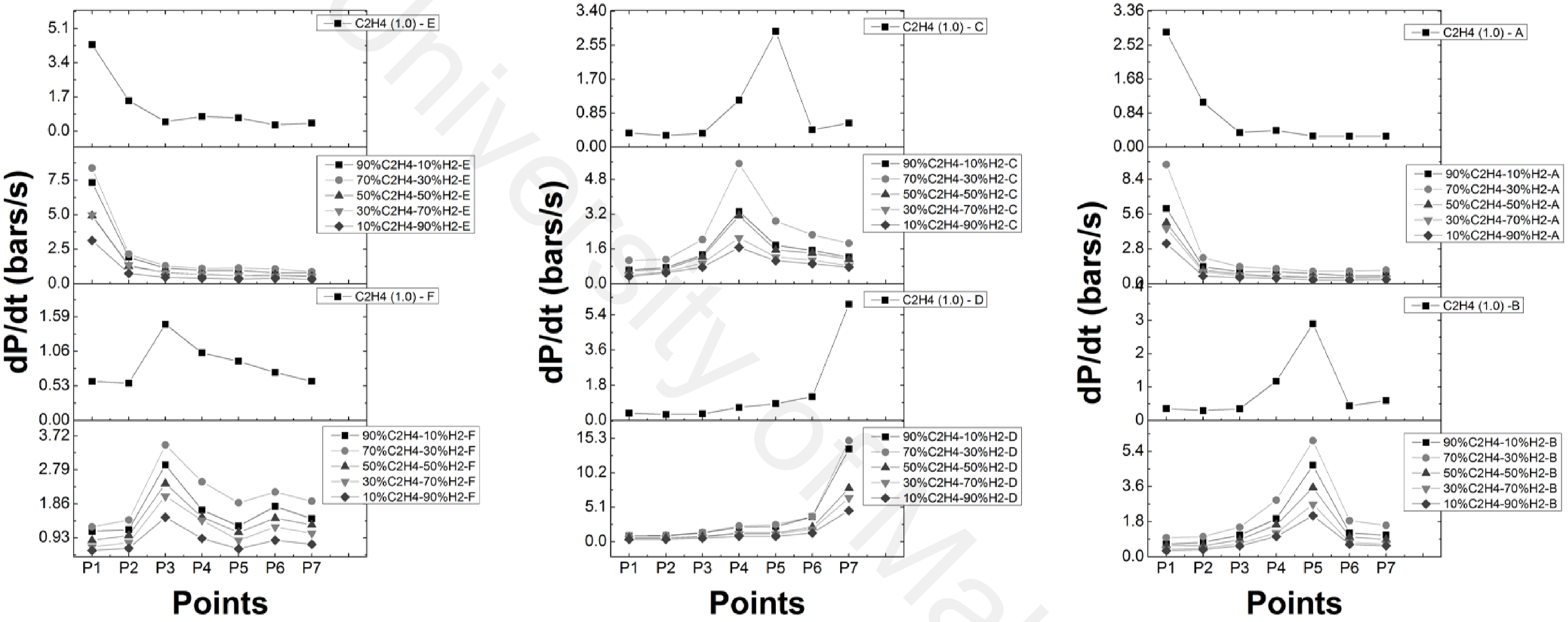

Figure 4. 15 Rate of pressure rise vs. the recorded points at different ignition positions

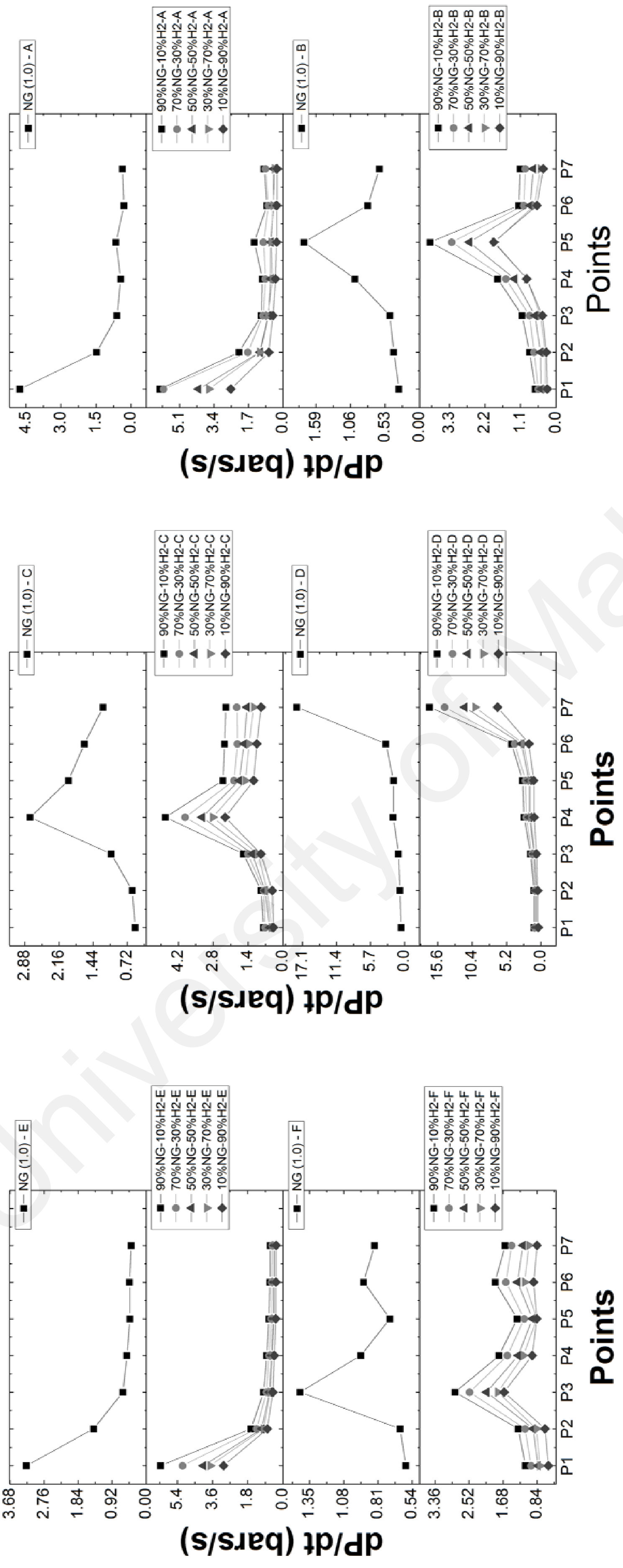

Figure 4. 15 Continued

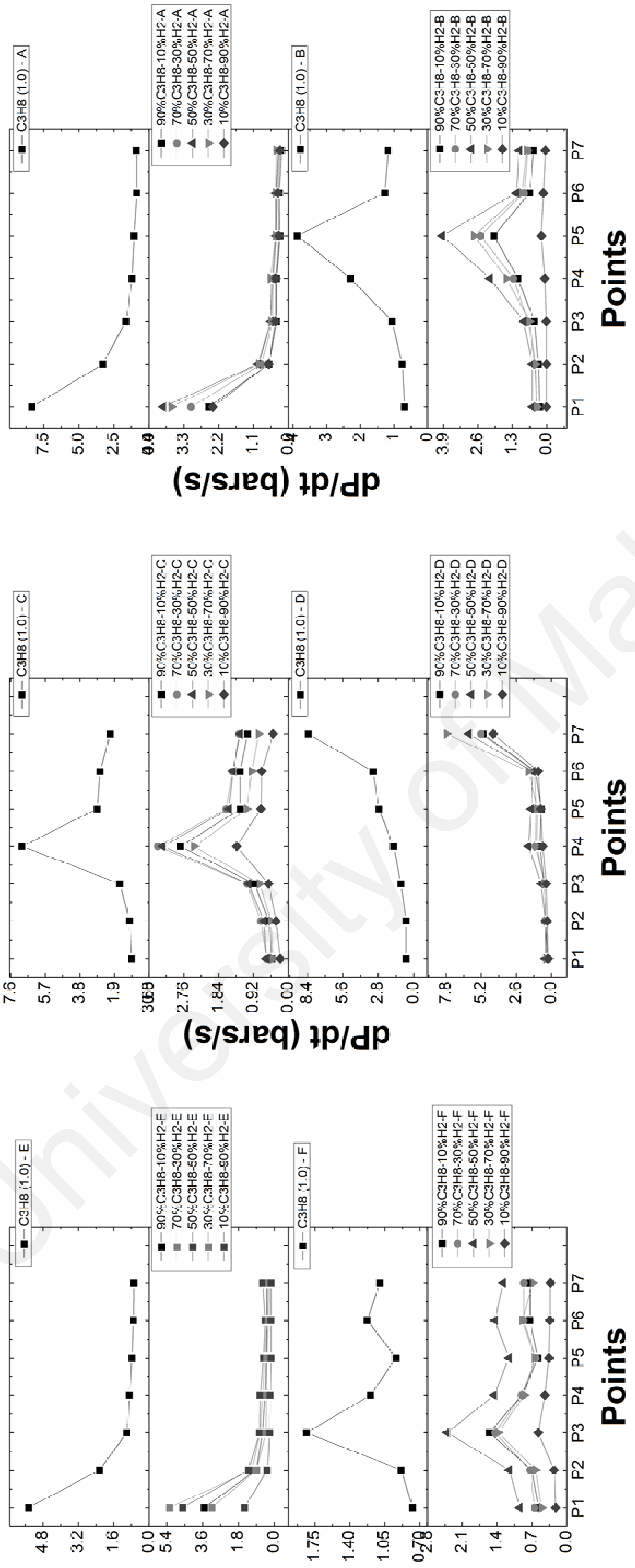

Figure 4. 15 Continued

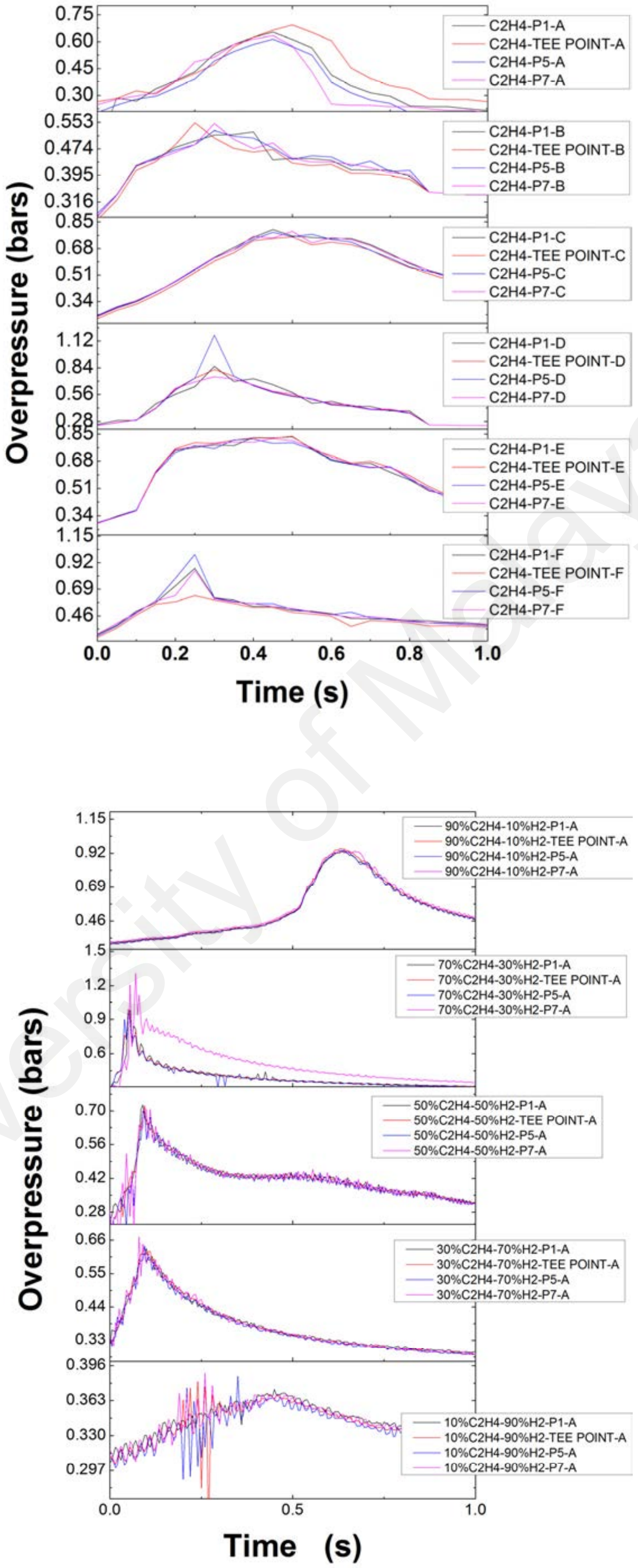

Figure 4. 16 Blast waves - C_2H_4/air and C_2H_4-H_2/air mixtures

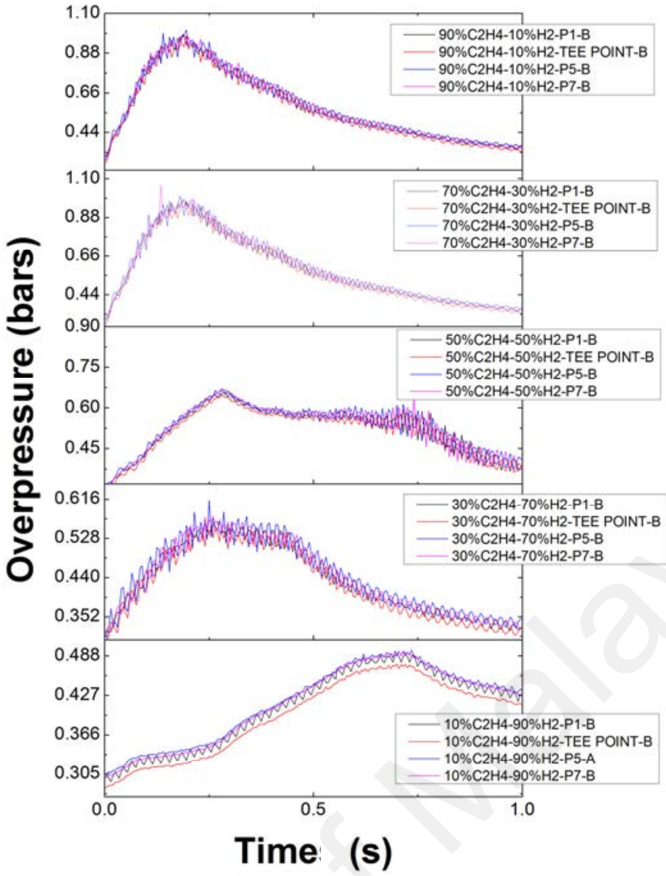

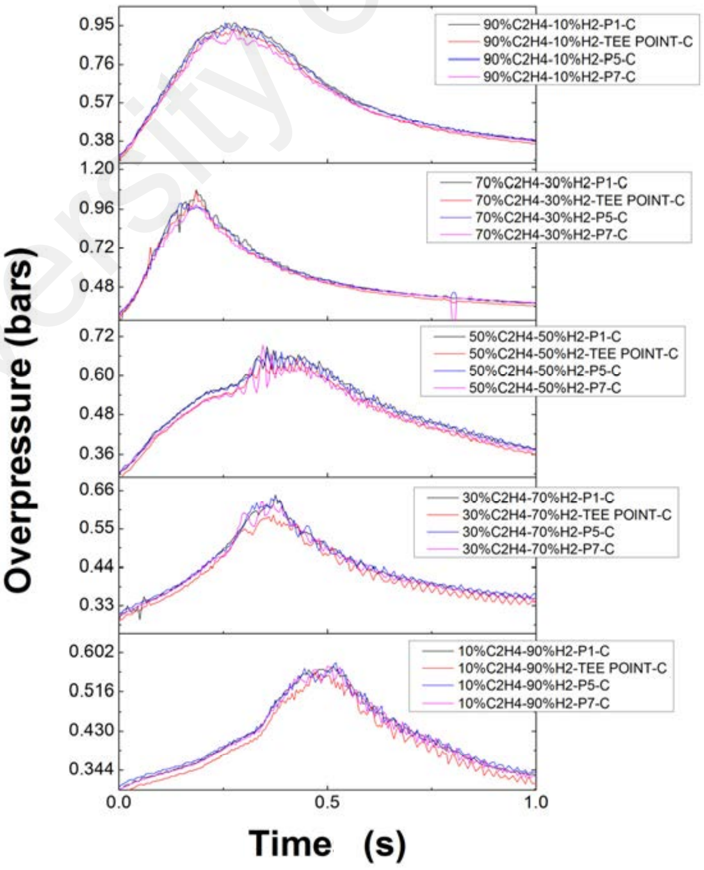

Figure 4. 16 continued

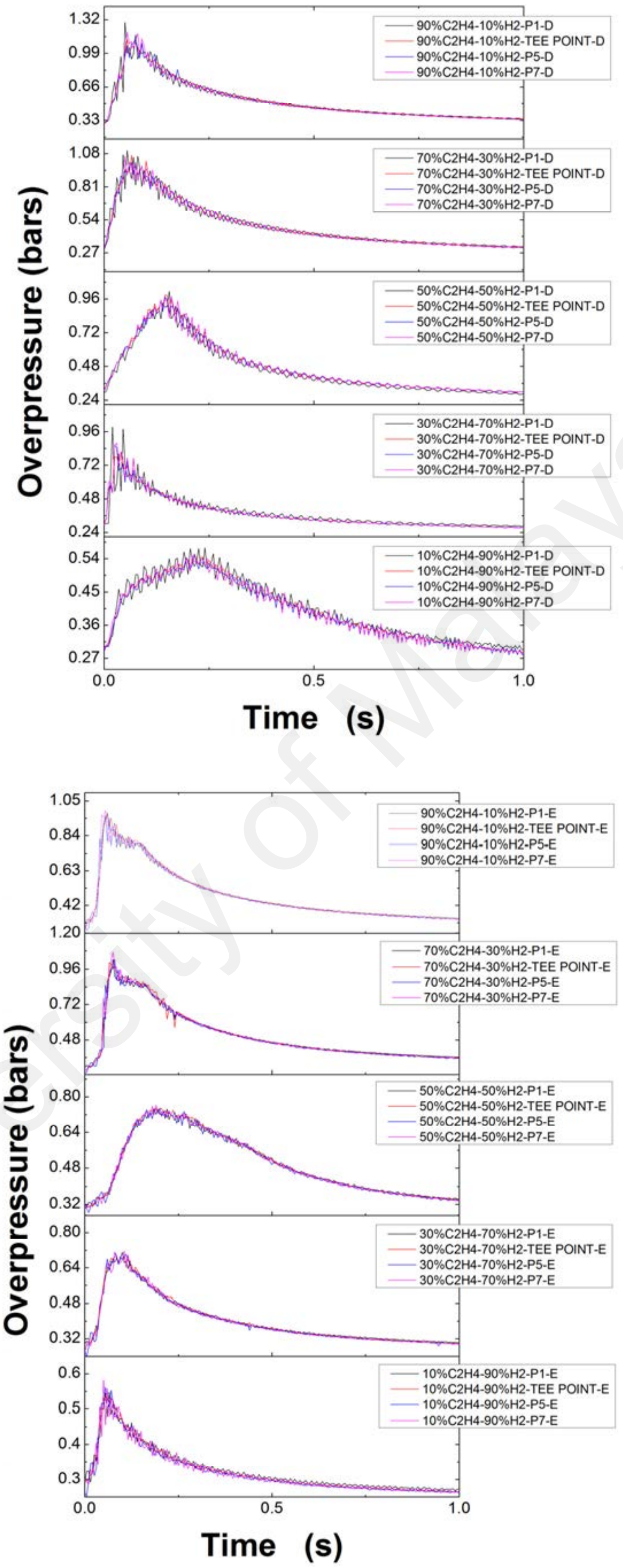

Figure 4. 16 continued

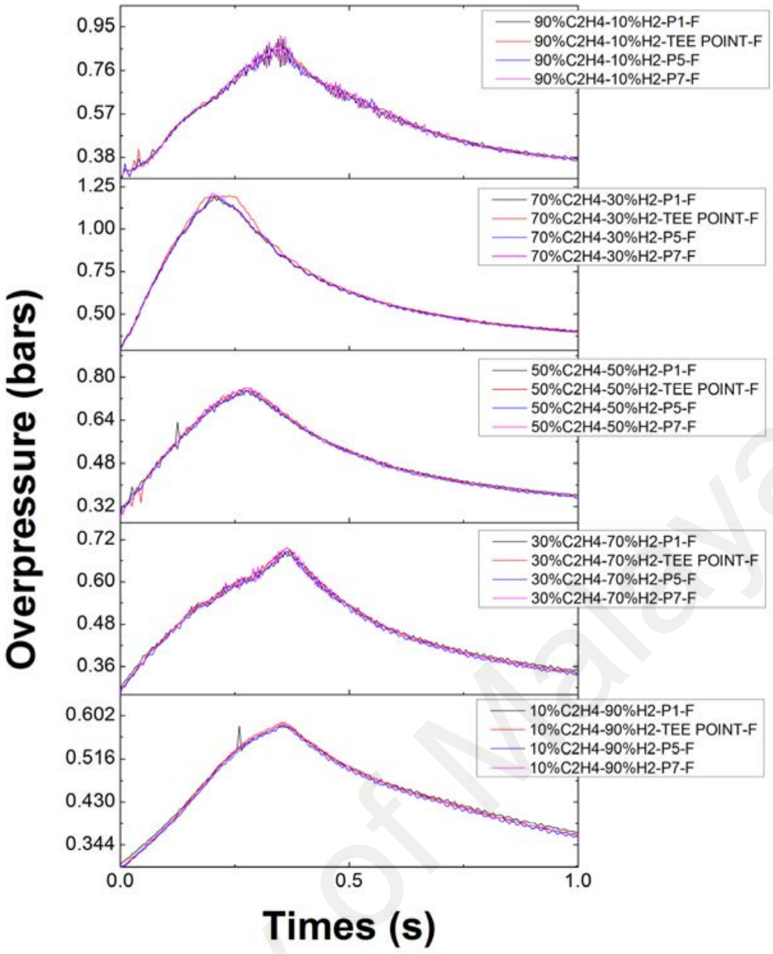

Figure 4. 16 continued

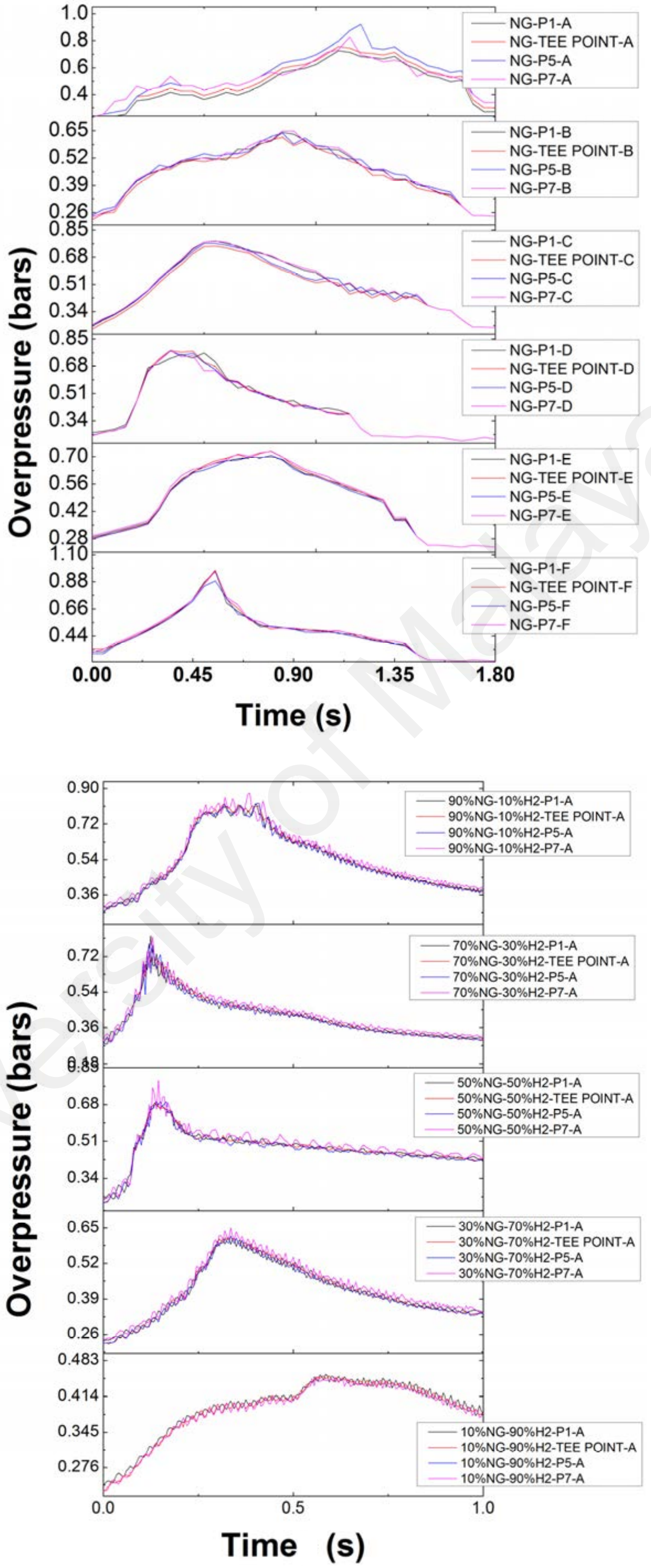

Figure 4. 17 Blast waves - NG/air and NG-H_2/air mixtures

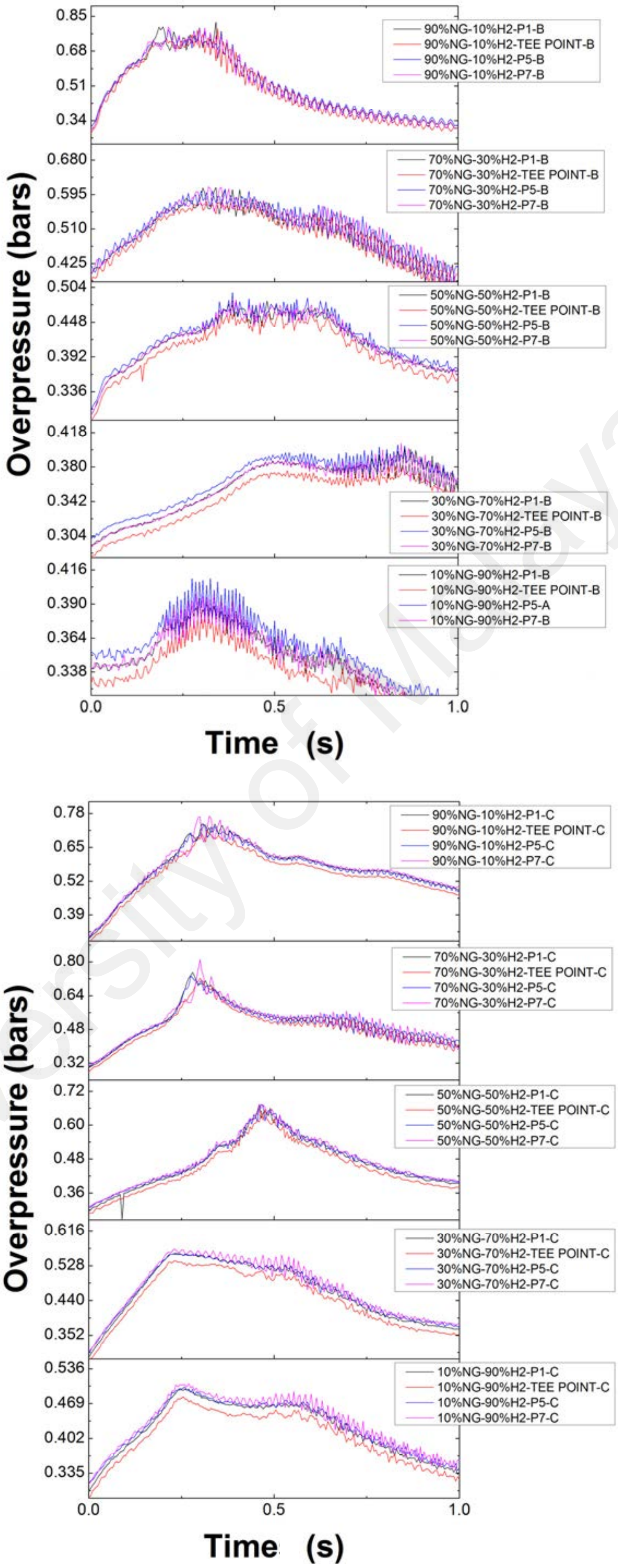

Figure 4 17 Continued

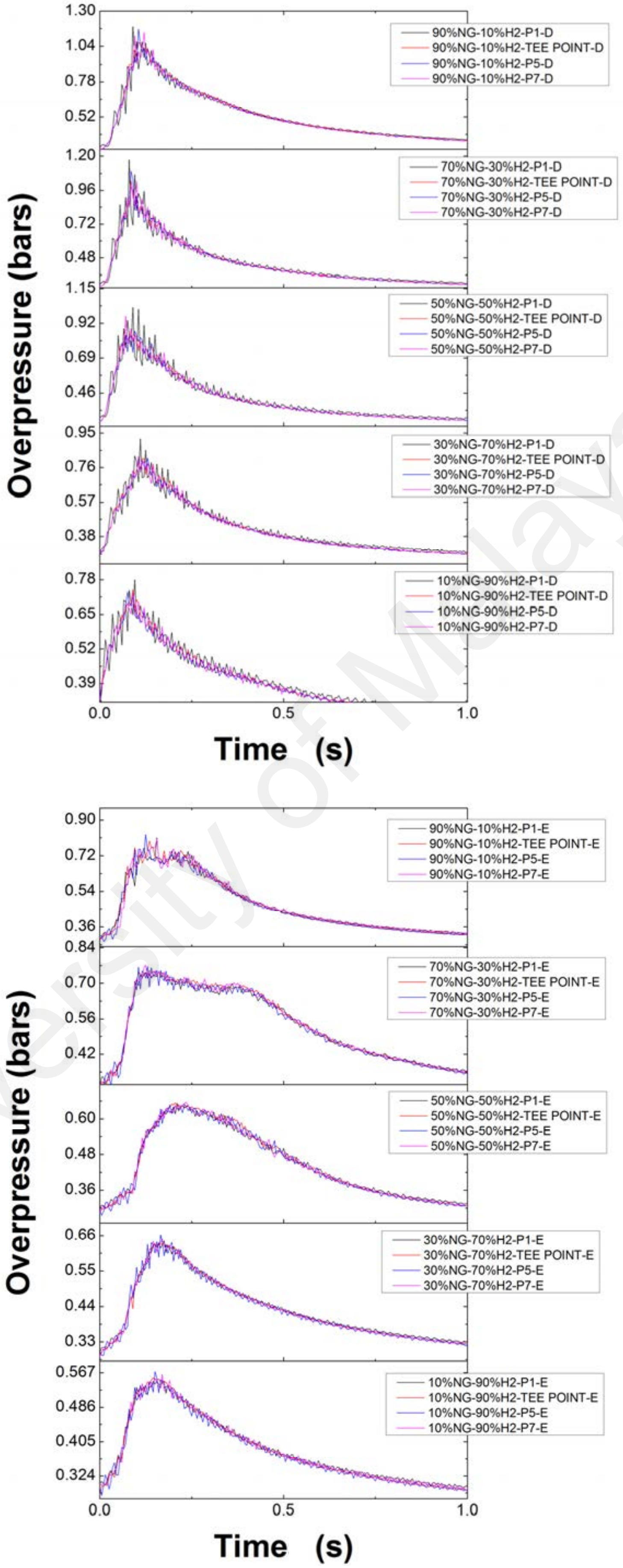

Figure 4. 17 Continued

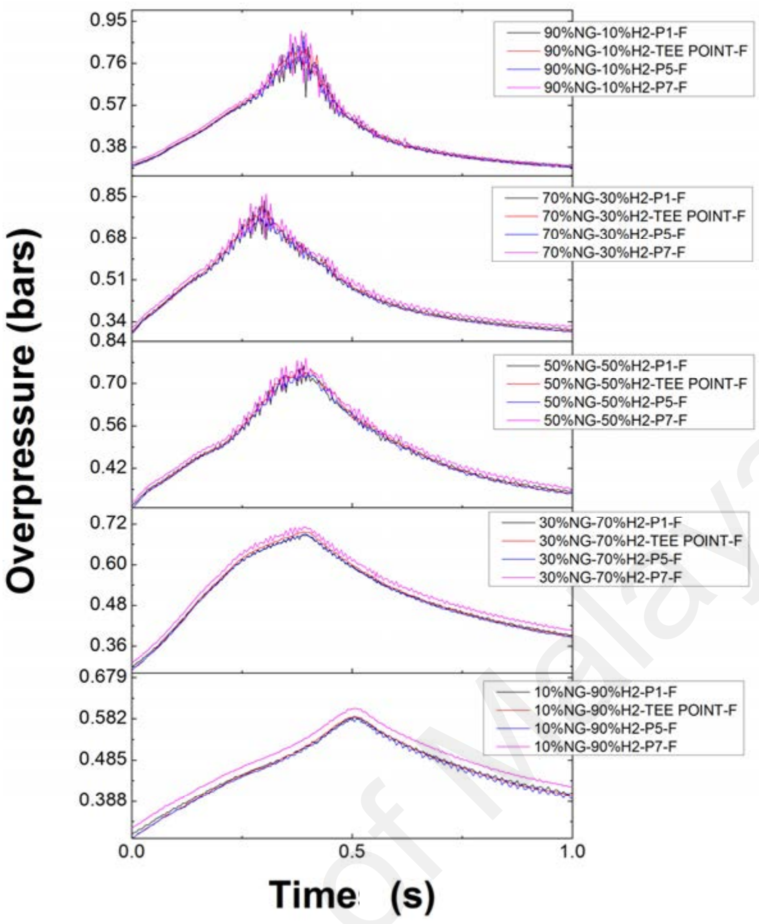

Figure 4. 17 Continued

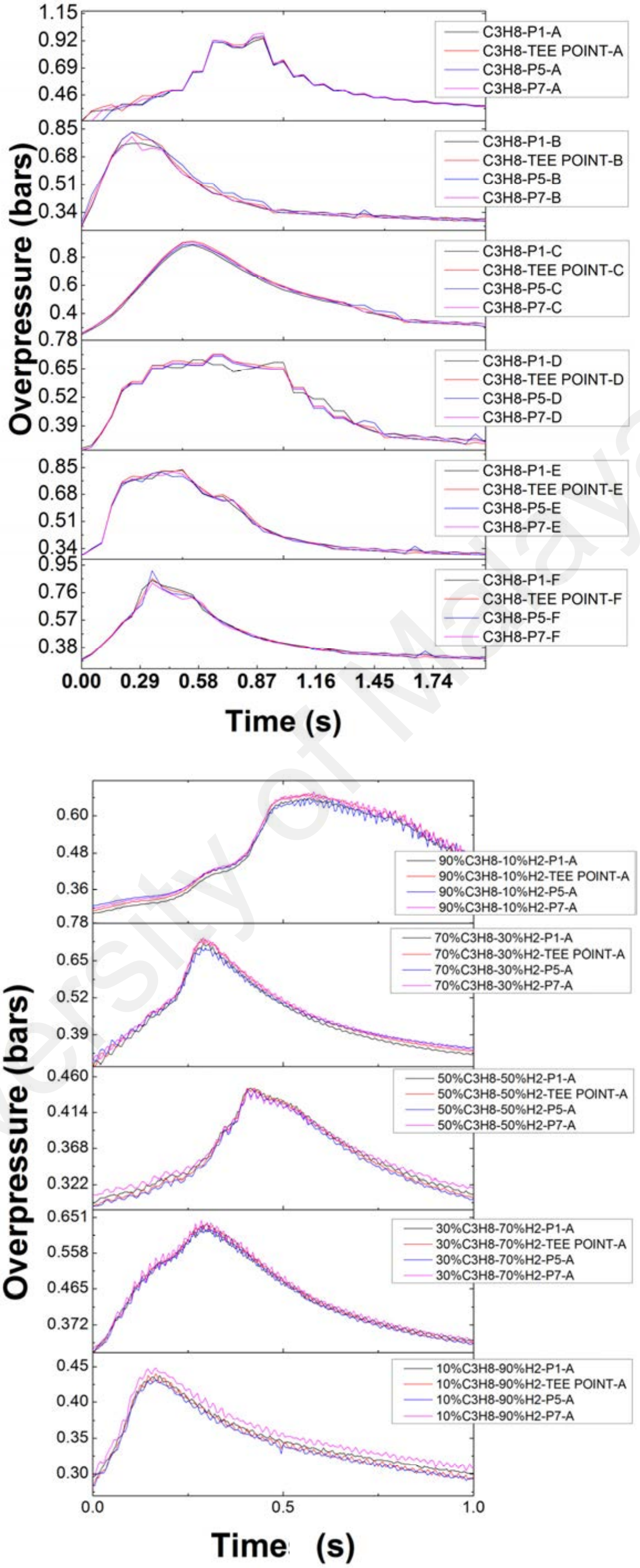

Figure 4. 18 Blast waves – C_3H_8/air and C_3H_8-H_2/air mixtures

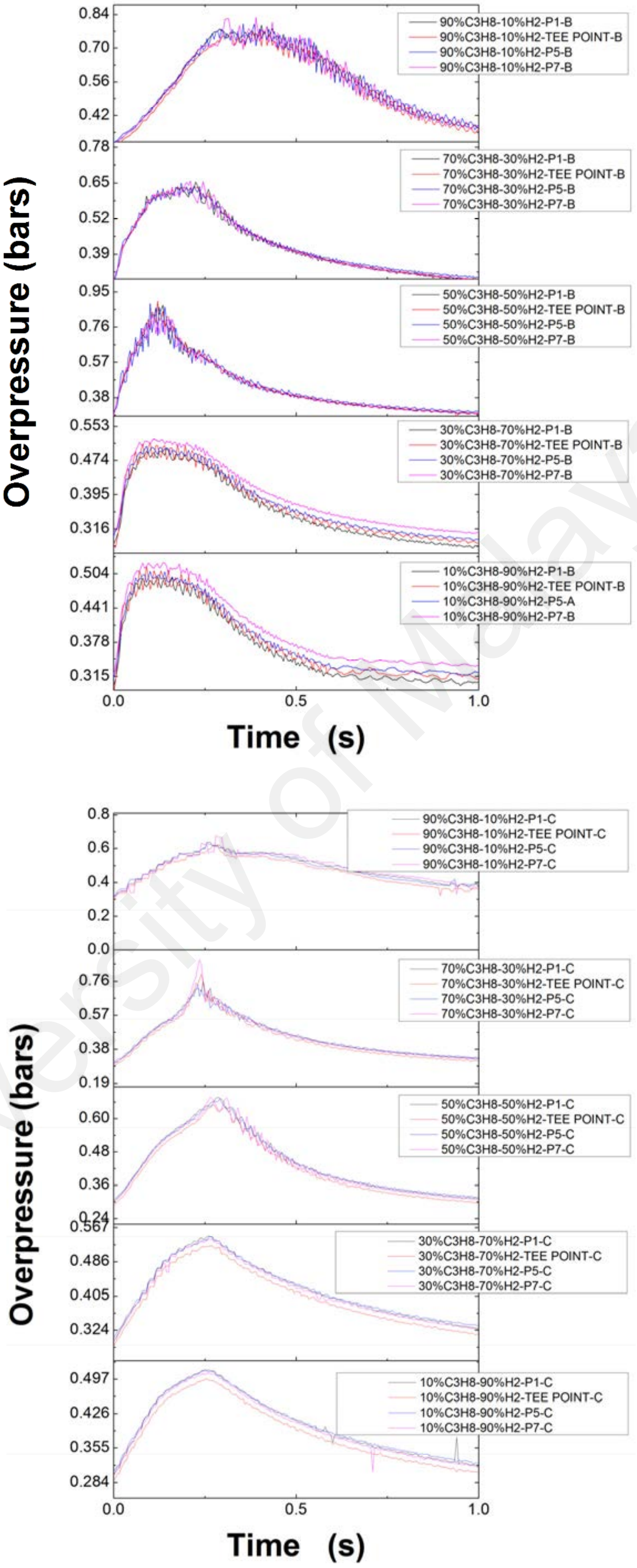

Figure 4. 18 Continued

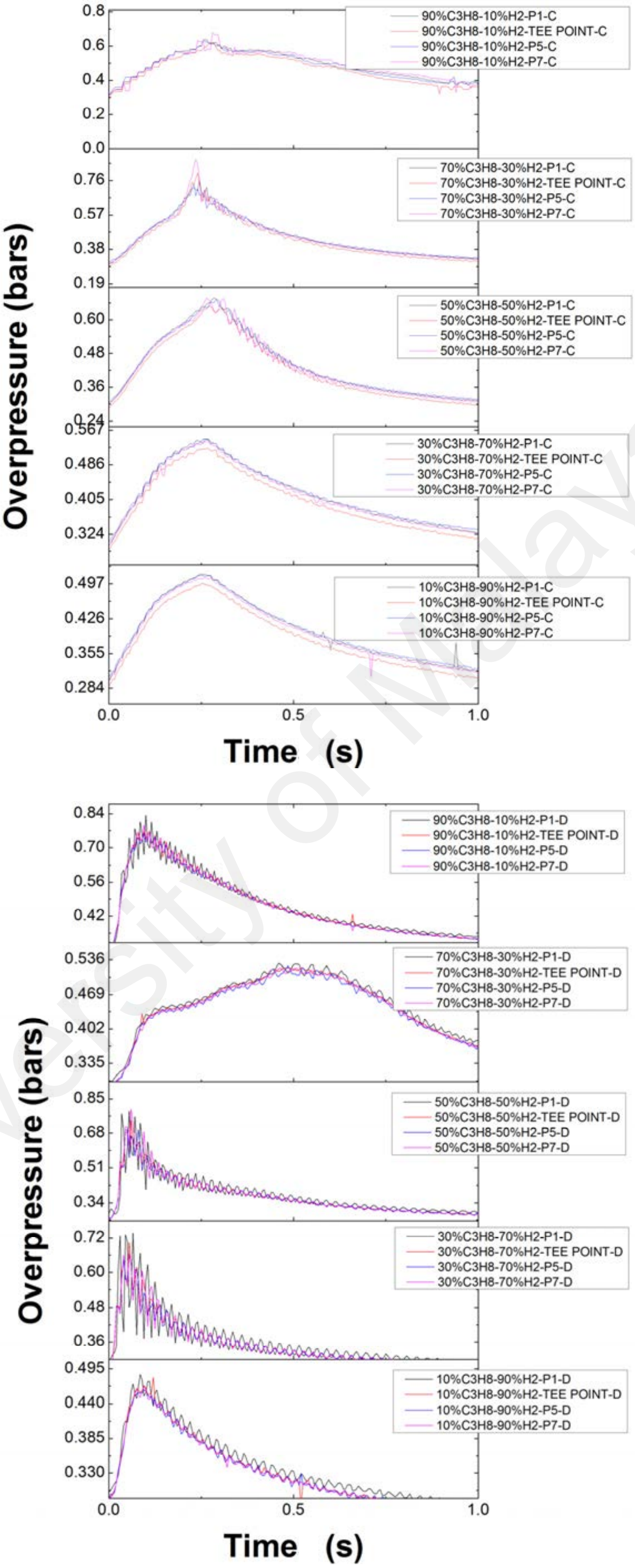

Figure 4. 18 Continued

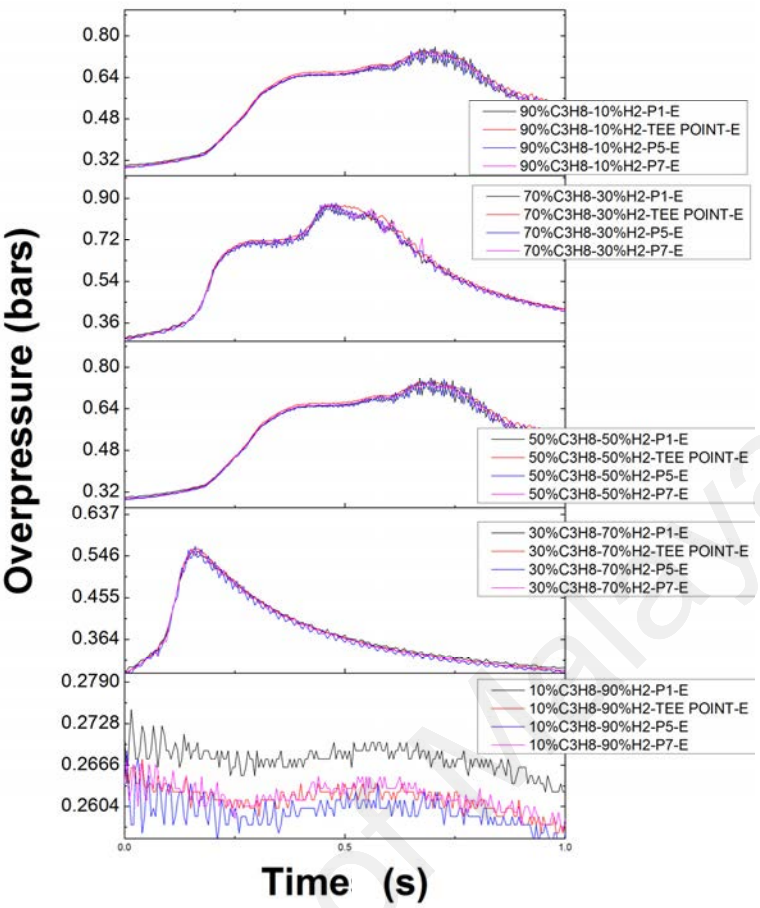

Figure 4. 18 Continued

The Lewis number can justify the inconsistent overpressure of the studied fuels (Figure 4.19). It is associated with the diffusivity rate of species to unburnt gases, which correspond to the mass burning rate. This is the most important factor that affects the burning velocity and heat release rate during flame propagation (Movileanu et al., 2013). Figure 4.15 shows that the value of the Lewis number for all of the ethylene-hydrogen/air and NG-hydrogen/air mixtures was lower than one. This indicates that these mixtures were affected by thermal diffusivity. This is due to the fact that the diffusion coefficient at normal conditions for hydrogen gives a higher ratio of flame temperature and diffusion coefficient (Cussler, 2009). Consequently, the addition of H_2, ethylene and NG tends to diffuse more into the mixtures. Considering the maximum overpressures and flame speeds of the hydrocarbon fuels, it can be said that the flame acceleration of C_3H_8/air was much higher than the others. Furthermore, based on the molecular structure of the fuels, the required energy for the oxidation of C_3H_8/air was lower than the NG/air and C_2H_4/air, respectively. Previous literature has discussed this in detail (Gamezo et al., 2012; Hjertager et al., 1988; Kasmani et al., 2013; Liu et al., 2015; Movileanu et al., 2012; Suga, 1958). However, the results of the propane-hydrogen/air mixtures indicate that their flame acceleration phenomenon was mainly affected by kinetic processing. In the current research, thermal diffusion had insignificant effects, since the diffusion coefficient of the propane was higher than the other studied hydrocarbon fuels. This statement is also in agreement with previous research studies (Lohrer et al., 2008; Razus et al., 2010a).

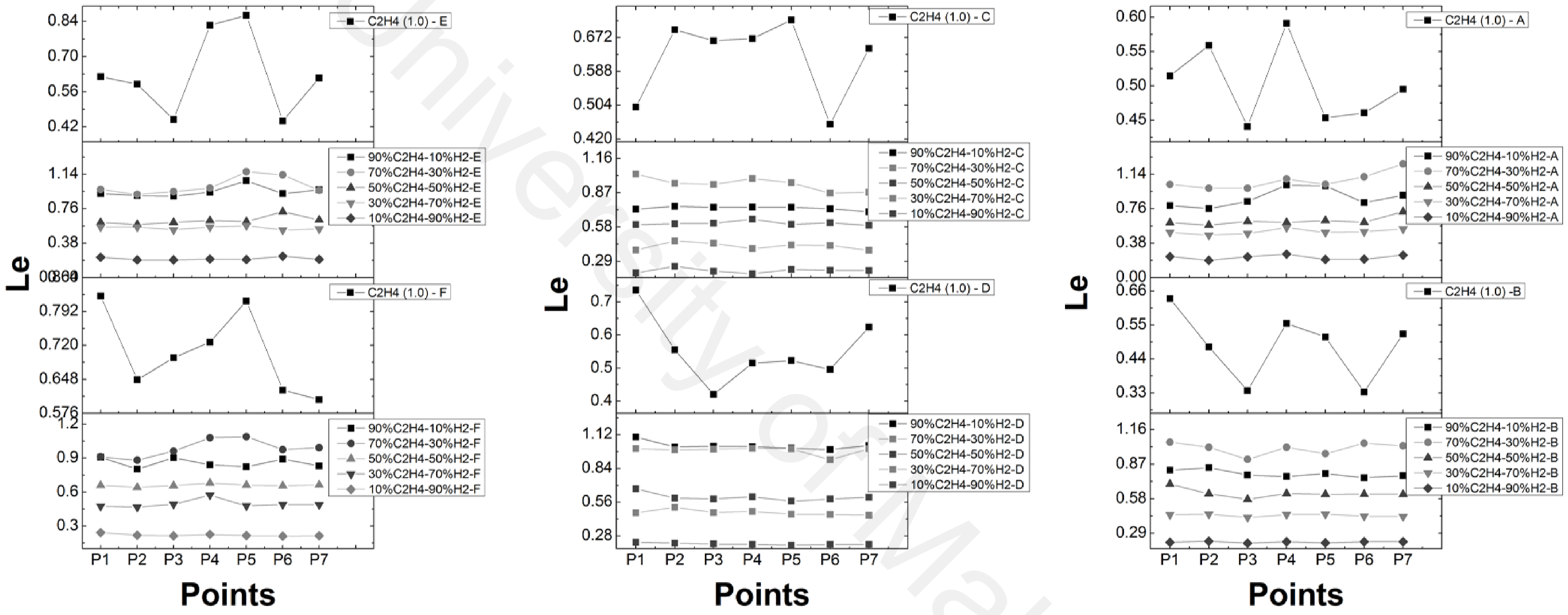

Figure 4. 19 Lewis number vs. the recorded points at different ignition positions

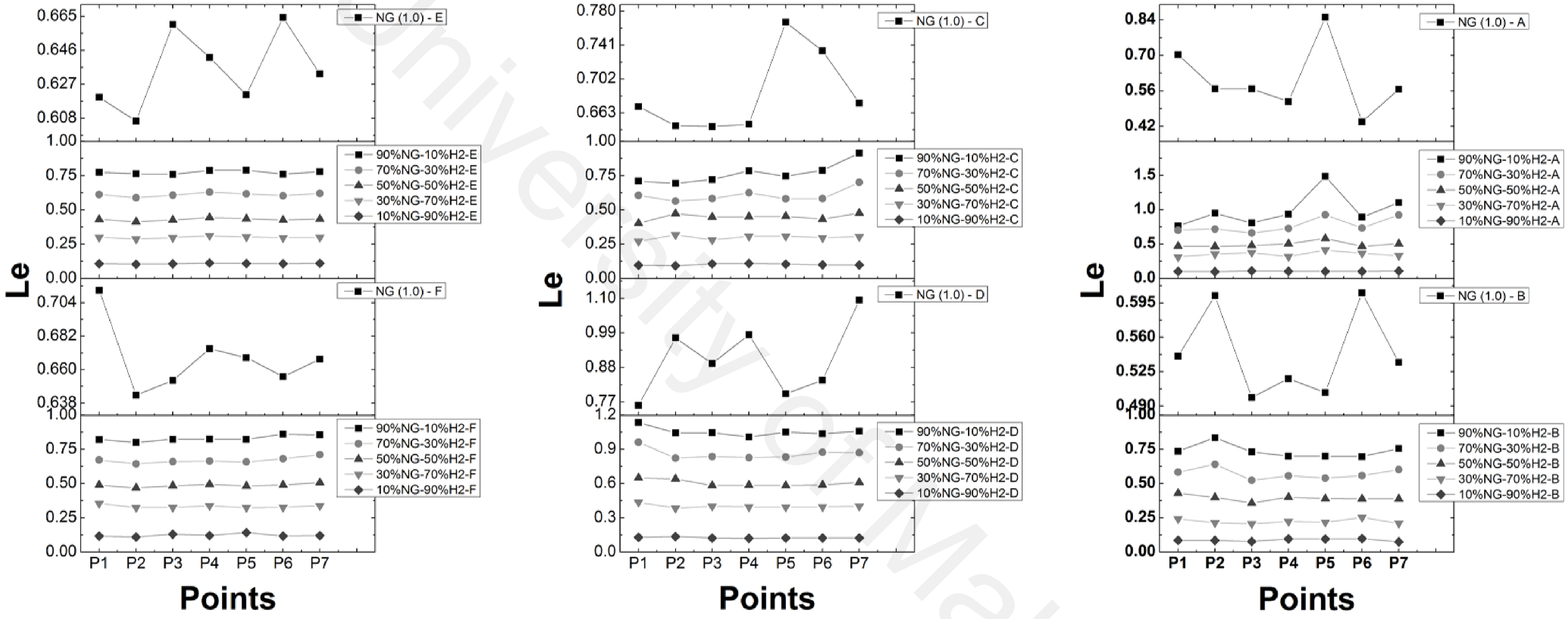

Figure 4. 19 Continued

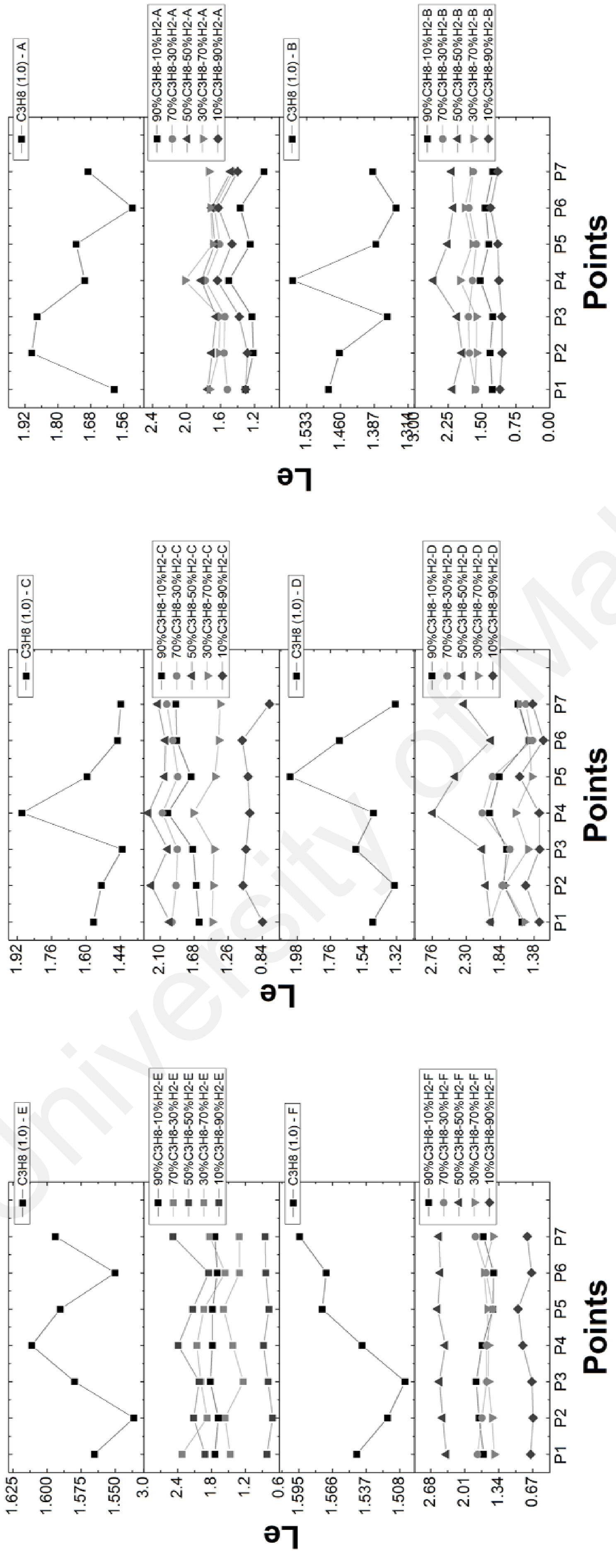

Figure 4. 19 Continued

For the overall observation, the explanation that is offered indicates that the flame reactivity of ethylene-hydrogen/air and NG-hydrogen/air is much higher than others. This is not only because of the kinetic reaction of these mixtures but also, the dynamics of flame deployment in tee junctions have significant effects on the recorded maximum overpressure and flame speeds along the pipes. In comparison with straight and 90 degree pipes, the value of maximum overpressure of hydrogen/air mixture in tee pipes are almost three times lower (Blanchard et al., 2010; Emami et al., 2013). Some investigations have shown that the burning rate increases when the flame front travels through the 90 degree bend (Clanet & Searby, 1996b; Emami et al., 2013; Zhou et al., 2006). Consequently, the value of both the flame speeds and the overpressure were lower at the tee junction compared to similar experiments that were carried out in a straight pipe and 90 degree pipe (Blanchard et al., 2010; Cheng et al., 2009; Emami et al., 2013; Phylaktou et al., 1993). There is no doubt that the presence of the obstacle in the pipe randomizes the flow, thus increasing the flame speed and overpressure, compared to the straight pipe/tube (Phylaktou et al., 1993). However, in a closed pipe/tube, the end wall acts as an obstacle, which has the propensity to initiate the flame perturbation and affect the explosion behaviour (Liberman et al., 2010; Thomas et al., 2010; Zhu et al., 2012). On the other hand, due to the various flame instabilities mechanisms (hydrodynamic instability, thermal diffusion, Darrius-Landau) that are involved in propagation, turbulent flame is developed by generating turbulent flame with the interactions of flame front and the acoustic waves (Bradley et al., 2008; Ciccarelli & Dorofeev, 2008; Gamezo et al., 2008; Liberman et al., 2010). This is because the addition of H2 extends the flammability limits that are associated with hydrocarbons/air triple flames. This is achieved by improving the interactions between the reaction zones (Briones et al., 2008). Consequently, in the current study, while the tee points act like obstacles, the recorded maximum overpressure and flame speed in the tee pipes were lower than the straight and 90 degree pipes. This is due to the free paths after the tee point in two directions (along the pipe and tee junction). Investigations on parallel pipes have also shown a similar phenomenon (Zhu et al., 2012).

However, the effects of tee junction placement on the flame acceleration of fuel gases in tee pipes are undeniable. The recorded data from ignition A and E, as the reference ignition points, shows that the lower distance of tee junction to ignition point causes higher explosion severity, i.e., a high rate of pressure rise. When looking at the overall plots, the fluctuation of maximum overpressures and flame speeds of all of the flames at ignition A was much higher than at ignition E. This condition is due to the influence of dynamic effect during the explosion development, i.e., thermo diffusivity, rapid mixing of the induced turbulence, fast flame downstream, a strong interaction of reflective waves and fast flames from the end points on the flame acceleration of the fuels. These factors cause retonation. In this particular configuration, detonation occurred (Qiao et al., 2005). A similar observation was also reported in parallel pipes with different lengths (Zhu et al., 2012). However, by placing the tee junction on the centre of the horizontal pipe (Figure 3.1b), which was ignited at E, the flame acceleration of the fuel gases showed the lowest intensity on both the overpressures and flame speeds. This is because the flames expended and accelerated almost in a similar distance after the tee junction. Consequently, in this configuration, the interaction of the reflective waves and fast flames from the end points was insignificant. Hassan et al. (1998) and Kolbe and Baker (Kolbe & Baker, 2005) have given a fair discussion on this phenomenon. Furthermore, it should be noted that the different flame paths greatly depend on the ignition location. This varies the flame propagation mechanism on each of the ignition positions. There is another interesting observation that is worth mentioning.

To facilitate the explanation of the findings, the unburnt gas velocity (Sg) was calculated and plotted for all of the mixture compositions, as given in Figure 4.20. As presented, in terms of overpressure and flame speeds, the hydrocarbons/air flames had a minimum fluctuation along the tee pipes at the entire ignition positions (refer to Figures 4.11-4.14). In this condition, it seems that the ignition position played a significant role in determining the maximum overpressure of these mixtures. As can be observed from the figures, the maximum overpressures were recorded in the early stages after ignition, before travelling in a smooth speed afterwards. By giving more attention to the Sg of these flames, it can be understood that the conflicts between the flame front and unburnt gases in these particular mixtures were insignificant. Consequently, this particular gas could not produce shock waves, since its overdriven detonations were not strong enough (Blanchard et al., 2011). The associated flame speed and rate of pressure rise at the same orientations followed the trends of the overpressures at all of the ignition points. This statement is also in agreement with previous investigations on the flame acceleration of hydrocarbon fuels (Cho & He, 2007; Kumar et al., 2007; Movileanu et al., 2011a, 2011b; Prince & Williams, 2012). Furthermore, the recorded blast waves of the flame also showed the linearity of the flame acceleration of hydrocarbons/air fuels in the tee pipe. However, it depends on many factors, i.e., the location of the tee junction and ignition points, and the duration of the acceleration of the flames. This is due to the direction and starting point of the flame acceleration. It is worth mentioning that the flame reactivity of ethylene/air and NG/air increased by adding hydrogen. Hence, the flame front and unburnt gases increased, since the concentrations of H and OH radicals increased (Cammarota et al., 2009; Cammarota et al., 2010; Hu et al., 2009b; Hu et al., 2009c; Miao et al., 2008; Salzano et al., 2012). As mentioned earlier, the flame reactivity of C_2H_4-H_2/air and NG-H_2/air, with ratios of 90:10 and 70:30, were most pronounced. This is due to the dynamic effect, i.e., the thermo diffusivity, rapid mixing of the induced turbulence and fast flame downstream. Since the induced maximum value of Sg was calculated to be less than 340 m/s, the flame travelled with a slight impact at the end pipe. Consequently, the fluctuation rate of each monitoring point, depending on the mixture and ignition position, more or less had wrinkling in terms of pressure changes in the specific time period.

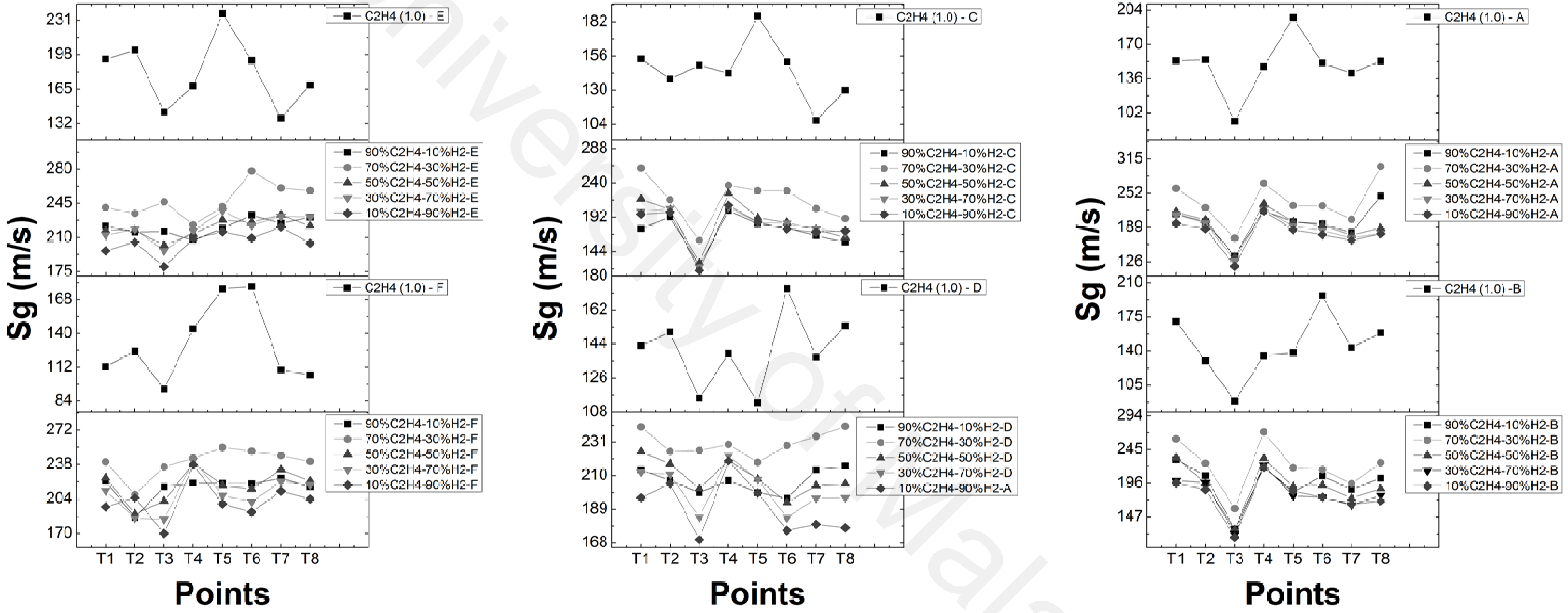

Figure 4. 20 Unburned gas flame speed vs. the recorded points at different ignition positions

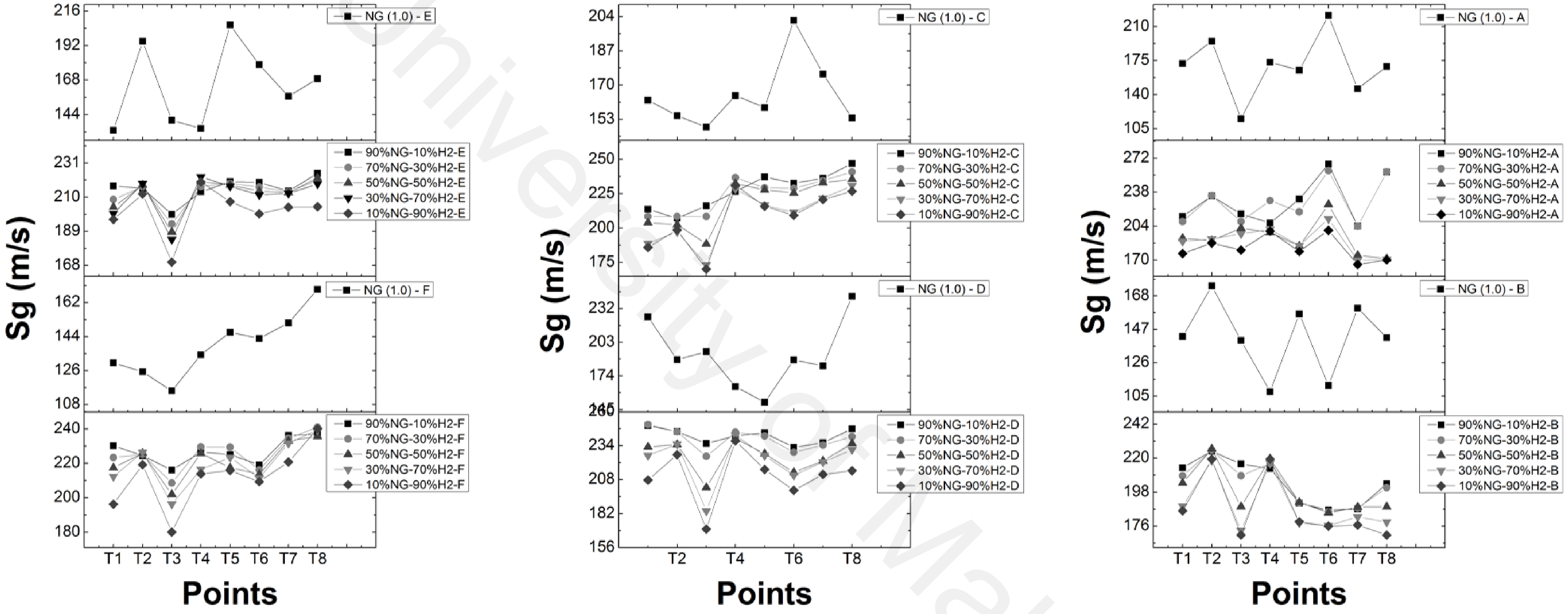

Figure 4. 20 Continued

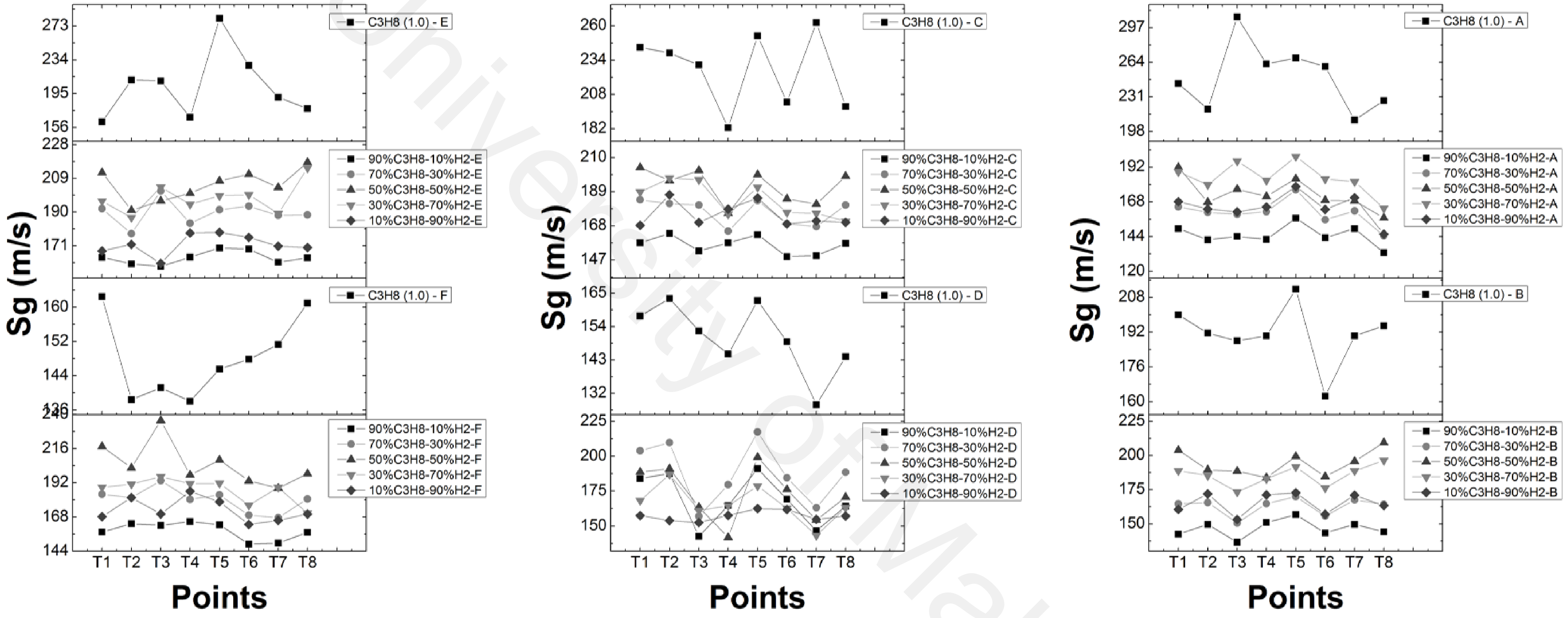

Figure 4. 20 Continued

4.4. Effectiveness of Inhibitors on Flame Acceleration of Hydrogen

4.4.1. Effect of Inhibitors to Pressure and Flame Speed in Explosion Development

A set of recorded maximum overpressures along the tee pipe at different ignition positions are presented in Figure 4.21. These are in reference to the stoichiometric hydrogen/air mixtures, which were diluted with various amounts of CO_2, Ar and N_2. As a function of the recorded points, the corresponding flame speed and rate of pressure rise (dP/dt) are plotted in Figure 4.22 and Figure 4.23. Considering the hydrogen/air as a prime fuel, it is found that the pressure drop and flame linearity were more significant in the presence of CO_2, i.e., 95%H_2-5%CO_2/air, 95%H_2-2.5%CO_2-2.5%N_2/air and 95%H_2-2.5%Ar-2.5%CO_2/air. As reported by Di Benedetto et al. (2009), the presence of free radicals, including O, H, CO, HCO, OH, HO_2 and CO_2, causes the rate of overpressure, flame speed and rate of pressure rise to decrease significantly, as illustrated in Figure 4.21-4.23. Among the inhibitors, the argon in the hydrogen/air mixtures gave a higher overpressure, compared to the others. Based on the work carried out by Movileanu et al. (2013), the presence of additives changes the thermo-physical properties of unburned mixtures (thermal conductivity and heat capacity) and this directly affects the overall reaction rate in the reaction zone (in the flame front). Kwon and Faeth's (2001) investigation also showed that, even though nitrogen and argon have almost similar transport properties, the addition of argon into hydrogen could cause a higher laminar burning velocity due to the higher flame temperature. This mechanism suggests that the effectiveness of inhibitors should be in the order of $Ar < N_2 < CO_2$.

On the other hand, from Figure 4.22, it can be said that there was a significant change in the flame speed rate along the centreline of the pipe and end points at all of the ignition positions. This is due to the fuels' reactivity (Zhu et al., 2010). The highest flame speed recorded was at the average of 736, 719, 706 and 703 m/s on 95% H_2-2.5%Ar-2.5%N_2/air,

$95\%H_2$-$5\%N_2$/air, H_2/air and $95\%H_2$-$5\%Ar$/air mixtures, respectively for all of the ignition positions. This was also in agreement with a previous studies (Kwon & Faeth, 2001; Qiao et al., 2005). Moreover, by comparing the flame speed of these mixtures with the $95\%H_2$-$5\%CO_2$/air at a similar condition, the linearity of this mixture was higher, since the average recorded maximum flame speed of 599 m/s for this particular mixture was lower for all of the ignition positions. This suggests that the addition of CO_2 into hydrogen mixtures caused the heat release rate to decrease and consequently, the average value of the flame speed for this mixture to be lower. This observation is also in agreement with previous research studies regarding the lower concentration of CO_2 in a mixture (Di Benedetto et al., 2009).

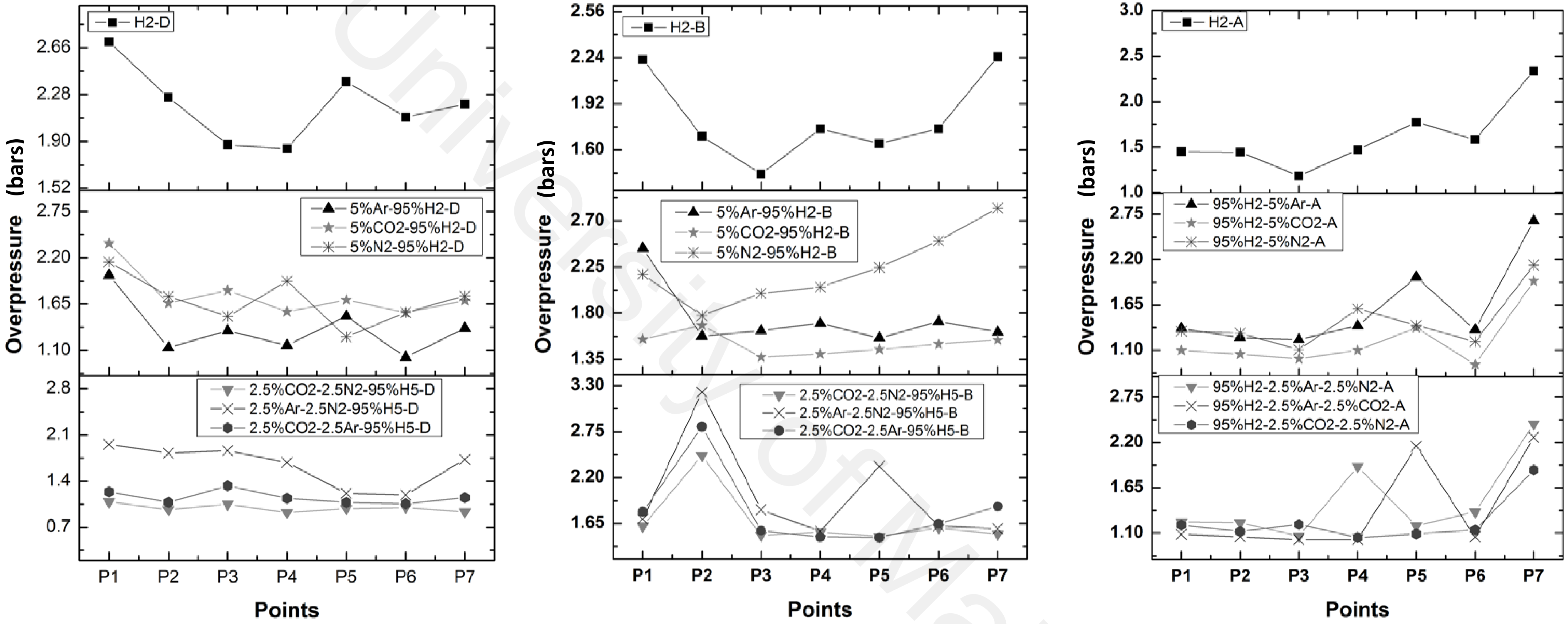

Figure 4. 21 Maximum overpressure vs. the recorded points in a Tee pipe at different ignition positions.

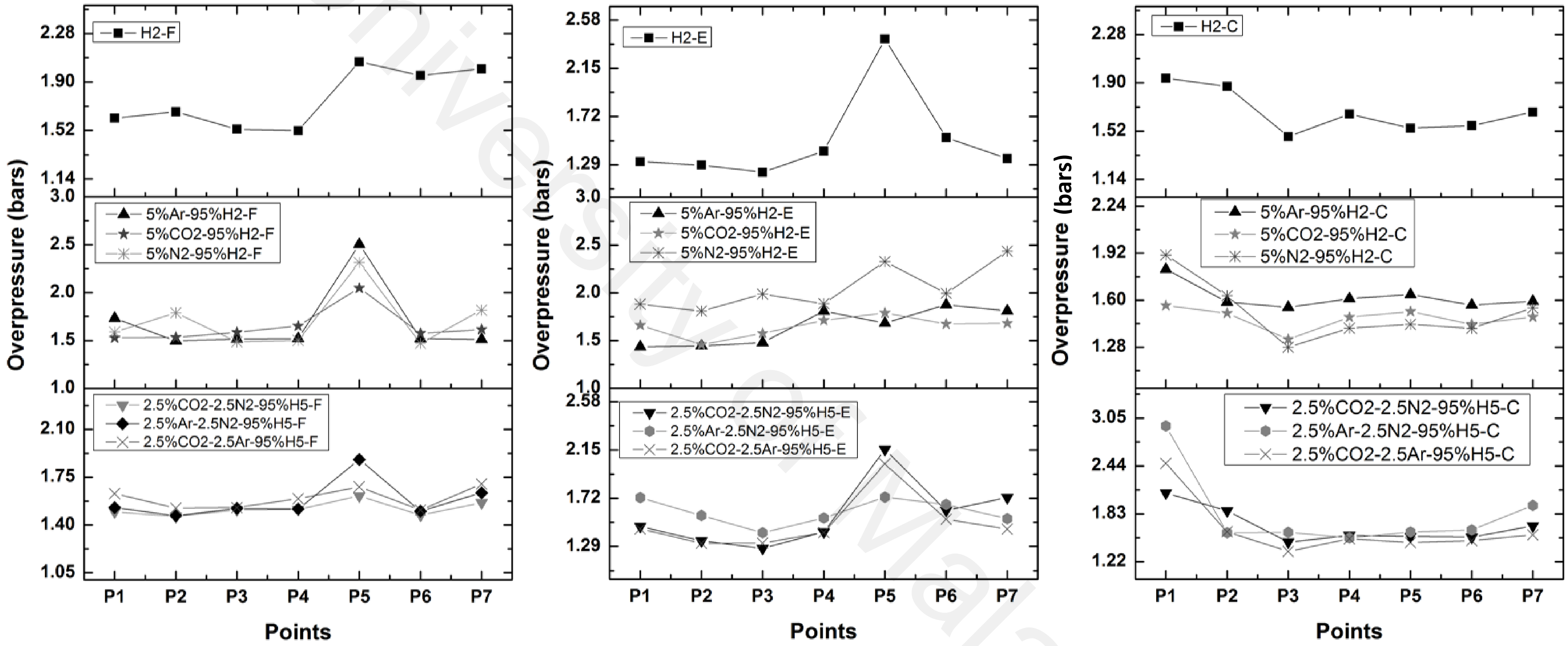

Figure 4.21 Continued

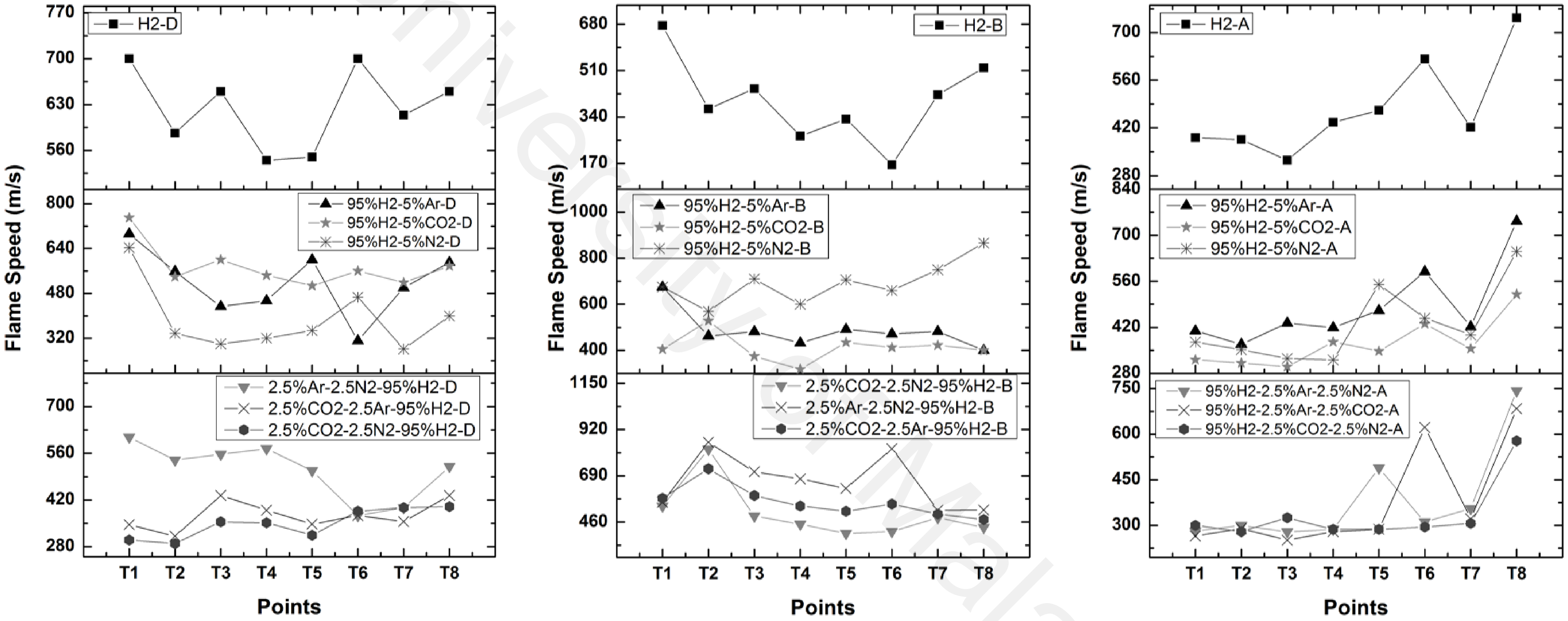

Figure 4. 22 Maximum flame speed vs. the recorded points in a Tee pipe at different ignition positions

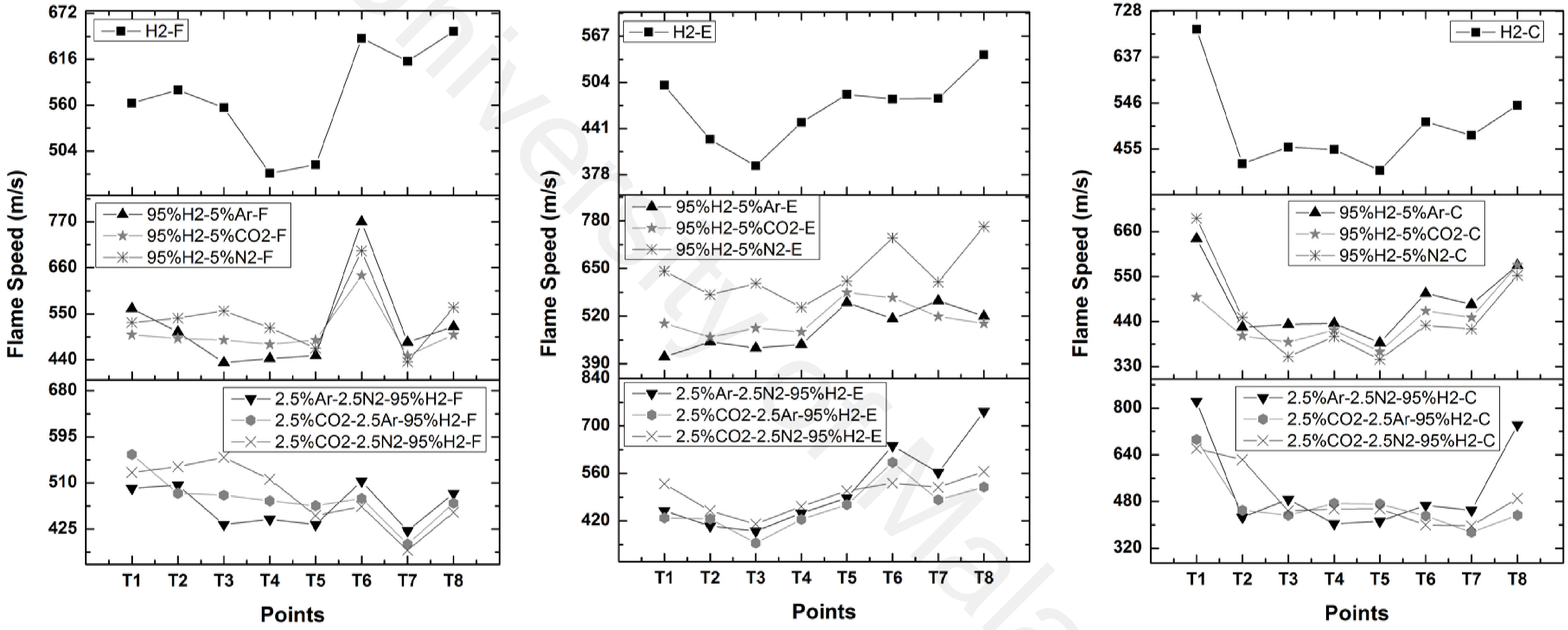

Figure 4. 23 Continued

The effect of inhibitors on the explosion development on stoichiometric hydrogen/air mixtures can be better explained by plotting Lewis numbers (see Figure 4.23). The Lewis number is associated with the diffusivity rate of species to unburnt gases, corresponding to the mass burning rate. This is the most important factor that affects the burning velocity and heat release rate during flame propagation (Movileanu et al., 2013). As it can be seen in Figure 4.23, the value of the Lewis number for all of the mixtures was lower than one. This indicates that all of the mixtures were affected by thermal diffusivity. However, this phenomenon is more significant for those mixtures that consisted of argon. This is due to the fact that the diffusion coefficient at normal conditions for argon ($2x10^{-5}$ $cm^2.s^{-1}$) was higher than N_2 ($1.88x10^{-5}$ $cm^2.s^{-1}$) and CO_2 ($1.92x10^{-5}$ $cm^2.s^{-1}$), giving a higher ratio of flame temperature and diffusion coefficient (Cussler, 2009). Consequently, by adding argon, H_2 tended to diffuse more into the mixtures.

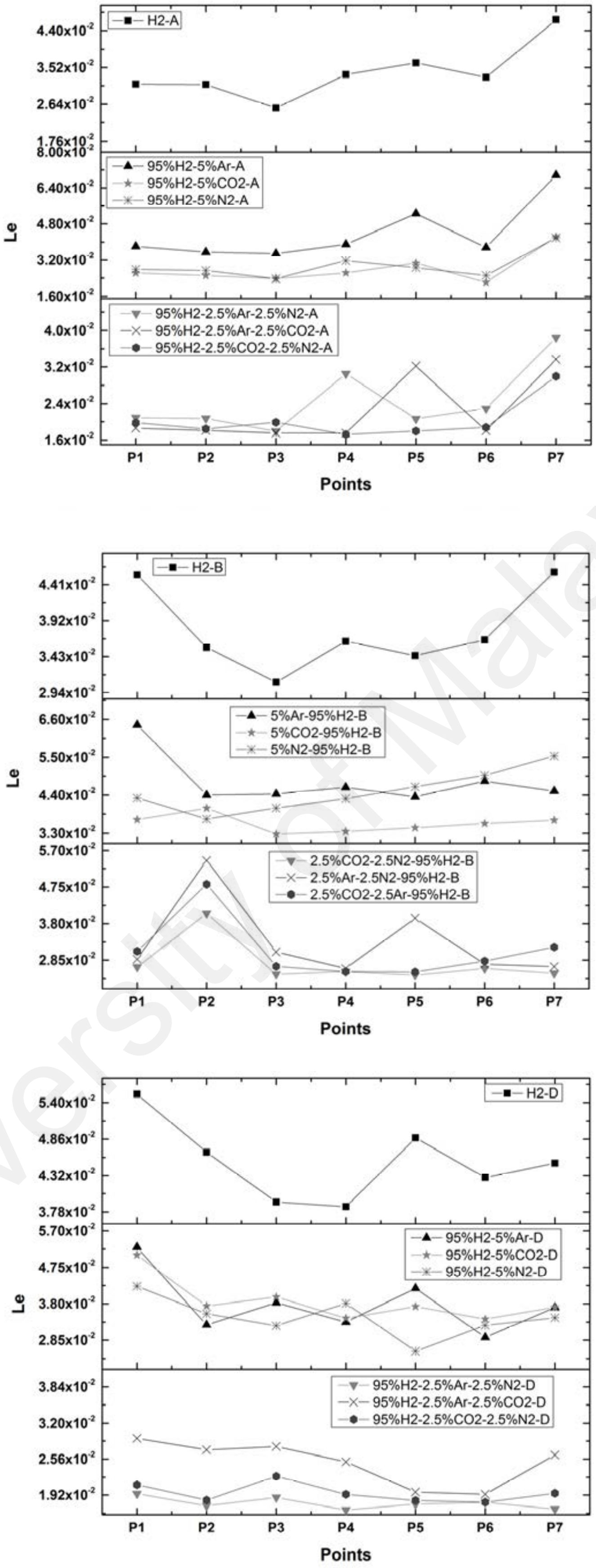

Figure 4. 23 Lewis number vs. the recorded points in a Tee pipe at different ignition points.

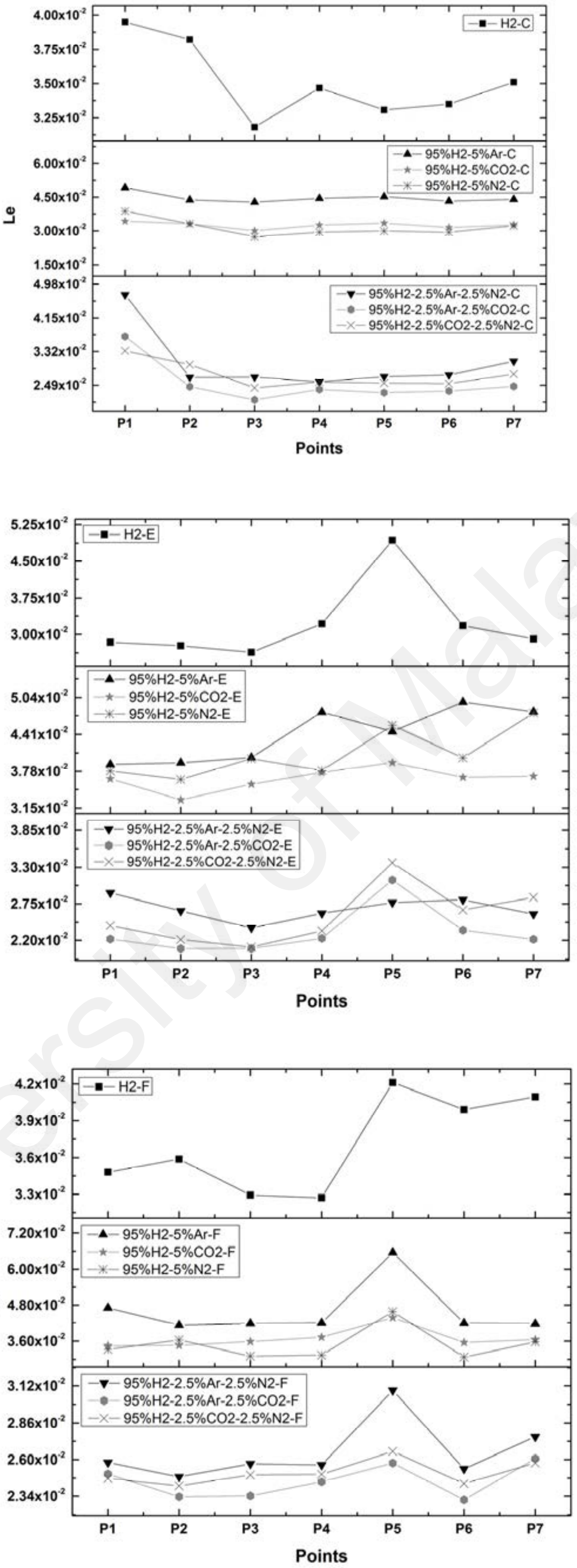

Figure 4. 23 Continued.

From the overall observations, it is noted that the overpressure plot of 95%H_2-5%N_2/air mixtures posed a different trend at all of the ignition positions. The maximum peak overpressure, flame speeds and rate of pressure rise allocated along the pipe were spotted at different points. An explanation for this can be offered as follows: the momentum movement of the N_2O, NNH and NO radicals gave variation on the explosion pressure development and this directly affected the rate of pressure rise and flame speed ratio. This is because the contribution of the N_2O intermediate route rose much faster than the other routes that were involved in the reaction (Guo et al., 2005a). Besides, it should be noted that the different flame paths greatly depended on the ignition location. This varied the flame propagation mechanism of each of the ignition positions. There is another interesting observation that is worth mentioning. The flame reactivity of 95%H_2-2.5%Ar-2.5%N_2/air mixtures gave higher values on the overall overpressure, flame speeds and rate of pressure rise - approximately two times higher than that of the 95%H_2-2.5%Ar-2.5% CO_2 composition (Figure 4.24). As mentioned earlier, with regards to the effect of N_2 on the inhibitors-fuel mixtures, the unique dynamic properties (flame diffusivity and thermal conductivity) of argon also played an important role in intensifying the combustion of the mixtures.

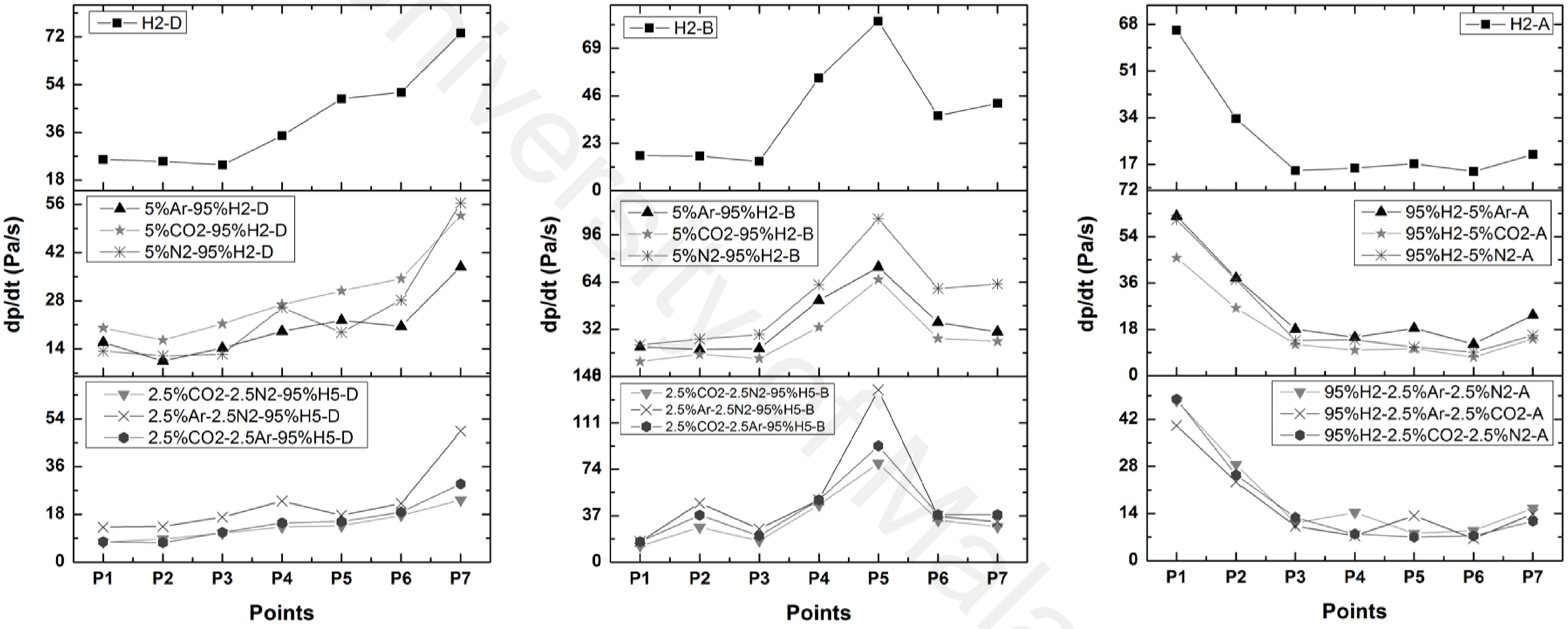

Figure 4. 24 Rate of pressure rise vs. the recorded points in a Tee pipe at different ignition positions

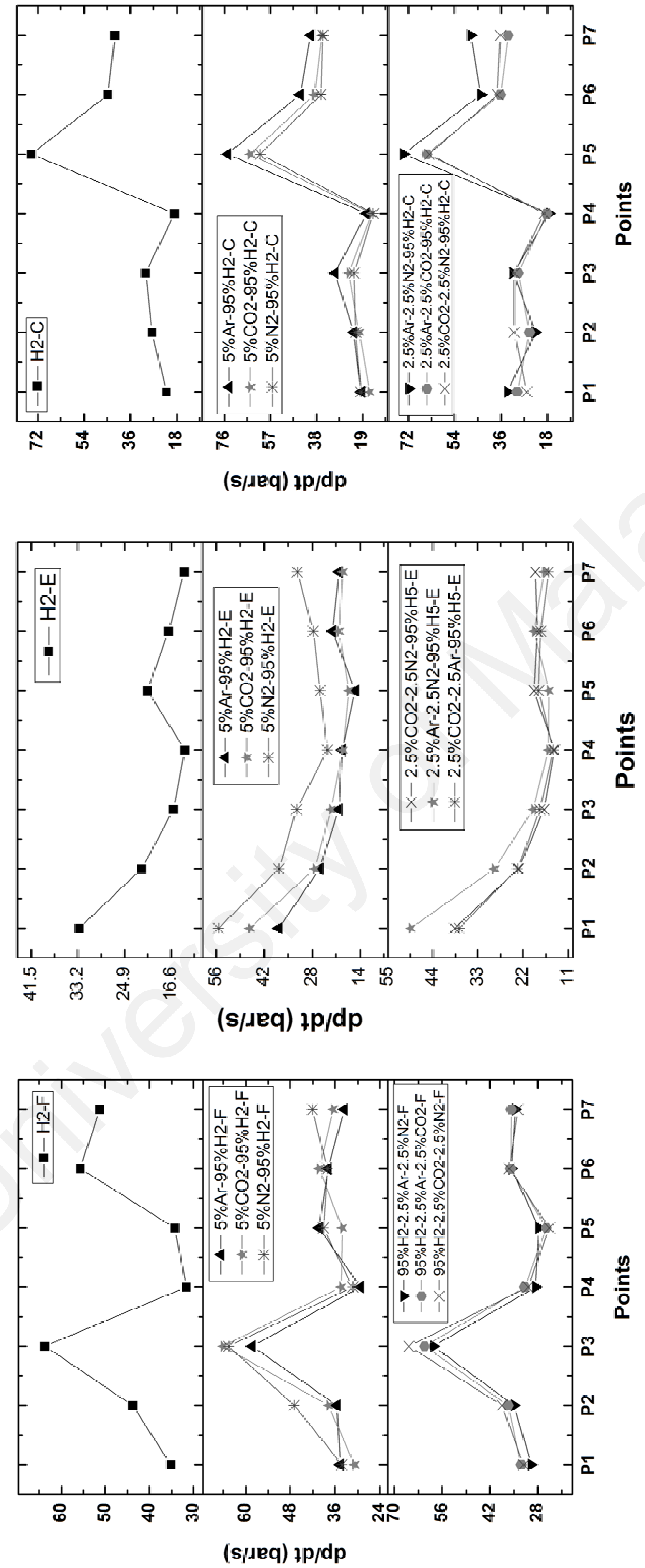

Figure 4. 24 Continued

4.4.2. The Influence of Ignition Positions to Overall Explosion Development

To facilitate the explanation of the findings, the unburnt gas velocity (Sg) was calculated and plotted for all of the mixture compositions, as given in Figures 4.25 and 4.26. As mentioned earlier, the flame reactivity of 5%Ar-95%H_2/air and, partially, 5%N_2-95%H_2/air and 2.5%Ar-2.5%N_2-95%H_2/air were mostly affected due to the dynamic effect, i.e., mass diffusivity and rapid mixing of the induced turbulence and fast flame downstream. Since the induced maximum value of Sg was calculated to be more than 340 m/s, the flame travelled with a higher speed, giving a massive compression impact at the end pipe and hence, promoting a strong interaction between the fast flame and reflective wave. This phenomenon is known as retonation and was markedly sound if the ignition started at position A and D. Previous research studies (Sabard et al., 2013; Di Benedetto et al., 2009) gave a similar observation on this phenomenon. However, the ignition position B had an opposite impact on both the pressure and flame development in the Tee pipe configuration. The blended inhibitors-fuel/air mixtures did not guarantee that the explosion risk posed on the obstacles would be minimized. Application of the inerting method is a recommended protection and mitigation measure for an explosion hazard. Instead, in this study, when the method was considered at this particular ignition point, it gave a 'vulnerable condition'. As shown in Figure 4.25, the maximum overpressure for 2.5%CO_2-2.5%N_2-95%H_2/air, 2.5%Ar-2.5%N_2-95%H_2/air and 2.5%CO_2-2.5%Ar-95%H_2/air were observed at P2 for the ignition initiated at B. Previous studies show that, with a wider fuel variation, i.e., composition of the blended mixtures, the Lewis number is directly proportional with the wider Markstein numbers (Bell et al., 2007). Based on this justification, it can be said that the flame acceleration, which was ignited at position B, was mainly affected by thermal diffusivity. It further indicates that the transition of the flame deformation into detonation and a strong interaction of reflective waves and fast flames from the end point could be possible causes for the maximum overpressure that was experienced at P2. Furthermore, at position B, the mixtures consisting of 5%N_2-95%H_2/air and 2.5%Ar-2.5%N_2-95%H_2/air gave overpressure, which was also picked at P5 and P7 in the former and at P5 in the latter. This is not only due to the mentioned reasons but also, the mixtures experienced strong thermal diffusivity in the presence of Ar and N_2, as explained in the previous section. This phenomenon is also discussed by Qiao et al. (2005).

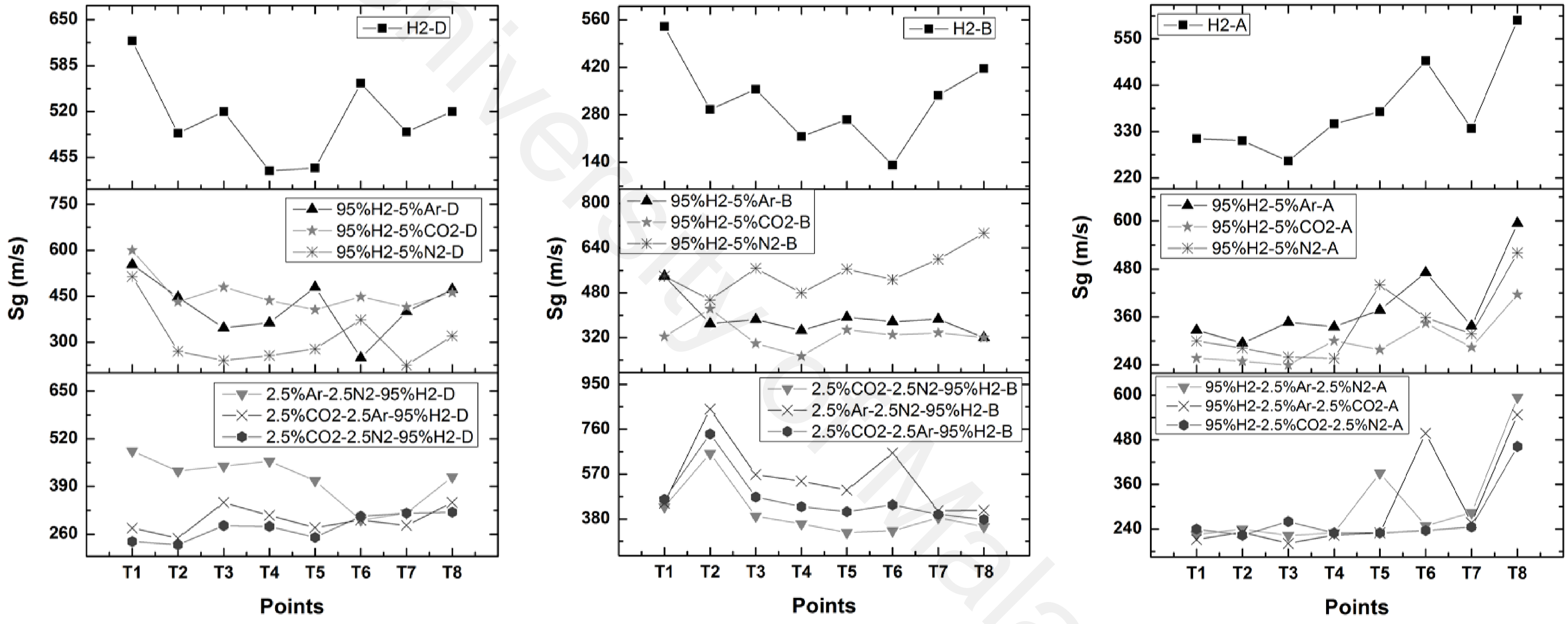

Figure 4. 25 Unburnt gas flame speed vs. the recorded points in a Tee pipe at ignition points A, B and D

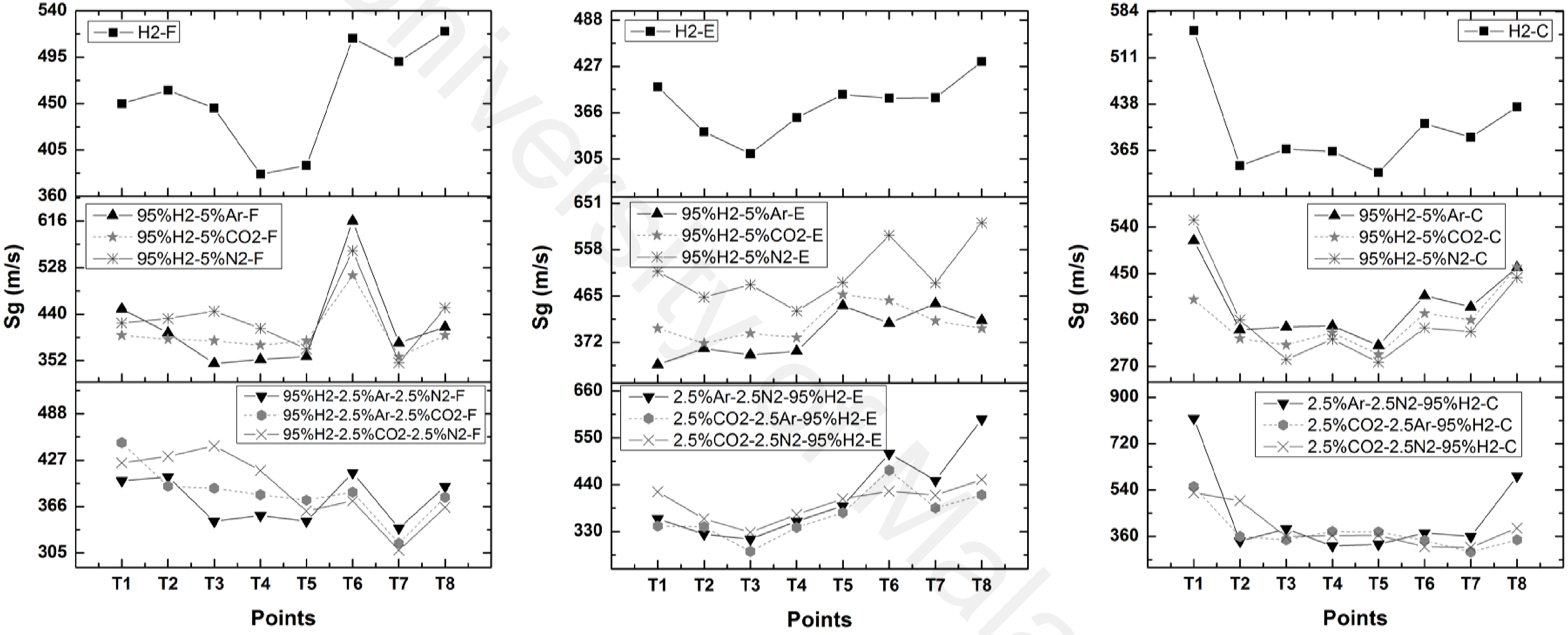

Figure 4. 26 Unburnt gas flame speed Vs. recorded points in a Tee pipe at ignition points C, E and F

Giving more attention to overpressure trends of all mixtures at C, E and F ignition positions, it can be found that the trends and pick point for all mixtures at same ignition position are almost same. As shown in figure 4.21, the maximum overpressures were recorded at P1 for ignition C and, at P5 for latter ignitions. It indicates that the flames tend to growth in the direction with longer distance. It is also in agreement with previous investigations (Kindracki et al., 2007; Zhang et al., 2011). Same as ignition position A and D, retonation phenomenon happens for ignitions C, E and F due to a massive compression effect at the end pipes which is promoting a strong interaction between fast flame and reflective wave. For giving more clarification, the the fluctuation rate of all mixtures at P1, Tee point, P5 and P7 at t =1 ms are presented by blast wave in Figure 4.27 and 4.28. As fairy discussed in the literature, the flames of the mixtures with Lewis number lower than 1 were wrinkled by diffusional-thermal instability which cause higher flame speed and more overpressure intensity (Kim et al., 2014). As shown, hydrogen/air, 5%Ar-95%H_2/air, 5%N_2-95%H_2/air and 2.5%Ar-2.5%N_2-95%H_2/air mixtures travels with short duration to reach the end pipe and maximum overpressure in these ignition points, at consequent, the rate of pressure rise and flame speed are higher due to associated dynamic effect i.e. thermodiffusivity that has been discussed fairly earlier.

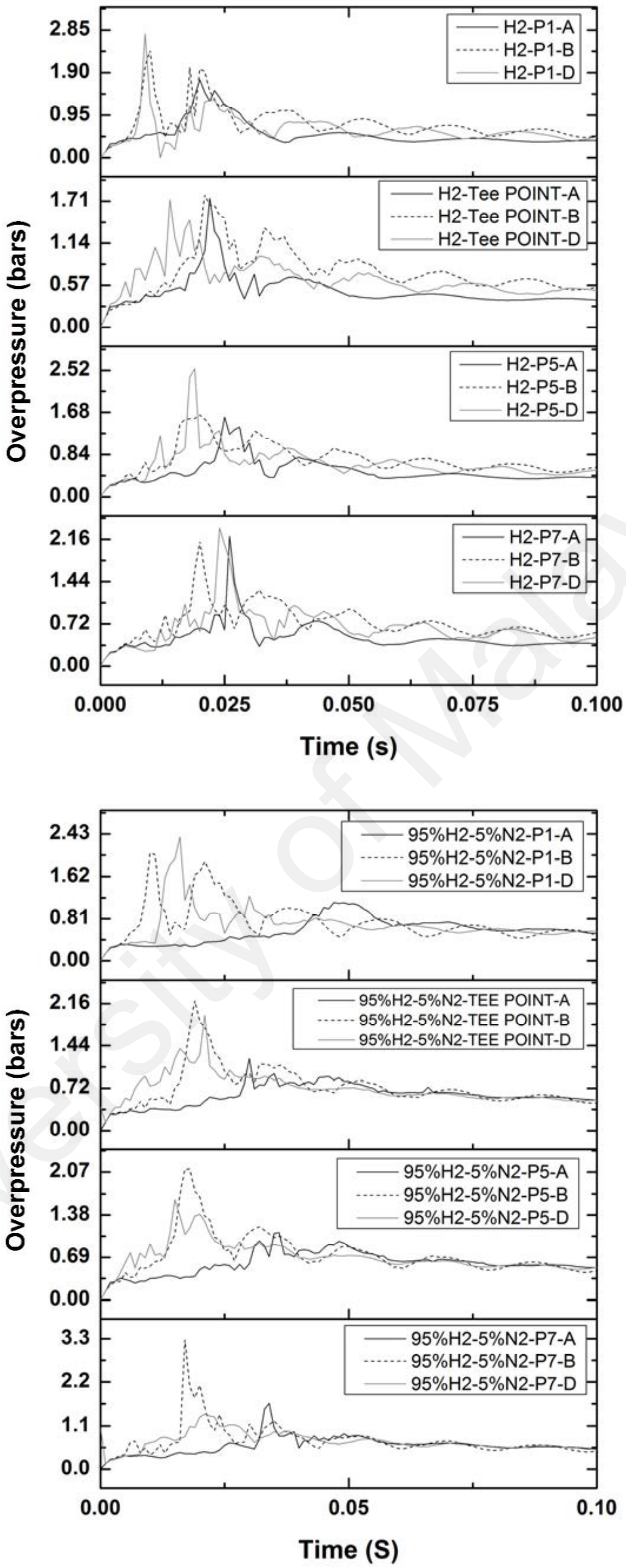

Figure 4. 27 Blast wave in P1, Tee point, P5 and P7 at ignition position A, B and D

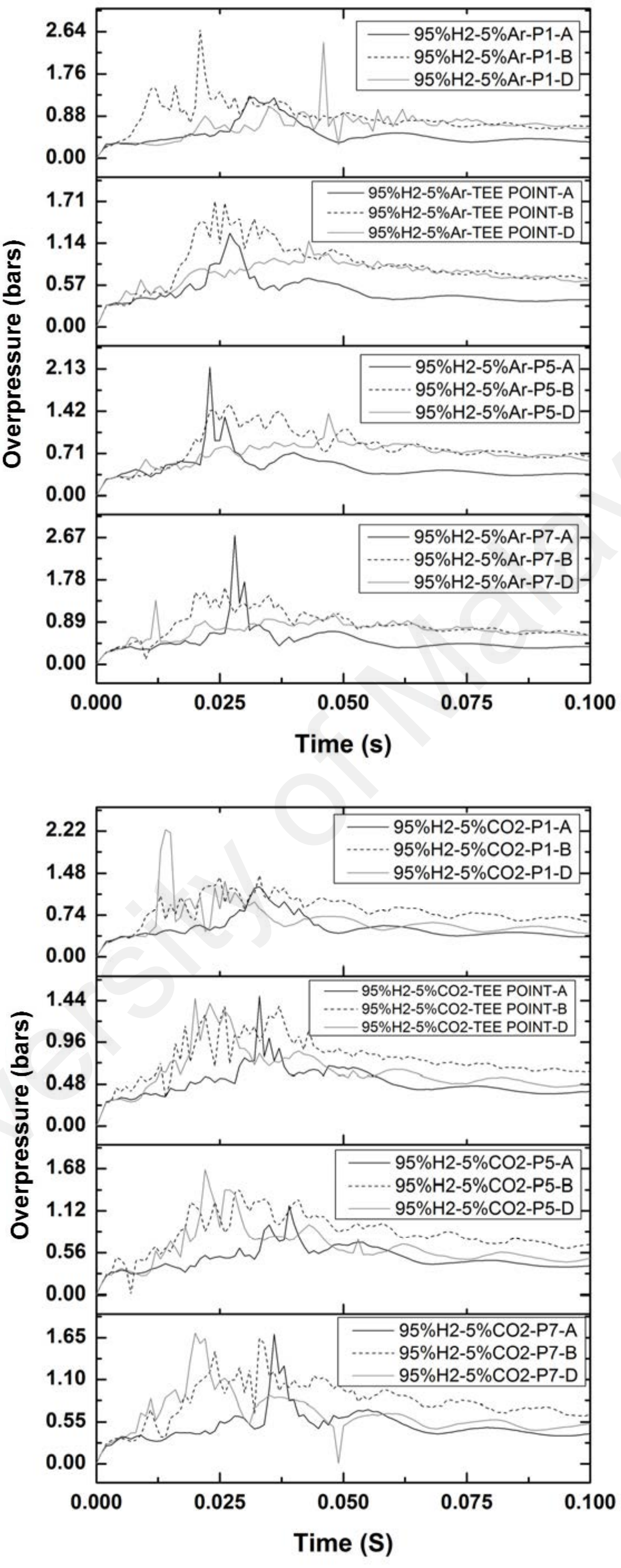

Figure 4. 27 Continued

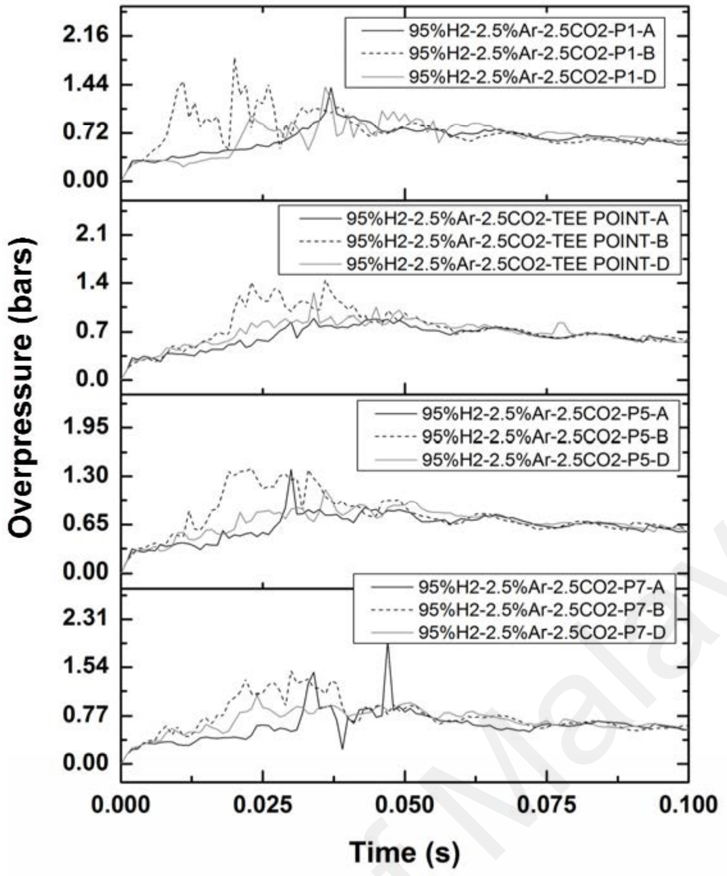

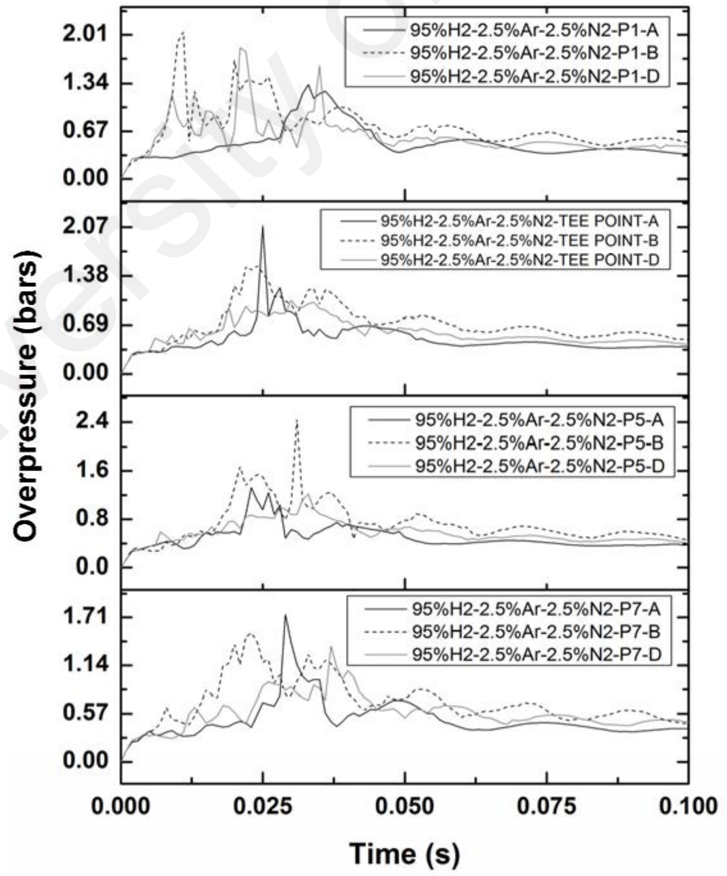

Figure 4. 27 Continued

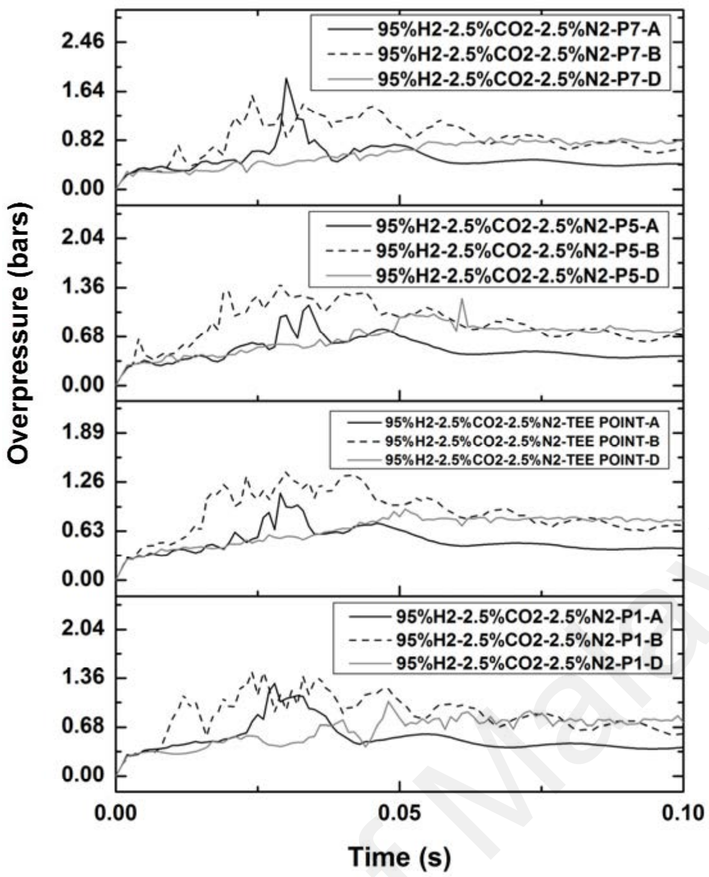

Figure 4. 27 Continued

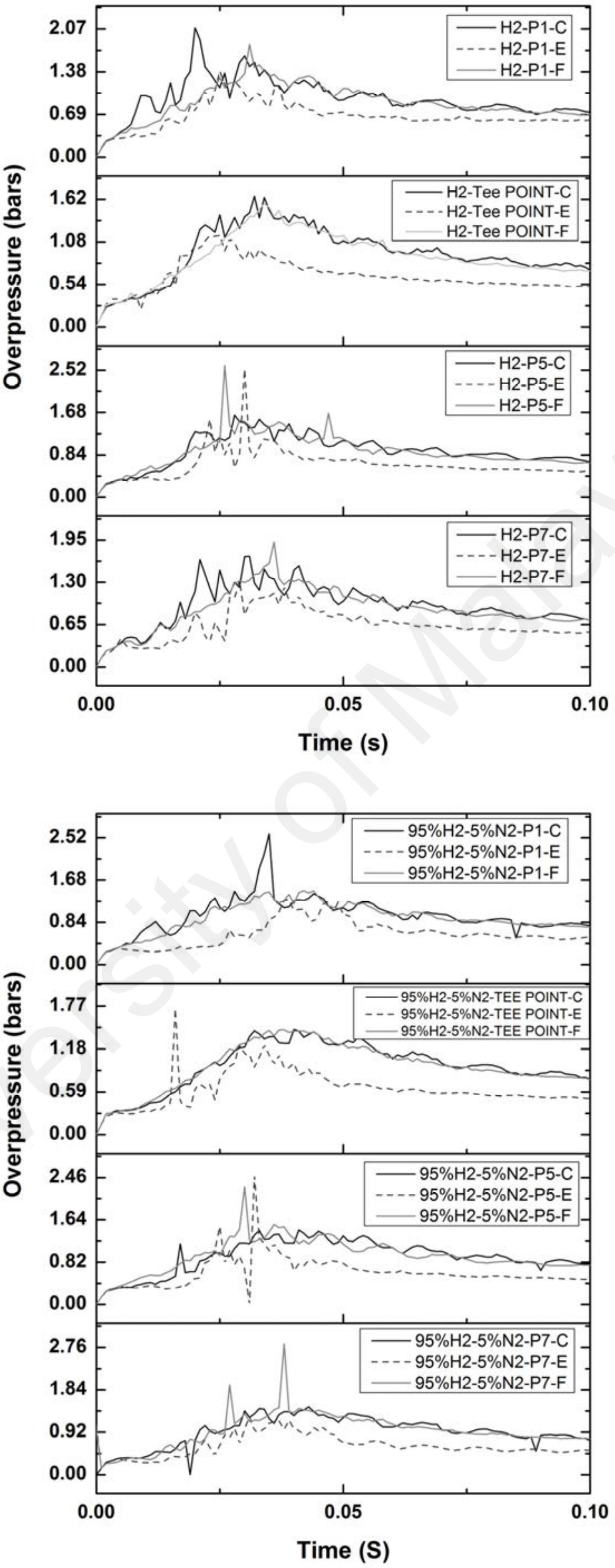

Figure 4. 28 Blast wave in P1, Tee point, P5 and P7 at ignition positions C, E and F

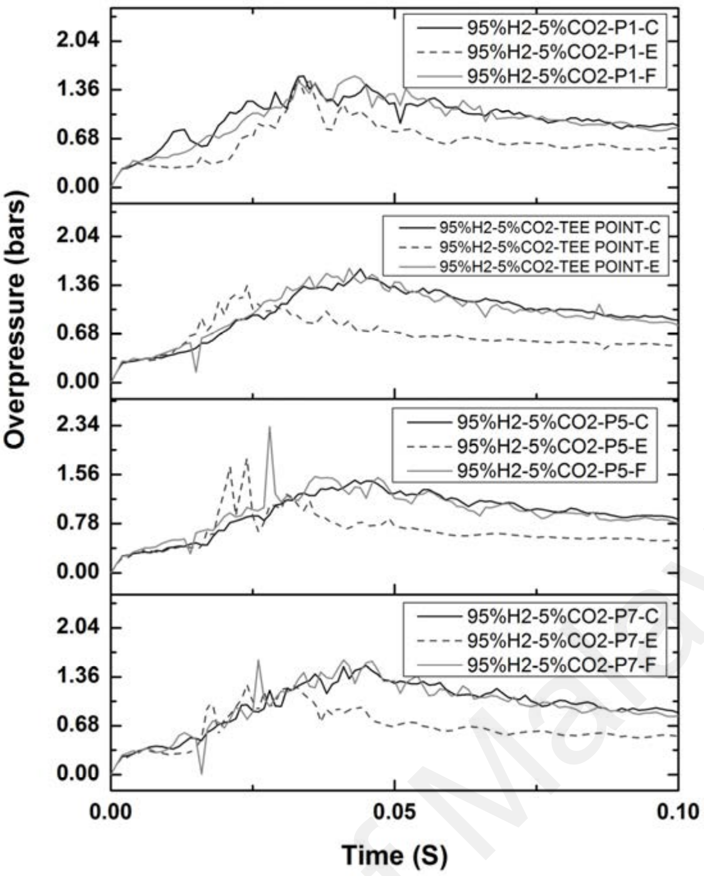

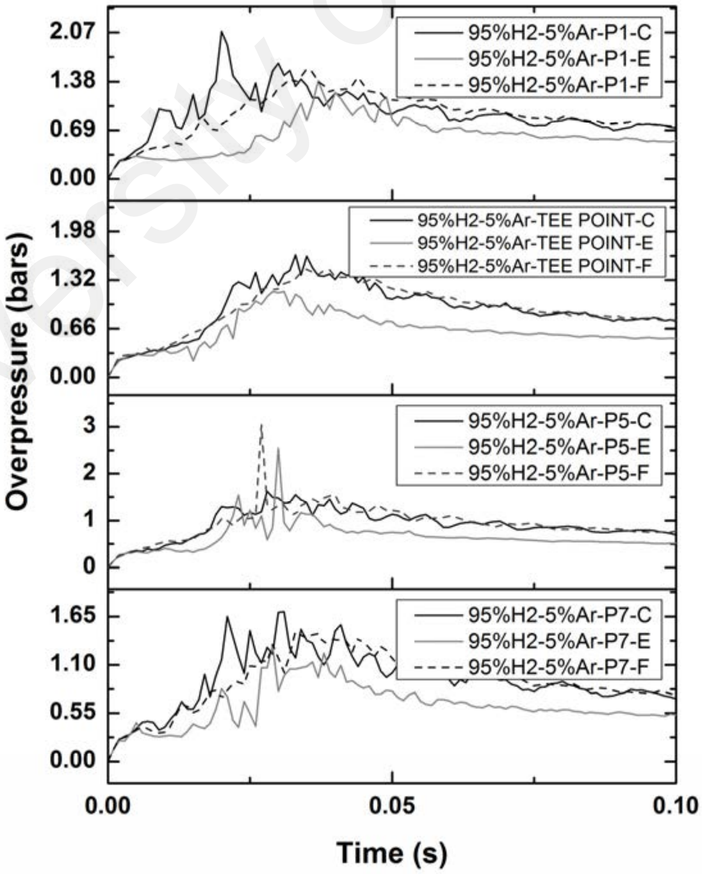

Figure 4. 28 Continued

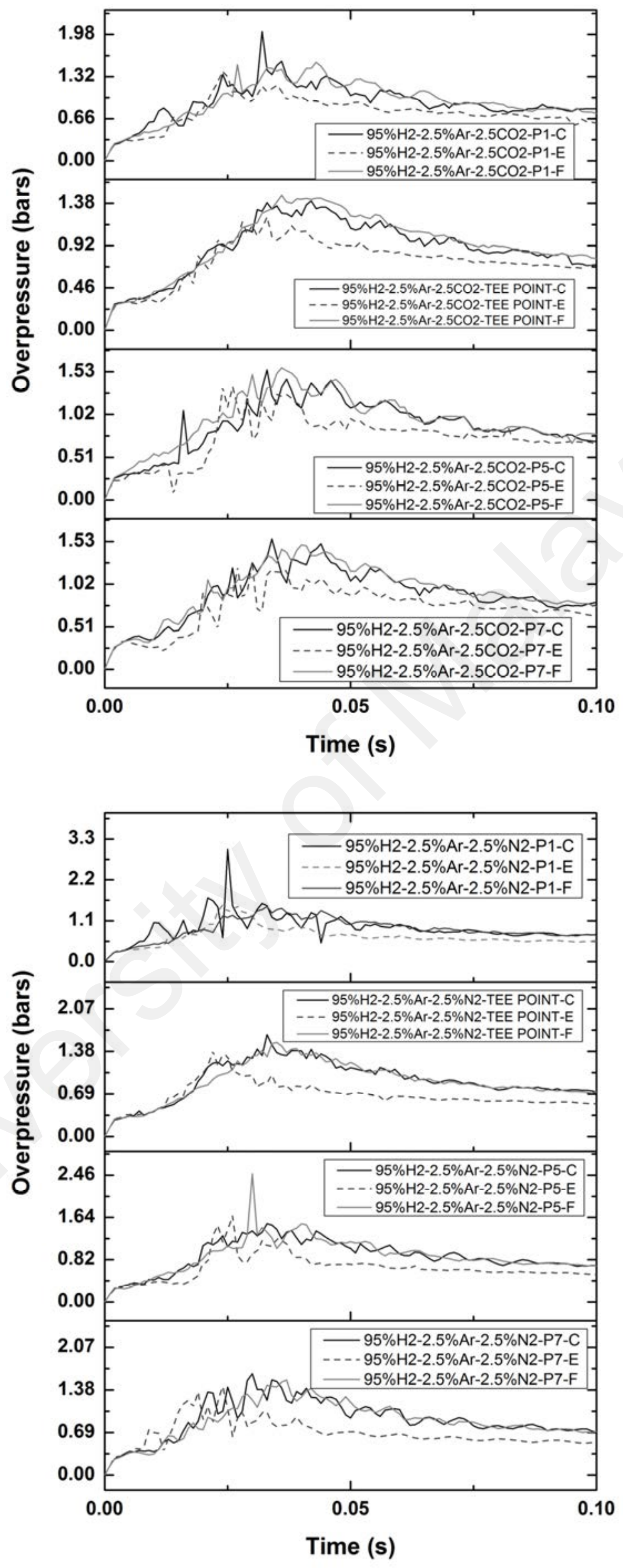

Figure 4. 28 Continued

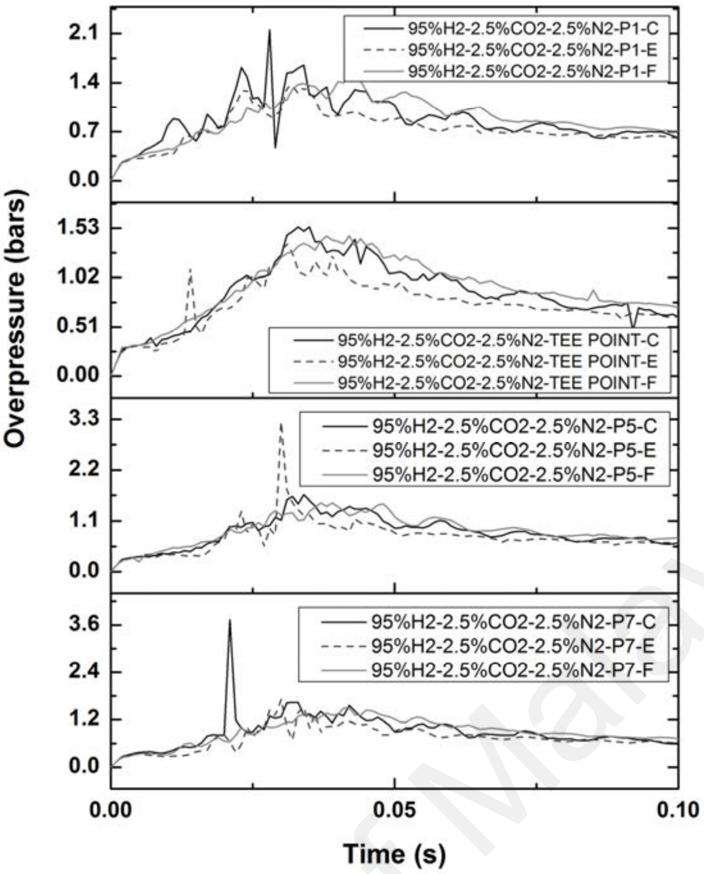

Figure 4. 28 Continued

4.4.3. The influence of tee junction position to overall explosion development

Giving more attention to recoreded data from two tee pipe cofiguratations (Figure 3.2 a & b), it can be found that tee junction allocation also has significant effect on flame development of hydrogen-inhibitors/air fuels. By comparing the obtained data from ignition C to F and, E to A and B, it can be found that the lower distance of tee junction to ignition point cause higher level of severity. For enstance, in overal, the obtained severity from ignition point B is 1.72 and 2.14 times higher than A and E, respectively. for all mixtures. The appearance of multiple peak overpressures indicates that, at a shorter distance between ignition point and obstacles, the flame experiences a strong interaction with the transverse pressure waves from the tee junction effect, inducing more turbulence and, consequently, attenuating the acceleration of the burning of the unreacted mixtures, which were trapped along the tee junction region. This, again, will increase the combustion rate and thus increase the flame speeds and overpressure. The findings of this study are in good agreement with previous studies (Kim et al., 2014).

By comparing the overpressure trends in early stage after ignition position (P5 for ignition position B and, P1 for ignition positions A and E) it can be noticed that turrbulence ratio in the early stage of flame development at ignition position B is much higher than ignitions A and E, respectively (Figures 4.21). It is due to the fact that the wrinkled flame ultimately transforms into a turbulent flame due to presence of the obstacle (tee junction) in the early stage of flame development at ignition position B. This phenomenon causes further flame acceleration due to the increase in surface area of the laminar flamelets inside the flame (Gamezo et al., 2008). In the next phases (along the pipe and tee junction), higher level of turbulence in the early stage of flame development at ignition B causes a distributed reaction zone destroyed and then replaced the flamelet structure which it leads the deflagration to detonation transition (DDT) happened via the shock wave amplification mechanism at end of the pipe due to the increase in flame area and the burning rate (Gamezo et al., 2008).

On the other hand, overpressure trends at ignition A and E showed that the turbulence ratio for former is higher (Figure 4.21). This is due the fact that the distortion of the flame surface happened in two different periods of time at ignition A. Firstly, it happened along the pipe before reaching the tee point and secondly, after passing the obstacle (tee point). Therefore, the interaction between the unburnt gas and the flame front is higher at ignition A since the burning velocity ratio increases (Clanet & Searby, 1996a; Zhou et al., 2006). It is a known fact that the presence of an obstacle in the pipe will randomize the flow, thus increasing the flame speed and overpressure (Phylaktou et al, 1993). This phenomenon is much significant in the tee junction at ignition A than at ignition E.

The stability of the flames is much higher if the tee junction is allocated centrally along the pipe (ignition E). By locating the tee junction at the central point, the flame acceleration along the pipe and in the tee junction showed almost the same behaviour since it passed the almost equal distance after the obstacle (tee point). Consequently, the overpressure and flame speed distribution in both directions are almost same. This phenomena is also in agreement with observations in parallel pipes (Zhu et al., 2012). However, due to the flame reactivity of the fuel, the reflective waves from the end walls had significant effect on turbulent ratio in both directions at ignition E.

4.5. Numerical analysis on explosion development in tee junctions using FLUENT

Due to defined benefits on simulators systems compare to experimental setups (Zalok et al., 2011), the main purpose of using FLUENT software in current research is to investigate the capability of this software for studying flame acceleration of gases fuel in medium scales sizing pipe for fuel transferring purposes based on associated standard models for combustion purposes.

As well-known, the location of flame at any time of burning depends on many physical and chemical characteristics such as initial mixture, pipe diameter, length of pipe, the position of tee junction, equivalence ratio of mixture, ignition position, spark power and spark duration. Therefore, the pressure in the pipe at any time of flame propagation is depended on the length of pipe and the position of the tee junction and ignition source. Figures 4.29-4.32 present the predicted pressure contour of hydrocarbons/air and hydrogen/air flames at their stoichiometric concentration ratio in tee pipes at four ignition positions. Red color indicates higher pressure and the amount of pressure decline according to color table beside the figures. As presented, the tee junction has very influential impact on flame behavior because of its pressure drop act. In fact, the tee junction acts as a venture pipe (ejector). The pressure increase across the pipe step by step and pressure waves move along till they pass the tee junction. The pressure drops suddenly after the tee junction and it can be a main factor in flame shedding and vortex flow in this section of pipe. Moreover, each ignition position produce pressure waves around itself naturally. This pressure deviation across the pipe during time and distance can play a main role in flame propagation and its tip forming. The amount of burned gas pressure and unburned gas changed during reaction model and burning process. Consequently, the associated turbulence in the unburned mixture ahead of the flame front represents the main mechanism for the flame acceleration, therefore, the obstacles randomize of the mean flow kinetic energy (E Salzano et al., 2002). It is due to this fact that turbulent burning velocity was dominated by three factors: (1) purely hydrodynamic factor, turbulence Reynolds number, (2) relative turbulence intensity to reaction speed, the ratio of turbulence intensity to unstretched laminar burning velocity, and (3) sensitivity of the flame to the stretch due to the thermo-diffusive effects (Kitagawa et al., 2008). This observation is more significant for hydrogen/air mixtures compare to hydrocarbons/air fuels (refer to Figure 4.36) due to its specific properties that has been discussed earlier fairly.

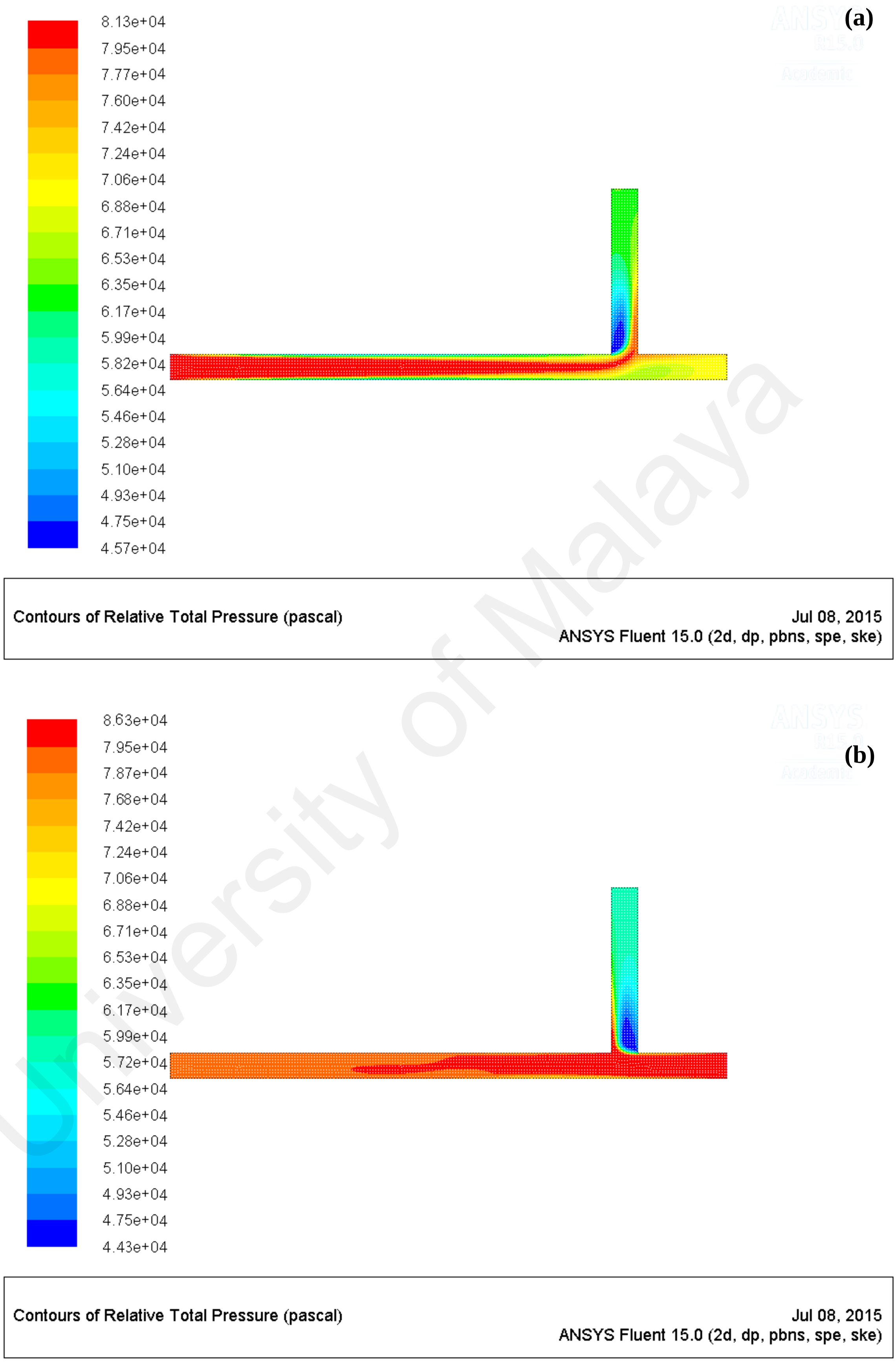

Figure 4. 29 simulated models of the pressure contour of C_2H_4/air (ϕ=1) mixture at ignition positions: (a)A, (b)B, (c)C and (d)E

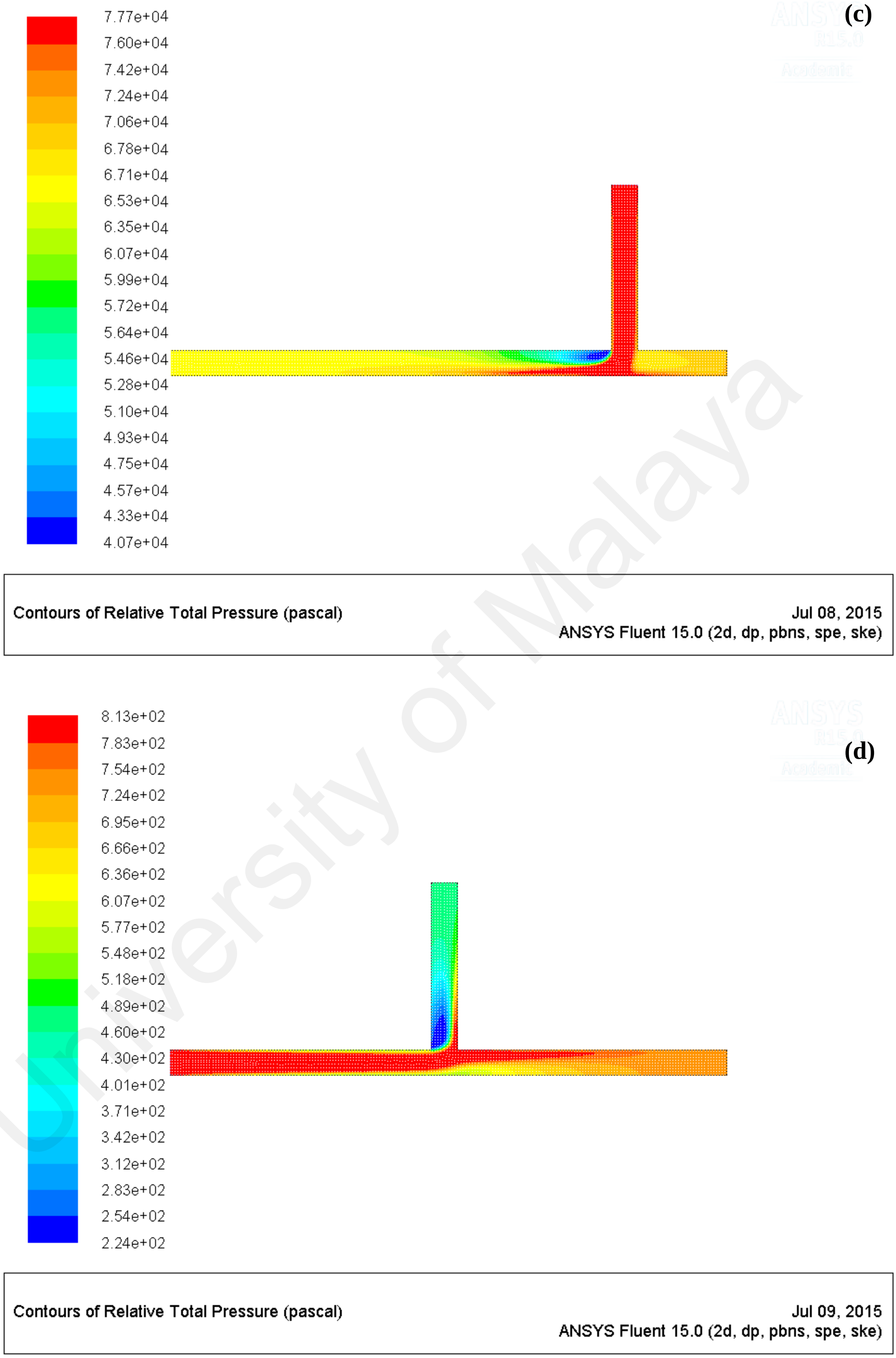

Figure 4. 29 Continued

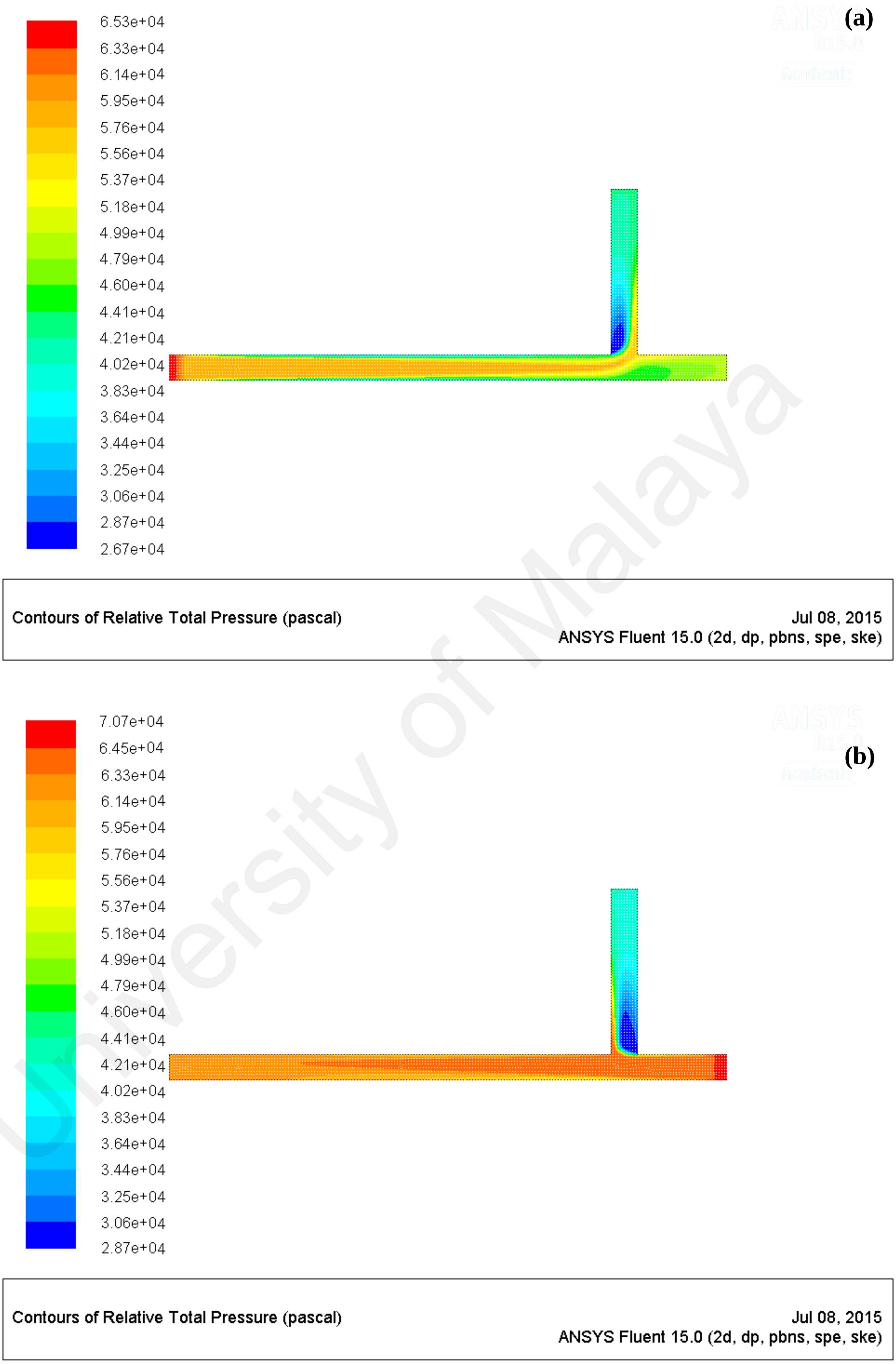

Figure 4. 30 simulated models of the pressure contour of NG/air (ϕ=1) mixture at ignition positions: (a)A, (b)B, (c)C and (d)E

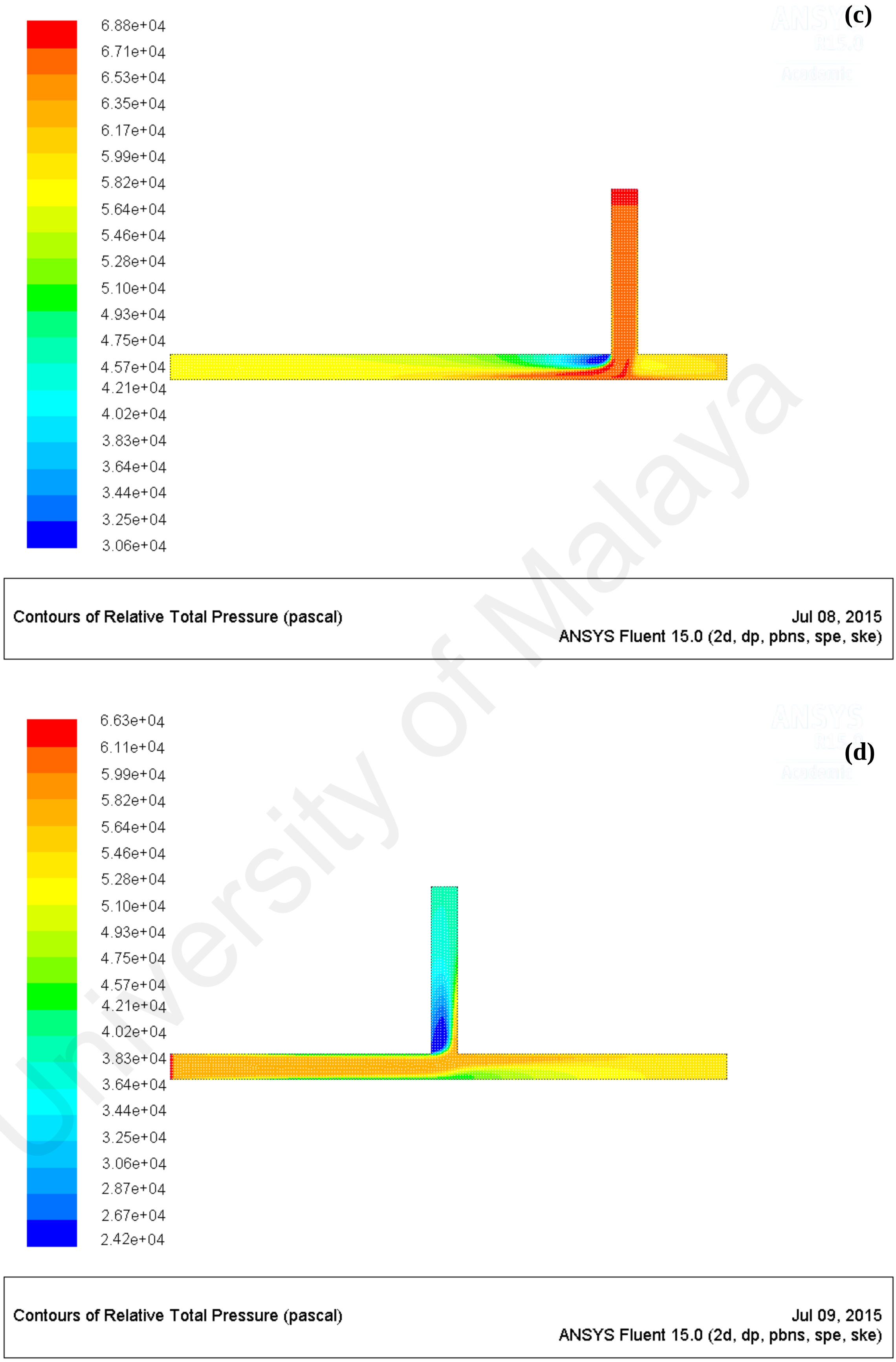

Figure 4. 30 Continued

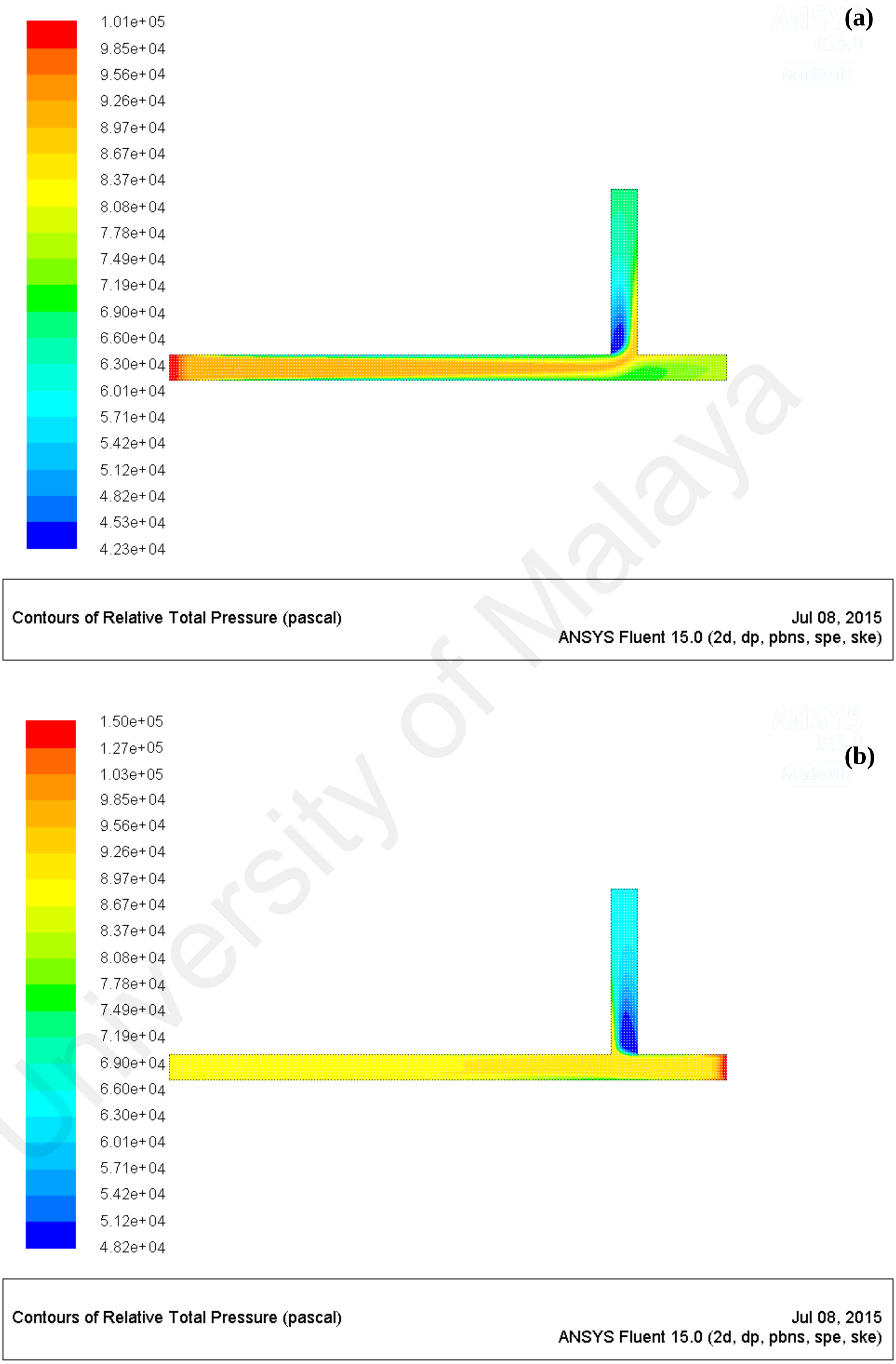

Figure 4. 31 simulated models of the pressure contour of C_3H_8/air (ϕ=1) mixture at ignition positions: (a)A, (b)B, (c)C and (d)E

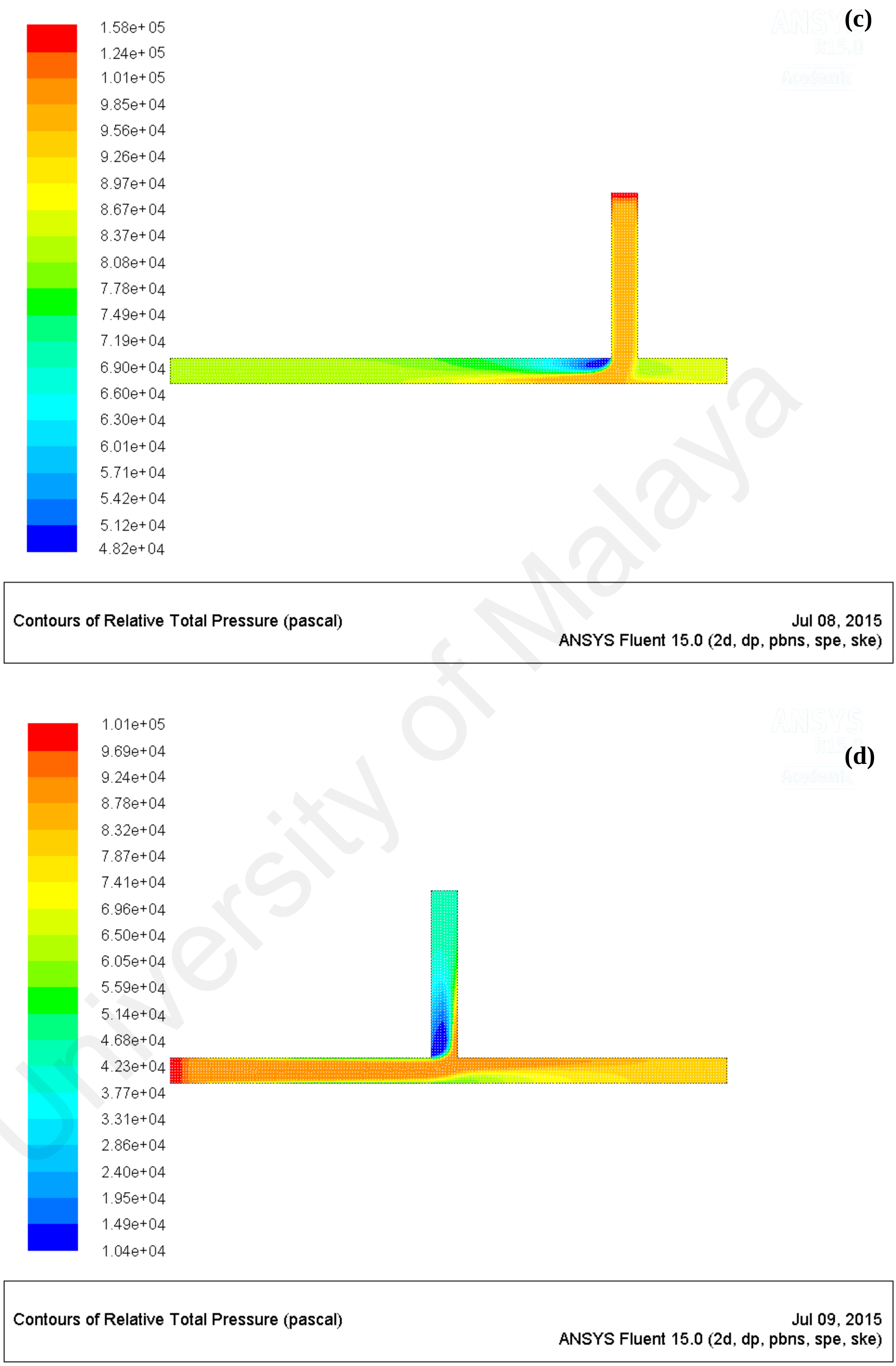

Figure 4. 31 Continued

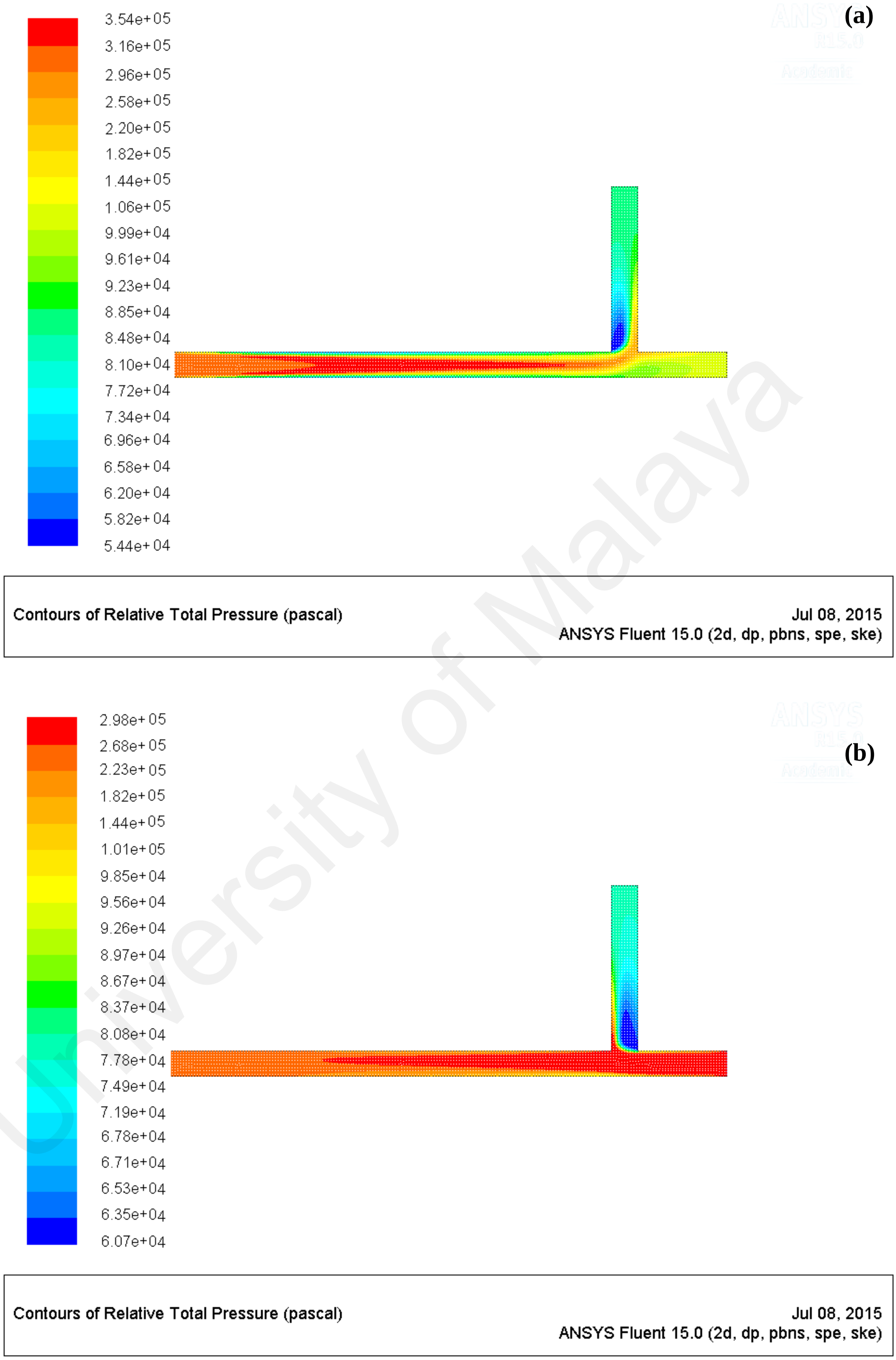

Figure 4. 32 simulated models of the pressure contour of H_2/air (ϕ=1) mixture at ignition positions: (a)A, (b)B, (c)C and (d)E

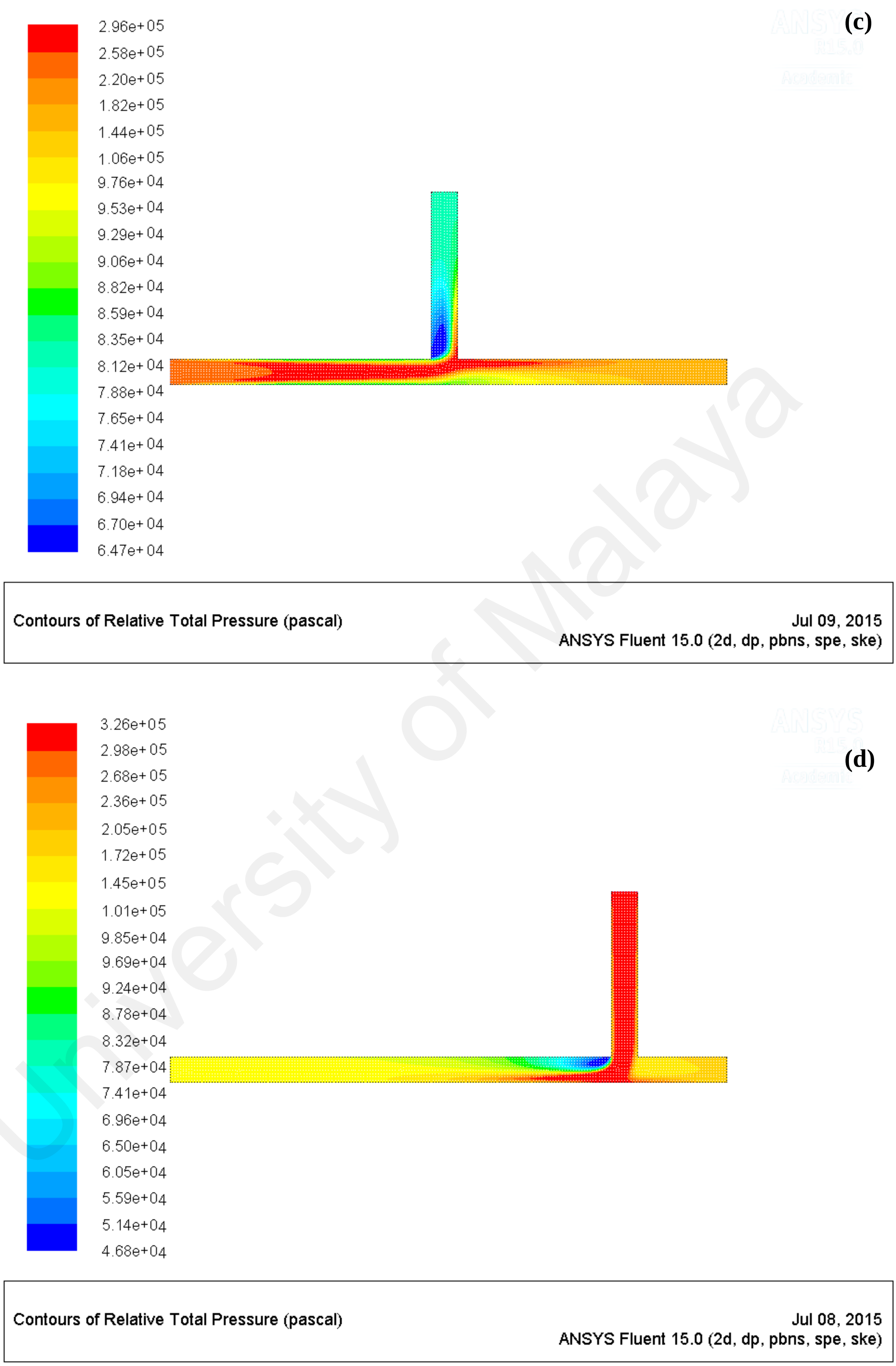

Figure 4. 32 Continued

On the other hand, the change of the flame shape in tee junction is also due to the side walls in vertical direction which obstruct the flame expanding freely as the flame approaches the side walls. This observation is also in agreement with previous study by Xiao et al. (2010). However, the generated pressure of the flames at end of the junction and along the pipes showed an increase due to associated reflective wave at end walls for all mixtures. On the other hand, when the tee junction was placed at an equal distance along the pipe, the flame acceleration of the fuel gases gave the lowest flame speed intensity, since the flames accelerate at almost the same distance after the tee junction region. In this instance, the interaction between the reflective waves and fast flames from the end points was insignificant; this phenomenon has been fairly widely discussed in the literature (Hassan et al., 2012; Kolbe & Baker, 2005).

Figures 4.37-4.40 compare the recorded pressure of hydrocarbons/air and hydrogen/air mixtures in the tee pipes based on CFD model and experimental results. It is noticeable that X and Y parameters are defined in Figure 3.3. There is difference between simulation values and experimental values. In average, the differences between recorded data from experiment and simulation was 0.236, 0.284, 0.598 and 1.57 bars for C_2H_4/air, NG/air, C_3H_8/air and H_2/air, respectively. Mostly, the simulation values are larger than experimental values. This may relate to the different setting of conditions of the pipe wall. In numerical simulation, the pipe wall was set to be smooth while the roughness of the real wall may cause some loss of energy, making the pressure value lower. However, the simulation values decreased near the exit, contrary to the experimental trend, and this is because in experiment, the exit was sealed with film so the pressure wave was influenced and the pressure value increased. Instead, in simulation there was no such handling, so the pressure value decreased after decompression (Zhian et al., 2012). However, among all mixtures, C_3H_8/air showed a slightly larger value in experimental data compared to simulation. It maybe because of the associated governing factors/parameters in FLUENT software may incongruent for this mixture in applied setup. Since the same setup was applied for all mixtures, the sudden increase of temperature of the domain may affect on reacting flows of propane/air. Other researchers (Yan et al., 1996; Sathiah et al., 2012) also argue this statement.

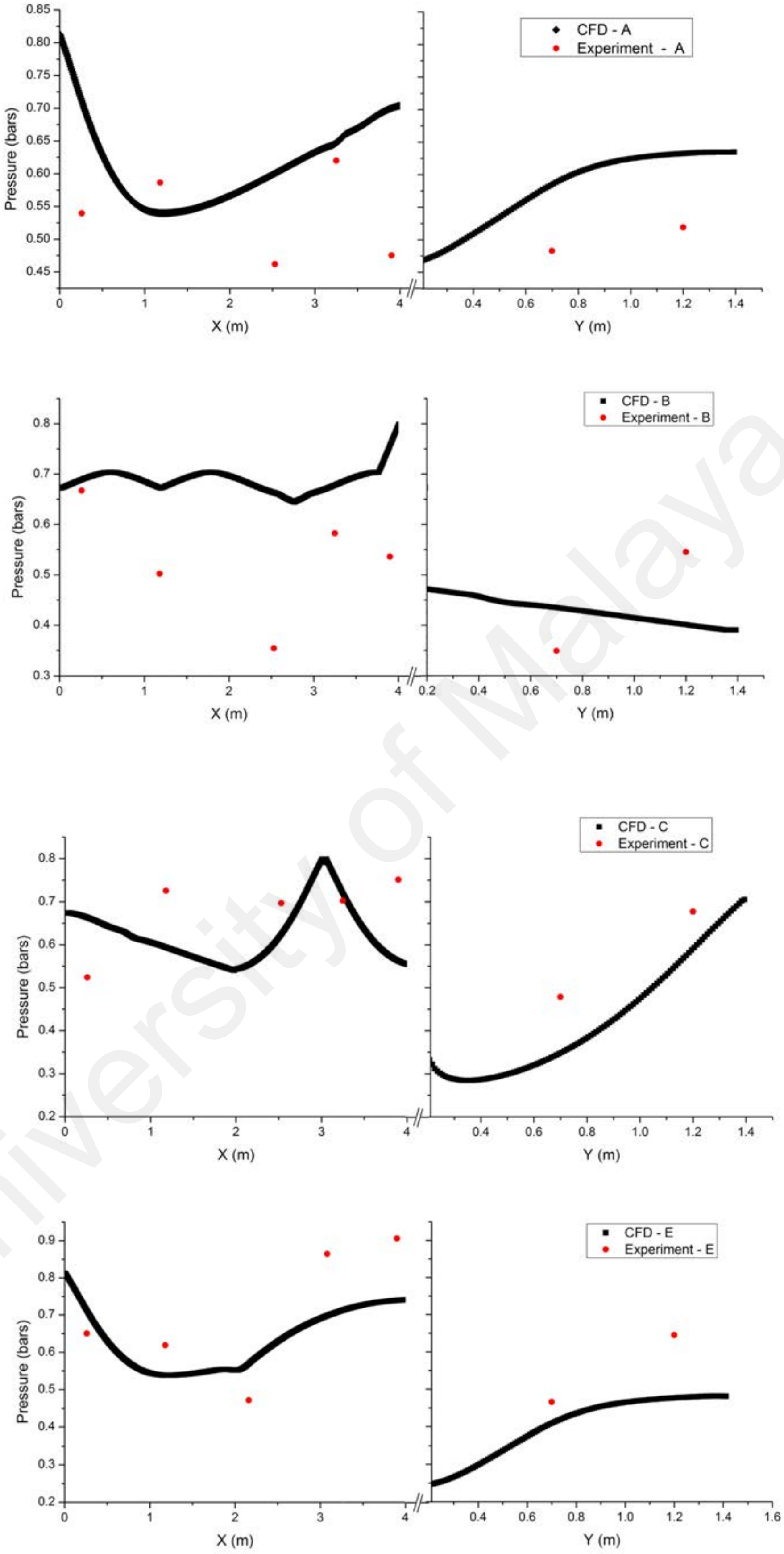

Figure 4. 33 Experimental and simulated overpressure vale of C_2H_4/air (ϕ=1) mixture at ignition positions A, B, C and E

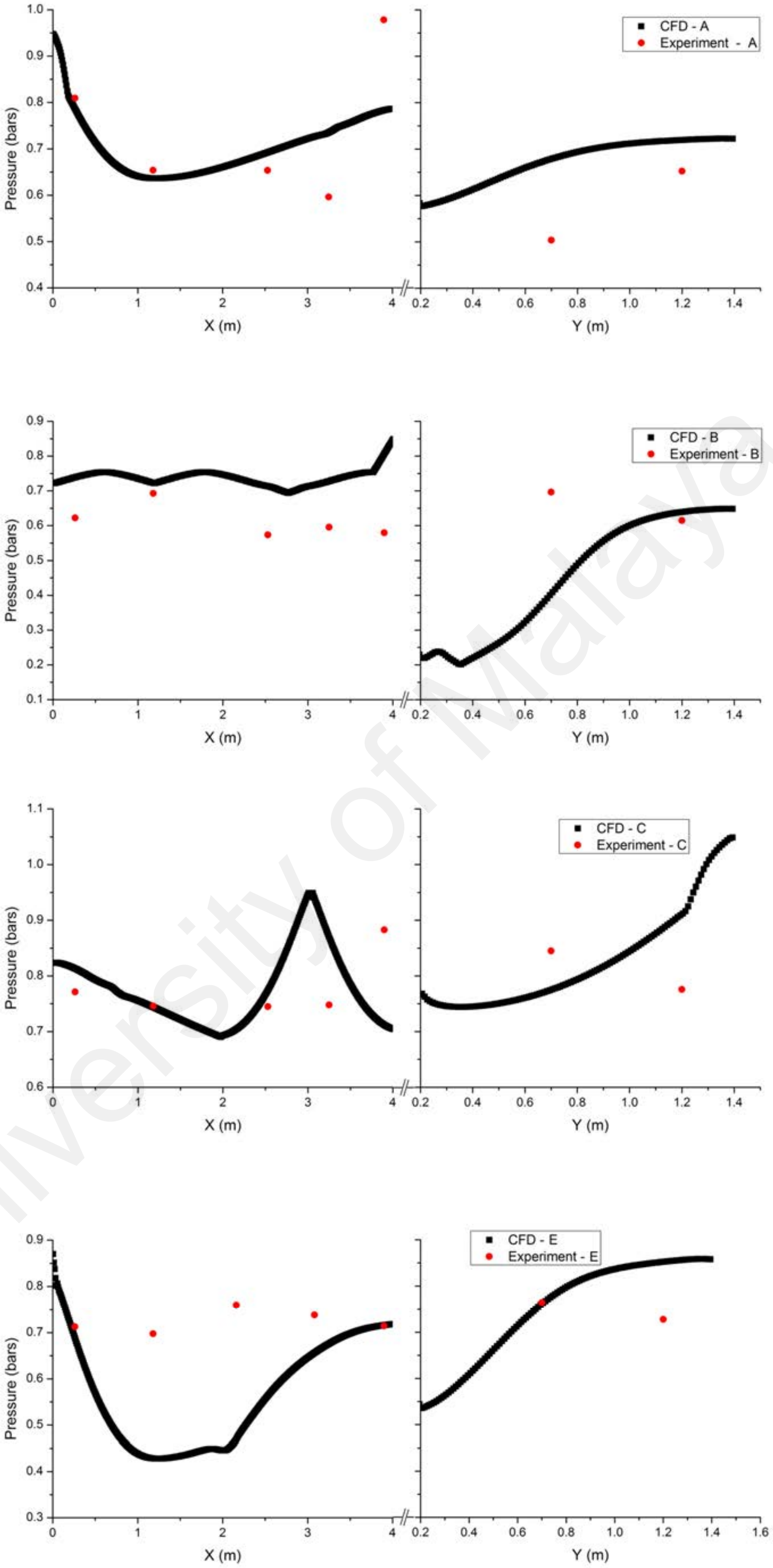

Figure 4. 34 Experimental and simulated overpressure vale of NG/air ($\phi=1$) mixture at ignition positions A, B, C and E

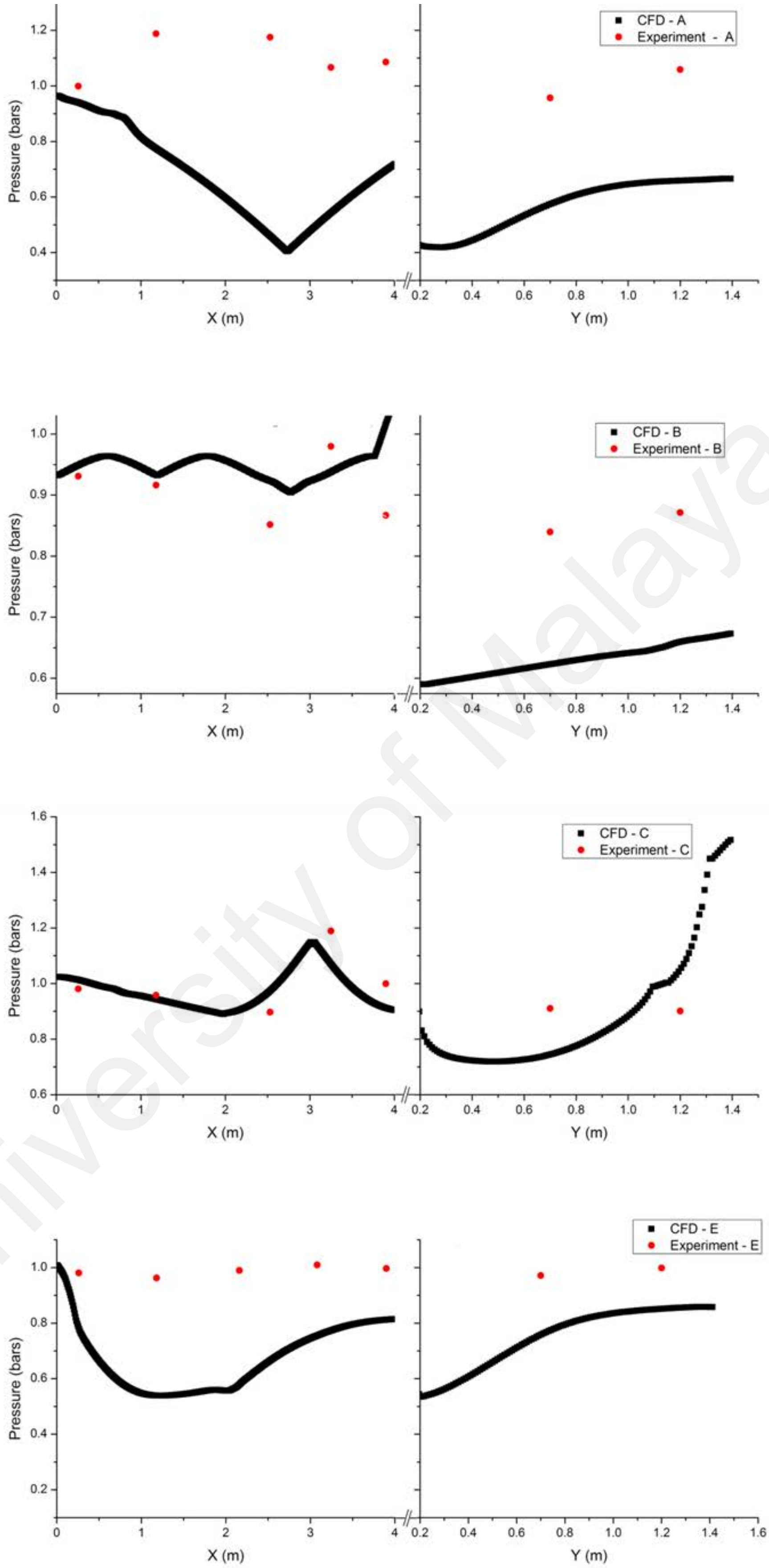

Figure 4. 35 Experimental and simulated overpressure vale of C_3H_8/air (ϕ=1) mixture at ignition positions A, B, C and E

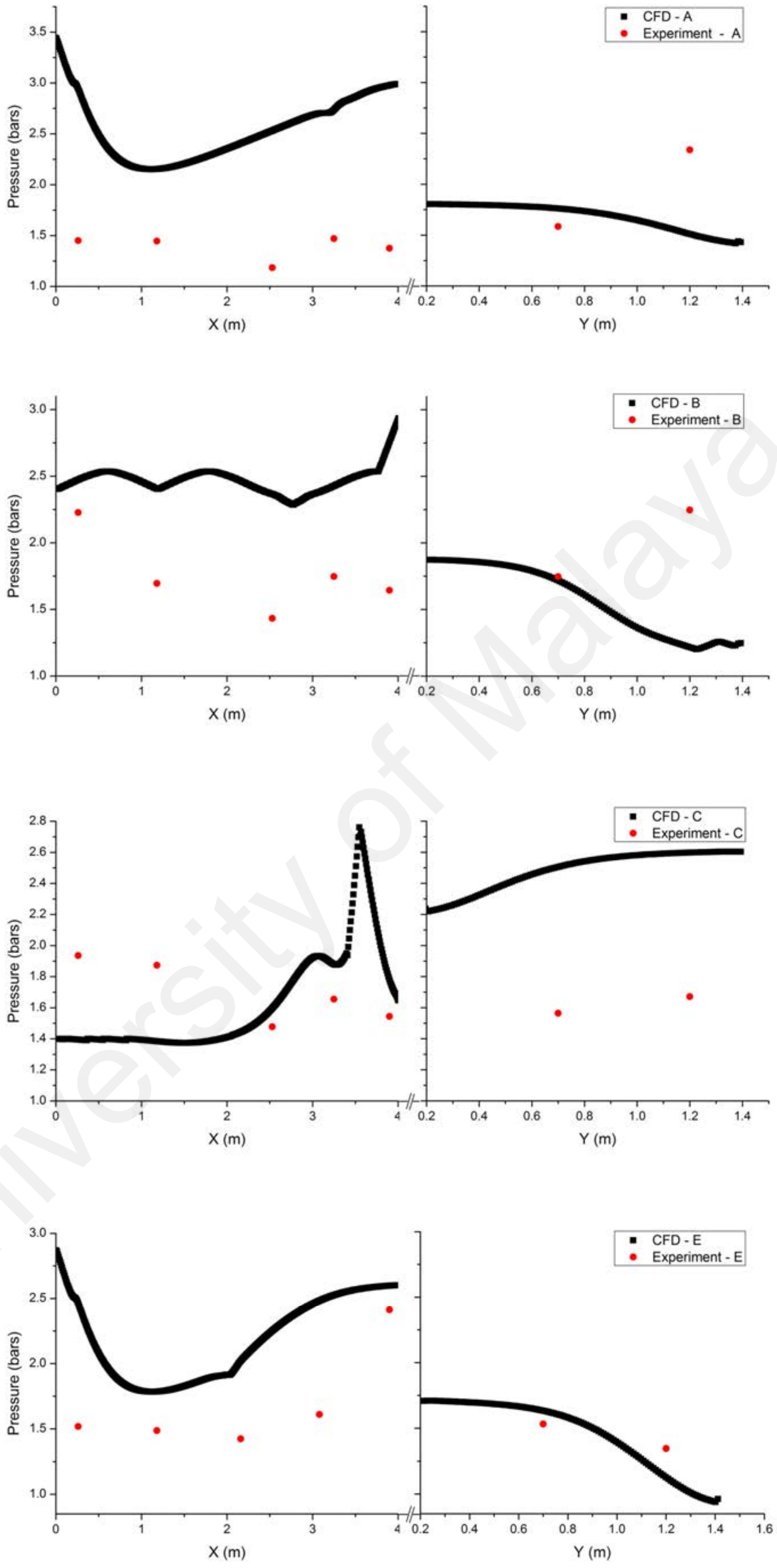

Figure 4. 36 Experimental and simulated overpressure vale of H_2/air (ϕ=1) mixture at ignition positions A, B, C and E

CHAPTER V: CONCLUSIONS AND RECOMMENDATIONS

5.1. Conclusions

A comprehensive study of the governing parameters involved in the flame propagation of hydrocarbons-air and hydrogen-air mixtures, in a wide range of equivalence ratios and in different pipe configurations, was carried out in this current research. The findings can be summarized as below:

- From the hydrogen-air pressure and flame speed results, hydrogen explosions gave both higher maximum overpressure and flame speed values compared to those of the hydrocarbon fuels (approximately twice as high for all studied pipe configurations). However, the recorded data also showed that the associated maximum overpressure and flame speed of ethylene-air were the highest among all the hydrocarbon-air fuels, followed by NG-air and propane-air, respectively, since the diffusivity of propane is significantly smaller than its thermal conductivity, which allows the fuel to be preferentially heated more rapidly at the preheated zone compared to other hydrocarbon fuels.
- It is interesting to note that the maximum pressure of hydrogen-air mixtures experienced its highest value (~7.2 bars) at the bending region, compared to the straight pipe and both tee junction configurations. Therefore, pipe bends pose the highest explosion severity in terms of the rate of pressure rise when compared to other pipe obstacles.
- There are two distinct overpressure peaks recorded at two different positions in the bent pipe explosions for all studied mixtures: first, at the bending position, and second, near the end wall (0.9 m from the pipe end wall). The presence of a bend can be observed to attenuate flame stretching and intensify the turbulence. This condition promotes further strong mixing of reflection and diffraction

acoustic/shock waves, entering into the reaction zone, enhancing the burning rate and increasing the flame speed.

- The trend for all fuels is consistent in the straight pipe, with the maximum overpressure occurring at a distance of x = 2.02 m (P3) from the ignition position. The associated maximum overpressure and flame speed resulting from the highest burning rate is due to the flame cellularity/wrinkling, i.e., the distortion of the flame surfaces to become larger, hence increasing the burning velocity.
- Within the examined range of hydrocarbons-air and hydrogen-air concentrations, the values for the maximum overpressure and maximum flame speed were almost the same for both tee pipe configurations, only they were attained at different locations. Moreover, the appearance of multiple peak overpressures indicates that, at a shorter distance from the obstacles, the flame experiences a strong interaction with the transverse pressure waves resulting from the tee junction effect, inducing more turbulence and, consequently, attenuating the acceleration of the substantial unburned gases trapped around the tee junction region. This results in a rise in flame speeds and thus enhances the maximum pressure and rate of pressure rise.

Another aim of this study was to provide an understanding of the explosion development in the geometry of tee pipes on a medium scale system, where ignition occurs at different locations for hydrocarbons-hydrogen/air mixtures. The results showed that:

- The flame reactivity of the ethylene-hydrogen/air and NG-hydrogen/air were much higher than the propane-hydrogen/air mixture. This was not only because of the kinetic reaction of these mixtures but also, the dynamics of flame deployment in the tee junctions had significant effects on the recorded maximum overpressure and flame speeds along the pipes.

- The recorded data from ignition A and E, as the reference ignition points, show that the lower distance of tee junction to ignition point caused higher explosion severity in terms of the rate of pressure rise. When looking at the overall plots, the fluctuation of the maximum overpressures and flame speeds of all of the flames at ignition A was much higher than ignition E. This is due to the influence of the dynamic effect, i.e., thermo diffusivity, rapid mixing of the induced turbulence, fast flame downstream and a strong interaction of reflective waves and fast flames from the end points on flame acceleration of the fuels. These factors caused retonation and, in this particular configuration, detonation occurred.
- Within the examined range of hydrocarbons/air and hydrocarbons-hydrogen/air concentrations, the value of the maximum overpressure and flame speed was almost the same at all of the ignition positions. We only recorded the peak overpressure and flame speeds at the different locations. It can be suggested that the different values of maximum overpressure and flame speed on each of the mixtures at all of the ignition points may have been due to the stratification of gases on the pipe bed or sedimentation phenomenon.

With regards to the importance of hydrogen fuel for future transportation, this research study was conducted to investigate the effectiveness of argon, nitrogen and carbon dioxide on hydrogen/air flame acceleration in a tee pipe configuration. Based on the findings, it can be summarized that:

- The ignition position and initial fuel composition had a strong influence on the overpressure, flame speed and rate of pressure rise. The blending of the two inhibitors gave a lower severity to all of the investigated compositions of hydrogen/air mixtures. From the study, CO_2 is the most efficient, followed by N_2 and Argon.

- The noticable observation is regarding to obtained severty of applied fuels if the ignition happens in the tee points of both cofigurations (ignition points C and E). it indicats that in any configuration of tee junctions, the risks pose by hydrogen-inhibitors/air mixtures is the highest if the ignition happened in tee points. Moreover, by comparing the obtained data from ignition C to F and, E to A, D and B, it can be found that the lower distance of tee junction to ignition point cause higher level of severity. Overal, the obtained severity, in terms of rate of pressure rise, from ignition point B is 1.72, 1.67 and 2.14 times higher than A, D and E, respectively.
- The explosion severity recorded at ignition position B was higher than at A or D. It is found that the flame acceleration, when ignited at position B, was mainly affected by mass diffusivity and consequently, it promoted the transition of the flames deformation into the detonation mode. However, flame acceleration at ignition position A and D was affected by the strong interaction of a reflective wave at the end pipe and fast induced flame, highlighting the retonation-like obstacles phenomenon.
- Among all of the studied mixtures, 95%H_2-2.5%Ar-2.5%N_2/air, 95%H_2-5%N_2/air, H_2/air and 95%H_2-5%Ar/air, respectively, showed higher risks, in terms of rate of pressure rise, compared to others. This is due to their dynamic properties. However, it was found that the mixtures containing CO_2 had lower severity, since the average recorded maximum flame speed for this particular mixture was lower for all ignition points (at the average of 599 m/s).

Numerical analysis on explosion development in tee junctions using FLUENT also showed that:

- There is difference between simulation values and experimental values. In average, the differences between recorded data from experiment and simulation was 0.236, 0.284, 0.598 and 1.57 bars for C_2H_4/air, NG/air, C_3H_8/air and H_2/air, respectively. Mostly, the simulation values are larger than the experimental values. This may relate to the different setting of conditions of the pipe wall. It can be concluded that the application of FLUENT for fuels with higher reactivity needs more scrutiny due to higher value of differences for medium scale sizing pipe for fuel transfer processing.

5.2. Recommendations

In order to ensure that better precautions are taken in relation to pipeline gas carriers, it is essential to fully characterize and quantify their explosion mechanisms and do some primary actions to avoid the unwanted combustion phenomena, such as deflagration to detonation transmission (DDT) (including decomposition flames), occurring in the process. For this study a number of recommendation for both industrial and academic concepts to reduce unpredictable accidents/incidents in fuel transferring processing can be made.

4.2.1. Recommendation for Industries

As the results shown, pipe bends pose the highest explosion severity in terms of the rate of pressure rise when compared to other pipe obstacles. Therefore, among all pipe configurations that have been investigated in current research, it is highly recommended to reduce the number of bend joins in piping design processing. Moreover, due to associated the lowest severity for tee pipes, especially for configuration where tee junction allocated in central (Figure 3.2b), it is recommended to giving more attention for allocation tee junction in piping processing. It is more preferred to allocate the tee junction at almost the central point of a horizontal/main pipe. Moreover, allocating flame arrestors before the bend joins and tee point joins from the initial vessel is another recommendation for piping design process to prevent DDT from initial vessel to end point vessel.

As mentioned earlier, transporting hydrogen as a gas carrier to end users could affect the integrity or durability of a pipeline network. It is due to this fact that the existing gas pipeline network is designed, constructed and operated using natural gas. Once it is introduced into the pipeline, the hydrogen mixes with other gases such as natural gas, inhibitors and act. The results at the current research also emphasis this issue. Therefore, it is highly recommended that the piping system should be purged fully before fuel transferring beginning. Moreover, controlling the purity of the initial fuel into the system is another recommendation for reducing the associated hazards of hydrogen fuel transferring.

4.2.2. Recommendation for Academic Research

It is recommended to do more experimental investigations on flame acceleration of gases fuels in different shaped pipes by considering different L/D ratio and the presence of obstacles. On the other hand, to better understand the effectiveness of tee point on flame acceleration of fuels, , it is recommended to investigate flow and fluid dynamics of flames intensely by considering the different initial mixtures, tee junction and ignition position.

To better understand the capability of simulation software on flame acceleration of fuels in piping processing, it is required to do comparison studies using available software, including ANSYS FLUENT, FLACS and ABAQUS, and compare with actual experimental data to reduce the value of errors which associated. Furthermore, while the simulation results showed almost the similar trends compare to experimental results for pure hydrogen/air and hydrocarbons/air mixtures, due to available limitation on FLUENT software, more investigations on applied turbulent models for predicting the flame acceleration of hydrogen-hydrocarbon/air and hydrogen-inhibitors/air mixtures are required.

List of Publications

Emami, S. D., et al. (2013). Experimental study on premixed hydrogen/air and hydrogen–methane/air mixtures explosion in 90 degree bend pipeline. International Journal of Hydrogen Energy.

*It is also issued by “Renewable Energy Global Innovations”

Emami, S. D., Kasmani, R. M., Hamid, M. D., Hassan, C. R. C., & Sulaiman, S. Z. (2016). Effect of inhibitor gases on hydrogen flame propagation in a confined tee pipe (Part I). *Fuel*.

Emami, S. D., Sulaiman, S. Z., Kasmani, R. M., Hamid, M. D., & Hassan, C. R. C. (2016). Effectiveness of pipe configuration on flame acceleration of hydrocarbons/air and hydrogen/air mixtures in constant volume. *Journal of Loss Prevention in the Process Industries.* Accepted.

Emami, S. D., et al. (2014). Kinetic and Dynamic Analysis of Hydrogen-enrichment Mixtures in Combustor Systems – A Review Paper. Renewable & Sustainable Energy Reviews. submitted

Emami, S. D., Kasmani, R. M., Hamid, M. D., & Hassan, C. R. C. (2015). Experimental study on flame acceleration of premixed hydrocarbons-hydrogen/air mixtures in Tee pipes. *International Journal of Hydrogen Energy*. Submitted.

Emami, S. D., et al. (2016). Effectiveness of Inhibitor Gases on Hydrogen Flame Propagation in Tee Pipe (Part II). *Fuel*. Submitted.

List of conferences

- ✓ Premixed Hydrogen/Air and Hydrogen-Methane/Air Mixtures Flame Acceleration in Bend Pipeline. 6th Regional Conference on Chemical Engineering (RCChE) on December 2-3, 2013 in Century Park Hotel, City of Manila, Philippines

- Experimental study on flame acceleration of premixed hydrocarbons-hydrogen/air mixtures in Tee pipes (July 2015). ANM2015.

References

Abbasi, T., & Abbasi, S. A. (2011). Decarbonization of fossil fuels as a strategy to control global warming. *Renewable and Sustainable Energy Reviews, 15*(4), 1828-1834.

Aggarwal, S. K., Awomolo, O., & Akber, K. (2011). Ignition characteristics of heptane–hydrogen and heptane–methane fuel blends at elevated pressures. *International Journal of Hydrogen Energy, 36*(23), 15392-15402. doi: http://dx.doi.org/10.1016/j.ijhydene.2011.08.065

Akansu, S. O., Dulger, Z., Kahraman, N., & Veziroğlu, T. N. (2004). Internal combustion engines fueled by natural gas—hydrogen mixtures. *International Journal of Hydrogen Energy, 29*(14), 1527-1539. doi: http://dx.doi.org/10.1016/j.ijhydene.2004.01.018

Alekseev, V. A., Christensen, M., & Konnov, A. A. (2014). The effect of temperature on the adiabatic burning velocities of diluted hydrogen flames: A kinetic study using an updated mechanism. *Combustion and Flame*(0). doi: http://dx.doi.org/10.1016/j.combustflame.2014.12.009

Aspden, A. J., Day, M. S., & Bell, J. B. (2011). Lewis number effects in distributed flames. *Proceedings of the Combustion Institute, 33*(1), 1473-1480. doi: http://dx.doi.org/10.1016/j.proci.2010.05.095

Aung, K. T., Hassan, M. I., Kwon, S., Tseng, L. K., Kwon, O. C., & Faeth, G. M. (2002). Flame/stretch interactions in laminar and turbulent premixed flames. *Combustion Science and Technology, 174*(1), 61-99. doi: 10.1080/713712909

Azatyan, V., Borisov, A., Merzhanov, A., Kalachev, V., Masalova, V., Mailkov, A., & Troshin, K. Y. (2005). Inhibition of various hydrogen combustion regimes in air by propylene and isopropanol. *Combustion, Explosion and Shock Waves, 41*(1), 1-11.

Azatyan, V., Gershenson, U., Sarkissyan, E., Sachyan, G., & Nalbandyan, A. (1969). *Investigation of low-pressure flames of a number of compounds containing sulfur by the ESR method.* Paper presented at the Symposium (International) on Combustion.

Azatyan, V. V., Shebeko, Y. N., & Shebeko, A. Y. (2010). A numerical modelling of an influence of CH4, N2, CO2 and steam on a laminar burning velocity of hydrogen in air. *Journal of loss prevention in the process industries, 23*(2), 331-336. doi: http://dx.doi.org/10.1016/j.jlp.2009.12.002

Barreto, L., Makihira, A., & Riahi, K. (2003). The hydrogen economy in the 21st century: a sustainable development scenario. *International Journal of Hydrogen Energy, 28*(3), 267-284.

Bauer, C., & Forest, T. (2001). Effect of hydrogen addition on the performance of methane-fueled vehicles. Part I: effect on SI engine performance. *International Journal of Hydrogen Energy, 26*(1), 55-70.

Bauwens, C., Chao, J., & Dorofeev, S. (2012). Effect of hydrogen concentration on vented explosion overpressures from lean hydrogen–air deflagrations. *International Journal of Hydrogen Energy, 37*(22), 17599-17605.

Bauwens, C. R., Chaffee, J., & Dorofeev, S. (2011). Vented explosion overpressures from combustion of hydrogen and hydrocarbon mixtures. *International Journal of Hydrogen Energy, 36*(3), 2329-2336.

Bell, J. B., Cheng, R. K., Day, M. S., & Shepherd, I. G. (2007). Numerical simulation of Lewis number effects on lean premixed turbulent flames. *Proceedings of the combustion institute, 31*(1), 1309-1317.

Bergthorson, J. M., & Dimotakis, P. E. (2007). Premixed laminar C 1–C 2 stagnation flames: Experiments and simulations with detailed thermochemistry models. *Proceedings of the combustion institute, 31*(1), 1139-1147.

Blanchard, R., Arndt, D., Grätz, R., Poli, M., & Scheider, S. (2010). Explosions in closed pipes containing baffles and 90 degree bends. *Journal of loss prevention in the process industries, 23*(2), 253-259.

Blanchard, R., Arndt, D., Grätz, R., & Scheider, S. (2011). Effect of ignition position on the run-up distance to DDT for hydrogen–air explosions. *Journal of loss prevention in the process industries, 24*(2), 194-199.

Bortnikov, L. (2007). Combustion of a gasoline-hydrogen-air mixture in a reciprocating internal combustion engine cylinder and determining the optimum gasoline-hydrogen ratio. *Combustion, Explosion, and Shock Waves, 43*(4), 378-383.

Bougrine, S., Richard, S., Colin, O., & Veynante, D. (2014). Fuel Composition Effects on Flame Stretch in Turbulent Premixed Combustion: Numerical Analysis of Flame-Vortex Interaction and Formulation of a New Efficiency Function. *Flow, turbulence and combustion, 93*(2), 259-281.

Boushaki, T., Dhué, Y., Selle, L., Ferret, B., & Poinsot, T. (2012). Effects of hydrogen and steam addition on laminar burning velocity of methane–air premixed flame: Experimental and numerical analysis. *International Journal of Hydrogen Energy, 37*(11), 9412-9422. doi: http://dx.doi.org/10.1016/j.ijhydene.2012.03.037

Bradley, D., Gaskell, P. H., & Gu, X. J. (1996). Burning velocities, markstein lengths, and flame quenching for spherical methane-air flames: A computational study. *Combustion and Flame, 104*(1–2), 176-198. doi: http://dx.doi.org/10.1016/0010-2180(95)00115-8

Bradley, D., Lawes, M., & Liu, K. (2008). Turbulent flame speeds in ducts and the deflagration/detonation transition. *Combustion and Flame, 154*(1–2), 96-108. doi: 10.1016/j.combustflame.2008.03.011

Briones, A. M., Aggarwal, S. K., & Katta, V. R. (2008). Effects of H2 enrichment on the propagation characteristics of CH4–air triple flames. *Combustion and Flame, 153*(3), 367-383. doi: http://dx.doi.org/10.1016/j.combustflame.2008.02.005

Burbano, H. J., Amell, A. A., & García, J. M. (2008). Effects of hydrogen addition to methane on the flame structure and CO emissions in atmospheric burners. *International Journal of Hydrogen Energy, 33*(13), 3410-3415. doi: http://dx.doi.org/10.1016/j.ijhydene.2008.04.020

Buxbaum, R. E. (2011). Hydrogen Explosions in Nuclear Reactors and a Passive Way to Prevent Them. from http://www.rebresearch.com/REB_Hydrogen_Nuclear.html

Cammarota, F., Di Benedetto, A., Di Sarli, V., Salzano, E., & Russo, G. (2009). Combined effects of initial pressure and turbulence on explosions of hydrogen-enriched methane/air mixtures. *Journal of loss prevention in the process industries, 22*(5), 607-613. doi: http://dx.doi.org/10.1016/j.jlp.2009.05.001

Cammarota, F., Di Benedetto, A., Di Sarli, V., Salzano, E., & Russo, G. (2010). The Effect of Initial Pressure on Explosions of Hydrogen-Enriched Methane/Air Mixtures. *Chemical Engineering Transactions, 19*, 273-278.

Chan, C., & Dewit, W. (1996). *Deflagration-to-detonation transition in end gases.* Paper presented at the Symposium (International) on Combustion.

Chatrathi, K., Going, J. E., & Grandestaff, B. (2001). Flame propagation in industrial scale piping. *Process Safety Progress, 20*(4), 286-294.

Chen-hua, X. (2008). Layout of Piping Connected with Reciprocating Compressor and Vibration Protection Method [J]. *Process Equipment & Piping, 5*, 013.

Chen, J.-L., Lv, H.-X., Shi, X., Zhu, D.-L., & Wang, W. (2011). Ana-lysis of water hammer process of tee pipe eonsidering local head loss by using characteristic line method. *Water Saving Irrigation, 10*, 17-20.

Cheng, Z., Bai-quan, L., Qing, Y., Xian-zhong, L., & Chuan-jie, Z. (2009). Influence of geometry shape on gas explosion propagation laws in bend roadways. *Procedia Earth and Planetary Science, 1*(1), 193-198.

Cho, H. M., & He, B.-Q. (2007). Spark ignition natural gas engines—A review. *Energy Conversion and Management, 48*(2), 608-618. doi: http://dx.doi.org/10.1016/j.enconman.2006.05.023

Choi, B. C., & Chung, S. H. (2012). Autoignited laminar lifted flames of methane/hydrogen mixtures in heated coflow air. *Combustion and Flame, 159*(4), 1481-1488. doi: http://dx.doi.org/10.1016/j.combustflame.2011.11.016

Choudhuri, A. R., & Gollahalli, S. R. (2003). Characteristics of hydrogen–hydrocarbon composite fuel turbulent jet flames. *International Journal of Hydrogen Energy, 28*(4), 445-454. doi: http://dx.doi.org/10.1016/S0360-3199(02)00063-0

Ciccarelli, G., & Dorofeev, S. (2008). Flame acceleration and transition to detonation in ducts. *Progress in Energy and Combustion Science, 34*(4), 499-550. doi: 10.1016/j.pecs.2007.11.002

Clanet, C., & Searby, G. (1996a). On the “tulip flame” phenomenon. *Combustion and Flame, 105*(1), 225-238.

Clanet, C., & Searby, G. (1996b). On the "tulip flame" phenomenon. *Combustion and Flame, 105*(1–2), 225-238. doi: http://dx.doi.org/10.1016/0010-2180(95)00195-6

Conte, E., & Boulouchos, K. (2006). Experimental investigation into the effect of reformer gas addition on flame speed and flame front propagation in premixed, homogeneous charge gasoline engines. *Combustion and Flame, 146*(1–2), 329-347. doi: http://dx.doi.org/10.1016/j.combustflame.2006.03.001

Coppens, F. H. V., De Ruyck, J., & Konnov, A. A. (2007). The effects of composition on burning velocity and nitric oxide formation in laminar premixed flames of CH4 + H2 + O2 + N2. *Combustion and Flame, 149*(4), 409-417. doi: http://dx.doi.org/10.1016/j.combustflame.2007.02.004

Cortright, R. D., Goddard, S. A., Rekoske, J. E., & Dumesic, J. A. (1991). Kinetic study of ethylene hydrogenation. *Journal of Catalysis, 127*(1), 342-353. doi: http://dx.doi.org/10.1016/0021-9517(91)90230-2

Cussler, E. L. (2009). *Diffusion: mass transfer in fluid systems*: Cambridge university press.

Dagaut, P., & Nicolle, A. (2005). Experimental and detailed kinetic modeling study of hydrogen-enriched natural gas blend oxidation over extended temperature and equivalence ratio ranges. *Proceedings of the combustion institute, 30*(2), 2631-2638. doi: http://dx.doi.org/10.1016/j.proci.2004.07.030

Dahoe, A. (2005). Laminar burning velocities of hydrogen–air mixtures from closed vessel gas explosions. *Journal of loss prevention in the process industries, 18*(3), 152-166.

Das, L. M. (1996). Hydrogen-oxygen reaction mechanism and its implication to hydrogen engine combustion. *International Journal of Hydrogen Energy, 21*(8), 703-715. doi: http://dx.doi.org/10.1016/0360-3199(95)00138-7

de Ferrières, S., El Bakali, A., Lefort, B., Montero, M., & Pauwels, J. F. (2008). Experimental and numerical investigation of low-pressure laminar premixed synthetic natural gas/O2/N2 and natural gas/H2/O2/N2 flames. *Combustion and Flame, 154*(3), 601-623. doi: http://dx.doi.org/10.1016/j.combustflame.2008.04.018

de Goey, L. P. H., Hermanns, R. T. E., & Bastiaans, R. J. M. (2007). Analysis of the asymptotic structure of stoichiometric premixed CH4–H2–air flames. *Proceedings of the combustion institute, 31*(1), 1031-1038. doi: http://dx.doi.org/10.1016/j.proci.2006.07.072

de Goey, L. P. H., van Oijen, J. A., Kornilov, V. N., & ten Thije Boonkkamp, J. H. M. (2011). Propagation, dynamics and control of laminar premixed flames. *Proceedings of the Combustion Institute, 33*(1), 863-886. doi: http://dx.doi.org/10.1016/j.proci.2010.09.006

Delattin, F., Lorenzo, G. D., Rizzo, S., Bram, S., & Ruyck, J. D. (2010). Combustion of syngas in a pressurized microturbine-like combustor: Experimental results. *Applied Energy, 87*(4), 1441-1452.

Di Benedetto, A., Di Sarli, V., Salzano, E., Cammarota, F., & Russo, G. (2009). Explosion behavior of CH4/O2/N2/CO2 and H2/O2/N2/CO2 mixtures. *International Journal of Hydrogen Energy, 34*(16), 6970-6978. doi: http://dx.doi.org/10.1016/j.ijhydene.2009.05.120

Di Benedetto, A., Di Sarli, V., Salzano, E., Cammarota, F., & Russo, G. (2009). Explosion behavior of CH 4/O2/N2/CO2 and H2/O2/N2/CO2 mixtures. *International Journal of Hydrogen Energy, 34*(16), 6970-6978.

Di Benedetto, A., Garcia-Agreda, A., Russo, P., & Sanchirico, R. (2011). Combined effect of ignition energy and initial turbulence on the explosion behavior of lean gas/dust-air mixtures. *Industrial & Engineering Chemistry Research, 51*(22), 7663-7670.

Di Benedetto, A., & Salzano, E. (2010). CFD simulation of pressure piling. *Journal of loss prevention in the process industries, 23*(4), 498-506. doi: http://dx.doi.org/10.1016/j.jlp.2010.03.003

Di Sarli, V., & Benedetto, A. D. (2007). Laminar burning velocity of hydrogen–methane/air premixed flames. *International Journal of Hydrogen Energy, 32*(5), 637-646. doi: http://dx.doi.org/10.1016/j.ijhydene.2006.05.016

Di Sarli, V., & Di Benedetto, A. (2013). Effects of non-equidiffusion on unsteady propagation of hydrogen-enriched methane/air premixed flames. *International Journal of Hydrogen Energy, 38*(18), 7510-7518. doi: http://dx.doi.org/10.1016/j.ijhydene.2013.03.126

Di Sarli, V., Di Benedetto, A., Long, E. J., & Hargrave, G. K. (2012). Time-Resolved Particle Image Velocimetry of dynamic interactions between hydrogen-enriched methane/air premixed flames and toroidal vortex structures. *International Journal of Hydrogen Energy, 37*(21), 16201-16213. doi: http://dx.doi.org/10.1016/j.ijhydene.2012.08.061

Di Sarlia, V., & Di Benedettob, A. (2013). Large Eddy Simulation of Transient Flame-Vortex Interactions during Explosions of Hydrogen-Enriched Methane/Air Mixtures. *CHEMICAL ENGINEERING, 31*.

Dinkelacker, F., Manickam, B., & Muppala, S. P. R. (2011). Modelling and simulation of lean premixed turbulent methane/hydrogen/air flames with an effective Lewis number approach. *Combustion and Flame, 158*(9), 1742-1749. doi: http://dx.doi.org/10.1016/j.combustflame.2010.12.003

Dunstan, T. D., & Jenkins, K. W. (2009). The effects of hydrogen substitution on turbulent premixed methane–air kernels using direct numerical simulation. *International Journal of Hydrogen Energy, 34*(19), 8389-8404. doi: http://dx.doi.org/10.1016/j.ijhydene.2009.07.087

Eckhoff, R., Ngo, M., & Olsen, W. (2010). On the minimum ignition energy (MIE) for propane/air. *Journal of Hazardous Materials, 175*(1), 293-297.

Egolfopoulos, F., Zhu, D., & Law, C. (1991). *Experimental and numerical determination of laminar flame speeds: Mixtures of C 2-hydrocarbons with oxygen and nitrogen.* Paper presented at the Symposium (International) on Combustion.

Emami, S. D., Rajabi, M., Che Hassan, C. R., Hamid, M. D. A., Kasmani, R. M., & Mazangi, M. (2013). Experimental study on premixed hydrogen/air and hydrogen–methane/air mixtures explosion in 90 degree bend pipeline. *International Journal of Hydrogen Energy, 38*(32), 14115-14120. doi: http://dx.doi.org/10.1016/j.ijhydene.2013.08.056

Ethylene is Explosive! (2015). from http://www.catalyticgenerators.com/explosions.html

Fang, L. (1996). Wang deng-bao, Li Dao-lin, Ge You-kang, Lo Yong-bao, Wu Zhen-yao.; Flow Distribution Studies of Superheaters and Reheaters of Large Utility Boilers with Tee-Junction Headers.[J]. *POWER ENGINEERING, 3*.

Federici, J., & Vlachos, D. (2008). A computational fluid dynamics study of propane/air microflame stability in a heat recirculation reactor. *Combustion and Flame, 153*(1), 258-269.

Ferrara, G., Di Benedetto, A., Salzano, E., & Russo, G. (2006). CFD analysis of gas explosions vented through relief pipes. *Journal of Hazardous Materials, 137*(2), 654-665.

Fotache, C. G., Kreutz, T. G., & Law, C. K. (1997). Ignition of hydrogen-enriched methane by heated air. *Combustion and Flame, 110*(4), 429-440. doi: http://dx.doi.org/10.1016/S0010-2180(97)00084-9

Frolov, S. M., Medvedev, S. N., Basevich, V. Y., & Frolov, F. S. (2013). Self-ignition of hydrocarbon–hydrogen–air mixtures. *International Journal of Hydrogen Energy, 38*(10), 4177-4184. doi: http://dx.doi.org/10.1016/j.ijhydene.2013.01.075

Gamezo, V. N., Ogawa, T., & Oran, E. S. (2008). Flame acceleration and DDT in channels with obstacles: Effect of obstacle spacing. *Combustion and Flame, 155*(1–2), 302-315. doi: 10.1016/j.combustflame.2008.06.004

Gamezo, V. N., Zipf, R. K., Sapko, M. J., Marchewka, W. P., Mohamed, K. M., Oran, E. S., Karnack, F. A. (2012). Detonability of natural gas–air mixtures. *Combustion and Flame, 159*(2), 870-881.

Gas explosion. (2012). from http://en.wikipedia.org/wiki/Gas_explosion

Grossel, S. S. (2002). *Deflagration and detonation flame arresters*: Center for Chemical Process Safety of the American Institute of Chemical Engineers.

Grossel, S. S. (2010). *Deflagration and detonation flame arresters* (Vol. 9): John Wiley & Sons.

Gu, X. J., Haq, M. Z., Lawes, M., & Woolley, R. (2000). Laminar burning velocity and Markstein lengths of methane–air mixtures. *Combustion and Flame, 121*(1–2), 41-58. doi: http://dx.doi.org/10.1016/S0010-2180(99)00142-X

Gülder, Ö. L., Snelling, D. R., & Sawchuk, R. A. (1996). Influence of hydrogen addition to fuel on temperature field and soot formation in diffusion flames. *Symposium (International) on Combustion, 26*(2), 2351-2358. doi: http://dx.doi.org/10.1016/S0082-0784(96)80064-6

Guo, H., & Neill, W. S. (2009). A numerical study on the effect of hydrogen/reformate gas addition on flame temperature and NO formation in strained methane/air diffusion flames. *Combustion and Flame, 156*(2), 477-483. doi: http://dx.doi.org/10.1016/j.combustflame.2008.07.009

Guo, H., Smallwood, G., Liu, F., Ju, Y., & Gulder, O. (2005a). The effect of hydrogen addition on flammability limit and NOx emission in ultra-lean counterflow CH4/air premixed flames. *Proceedings of the combustion institute, 30*, 303-311.

Guo, H., Smallwood, G. J., & Gülder, Ö. L. (2007). The effect of reformate gas enrichment on extinction limits and NOX formation in counterflow CH4/air premixed flames. *Proceedings of the combustion institute, 31*(1), 1197-1204. doi: http://dx.doi.org/10.1016/j.proci.2006.07.205

Guo, H., Smallwood, G. J., Liu, F., Ju, Y., & Gülder, Ö. L. (2005b). The effect of hydrogen addition on flammability limit and NOx emission in ultra-lean counterflow CH4/air premixed flames. *Proceedings of the combustion institute, 30*(1), 303-311. doi: http://dx.doi.org/10.1016/j.proci.2004.08.177

Hadjisophocleous, G. V., & Mehaffey, J. R. (2016). Fire Scenarios. In *SFPE Handbook of Fire Protection Engineering* (pp. 1262-1288). Springer New York.

Halter, F., Chauveau, C., Djebaïli-Chaumeix, N., & Gökalp, I. (2005). Characterization of the effects of pressure and hydrogen concentration on laminar burning velocities of methane–hydrogen–air mixtures. *Proceedings of the combustion institute, 30*(1), 201-208. doi: http://dx.doi.org/10.1016/j.proci.2004.08.195

Halter, F., Chauveau, C., & Gökalp, I. (2007). Characterization of the effects of hydrogen addition in premixed methane/air flames. *International Journal of Hydrogen Energy, 32*(13), 2585-2592. doi: http://dx.doi.org/10.1016/j.ijhydene.2006.11.033

Hamza, K. (2010). Hydrogen Explosion ACCIDENT AT U.S. , LESSONS !!!!!   , from http://science-hamza.blogspot.com/2010/12/hydrogen-explosion-accident-at-us.html

Harris, R. J. (1983). *The investigation and control of gas explosions in building and heating plant*. New York: E&F N Spon Ltd.

Hassan, M. I., Aung, K. T., & Faeth, G. M. (1998). Measured and predicted properties of laminar premixed methane/air flames at various pressures. *Combustion and Flame, 115*(4), 539-550. doi: http://dx.doi.org/10.1016/S0010-2180(98)00025-X

Hassan, Y., Mousseau, V., Sanyal, J., Durbin, S., Baglietto, E., Lucas, D., . . . Dreisbach, J. (2012). Technical session summaries.

Hawkes, E. R., & Chen, J. H. (2004). Direct numerical simulation of hydrogen-enriched lean premixed methane–air flames. *Combustion and Flame, 138*(3), 242-258. doi: http://dx.doi.org/10.1016/j.combustflame.2004.04.010

Heidari, A., & Wen, J. (2014). Flame acceleration and transition from deflagration to detonation in hydrogen explosions. *International Journal of Hydrogen Energy, 39*(11), 6184-6200.

Herrig Brothers Farm Propane Tank Explosion. (1998). from http://www.csb.gov/herrig-brothers-farm-propane-tank-explosion/

Hjertager, B., Fuhre, K., & Bjørkhaug, M. (1988). Concentration effects on flame acceleration by obstacles in large-scale methane-air and propane-air vented explosions. *Combustion Science and Technology, 62*(4-6), 239-256.

Hu, E., Huang, Z., He, J., & Miao, H. (2009a). Experimental and numerical study on laminar burning velocities and flame instabilities of hydrogen–air mixtures at elevated pressures and temperatures. *International Journal of Hydrogen Energy, 34*(20), 8741-8755. doi: http://dx.doi.org/10.1016/j.ijhydene.2009.08.044

Hu, E., Huang, Z., He, J., & Miao, H. (2009b). Experimental and numerical study on lean premixed methane–hydrogen–air flames at elevated pressures and temperatures. *International Journal of Hydrogen Energy, 34*(16), 6951-6960. doi: http://dx.doi.org/10.1016/j.ijhydene.2009.06.072

Hu, E., Huang, Z., He, J., Zheng, J., & Miao, H. (2009c). Measurements of laminar burning velocities and onset of cellular instabilities of methane–hydrogen–air flames at elevated pressures and temperatures. *International Journal of Hydrogen Energy, 34*(13), 5574-5584. doi: http://dx.doi.org/10.1016/j.ijhydene.2009.04.058

Hu, E., Huang, Z., Liu, B., Zheng, J., Gu, X., & Huang, B. (2009d). Experimental investigation on performance and emissions of a spark-ignition engine fuelled with natural gas–hydrogen blends combined with EGR. *International Journal of Hydrogen Energy, 34*(1), 528-539. doi: http://dx.doi.org/10.1016/j.ijhydene.2008.10.042

Hu, E., Huang, Z., Zheng, J., Li, Q., & He, J. (2009e). Numerical study on laminar burning velocity and NO formation of premixed methane–hydrogen–air flames. *International Journal of Hydrogen Energy, 34*(15), 6545-6557. doi: http://dx.doi.org/10.1016/j.ijhydene.2009.05.080

Huang, Z., Zhang, Y., Zeng, K., Liu, B., Wang, Q., & Jiang, D. (2006). Measurements of laminar burning velocities for natural gas–hydrogen–air mixtures. *Combustion and Flame, 146*(1–2), 302-311. doi: http://dx.doi.org/10.1016/j.combustflame.2006.03.003

Huntress Jr, W. T. (1972). Hydrogen atom scrambling in ion-molecule reactions of methane and ethylene.

Huzayyin, A., Moneib, H., Shehatta, M., & Attia, A. (2008). Laminar burning velocity and explosion index of LPG–air and propane–air mixtures. *Fuel, 87*(1), 39-57.

Hydrogen Airship Disasters. from http://www.airships.net/hydrogen-airship-accidents

Ibrahim, S., & Masri, A. (2001). The effects of obstructions on overpressure resulting from premixed flame deflagration. *Journal of loss prevention in the process industries, 14*(3), 213-221.

Ikegami, M., Miwa, K., & Shioji, M. (1982). A study of hydrogen fuelled compression ignition engines. *International Journal of Hydrogen Energy, 7*(4), 341-353.

Ilbas, M., Crayford, A. P., Yılmaz, İ., Bowen, P. J., & Syred, N. (2006). Laminar-burning velocities of hydrogen–air and hydrogen–methane–air mixtures: An experimental study. *International Journal of Hydrogen Energy, 31*(12), 1768-1779. doi: http://dx.doi.org/10.1016/j.ijhydene.2005.12.007

İlbas, M., Yılmaz, İ., & Kaplan, Y. (2005). Investigations of hydrogen and hydrogen–hydrocarbon composite fuel combustion and emission characteristics in a model combustor. *International Journal of Hydrogen Energy, 30*(10), 1139-1147. doi: http://dx.doi.org/10.1016/j.ijhydene.2004.10.016

Inaba, Y., Nishihara, T., Groethe, M. A., & Nitta, Y. (2004). Study on explosion characteristics of natural gas and methane in semi-open space for the HTTR hydrogen production system. *Nuclear engineering and design, 232*(1), 111-119.

Jackson, G. S., Sai, R., Plaia, J. M., Boggs, C. M., & Kiger, K. T. (2003). Influence of H2 on the response of lean premixed CH4 flames to high strained flows. *Combustion and Flame, 132*(3), 503-511. doi: http://dx.doi.org/10.1016/S0010-2180(02)00496-0

Jamal, Y., & Wyszynski, M. L. (1994). On-board generation of hydrogen-rich gaseous fuels—a review. *International Journal of Hydrogen Energy, 19*(7), 557-572. doi: http://dx.doi.org/10.1016/0360-3199(94)90213-5

Jianliang, Y., Wei, M., & Yajie, W. (2005). Experiment to Suppress Gas Explosion in Pipe with Structure of Multi-layer Wire Mesh. *Natural gas industry, 25*(6), 116.

Jo, Y.-D., & Ahn, B. J. (2005). A method of quantitative risk assessment for transmission pipeline carrying natural gas. *Journal of Hazardous Materials, 123*(1–3), 1-12. doi: http://dx.doi.org/10.1016/j.jhazmat.2005.01.034

Jo, Y.-D., & Ahn, B. J. (2006). Analysis of hazard area associated with hydrogen gas transmission pipelines. *International Journal of Hydrogen Energy, 31*(14), 2122-2130. doi: 10.1016/j.ijhydene.2006.01.008

Jo, Y.-D., & Crowl, D. A. (2008). Individual risk analysis of high-pressure natural gas pipelines. *Journal of loss prevention in the process industries, 21*(6), 589-595. doi: http://dx.doi.org/10.1016/j.jlp.2008.04.006

Jo, Y. D., & Ahn, B. J. (2002). Analysis of hazard areas associated with high-pressure natural-gas pipelines. *Journal of loss prevention in the process industries, 15*(3), 179-188. doi: http://dx.doi.org/10.1016/S0950-4230(02)00007-4

Jomaas, G., Zheng, X., Zhu, D., & Law, C. (2005). Experimental determination of counterflow ignition temperatures and laminar flame speeds of C 2–C 3 hydrocarbons at atmospheric and elevated pressures. *Proceedings of the combustion institute, 30*(1), 193-200.

Ju, Y., & Niioka, T. (1994). Reduced kinetic mechanism of ignition for nonpremixed hydrogen/air in a supersonic mixing layer. *Combustion and Flame, 99*(2), 240-246. doi: http://dx.doi.org/10.1016/0010-2180(94)90127-9

Kahraman, N., Çeper, B., Akansu, S. O., & Aydin, K. (2009). Investigation of combustion characteristics and emissions in a spark-ignition engine fuelled with natural gas–hydrogen blends. *International Journal of Hydrogen Energy, 34*(2), 1026-1034. doi: http://dx.doi.org/10.1016/j.ijhydene.2008.10.075

Karim, G. A., Wierzba, I., & Al-Alousi, Y. (1996). Methane-hydrogen mixtures as fuels. *International Journal of Hydrogen Energy, 21*(7), 625-631. doi: http://dx.doi.org/10.1016/0360-3199(95)00134-4

Kasmani, R., Andrews, G., & Phylaktou, H. (2013). Experimental study on vented gas explosion in a cylindrical vessel with a vent duct. *Process Safety and Environmental Protection, 91*(4), 245-252.

Kasmani, R., Andrews, G., Phylaktou, H., & Willacy, S. (2007). *Influence of static burst pressure and ignition position on duct-vented gas explosions.* Paper presented at the 5th International Seminar on Fire and Explosion Hazards.

Khan, F. I., & Abbasi, S. A. (2001). An assessment of the likelihood of occurrence, and the damage potential of domino effect (chain of accidents) in a typical cluster of industries. *Journal of Loss Prevention in the Process Industries, 14*(4), 283-306.

Kim, H. S., Arghode, V. K., & Gupta, A. K. (2009). Combustion characteristics of a lean premixed LPG–air combustor. *International Journal of Hydrogen Energy, 34*(2), 1045-1053. doi: http://dx.doi.org/10.1016/j.ijhydene.2008.10.036

Kim, W. K., Mogi, T., & Dobashi, R. (2013). Fundamental study on accidental explosion behavior of hydrogen-air mixtures in an open space. *international journal of hydrogen energy*, *38*(19), 8024-8029.

Kim, W. K., Mogi, T., & Dobashi, R. (2014). Effect of propagation behaviour of expanding spherical flames on the blast wave generated during unconfined gas explosions. *Fuel, 128,* 396-403.

Kindracki, J., Kobiera, A., Rarata, G., & Wolanski, P. (2007). Influence of ignition position and obstacles on explosion development in methane–air mixture in closed vessels. *Journal of loss prevention in the process industries, 20*(4), 551-561.

Kitagawa, T., Nakahara, T., Maruyama, K., Kado, K., Hayakawa, A., & Kobayashi, S. (2008). Turbulent burning velocity of hydrogen–air premixed propagating flames at elevated pressures. *International Journal of Hydrogen Energy, 33*(20), 5842-5849. doi: http://dx.doi.org/10.1016/j.ijhydene.2008.06.013

Kolbe, M., & Baker, Q. (2005). *Gaseous explosions in pipes.* Paper presented at the ASME 2005 Pressure Vessels and Piping Conference.

Konnov, A. A., Riemeijer, R., & de Goey, L. P. H. (2010). Adiabatic laminar burning velocities of CH4 + H2 + air flames at low pressures. *Fuel, 89*(7), 1392-1396. doi: http://dx.doi.org/10.1016/j.fuel.2009.11.002

Kumar, K., Mittal, G., Sung, C., & Law, C. (2007). *An experimental Investigation on ethylene/oxygen/diluent mixtures: Laminar flame speeds with preheat and ignition delays at high pressures.* Paper presented at the 5th US Combustion Meeting.

Kwon, O., & Faeth, G. (2001). Flame/stretch interactions of premixed hydrogen-fueled flames: measurements and predictions. *Combustion and Flame, 124*(4), 590-610.

Lafay, Y., Renou, B., Cabot, G., & Boukhalfa, M. (2008). Experimental and numerical investigation of the effect of H2 enrichment on laminar methane–air flame thickness. *Combustion and Flame, 153*(4), 540-561. doi: http://dx.doi.org/10.1016/j.combustflame.2007.10.002

Law, C. K., & Kwon, O. C. (2004). Effects of hydrocarbon substitution on atmospheric hydrogen–air flame propagation. *International Journal of Hydrogen Energy, 29*(8), 867-879. doi: http://dx.doi.org/10.1016/j.ijhydene.2003.09.012

Lee, J. G., Kim, K., & Santavicca, D. (2000). Measurement of equivalence ratio fluctuation and its effect on heat release during unstable combustion. *Proceedings of the combustion institute, 28*(1), 415-421.

Lee, T.-W., Jain, V., & Kozola, S. (2001). Measurements of minimum ignition energy by using laser sparks for hydrocarbon fuels in air: propane, dodecane, and jet-A fuel. *Combustion and Flame, 125*(4), 1320-1328.

Levy, A. (1955). *The fast and slow reactions of hydrogen-oxygen-propane mixtures.* Paper presented at the Symposium (International) on Combustion.

Lewis, B., & Von Elbe, G. (2012). *Combustion, flames and explosions of gases*. Elsevier.

Li, G., Zhang, Z., Liang, J., Dong, F., Li, Y., & Gao, X. (2012). Effects of hydrogen addition on the premixed laminar-flames of ethanol–air gaseous mixtures: An experimental study. *International Journal of Hydrogen Energy, 37*(5), 4490-4501. doi: http://dx.doi.org/10.1016/j.ijhydene.2011.11.126

Liao, S., Jiang, D., Gao, J., & Huang, Z. (2004). Measurements of Markstein numbers and laminar burning velocities for natural gas-air mixtures. *Energy & fuels, 18*(2), 316-326.

Liberman, M. A., Ivanov, M. F., Kiverin, A. D., Kuznetsov, M. S., Chukalovsky, A. A., & Rakhimova, T. V. (2010). Deflagration-to-detonation transition in highly reactive combustible mixtures. *Acta Astronautica, 67*(7–8), 688-701. doi: 10.1016/j.actaastro.2010.05.024

Lide, D., & Haynes, W. (2009). *CRC handbook of chemistry and physics: a ready-reference book of chemical and physical data-/editor-in-chief, David R. Lide; ass. ed. WM" Mickey" Haunes*: Boca Raton, Fla: CRC.

List of pipeline accidents. (3 March 2015). from http://en.wikipedia.org/wiki/List_of_pipeline_accidents

Liu, Q., Zhang, Y., Niu, F., & Li, L. (2015). Study on the flame propagation and gas explosion in propane/air mixtures. *Fuel, 140*, 677-684.

LIU, S., ZHANG, Y., SONG, K., & GAO, J. (2011). Finite Element Analysis of Internal Pressure bulging Process for T-tube. *Hot Working Technology, 21*, 020.

Lohrer, C., Drame, C., Schalau, B., & Grätz, R. (2008). Propane/air deflagrations and CTA measurements of turbulence inducing elements in closed pipes. *Journal of loss prevention in the process industries, 21*(1), 1-10.

Ma, F., & Wang, Y. (2008). Study on the extension of lean operation limit through hydrogen enrichment in a natural gas spark-ignition engine. *International Journal of Hydrogen Energy, 33*(4), 1416-1424. doi: http://dx.doi.org/10.1016/j.ijhydene.2007.12.040

Ma, F., Wang, Y., Liu, H., Li, Y., Wang, J., & Ding, S. (2008). Effects of hydrogen addition on cycle-by-cycle variations in a lean burn natural gas spark-ignition engine. *International Journal of Hydrogen Energy, 33*(2), 823-831. doi: http://dx.doi.org/10.1016/j.ijhydene.2007.10.043

Ma, F., Wang, Y., Liu, H., Li, Y., Wang, J., & Zhao, S. (2007). Experimental study on thermal efficiency and emission characteristics of a lean burn hydrogen enriched natural gas engine. *International Journal of Hydrogen Energy, 32*(18), 5067-5075. doi: http://dx.doi.org/10.1016/j.ijhydene.2007.07.048

Mandilas, C., Ormsby, M. P., Sheppard, C. G. W., & Woolley, R. (2007). Effects of hydrogen addition on laminar and turbulent premixed methane and iso-octane–air flames. *Proceedings of the combustion institute, 31*(1), 1443-1450. doi: http://dx.doi.org/10.1016/j.proci.2006.07.157

Mardani, A., & Tabejamaat, S. (2010). Effect of hydrogen on hydrogen–methane turbulent non-premixed flame under MILD condition. *International Journal of Hydrogen Energy, 35*(20), 11324-11331. doi: http://dx.doi.org/10.1016/j.ijhydene.2010.06.064

Markstein, G. H. (2014). *Nonsteady Flame Propagation: AGARDograph* (Vol. 75): Elsevier.

Masri, A. R., Dibble, R. W., & Barlow, R. S. (1992). Chemical kinetic effects in nonpremixed flames of H2/CO2 fuel. *Combustion and Flame, 91*(3–4), 285-309. doi: http://dx.doi.org/10.1016/0010-2180(92)90059-X

Merlin, C., Domingo, P., & Vervisch, L. (2012). Large Eddy Simulation of turbulent flames in a Trapped Vortex Combustor (TVC)–A flamelet presumed-pdf closure preserving laminar flame speed. *Comptes Rendus Mécanique, 340*(11), 917-932.

Metghalchi, M., & Keck, J. (1980). Laminar burning velocity of propane-air mixtures at high temperature and pressure. *Combustion and Flame, 38*, 143-154.

Miao, H., Jiao, Q., Huang, Z., & Jiang, D. (2008). Effect of initial pressure on laminar combustion characteristics of hydrogen enriched natural gas. *International Journal of Hydrogen Energy, 33*(14), 3876-3885. doi: http://dx.doi.org/10.1016/j.ijhydene.2008.04.029

Miao, H., Jiao, Q., Huang, Z., & Jiang, D. (2009). Measurement of laminar burning velocities and Markstein lengths of diluted hydrogen-enriched natural gas. *International Journal of Hydrogen Energy, 34*(1), 507-518. doi: http://dx.doi.org/10.1016/j.ijhydene.2008.10.050

Miao, H., Lu, L., & Huang, Z. (2011). Flammability limits of hydrogen-enriched natural gas. *International Journal of Hydrogen Energy, 36*(11), 6937-6947. doi: http://dx.doi.org/10.1016/j.ijhydene.2011.02.126

Middha, P., Hansen, O. R., & Schneider, H. (2007). *Deflagration to detonation transition (DDT) in jet ignited hydrogen-air mixtures: large scale experiments and FLACS CFD predictions.* Paper presented at the Proceedings of 12th International Symposium on Loss Prevention and Safety Promotion in the Process Industries, Edinburgh, UK.

Mohammed, S. E. L., Baharom, M. B., & Aziz, A. R. A. (2011). Analysis of engine characteristics and emissions fueled by in-situ mixing of small amount of hydrogen in CNG. *International Journal of Hydrogen Energy, 36*(6), 4029-4037. doi: http://dx.doi.org/10.1016/j.ijhydene.2010.12.065

Movileanu, C., Gosa, V., & Razus, D. (2012). Explosion of gaseous ethylene–air mixtures in closed cylindrical vessels with central ignition. *Journal of Hazardous Materials, 235*, 108-115.

Movileanu, C., Razus, D., & Oancea, D. (2011a). Additive effects on explosion pressure and flame temperature of stoichiometric ethylene–air mixture in closed vessels. *Rev. Roumaine Chim, 56*, 11-17.

Movileanu, C., Razus, D., & Oancea, D. (2011b). Additive effects on the burning velocity of ethylene–air mixtures. *Energy & fuels, 25*(6), 2444-2451.

Movileanu, C., Razus, D., & Oancea, D. (2013). Additive effects on the rate of pressure rise for ethylene–air deflagrations in closed vessels. *Fuel, 111*, 194-200.

Muramatsu, T. (2004). *Numerical Simulation of Non-Stationary Heat Transfer Process Related to Thermal Striping Phenomena.* Paper presented at the ASME/JSME 2004 Pressure Vessels and Piping Conference.

Na'inna, A. M., Somuano, G. B., Phylaktou, H. N., & Andrews, G. E. (2015). Flame acceleration in tube explosions with up to three flat-bar obstacles with variable obstacle separation distance. *Journal of loss prevention in the process industries, 38*, 119-124. doi: http://dx.doi.org/10.1016/j.jlp.2015.08.009

Naha, S., & Aggarwal, S. K. (2004). Fuel effects on NOx emissions in partially premixed flames. *Combustion and Flame, 139*(1–2), 90-105. doi: http://dx.doi.org/10.1016/j.combustflame.2004.07.006

Naha, S., Briones, A. M., & Aggarwal, S. K. (2005). Effect of fuel blends on pollutant emissions in flames. *Combustion Science and Technology, 177*(1), 183-220.

Ng, H. K., & Gan, S. (2010). Combustion performance and exhaust emissions from the non-pressurised combustion of palm oil biodiesel blends. *Applied Thermal Engineering, 30*(16), 2476-2484.

Nguyen, T. A., & Mikami, M. (2013). Effect of hydrogen addition to intake air on combustion noise from a diesel engine. *International Journal of Hydrogen Energy, 38*(10), 4153-4162. doi: http://dx.doi.org/10.1016/j.ijhydene.2013.01.082

Noble, D. R., Zhang, Q., & Lieuwen, T. (2006). Hydrogen effects upon flashback and blowout. *Proc. ICEPAG*.

Norman, F., Van den Schoor, F., & Verplaetsen, F. (2006). Auto-ignition and upper explosion limit of rich propane–air mixtures at elevated pressures. *Journal of Hazardous Materials, 137*(2), 666-671.

Norton, D. G., & Vlachos, D. G. (2004). A CFD study of propane/air microflame stability. *Combustion and Flame, 138*(1), 97-107.

Oh, K.-H., Kim, H., Kim, J.-B., & Lee, S.-E. (2001). A study on the obstacle-induced variation of the gas explosion characteristics. *Journal of loss prevention in the process industries, 14*(6), 597-602.

Ozcan, H. (2010). Hydrogen enrichment effects on the second law analysis of a lean burn natural gas engine. *International Journal of Hydrogen Energy, 35*(3), 1443-1452. doi: http://dx.doi.org/10.1016/j.ijhydene.2009.11.039

Papagiannakis, R. G., Rakopoulos, C. D., Hountalas, D. T., & Rakopoulos, D. C. (2010). Emission characteristics of high speed, dual fuel, compression ignition engine operating in a wide range of natural gas/diesel fuel proportions. *Fuel, 89*(7), 1397-1406. doi: http://dx.doi.org/10.1016/j.fuel.2009.11.001

Park, J., Lee, K., & Lee, E. (2001). Effects of CO2 addition on flame structure in counterflow diffusion flame of H2/CO2/N2 fuel. *International Journal of Energy Research, 25*(6), 469-485.

Petchenko, A., Bychkov, V., Akkerman, V. y., & Eriksson, L.-E. (2007). Flame–sound interaction in tubes with nonslip walls. *Combustion and Flame, 149*(4), 418-434. doi: http://dx.doi.org/10.1016/j.combustflame.2007.02.003

Petukhov, V., Naboko, I., & Fortov, V. (2009). Explosion hazard of hydrogen–air mixtures in the large volumes. *International Journal of Hydrogen Energy, 34*(14), 5924-5931.

Phylaktou, H. (1993). *Explosion development in T- piece*.

Phylaktou, H., & Andrews, G. (1991). Gas explosions in long closed vessels. *Combustion Science and Technology, 77*(1-3), 27-39.

Phylaktou, H., & Andrews, G. E. (1991). The acceleration of flame propagation in a tube by an obstacle. *Combustion and Flame, 85*(3–4), 363-379. doi: 10.1016/0010-2180(91)90140-7

Phylaktou, H., Foley, M., & Andrews, G. (1993). Explosion enhancement through a 90° curved bend. *Journal of loss prevention in the process industries, 6*(1), 21-29.

Phylaktou, H., Foley, M., & Andrews, G. E. (1993). Explosion enhancement through a 90° curved bend. *Journal of Loss Prevention in the Process Industries, 6*(1), 21-29. doi: 10.1016/0950-4230(93)80016-f

Prince, J. C., & Williams, F. A. (2012). Short chemical-kinetic mechanisms for low-temperature ignition of propane and ethane. *Combustion and Flame, 159*(7), 2336-2344.

Qiao, L., Kim, C., & Faeth, G. (2005). Suppression effects of diluents on laminar premixed hydrogen/oxygen/nitrogen flames. *Combustion and Flame, 143*(1), 79-96.

Qing, Y., Bai-quan, L., Zhen-zhen, J., & Chuan-jie, Z. (2009). Propagation law and analysis of gas explosion in bend duct. *Procedia Earth and Planetary Science, 1*(1), 316-321.

Rai, K., Bjerketvedt, D., & Gaathaug, A. V. (2014). Gas explosion field test with release of hydrogen from a high pressure reservoir into a channel. *International Journal of Hydrogen Energy, 39*(8), 3956-3962.

Razus, D., Brinzea, V., Mitu, M., Movileanu, C., & Oancea, D. (2011). Temperature and pressure influence on maximum rates of pressure rise during explosions of propane–air mixtures in a spherical vessel. *Journal of Hazardous Materials, 190*(1), 891-896.

Razus, D., Brinzea, V., Mitu, M., & Oancea, D. (2010a). Temperature and pressure influence on explosion pressures of closed vessel propane–air deflagrations. *Journal of Hazardous Materials*, *174*(1), 548-555.

Razus, D., Movileanu, C., Brinzea, V., & Oancea, D. (2006). Explosion pressures of hydrocarbon–air mixtures in closed vessels. *Journal of Hazardous Materials, 135*(1), 58-65.

Razus, D., Oancea, D., Brinzea, V., Mitu, M., & Movileanu, C. (2010b). Experimental and computed burning velocities of propane–air mixtures. *Energy Conversion and Management, 51*(12), 2979-2984.

Refael, S., & Sher, E. (1989). Reaction kinetics of hydrogen-enriched methane-air and propane-air flames. *Combustion and Flame, 78*(3–4), 326-338. doi: http://dx.doi.org/10.1016/0010-2180(89)90021-7

Remennikov, A. M., & Rose, T. A. (2005). Modelling blast loads on buildings in complex city geometries. *Computers & Structures, 83*(27), 2197-2205.

Ren, J. Y., Qin, W., Egolfopoulos, F. N., Mak, H., & Tsotsis, T. T. (2001). Methane reforming and its potential effect on the efficiency and pollutant emissions of lean methane–air combustion. *Chemical Engineering Science, 56*(4), 1541-1549. doi: http://dx.doi.org/10.1016/S0009-2509(00)00381-X

Sabard, J., Chaumeix, N., & Bentaib, A. (2013). Hydrogen explosion in ITER: Effect of oxygen content on flame propagation of H2/O2/N2 mixtures. *Fusion Engineering and Design, 88*(9–10), 2669-2673. doi: http://dx.doi.org/10.1016/j.fusengdes.2013.02.128

Sabia, P., de Joannon, M., Lavadera, M. L., Giudicianni, P., & Ragucci, R. (2014). Autoignition delay times of propane mixtures under MILD conditions at atmospheric pressure. *Combustion and Flame, 161*(12), 3022-3030.

Salzano, E., Cammarota, F., Di Benedetto, A., & Di Sarli, V. (2012). Explosion behavior of hydrogen–methane/air mixtures. *Journal of loss prevention in the process industries, 25*(3), 443-447. doi: http://dx.doi.org/10.1016/j.jlp.2011.11.010

Salzano, E., Marra, F., Russo, G., & Lee, J. (2002). Numerical simulation of turbulent gas flames in tubes. *Journal of Hazardous Materials, 95*(3), 233-247.

Sanchirico, R., Di Benedetto, A., Garcia-Agreda, A., & Russo, P. (2011). Study of the severity of hybrid mixture explosions and comparison to pure dust–air and vapour–air explosions. *Journal of loss prevention in the process industries, 24*(5), 648-655.

Sankaran, R., & Im, H. G. (2006). Effects of hydrogen addition on the markstein length and flammability limit of stretched methane/air premixed flames. *Combustion Science and Technology, 178*(9), 1585-1611.

Saravanan, N., & Nagarajan, G. (2008). An experimental investigation of hydrogen-enriched air induction in a diesel engine system. *International Journal of Hydrogen Energy, 33*(6), 1769-1775. doi: http://dx.doi.org/10.1016/j.ijhydene.2007.12.065

Sathiah, P., Komen, E., & Roekaerts, D. (2012). The role of CFD combustion modeling in hydrogen safety management—Part I: Validation based on small scale experiments. *Nuclear Engineering and Design, 248*, 93-107.

Schefer, R., Wicksall, D., & Agrawal, A. (2002). Combustion of hydrogen-enriched methane in a lean premixed swirl-stabilized burner. *Proceedings of the combustion institute, 29*(1), 843-851.

Schefer, R. W. (2003). Hydrogen enrichment for improved lean flame stability. *International Journal of Hydrogen Energy, 28*(10), 1131-1141. doi: http://dx.doi.org/10.1016/S0360-3199(02)00199-4

Schefer, R. W., Wicksall, D. M., & Agrawal, A. K. (2002). Combustion of hydrogen-enriched methane in a lean premixed swirl-stabilized burner. *Proceedings of the combustion institute, 29*(1), 843-851. doi: http://dx.doi.org/10.1016/S1540-7489(02)80108-0

Scholte, T. G., & Vaags, P. B. (1959). Burning velocities of mixtures of hydrogen, carbon monoxide and methane with air. *Combustion and Flame, 3*(0), 511-524. doi: http://dx.doi.org/10.1016/0010-2180(59)90057-4

Selim, H., Al Shoaibi, A., & Gupta, A. K. (2011). Effect of H2S in methane/air flames on sulfur chemistry and products speciation. *Applied Energy, 88*(8), 2593-2600. doi: http://dx.doi.org/10.1016/j.apenergy.2011.02.032

Selim, H., Gupta, A. K., & Al Shoaibi, A. (2012). Effect of CO2 and N2 concentration in acid gas stream on H2S combustion. *Applied Energy, 98*(0), 53-58. doi: http://dx.doi.org/10.1016/j.apenergy.2012.02.072

Selim, H., Ibrahim, S., Al Shoaibi, A., & Gupta, A. (2013). Effect of oxygen enrichment on acid gas combustion in hydrogen/air flames under claus conditions. *Applied Energy, 109*, 119-124.

Sepman, A. V., Mokhov, A. V., & Levinsky, H. B. (2011). The effects of hydrogen addition on NO formation in atmospheric-pressure, fuel-rich-premixed, burner-stabilized methane, ethane and propane flames. *International Journal of Hydrogen Energy, 36*(7), 4474-4481. doi: http://dx.doi.org/10.1016/j.ijhydene.2010.12.117

Sher, E., & Ozdor, N. (1992). Laminar burning velocities of n-butane/air mixtures enriched with hydrogen. *Combustion and Flame, 89*(2), 214-220. doi: http://dx.doi.org/10.1016/0010-2180(92)90029-O

Shiga, S., Ozone, S., Machacon, H. T. C., Karasawa, T., Nakamura, H., Ueda, T., . . . Kono, M. (2002). A study of the combustion and emission characteristics of compressed-natural-gas direct-injection stratified combustion using a rapid-compression-machine. *Combustion and Flame, 129*(1–2), 1-10. doi: http://dx.doi.org/10.1016/S0010-2180(01)00367-4

Shih, H.-Y. (2009). Computed extinction limits and flame structures of H2/O2 counterflow diffusion flames with CO2 dilution. *International Journal of Hydrogen Energy, 34*(9), 4005-4013. doi: http://dx.doi.org/10.1016/j.ijhydene.2009.03.013

Shirk, M. G., McGuire, T. P., Neal, G. L., & Haworth, D. C. (2008). Investigation of a hydrogen-assisted combustion system for a light-duty diesel vehicle. *International Journal of Hydrogen Energy, 33*(23), 7237-7244. doi: http://dx.doi.org/10.1016/j.ijhydene.2008.07.128

Shy, S. S., Chen, Y. C., Yang, C. H., Liu, C. C., & Huang, C. M. (2008). Effects of H2 or CO2 addition, equivalence ratio, and turbulent straining on turbulent burning velocities for lean premixed methane combustion. *Combustion and Flame, 153*(4), 510-524. doi: http://dx.doi.org/10.1016/j.combustflame.2008.03.014

Smith, P. D., & Rose, T. A. (2006). Blast wave propagation in city streets—an overview. *Progress in structural engineering and materials, 8*(1), 16-28.

Solberg, D., Pappas, J., & Skramstad, E. (1979). Experimental Investigations of Partly Confined Gas Explosions Analysis of Pressure Loads, Part 1. *Det Norske Veritas Research Division Technical Report No. 79-0483*.

Strakey, P., Sidwell, T., & Ontko, J. (2007). Investigation of the effects of hydrogen addition on lean extinction in a swirl stabilized combustor. *Proceedings of the combustion institute, 31*(2), 3173-3180. doi: http://dx.doi.org/10.1016/j.proci.2006.07.077

Suga, M. (1958). Studies on explosive reaction of ethylene mixed with oxygen or air. I. Explosion limit at low pressure. *Bulletin of the Chemical Society of Japan, 31*(5), 515-521.

Sulaiman, S. Z. (2015). *Computational study on the explosion mechanism in the pipelines using FLUENT and FLACS.* (PhD), UTM.

Tahtouh, T., Halter, F., & Mounaïm-Rousselle, C. (2011). Laminar premixed flame characteristics of hydrogen blended iso-octane–air–nitrogen mixtures. *International Journal of Hydrogen Energy, 36*(1), 985-991. doi: http://dx.doi.org/10.1016/j.ijhydene.2010.08.148

Tahtouh, T., Halter, F., Samson, E., & Mounaïm-Rousselle, C. (2009). Effects of hydrogen addition and nitrogen dilution on the laminar flame characteristics of premixed methane–air flames. *International Journal of Hydrogen Energy, 34*(19), 8329-8338. doi: http://dx.doi.org/10.1016/j.ijhydene.2009.07.071

Tang, C., He, J., Huang, Z., Jin, C., Wang, J., Wang, X., & Miao, H. (2008). Measurements of laminar burning velocities and Markstein lengths of propane–hydrogen–air mixtures at elevated pressures and temperatures. *International Journal of Hydrogen Energy, 33*(23), 7274-7285. doi: http://dx.doi.org/10.1016/j.ijhydene.2008.08.053

Tang, C., Zhang, S., Si, Z., Huang, Z., Zhang, K., & Jin, Z. (2014). High methane natural gas/air explosion characteristics in confined vessel. *Journal of Hazardous Materials, 278*, 520-528.

Thomas, G., Oakley, G., & Bambrey, R. (2010). An experimental study of flame acceleration and deflagration to detonation transition in representative process piping. *Process Safety and Environmental Protection, 88*(2), 75-90.

Tinaut, F. V., Melgar, A., Giménez, B., & Reyes, M. (2011). Prediction of performance and emissions of an engine fuelled with natural gas/hydrogen blends. *International Journal of Hydrogen Energy, 36*(1), 947-956. doi: http://dx.doi.org/10.1016/j.ijhydene.2010.10.025

Toronto propane explosion. (2008, 2015). from http://en.wikipedia.org/wiki/Toronto_propane_explosion

Tuncer, O., Acharya, S., & Uhm, J. H. (2009). Dynamics, NOx and flashback characteristics of confined premixed hydrogen-enriched methane flames.

International Journal of Hydrogen Energy, 34(1), 496-506. doi: http://dx.doi.org/10.1016/j.ijhydene.2008.09.075

Turrio-Baldassarri, L., Battistelli, C. L., Conti, L., Crebelli, R., De Berardis, B., Iamiceli, A. L., Iannaccone, S. (2006). Evaluation of emission toxicity of urban bus engines: Compressed natural gas and comparison with liquid fuels. *Science of The Total Environment, 355*(1–3), 64-77. doi: http://dx.doi.org/10.1016/j.scitotenv.2005.02.037

Vagelopoulos C, E. F., Law CK. (1994). *Further considerations on the determination of laminar flame speeds with the counter-flow twin-flame technique*. Paper presented at the 25th Symposium (international) on combustion, Pittsburgh, PA: The Combustion Institute.

Vasanth, S., Tauseef, S. M., Abbasi, T., Rangwala, A. S., & Abbasi, S. A. (2014). Assessment of the effect of pool size on burning rates of multiple pool fires using CFD. *Journal of Loss Prevention in the Process Industries, 30,* 86-94.

Verhelst, S., & Wallner, T. (2009). Hydrogen-fueled internal combustion engines. *Progress in Energy and Combustion Science, 35*(6), 490-527.

Vu, T. M., Park, J., Kim, J. S., Kwon, O. B., Yun, J. H., & Keel, S. I. (2011a). *Experimental Study in H2/CO/CH4-Air and H2/CO/C3H8-Air Premixed Flames. Part 1: Laminar Burning Velocities and Markstein Lengths.* Paper presented at the Materials Science Forum.

Vu, T. M., Park, J., Kim, J. S., Kwon, O. B., Yun, J. H., & Keel, S. I. (2011b). Experimental study on cellular instabilities in hydrocarbon/hydrogen/carbon monoxide–air premixed flames. *International Journal of Hydrogen Energy, 36*(11), 6914-6924. doi: http://dx.doi.org/10.1016/j.ijhydene.2011.02.085

Vu, T. M., Song, W. S., Park, J., Bae, D. S., & You, H. S. (2011c). Measurements of propagation speeds and flame instabilities in biomass derived gas–air premixed flames. *International Journal of Hydrogen Energy, 36*(18), 12058-12067. doi: http://dx.doi.org/10.1016/j.ijhydene.2011.06.082

Wang, J., Chen, H., Liu, B., & Huang, Z. (2008a). Study of cycle-by-cycle variations of a spark ignition engine fueled with natural gas–hydrogen blends. *International Journal of Hydrogen Energy, 33*(18), 4876-4883. doi: http://dx.doi.org/10.1016/j.ijhydene.2008.06.062

Wang, J., Huang, Z., Miao, H., Wang, X., & Jiang, D. (2008b). Characteristics of direct injection combustion fuelled by natural gas–hydrogen mixtures using a constant volume vessel. *International Journal of Hydrogen Energy, 33*(7), 1947-1956. doi: http://dx.doi.org/10.1016/j.ijhydene.2008.01.007

Wang, J., Huang, Z., Miao, H., Wang, X., & Jiang, D. (2008c). Study of cyclic variations of direct-injection combustion fueled with natural gas–hydrogen blends using a constant volume vessel. *International Journal of Hydrogen Energy, 33*(24), 7580-7591. doi: http://dx.doi.org/10.1016/j.ijhydene.2008.09.041

Wang, J., Huang, Z., Zheng, J., & Miao, H. (2009). Effect of partially premixed and hydrogen addition on natural gas direct-injection lean combustion. *International Journal of Hydrogen Energy, 34*(22), 9239-9247. doi: http://dx.doi.org/10.1016/j.ijhydene.2009.09.018

Wang, W.-B., Li, J.-Y., & Wu, Q.-J. (2007). The design of a chemical virtual instrument based on LabVIEW for determining temperatures and pressures. *Journal of Analytical Methods in Chemistry, 2007*.

Wang, Y., Wang, Z., Wang, C., & Hu, B. (2000). Energy estimation on ethylene sphere explosion. *Journal of loss prevention in the process industries, 13*(3), 393-396.

Wen, J. X., Madhav Rao, V. C., & Tam, V. H. Y. (2010). Numerical study of hydrogen explosions in a refuelling environment and in a model storage room. *International Journal of Hydrogen Energy, 35*(1), 385-394. doi: http://dx.doi.org/10.1016/j.ijhydene.2009.10.052

Willacy, S., Phylaktou, H., Andrews, G., & Ferrara, G. (2007). Stratified Propane–Air Explosions in a Duct Vented Geometry: Effect of Concentration, Ignition and Injection Position. *Process Safety and Environmental Protection, 85*(2), 153-161.

Wiser, R., Bachrach, D., Bolinger, M., & Golove, W. (2004). Comparing the risk profiles of renewable and natural gas-fired electricity contracts. *Renewable and Sustainable Energy Reviews, 8*(4), 335-363. doi: http://dx.doi.org/10.1016/j.rser.2003.11.005

Wooley, R. M., Fairweather, M., Falle, S. A. E. G., & Giddings, J. R. (2008). Predictions of the consequences of natural gas-hydrogen explosions using a novel CFD approach. In B. Bertrand & J. Xavier (Eds.), *Computer Aided Chemical Engineering* (Vol. Volume 25, pp. 919-924): Elsevier.

Xianli, L. (1995). The microcomputer controlled filament-wound machine for tee pipe fitting. *Fiber Reinforced Plastics*, 01.

Xiao, H., He, X., Duan, Q., Luo, X., & Sun, J. (2014). An investigation of premixed flame propagation in a closed combustion duct with a 90° bend. *Applied Energy, 134*, 248-256.

Xiao, H., Makarov, D., Sun, J., & Molkov, V. (2012). Experimental and numerical investigation of premixed flame propagation with distorted tulip shape in a closed duct. *Combustion and Flame, 159*(4), 1523-1538.

Xiao, H., Wang, Q., He, X., Sun, J., & Shen, X. (2011). Experimental study on the behaviors and shape changes of premixed hydrogen–air flames propagating in horizontal duct. *International Journal of Hydrogen Energy, 36*(10), 6325-6336.

Xiao, H., Wang, Q., He, X., Sun, J., & Yao, L. (2010). Experimental and numerical study on premixed hydrogen/air flame propagation in a horizontal rectangular closed duct. *International Journal of Hydrogen Energy, 35*(3), 1367-1376. doi: http://dx.doi.org/10.1016/j.ijhydene.2009.12.001

Yan, Z., & Holmstedt, G. (1996). CFD and experimental studies of room fire growth on wall lining materials. *Fire safety journal, 27*(3), 201-238.

Yang, H., Yang, C., & Fan, B. (2002). Analysis of key process parameters in liquid bulge forming of four-arm tube and computer simulation. *Journal of University of Science and Technology Beijing, 24*(1), 72-75.

Yu, G., Law, C. K., & Wu, C. K. (1986). Laminar flame speeds of hydrocarbon + air mixtures with hydrogen addition. *Combustion and Flame, 63*(3), 339-347. doi: http://dx.doi.org/10.1016/0010-2180(86)90003-9

Zalok, E., and G. V. Hadjisophocleous. "Assessment of the use of Fire Dynamics Simulator in performance-based design." *Fire technology* 47.4 (2011): 1081-1100.

Zeng, W., Ma, H., Liang, Y., & Hu, E. (2014). Experimental and modeling study on effects of N 2 and CO 2 on ignition characteristics of methane/air mixture. *Journal of Advanced Research*.

Zhang, L.-w., Jie, T., Xunzhong, G., Ming, L., & Xianjun, S. (2010). Cold deformation and heat treatment process of Ti/Al bimetallic tee pipe fitting. *Heat Treatment of Metals, 35*(8), 65-69.

Zhang, Q., Jiang, J., You, M., Yu, Y., & Cui, Y. (2013). Experimental study on gas explosion and venting process in interconnected vessels. *Journal of loss prevention in the process industries, 26*(6), 1230-1237.

Zhang, Q., Li, W., & Liang, H.-M. (2012). Effect of spark duration on explosion parameters of methane/air mixtures in closed vessels. *Safety science, 50*(9), 1715-1721.

Zhang, Q., Li, W., Lin, D.-C., Duan, Y., & Liang, H.-M. (2011). Experimental study of gas deflagration temperature distribution and its measurement. *Experimental Thermal and Fluid Science, 35*(3), 503-508.

Zhao, Z., Kazakov, A., Li, J., & Dryer, F. L. (2004). The initial temperature and N2 dilution effect on the laminar flame speed of propane/air. *Combustion Science and Technology, 176*(10), 1705-1723.

Zhao, Z., Zhenyuan, J., & Haizhu, L. (2015). Characteristics of gas explosion flow fields in complex pipelines. *International Journal of Mining Science and Technology, 25*(1), 157-164.

Zhen, H. S., Cheung, C. S., Leung, C. W., & Choy, Y. S. (2012a). A comparison of the emission and impingement heat transfer of LPG–H2 and CH4–H2 premixed flames. *International Journal of Hydrogen Energy, 37*(14), 10947-10955. doi: http://dx.doi.org/10.1016/j.ijhydene.2012.04.055

Zhen, H. S., Cheung, C. S., Leung, C. W., & Choy, Y. S. (2012b). Effects of hydrogen concentration on the emission and heat transfer of a premixed LPG-hydrogen flame. *International Journal of Hydrogen Energy, 37*(7), 6097-6105. doi: http://dx.doi.org/10.1016/j.ijhydene.2011.12.130

Zhian, H., Zhigang, L., Shengguo, C., Yansong, Z., & Yinghua, Z. (2012). Numerical simulation and study on the transmission law of flame and pressure wave of pipeline gas explosion. *Safety Science, 50*(4), 806-810. doi: http://dx.doi.org/10.1016/j.ssci.2011.08.029

Zhou, B., Sobiesiak, A., & Quan, P. (2006). Flame behavior and flame-induced flow in a closed rectangular duct with a 90° bend. *International Journal of Thermal Sciences, 45*(5), 457-474. doi: http://dx.doi.org/10.1016/j.ijthermalsci.2005.07.001

Zhu, C., Lin, B., & Jiang, B. (2012). Flame acceleration of premixed methane/air explosion in parallel pipes. *Journal of loss prevention in the process industries, 25*(2), 383-390.

Zhu, C., Lu, Z., Lin, B., & Jiang, B. (2010). Effect of variation in gas distribution on explosion propagation characteristics in coal mines. *Mining Science and Technology (China), 20*(4), 516-519.

Appendix A – Operation Check List

Date:	**description**	**Fuel:**
Test No:		**Concentration:**
Authorized by:		**Ignition:**
		Injection:

Procedure: EXPLOSION TEST **Sheet: premixed fuel gases**

Tick	**operation**	**Instruction**	**Action/Remarks**
	Initial Start State		
☐	System purged		
	Pretest conditions		
☐	Load data logger software		
☐	Close the butterfly valve		
☐	Record the data	Ambient P: bar	
		Ambient T: °C	
		Humidity : %	
		Time base: ms	
☐	Valves closed		
☐	**Pretest checks**		
☐	Power to spark		
☐	Audible test to spark		
☐	Check the bottle pressure		Ensure enough fuel>5 bar
☐	Open and set regulator F2		Set to =2 bar
☐	Open and set regulator F3		
	Operating State **Connect and Evacuation**		
	Connect		
☐	CP1 TO V1		
☐	Open V1		
☐	CP2 TO V2		
☐	Open V3 to test vessel		Check the vessel pressure
	Evacuation		
☐	Open CB1		
☐	Start vacuum	Vacuum to <300 mbar	
☐	Close CB1		
☐	Stop vacuum		
☐	Is leak rate < 2 mbar/min		If No: see S/P 1
	Operating State		
☐	Note and record Vac P	% fuel required=	
☐		Vac P=	
☐		Fuel P required=	
☐		Total fill (vac P+fuel)=	
☐		Vf= litre	tf= second
☐	Open V2		
☐	Meter to total fill P	Actual pressure=	
☐	Close F1,F2,F3		
	Disconnect		
☐	CP2 from V2		
☐	**Ari filling**		
☐	Record required P	Final pretest P= mbars	(day ambient pressure)
☐	Crack V2 for initial air fill	Fill to 50 mbar less than pretest P	
☐	Close V2		
☐		Pretest P (driver vessel)= mbars	
☐	Close V1		
☐	Close V2		
	Check System		
☐	All valves are closed		
	Ignition State: Sequence		
☐	Checking ignition source		
☐	Start, Arm data logger		
☐	Open GV4		
☐	ignition	Ignition time =	
☐	Data logging ends		
☐	Save data		
	Purging End State		
☐	**Purging the test vessel**		
☐	Open V1		
☐	Open CB2		

☐	Start Vac B		
☐	Crack V5		
☐	Open V2		
☐	Allow Vac to run for >10 mins		
☐	Stop Vac B		
☐	Close CB2		
☐	Allow vessel pressure to reach ambient		
☐	Close V2		
☐	Close V1		
☐	Disconnect CP1 from V1		
	Data Check		
	Load test results		
	T/C and P data indicate ignition If No record: see S/P 2	**Recorded (P0)= bars**	
		Recorded (P1)= bars	
		Recorded (P2)= bars	
		Recorded (P3)= bars	
		Recorded (P4)= bars	
		Recorded (P5)= bars	
		Recorded (P6)= bars	
		Recorded (P7)= bars	
Y/N	Is the maximum recorded pressure lower than the maximum predicted one?		If no: see S/P3

Flame arrival Times		**Comments:**
thermocouples	Time	
T0		
T1		
T2		
T3		
T4		
T5		
T6		
T7		
T8		

Special Procedures (S/P) Sheet		**Authorized by**
No.	**Cause/Description**	**Action**
1	Leak to ambient	Close all valves Abandon test Collect leak
2	No ignition: fault in ignition circuit	Vessel contains exposable mixture Connect N2 supply Isolate barocel Fill vessel up 1.5 bars Open CB1, Start Vac B Evacuate vessel to <50 mbar Open V2,V3 and V4 (return vessel to ambient pressure) Re-integrate barocel Isolate N2 supply and follow purge procedure
3	Maximum pressures were underestimated	Go back to risk assessment stage Get more accurate pressure predictions